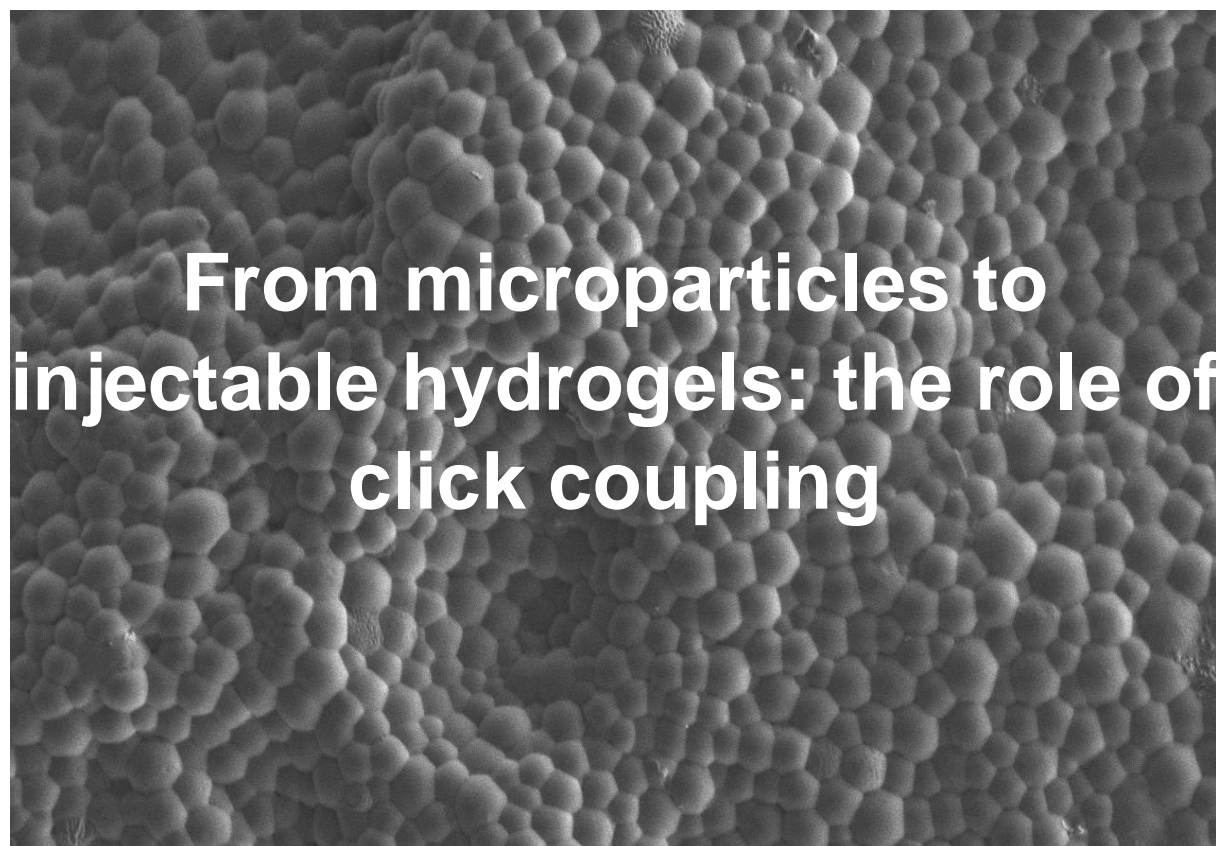


Faculty of Sciences
Department of Chemistry
Service des matériaux polymères
et composites

Faculty of Sciences
Departement of Organic and
Macromolecular Chemistry
Polymer Chemistry Research Group



From microparticles to injectable hydrogels: the role of click coupling

Absil Rémi

Promotor: Dr Laetitia Mespouille
Co-promotor: Prof. Dr. Filip Du Prez

Mons, 2017

Thesis submitted to obtain the degree of Doctor of Science: Chemistry

Exam Commission

Dr. Sylvain Gabriele (University of Mons)

Prof. Dr. Philippe Dubois (University of Mons)

Prof. Dr Roberto Lazzaroni (University of Mons)

Prof. Dr. Sandra Van Vlierberghe (Ghent University)

Prof. Dr. Andrij Pich (Aachen University)

Prof. Dr. Christopher Barner-Kowollik (Karlsruhe Institute of Technology)

Prof. Dr. Filip Du Prez (Ghent University)

Dr. Laetitia Mespouille (University of Mons)

Table of contents

Acknowledgements	
Abbreviations.....	
Symbols.....	
Chapter I: Introduction, aim and outline	1
I.1. Introduction and aim	1
I.2. Outline	1
I.3. Bibliography	3
Chapter II: Hydrogels in their diversities: definition and description	4
II.1. General introduction	4
II.2. Hydrogel structuration: the link between hierarchisation and physico-chemical properties	6
II.2.1. Chemical crosslinking	6
II.2.2. Physical crosslinking: generalities on physical stimuli	24
II.3. Doubly crosslinked networks	25
II.4. Advantages and limitations of the crosslinking methods	26
II.5. Shape and size designed hydrogels: the case of nano and microgels	27
II.5.1. Nano and microgels: description and applications	27
II.5.2. Synthetic processes for nano and microgels	31
II.5.3. Surface modifications	41
II.6. Doubly-crosslinked hydrogels as new injectable materials	44
II.6.1. Injectable hydrogels: breakthrough and challenges	44
II.6.2. The case of doubly crosslinked networks	46
II.6.3. From microgels to macrogels: gelation mechanisms	47
II.7. Bibliography	49
Chapter III: Synthesis of doubly crosslinked microgels by RAFT Hetero Diels-Alder click conjugation	61
III.1 Synthesis of click functionalized microgels by free radical suspension polymerization	61
III.1.1. Introduction to microgel synthesis and their surface modification	61
III.1.2. Synthesis of microgels by free radical suspension polymerization	64
III.1.3. Cyclopentadiene functionalization of microgels	70
III.1.4. Cytocompatibility of the Cp functionalized microgels	75
III.2. Doubly crosslinked microgels by RAFT-HDA click chemistry	77
III.2.1. Introduction on DX-gel	77
III.2.2. Synthesis and characterization of RAFT crosslinkers	79

III.2.3. Reactivity tests of various RAFT crosslinkers	88
III.2.4. DX gel synthesis	92
III.3. Conclusions	95
III.4. Experimental section	96
III.5. Bibliography	103
Chapter IV: Synthesis and characterization of DX hydrogels by TAD click chemistry in organic conditions	106
IV.1. Introduction	106
IV.2. DX-gel synthesis using TAD click chemistry in organic medium and characterization	107
IV.3. Investigation of the mechanical properties of doubly crosslinked gels	113
IV.2.1. Introduction and generalities	113
IV.2.2. Morphology of DX-gels and their swelling properties	116
IV.2.3. Investigation of mechanical properties of the DX-gels	119
IV.4. Conclusions	132
IV.5 Experimental section	133
IV.6. Bibliography	135
Chapter V: Synthesis of doubly crosslinked gels by TAD based HDA click chemistry in aqueous conditions	138
V.1. Introduction	138
V.2. DX-gel synthesis using TAD click chemistry in aqueous medium and characterization	139
V.2. Morphology of DX-gels and their swelling properties	141
V.2.1. Morphology investigations by SEM	141
V.2.2. Swelling behavior of the DX-gels	141
V.3 Biocompatibility proof of concept	142
V.4. Conclusions	143
V.5. Experimental section	144
V.6. Bibliography	145
Chapter VI: Microfluidics as a new synthetic road towards monodisperse click functionalized microgels	147
VI.1 Microfluidics: a key technique for monodisperse microgels production	147
VI.1.1 Introduction	147
VI.1.2. Monodisperse microgels produced by microfluidics	151
VI.2. Preparation of DX-gels from monodisperse microgels as-obtained by microfluidics	157
VI.3. Conclusions	159
VI.4. Experimental section	159

VI.5. Bibliography	161
Chapter VII: Conclusions and perspectives.....	164
VII.1. General conclusions	164
VII.2. Perspectives	167
Curriculum vitae	169
List of publications	169
List of poster presentation	169
List of oral presentation	170
Academic Visits.....	170

Acknowledgements

It is entirely fair to say that I've received more help and support in completing this thesis than at any other time of my life. I'm indebted to a great number of people and would like to extend my gratitude to the many people who have contributed

At first I would like to thank my promotor Dr. Laetitia Mespouille for providing me the opportunity to work on exciting and challenging projects as well as giving me the chance to pursue my own ideas. Your never-ending enthusiasm and optimism made it highly enjoyable to work with you. Thank you for your follow-up, your support and for the freedom you granted me during this 4 years.

At the same level, I would like to thank my co-promotor professor dr. Filip Du Prez. His ongoing commitment and dedication to research have created a dynamic and active atmosphere in his group, where creativity and ideas are highly stimulated. I would like also to thank you for your advice and critical look on my work and scientific discussion.

Thanks to my promotor, I was able present my work at national and international congresses, experiences that were enormously instructive.

I have to thank several post-docs of course as well that helped me during this PhD, so thank you Dr. Seda Çakır, Dr. Lucie Imbernon, Dr. Guadalupe Rivero, Dr. Roberto Teixeira, Dr. Richard Tood, Dr Sarah Tempelaar.

A special thanks to my two labs, both SMPC and PCR, for the discussion, interest, their advices, kindness during this 4 years.

Many thanks are given to all those who performed measurements and for the scientific discussion. As there are: Dr. Sylvain Gabriele (Fluorescent microscopy), Dr. Julien De

Winter (MALDI-ToF), Dr. Philippe Leclercq (AFM), Yoann Paint (SEM), Daniel Frank (Hr-MAS-NMR) and Fabienne Danhier for the toxicity test.

A special thanks as well to Nathalie and Queenie for all their help concerning administration regarding the last four years.

A special thanks as well to professor Christopher Barner-Kowollik who was so kind to invite me to work for three months in his lab in Karlsruhe, Germany. It was a wonderful experience to work with you and I enjoyed every the time spend in Karlsruhe.

I would like to thank my parents, brother, sister and family (in-law) for always being supportive and taking an interest in what I was doing. It was not always easy to explain what I was working on.

Also a big thanks to my friends that made these last four years so enjoyable. And last but not least, I would like to take the opportunity to thank the most important person in my life: Louise. In a couple of month, I will proudly call you my wife. Thanks to your endless support, bad moments disappeared with a single smile while sharing the good moments made it even more special. You are the biggest reason that I was able to finish this thesis and I will love you until the end of time.

Abbreviations

AA	Acrylic acid
ABCVA	4,4'-azobis(4-cyanovaleric acid)
AFM	Atomic force microscopy
APS	Ammonium persulfate
ATRP	Atom transfer radical polymerization
BSA	Bovin serum albumin
BDDA	1,4-butanediol diacrylate
CDCl ₃	Chloroform-d
CMG	Microgel concentration
CNT	Carbon nanotube
Cu	Copper
CuAAC	Copper catalyzed alkyne-azide cycloaddition
Cp	Cyclopentadiene
CV	Coefficient of variation
(H)DA	(Hetero) Diels Alder
DCC	<i>N,N'</i> -Dicyclohexylcarbodiimide
DCM	Dichloromethane
DMAc	Dimethylacetamide
DMAP	4-Dimethylaminopyridine
DMEM	Dulbecco Modified Eagle's medium
DMSO	Dimethyl sulfoxide
DVB	Divinylbenzene
DX	Doubly crosslinked
EA	Ethyl acetate
EAS	Electrophilic aromatic substitution
EDG	Electron donating group
EDMA	Ethylene dimethacrylate
EtoH	Ethanol
EWG	Electron withdrawing group

FDA	Food and drug administration
FRP	Free Radical polymerization
G'	Storage modulus
G''	Loss modulus
GMA	Glycidyl methacrylate
HA	Hyaluronic acid
HD-OH	Trans,trans hexadiene-1-ol
HCl	Hydrochloric acid
HDA	Hetero Diels-Alder
HLB	Hydrophilic-lipophilic balance
HEMA	2-hydroxyethyl methacrylate
HOMO	Highest occupied molecular orbital
k	Rate constant
LCST	Lower critical solution temperature
LUMO	Lower unoccupied molecular orbital
MALA	Maleamic acid
MDI-TAD	4,4'-(4,4'-diphenylmethylene)-bis-(1,2,4-triazoline-3,5-dione)
MG	Microgel
MMA	Methyl methacrylate
MALDI-ToF	Matrix assisted laser desorption ionization time of flight
M_n	Numeric average molecular weight
M_p	Peak maximum molecular mass
MTT	(3-(4,5-dimethylthiazol-2-yl)-2,5-diphenyltetrazolium bromine
NMP	Nitroxide mediated polymerization
NMR	Nuclear magnetic resonance
O/W	Oil in water
PAA	Poly(acrylic acid)
PAE	Poly(β -amino ester)

PCL	Poly(ϵ -caprolactone)
PCS	Photon correlation spectroscopy
PDMAEMA	Poly(<i>N,N</i> -dimethylamino-2-ethyl methacrylate)
PDMS	Polydimethylsiloxane
PEAI	Poly(<i>N</i> -acetyethyleimine)
PEG	Poly(ethylene Glycol)
PEGDA	Poly(polyethylene glycol diacrylate)
PEGMA	Poly(ethylene glycol) methyl ether methacrylate
PIV	Particle image velocimetry
PLA	Poly(lactic acid)
PMMA	Poly(methyl methacrylate)
PNiPAM	Poly(<i>N</i> -isopropylcrylamide)
PS	Polystyrene
PTAD	4-phenyl-1,2,4-triazoline-3,5-dione
Pyr-Mal	<i>N</i> -(1-pyrene) maleimide
P(VC)	Poly(vinyl carbazole)
RAFT	Reversible addition-fragmentation chain transfer
RDRP	Reversible deactivation radical polymerizations
ROP	Ring opening polymerization
Rpm	Rotation per minute
SEC	Size exclusion chromatography
SEM	Scanning electron microscopy
SPAAC	Strain-promoted alkyne-azide cycloaddition
SX	Singly crosslinked
TAD	Triazolinedione
TFA	Trifluoro acetic acid
THF	Tetrahydrofurane
TEMED	<i>N,N,N',N'</i> -tetramethylethylene diamine
VC	9-vinylcarbazole
W/O	Water in oil

Symbols

σ_{eq}	Swelling ratio at equilibrium
ϕ	Volume fraction
m	Mass
ρ	Density
α	Deswelling ratio
d	Diameter
μ	Chemical potential
V	Volume
X	Mole fraction
M	Molecular weight
\mathfrak{D}	Dispersity
γ_c	Critical strain

Chapter I: Introduction, aim and outline

I.1. Introduction and aim

Injectable polymer networks are gaining increasing attention as scaffolds for drug release or tissue engineering owing to their ability to fill ill-defined locations upon injection. In that context, doubly crosslinked gels (DX gels) appear as a highly interesting candidate as primarily crosslinked microbeads can be injected with a reactive crosslinker to generate *in situ* macroscopic networks filling and fitting cavities at perfection to optimize their action. Compared to other injectable networks, this new class of injectable hydrogels offers a better tuning of hydrogel hierarchisation, swelling and mechanical properties.^[1] However, these DX-gels are mainly obtained by radical coupling of vinyl functionalized particles, making this gelation mechanism inconvenient for *in vivo* applications.^[1-4]

This thesis aims to investigate two major points: 1) to assess the potential of copper-free click reactions in the synthesis of DX-gels in mild and fast conditions and 2) to evaluate the microgel synthetic process in terms of microgel size distribution.

To favor the installation of click reactive functionalities onto the starting microgels, our strategy relies on the preparation of glycidyl-functionalized microgels by copolymerization of glycidyl methacrylate and PEG-based methacrylate through a free radical approach. The epoxide functions retained in the glycidyl monomer offer an opportunity for post-derivatization of microgels shells by epoxide ring-opening reaction. In the particular framework of this thesis, cyclopentadiene functionalized microgels will be prepared as this moiety is readily reactive in hetero Diels-Alder click reactions. Crosslinking between the beads will be achieved by introducing in the medium a crosslinker functionalized with the complementary click reactive function. Based on the literature, our choice went to a RAFT-functionalized PEG-based linker on the one hand and a triazolinedione (TAD)-based linker on the other hand.

I.2. Outline

The Research and Discussion part of this thesis is subdivided into 4 chapters (starting from chapter 2) preceded by a literature review.

Chapter 2 details a general method for the preparation of cyclopentadienyl (Cp) functional microgels by conventional water in oil radical suspension copolymerization of poly(ethylene glycol methyl ether methacrylate) with glycidyl methacrylate and ethylene glycol dimethacrylate as crosslinkers. Post-modification with sodium cyclopentadiene of the microgels was subsequently achieved by taking advantages of the glycidyl functions via the opening of the epoxide function. The effectiveness of the epoxide opening reaction in providing cyclopentadiene functionalization was examined to confirm the efficiency of the functionalization and the reactivity of the Cp group onto the microgels surface. In this chapter, RAFT-HDA was chosen as click reaction to promote doubly crosslinked microgels. Several RAFT-functionalized PEG-based crosslinkers were prepared. Their structures and reactivities were analyzed through various techniques and finally tested for the synthesis of DX-gels.

In chapter 3, three cyclopentadiene-functionalised microgel systems are prepared by the emulsion co-polymerisation of each of the monomers involved in chapter 2. In this chapter, we describe a new approach towards DX-gels synthesis by making use of the ultrafast triazolidione (TAD)-based click reaction to promote the formation of DX-gel networks. The click functionalization of the microgels, allows for the formation of polymer gel networks containing both intra-particle and inter-particle crosslinking by using the TAD-Diels Alder click chemistry. These so-called double crosslinked gels show greater mechanical properties than single crosslinked microgels. The relationship between the relative Cp/TAD ratio and gel mechanical properties is discussed, as it offers the possibility to control not only the kinetics of the gelation but also the final gel mechanical properties. Finally, the various batches made for this chapter were used to investigate the influence of several parameters over the final mechanical properties of the DX-gels such as the microgel's intracrosslinking, the microgel size and the size distribution, and finally the initial microgel's concentration. In the same range of ideas, physical parameter like setting pressure during the DX-gel preparation was also experienced to evidence impact on the final properties.

Chapter 4 is dedicated to the early promising tests of DX-gel synthesis in water solution. As a prerequisite for biomedical application, a proof of concept was established. Interestingly enough, biocompatibility tests of the resulting DX-gel was evaluated *in vivo* after implantation into mice.

Chapter 5 detailed a new procedure for the synthesis of monodispersed microgels by a microfluidic process and its subsequent functionalization with sodium cyclopentadiene. Several parameters including monomer concentration, needle size, surfactant quantity and nature, flows of both continuous and discrete phase are discussed in this chapter. Finally, doubly crosslinked gels using those highly monodisperse microgels are prepared and analyzed using SEM.

I.3. Bibliography

1. Liu, R.X., et al., *Tuning the swelling and mechanical properties of pH-responsive doubly crosslinked microgels using particle composition*. Soft Matter, 2011. **7**(19): p. 9297-9306.
2. Milani, A.H., et al., *Swelling and mechanical properties of hydrogels composed of binary blends of inter-linked pH-responsive microgel particles*. Soft Matter, 2015. **11**(13): p. 2586-2595.
3. Lane, T., et al., *Double network hydrogels prepared from pH-responsive doubly crosslinked microgels*. Soft Matter, 2013. **9**(33): p. 7934-7941.
4. Farley, R., et al., *Using click chemistry to dial up the modulus of doubly crosslinked microgels through precise control of microgel building block functionalisation*. Polymer Chemistry, 2015. **6**(13): p. 2512-2522.

Chapter II: Hydrogels in their diversities: definition and description

II.1. General introduction

Since the pioneering works of Wichterle and Lim in the early 1950s, hydrogels in their diversities have known an explosive interest and development in various applicative fields. In their infancy, the first hydrogels were designed for applications in ophthalmology. The main features that synthetic materials must meet to satisfy biomedical requirements were: (a) shape stability and softness similar to that of the soft surrounding tissue; (b) chemical and biochemical stability; (c) absence of extractable; and (d) high permeability for water-soluble nutrients and metabolites. Based on this rationale, in 1953, Drahoslav and Lim synthesized the first hydrogels by copolymerization of 2-hydroxyethyl methacrylate (HEMA) with ethylene dimethacrylate (EDMA). These polymers were described in a seminal paper published in *Nature* in 1960.^[1] Meanwhile, Otto Wichterle prepared the first soft (hydrogel-based) contact lenses by the spin casting process.^[2] Interestingly, the first studies on hydrogel biocompatibility were published in 1959 and 1960.^[3, 4]

Since then, progresses realized in macromolecular engineering together with the development of manufacturing techniques, have led to a variety of new hydrogel based-materials presenting outstanding properties owing to an adequate combination of starting polymers and/or fillers, opening the doors to a plethora of new applications encompassing biomedical ones. Nowadays, the wide range of hydrogel materials can be classified according to different criteria as the material source (natural, synthetic or hybrid), the nature of the crosslinking (chemical or physical), the range size of the material (from nano to macro), the resulting properties (magnetic, electroconductive, pH-sensitive, temperature-sensitive, drug-sensitive), the type of gel hierarchisation (homopolymer networks, copolymer networks, (semi)-interpenetrating networks, or double networks), the pore sizes (homogeneous (optically transparent) hydrogels, microporous and macroporous hydrogels) and their fate in the organism (degradable and non-degradable hydrogels).^[5]

Over the past 30 years, the design of hydrogels has remarkably progressed owing to their appealing properties extending their applications in various fields. Benefits for the biomedical ones are clearly exemplified through the massive publications arising in literature, with particular preferences for drug delivery and regenerative medicine. In particular, their tuneable chemical and three-dimensional physical structure, their high water content, smartness, good mechanical properties and biocompatibility allow to evolve towards materials in contact with *in vivo* medium and successful clinical applications as for example the VivaGel™ (SPL7013 Gel) used as microbicides for the protection against sexually transmitted infections.

While a plethora of advanced applications are accessible to hydrogels, one of the most important parameters that will orient the fate of the hydrogel-based materials is the crosslinking organization. The crosslinks, or in other words the nodes connecting polymer chains to form a network structure, will regulate the water content, the resulting mechanical properties, their deformability, the kinetics of degradation if any, their shape stability or even their moldability. Therefore, controlling the intimate structuring of the hydrogels is extremely important since it conditions their resulting properties and their field of use. **Injectable hydrogels** are a subgroup of the hydrogel family but predominantly used in research and clinical applications for several reasons. A major limitation of most scaffold materials used for tissue engineering is the need for surgical implantation. For many clinical uses, injectable *in situ* crosslinkable hydrogels would be strongly preferred for three main reasons. Firstly, an injectable material could be formed into any **desired shape** at the site of injury and formed complex shapes by subsequent crosslink of the solution or moldable putties. Secondly, the gel formed would adhere to the environmental tissue during the crosslink. Therefore a mechanical interlocking would arise from surface microroughness and strengthen the tissue-hydrogel interface. In the case of drug delivery, this close contact would also maximize the contact with diseased tissues aiming an easier drug release. Thirdly, introduction of an *in situ* crosslinkable hydrogel could be accomplished by injection or laparoscopic methods and thereby minimizing the invasiveness of the procedure.^[6]

Development of an injectable hydrogel for tissue repair or tissue regeneration also comes with considerable challenges. The gelation conditions for *in vivo* use are limited to a narrow range of physiologically acceptable temperatures, and the crosslinking

must occur with **no byproducts** in a sensitive aqueous environment. Reagents must be nontoxic reagents and tolerant of moist, oxygen-rich environments. Furthermore, gelation must occur at a sufficiently **rapid rate** for clinical use in an outpatient or operating suite setting. Yet, it must be sufficiently slow to complete mixing prior to gelation. Various crosslinking approaches to prepare hydrogels are used in order to achieve specific properties, such as gelation time, mechanical modulus, and biocompatibility of the ensuing hydrogels that are important for tissue engineering applications.

II.2. Hydrogel structuration: the link between hierarchisation and physico-chemical properties

Hydrogels are by definition three-dimensional polymer networks that can retain a large amount of water without dissolution. This ability to hold a large quantity of water while preserving their 3D structure arises from the reticulation nodes occurring between the polymer chains. These nodes are named crosslinking points and can be of different nature depending on the kind of link established. We distinguish chemical crosslinkings that are covalent bonds from physical crosslinkings that arise from weak secondary interactions.

II.2.1. Chemical crosslinking

II.2.1.1. From functional and reactive polymer precursors to polymer networks

Hydrogels are referred as permanent or chemical hydrogels when the crosslinking is the result of covalent bonds. Therefore, these gels do not dissolve in water or in any organic solvents. There are two different approaches to synthesize chemical hydrogels: by polymerizing a water-soluble monomer in the presence of a bi- or multifunctional crosslinker agents or by crosslinking of water-soluble and reactive polymer precursors using typical organic chemical reactions that involve the functional groups of the polymer (Figure II.1A & B).

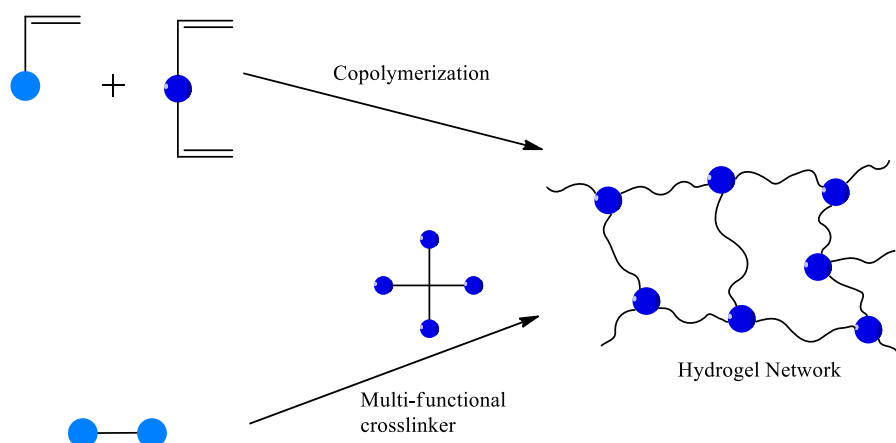


Figure II.1.A: Synthesis of chemically crosslinked hydrogels by free radical (co)polymerization.

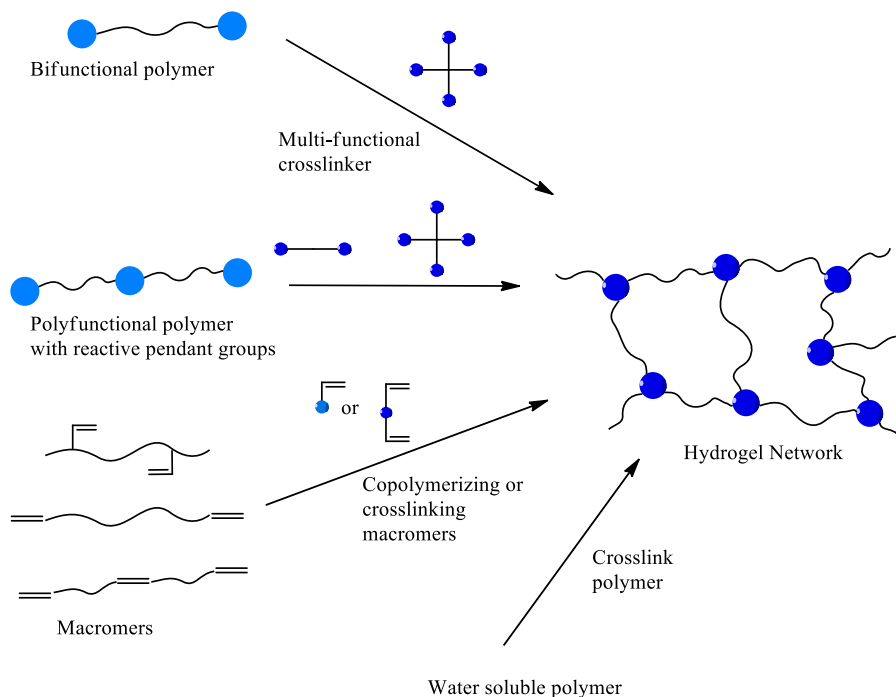


Figure II.1.B: Synthesis of chemically crosslinked hydrogels from the functional polymer precursor approach.

The chemical crosslinking prevents the polymer network from dissolution when immersed in a solvent. These solid nodes allow the gel to swell until it reaches its saturation, named swelling ratio at equilibrium (σ_{eq}). This swelling ratio at equilibrium is the result of two opposing phenomena: on one hand, the interactions between the polymer and the solvent that contribute to the swelling and on the other hand, the

retractile elastic forces which take their origins in the crosslinking density. In contrast to physical hydrogels (as discussed in the next section), chemical hydrogels have a better organized structure owing to the local nature of the covalent crosslink points compared to physical junctions, that are more diffuse as they involve polymer segments (Figure II.2).^[7]

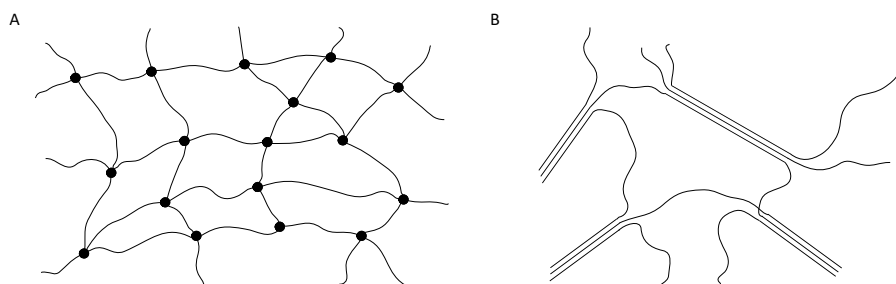


Figure II.2: (A) Schematic description of a chemical gel with covalent crosslinked points and (B) Schematic description of a physical gels with multiple junction zones.

However, free chain ends and formation of “loops” can occur and are depicted as gel network “defects”, which can highly impact on the elasticity of the network (Figure II.3).

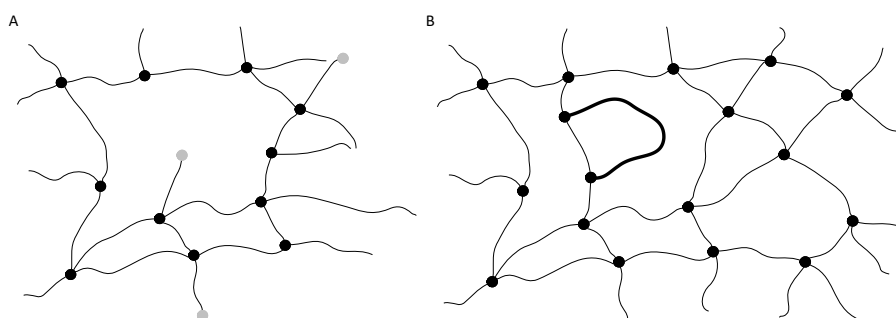


Figure II.3: (A) Schematic representation of network defects (●) and (B) loop chain defects (in bold).

1.2.1.2. Implementation of the click chemistry reaction in polymer network synthesis

1.2.1.2.1. Click chemistry: definition and recent developments

“Click” chemistry’ is a term introduced by K. B. Sharpless and coworkers in 2001 ^[8] to describe a set of highly efficient reactions between modular building "blocks" for the synthesis of novel molecules. The authors defined a set of stringent criteria that a reaction must meet to be qualified of “Click process”:

- be modular
- wide in scope
- give very high yield
- generate only inoffensive byproducts
- be stereospecific.

In addition, the process must present particular characteristics as:

- simple reaction conditions
- high thermodynamic driving forces
- readily available starting materials and reagents
- use of no solvent or a solvent that is benign or can easily be removed
- simple product isolation by non-chromatographic methods.^[8]

Click chemistry is not limited to a specific type of reaction, but stands as a synthetic philosophy that comprises a range of reactions, with different reaction mechanisms but common reaction trajectories (Figure II.4). Owing to these outstanding features, Click chemistry reactions are ideal candidates for biomaterial synthesis.

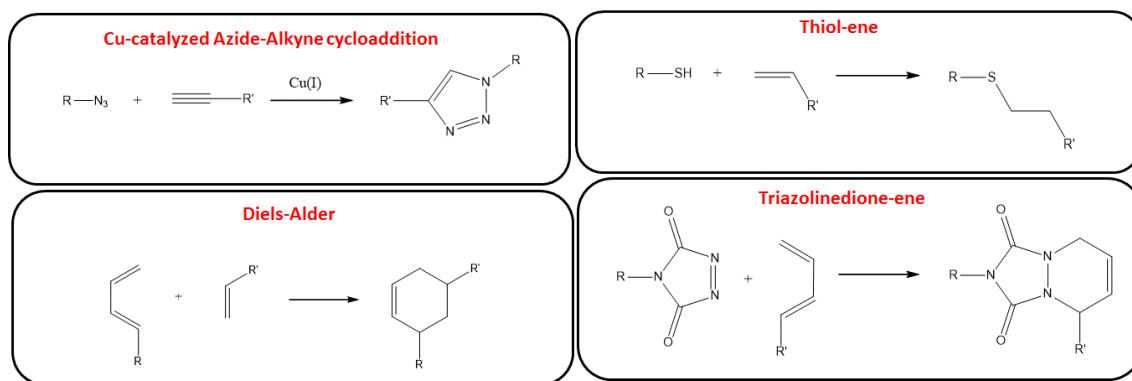


Figure II.4: List of widely exploited chemical reactions that fall within the framework of click Chemistry and recent advances in click chemistry.

Since then many organic reactions have been identified to belong to the Click reaction family (Figure II.4) and applied in polymer science to design various polymer architectures as flexible and efficient methods to connect functionalized molecules. Thanks to these advantages, click chemistry has become a great tool in the fabrication

of hydrogels, nanogels and microgels as emerging platforms for tissue engineering and drug delivery.^[9] Since their introduction, a large amount of examples can be found in literature using click chemistry for the synthesis of hydrogels.

II.2.1.2.2. Cu-catalyzed Huisgens cycloaddition applied to hydrogel synthesis

The Huisgen cycloaddition reaction is a process in which monosubstituted azides and alkynes combine their π electrons to form a stable 1,2,3-triazole molecule. Sigma bonds are formed between the termini of π systems following a concerted mechanism. Azides and alkynes functions are functions easy to install and are also lower reactive species in organic chemistry. For this reason, the reaction requires high temperature and long reaction time. Moreover, the reaction yields to two disubstituted isomers in 1,4 and 1,5 positions. However, the process can be greatly accelerated by using a catalyst. This is the prime example of a click reaction reported by Sharpless and Medal laboratories demonstrating a dramatic increase in reaction rate for the traditional Huisgen cycloaddition using a copper catalyst.^[10, 11] Another important aspect of the success of this reaction pertaining to materials science and biotechnology is that the starting materials, azides and terminal alkynes, are exceptionally stable and can be introduced in a wide range of macromolecules. This new reaction, termed copper catalyzed alkyne-azide cycloaddition (CuAAC), has since become the actual main reaction of click chemistry. A proposed dinuclear copper intermediary mechanism is displayed in Figure II.5. The value of click chemistry for materials synthesis possibly becomes most apparent in the area of polymer chemistry where several reviews have described the use of Cu-catalyzed azide-alkyne cycloaddition (CuAAC) for the synthesis of dendritic, branched, linear and cyclic co-polymers.^[12-15]

As one of the best click reactions to date, the copper-catalyzed azide-alkyne cycloaddition features an enormous rate acceleration of 10^7 to 10^8 compared to the uncatalyzed 1,3-dipolar cycloaddition. It succeeds over a broad temperature range, is insensitive to aqueous conditions and a pH range over 4 to 12, and tolerates a broad range of functional groups. Pure products can be isolated by simple filtration or extraction without the need for chromatography or recrystallization.

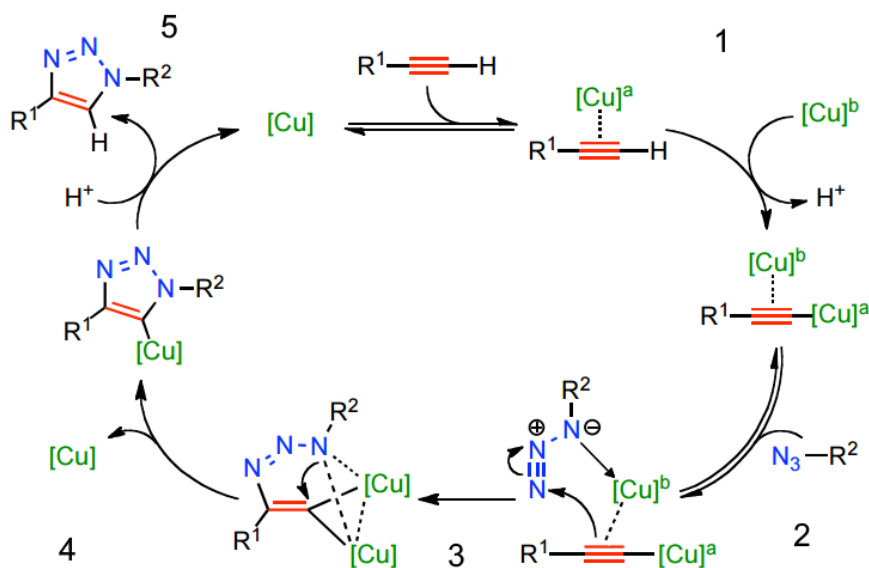


Figure II.5: Mechanism of the Cu-catalyzed Huisgen cycloaddition reproduced from [16].

In recent years, this widely used chemistry has been applied for the synthesis of a large variety of hydrogels for multiple applications. In 2006, a PEG based hydrogel has been synthesized by coupling azide derivatized and alkyne derivatized PEG and showed to result in well-defined networks having significantly improved mechanical properties.^[17] Mespouille *et al.* prepared adaptative and amphiphilic polymer conetworks based on hydrophilic poly(*N,N*-dimethylamino-2-ethyl methacrylate) (PDMAEMA) and hydrophobic poly(ϵ -caprolactone) (PCL) by combining ATRP, ROP, and “click chemistry” where the adaptative and amphiphilic properties of hydrogels were highlighted.^[18] Illustration of the synthesis is depicted in Figure II.6.

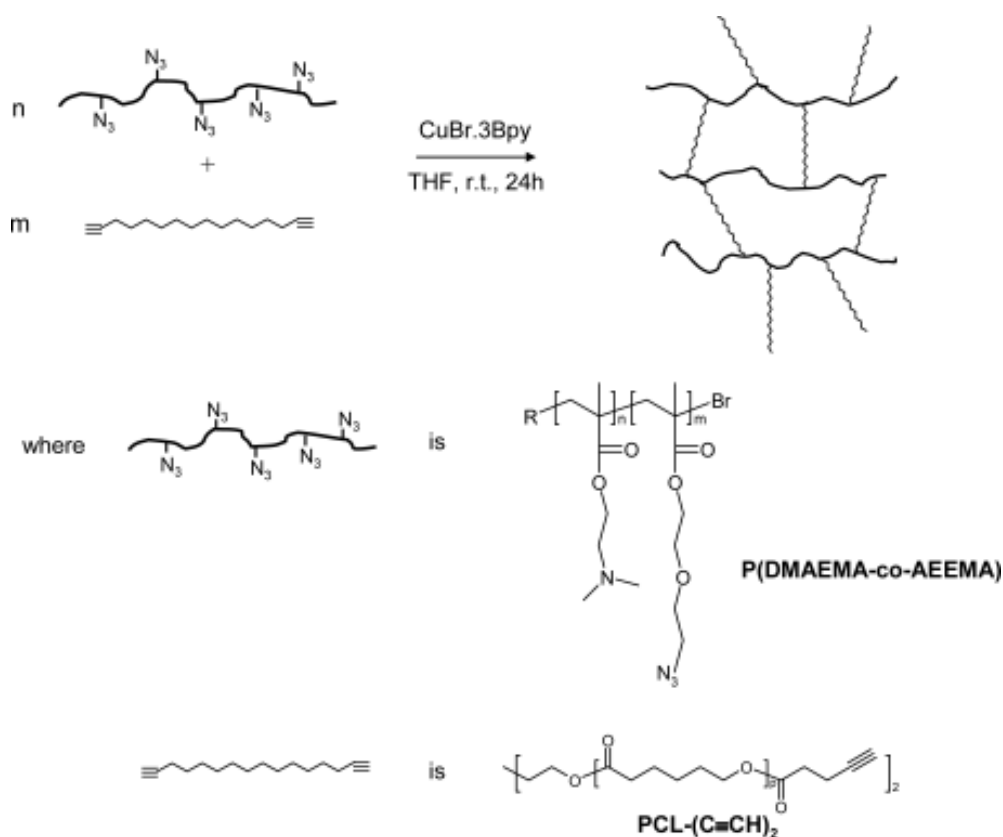


Figure II.6: Illustration of the synthesis of an hydrogel using Huisgen cycloaddition.^[18]

More recently, in order to mimic the natural cartilage tissue, a biological hydrogel made of hyaluronic acid, chondroitin sulfate and gelatin was synthesized using grafted azide and alkyne. Interestingly, *in vitro* cell culture showed that the hydrogel could support the adhesion and proliferation of chondrocytes.^[19] In the same range of ideas, cellulose based click hydrogels were prepared using cellulose derivatized respectively by sodium azide and propargylamine. Gel formation occurred after mixing the aqueous solutions of both components and copper(I) catalyst. The gelation time depended on both the degree of functionalization and the amount of copper(I) catalyst.^[20]

Copper (I) ion being toxic, alternative metal-free approaches have been developed in the literature by taking advantage of ring strain to promote the dipolar 1,3-cycloaddition between azide and alkyne. In this context, the reaction occurs between cyclooctyne compounds, the smallest ring retaining alkyne function, and an azide. This approach, called “strain-promoted alkyne-azide cycloaddition (SPAAC)”, is efficient in physiological conditions, without the need of extra reagents as illustrated in Figure II.7.^[21]

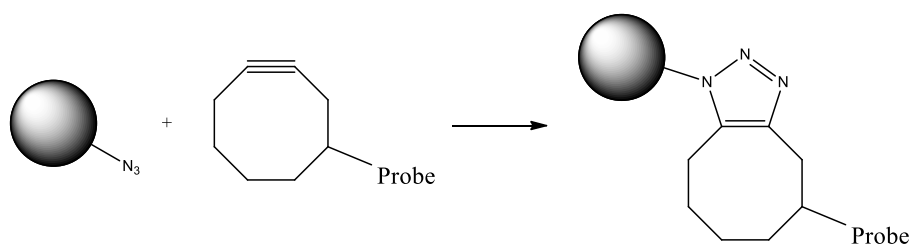


Figure II.7: Illustration of the SPAAC cycloaddition. Reproduced from [21].

Continuing on these promising results, several examples using the SPAAC chemistry have been applied to form injectable hydrogels. Indeed, without the presence of copper, the toxicity of this reaction should be greatly reduced. A first example of copper free click chemistry for the synthesis of hydrogels was published in Nature in 2009. In this work, macromolecular precursors react through a copper-free click chemistry allowing the direct encapsulation of cells within click hydrogels.^[22] In a next paper, they developed a strategy where step-growth networks are formed rapidly via a copper-free, azide-alkyne click chemistry between tetrafunctional poly(ethylene glycol) molecules and difunctionalized synthetic polypeptides. A sequential photochemically activated thiol-ene chemistry allowed subsequent functionalization of the network through reaction with pendant alkene moieties on the peptide. It exploited this alkene to create complex biochemical gradients of multiple peptides with well-defined magnitude and slope throughout the three-dimensional (3D) network.^[23] Based on their previous work, Anseth's team also developed programmable niches to study and direct cell function by modifying the local hydrogel environment.^[24] In the same range to have cell culture system dynamically tunable, a photocleavable PEG hydrogel was developed to control mechanical properties temporally and study the role of matrix signaling on stem cell function and fate.^[25] Another example of similar chemistry can be found in nature materials where Anseth's team exploited two bioorthogonal photochemistries to achieve reversible immobilization of bioactive full-length proteins with good spatial and temporal control within synthetic, cell-laden biomimetic scaffolds.^[26]

A biodegradable PEG based hydrogel was synthesized via copper-free, strain-promoted azide-alkyne cycloaddition (SPAAC) click chemistry owing to ester group introduced into the crosslinked networks. Azide and cyclooctyne moieties on the PEG

backbones underwent a rapid click reaction to trigger the formation of the hydrogel within several minutes.^[27]

II.2.1.2.3. The thiol-ene/thiol-yne reaction in hydrogel synthesis

There are several features associated with the thiol-ene reaction. This reaction proceeds in extremely high yields with fast kinetics, with good tolerance for functional groups, and can often be done without solvent, simplifying purification and making the reaction very user friendly and easy due to its insensitivity to oxygen. An illustrative review on thiol-ene polymerizations was given by Hoyle *et al.*^[28, 29]

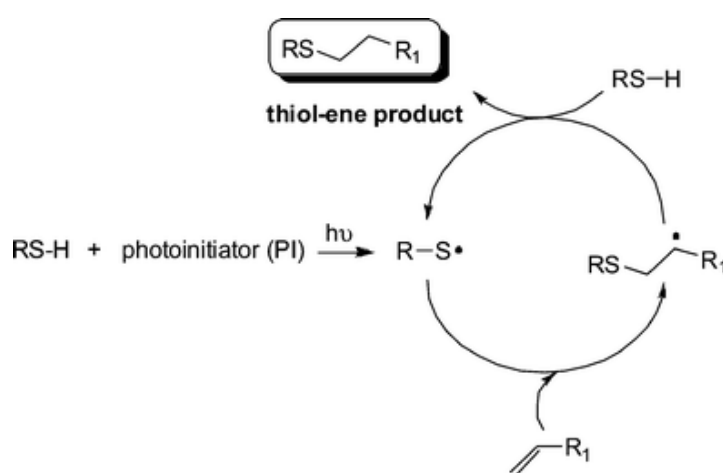


Figure II.8: The radical-mediated thiol-ene reaction mechanism, with initiation, propagation and chain transfer, and termination processes.

The thiol-ene system relies on a free-radical mechanism involving two steps as depicted in Figure II.8: the hydrogen abstraction of a thiol group to generate a thiyl radical function and its anti-Markovnikov addition onto an alkene to form a thioether bond. Termination occurs by radical– radical coupling.

Reactivity of the alkene is largely determined by the alkene structure, its reactivity being dependent on the degree of substitution. Classical examples of thiol-ene in hydrogels synthesis can be found in the paper of Dove *et al.*^[30] and Aimetti *et al.*^[31] They used poly-ene functionalized polymers that crosslink at the contact of difunctional thiol to promote hydrogel formation. An illustration of this method can be found in Figure II.9.

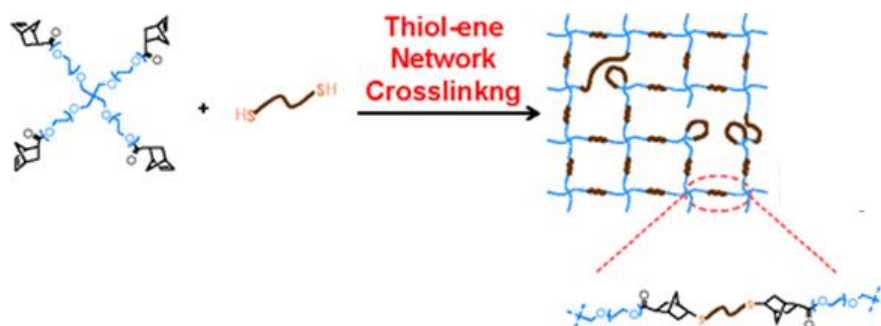


Figure II.9: Illustration of hydrogel synthesis using thiol-ene chemistry reproduced with modification from reference [31].

Light mediated thiol-ene radical reaction presents several benefits with the following advantages due to the photoinitiated process. Therefore, the reaction can be activated at specific location and time, offering a powerful tool for chemical synthesis and for tailorable materials fabrication.^[32-34] Moreover, the simplicity, robustness, and mechanism of the thiol-ene photopolymerization address each of the critical limitations of traditional photoinitiated systems by forming a homogeneous polymer network through a controllable combination of step-growth and chain-growth processes, with significantly simplified polymerization kinetics, reduced shrinkage and stress, and insensitivity towards oxygen. Due to these distinct advantages, the thiol-ene photopolymerization is at the heart of extensive fundamental research and of practical implementation in a number of novel applications in the last few years. In the hydrogel field, thiol-ene reaction has received directly a large success where PEG based modified hydrogel were synthesized.^[31, 35] PEG-based thiol-ene hydrogels are some of the most common types of hydrogels used in controlled release of therapeutic proteins. For example, Buwalda *et al.* cross-linked 8-arm PEG-poly(L-lactide)-acrylate block copolymers with multifunctional PEG-thiols for the encapsulation and release of the model proteins lysozyme and albumin.^[36] Protein diffusion out of the hydrogel was slowed relative to diffusion in water and took place on time scales of days to weeks, demonstrating controlled release. Recently, McCall and Anseth compared the efficiency of photoinitiated thiol-norbornene with photopolymerization of acrylate for the encapsulation of a model protein within PEG-based hydrogels.^[37] Interestingly, hydrogel degradation rates can be engineered to respond to microenvironment conditions such as the presence of enzymes, reducing conditions or pH. These conditions allow a triggered release of a protein therapeutic. For example, PEG-based

hydrogels formed by thiol-norbornene photopolymerization with cysteine functionalized and enzyme-sensitive peptide crosslinks were developed and used for protein release by Anseth and coworkers.^[31] An alternative approach to localized protein release was used by Kharkar *et al.* They formed PEG-based hydrogels sensitive to glutathione, which is elevated in tumors, using thiol-maleimide chemistry.^[38, 39] Hydrogels encapsulating BSA were formed with PEGmaleimide and PEG functionalized with different thiols modifying hydrogel degradability. Although PEG-based materials are often commercially available and a number of them are FDA approved,^[40] there is a limit to the possibility one can achieve simply by varying the end groups and functionality of PEG-based monomers. Langer and coworkers synthesized a large library of thiol-functionalized ethoxylated polyol esters and reacted them with PEG-diacrylate to form a library of hydrogels with highly tailorable rates of degradation.^[41]

II.2.1.2.4. Hetero Diels-Alder click reaction in hydrogel synthesis

Diels–Alder (DA) is a widely used reaction in organic synthesis where a diene reacts with a dienophile. This reaction was discovered by Otto Diels and Kurt Alder who received the Nobel Prize in 1950 for their discovery.^[42] The DA reaction is a concerted pericyclic reaction and its characteristics can be explained with the frontier molecular orbital (FMO) theory.^[43] Efficient DA reactions require the combination of electron-poor dienophiles and electron-rich dienes, (normal electron demand) or electron-rich dienophiles and electron-poor dienes (inverse electron demand) to realize a small HOMO-LUMO gap as depicted in Figure II.10.

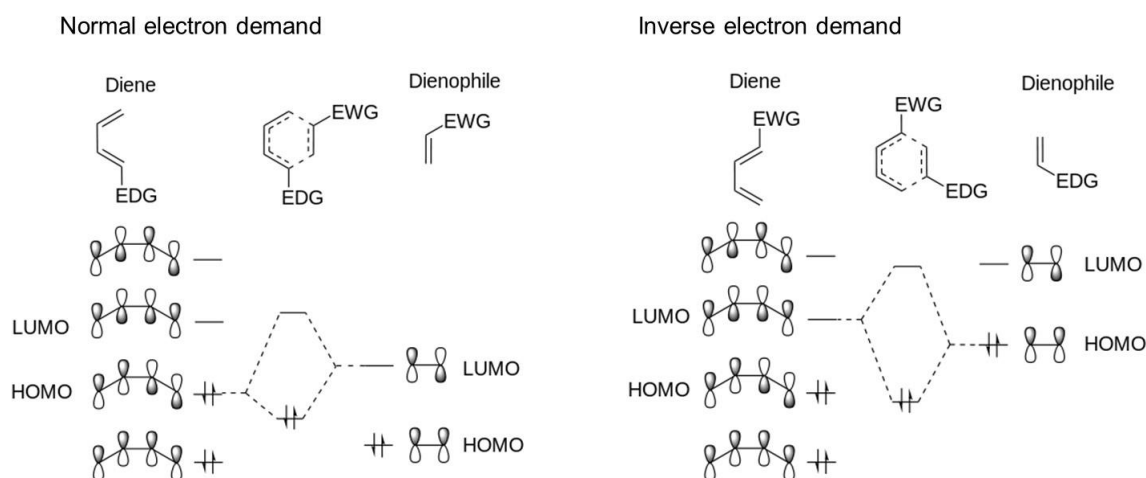


Figure II.10: Frontier orbital interactions in DA reactions with different electron demand. EWG = electron withdrawing group, EDG = electron donating group.

A substituted cyclohexene is formed in this reaction through the [4 + 2] cycloaddition of a diene and a dienophile. Due to the concerted mechanism DA reactions are highly stereospecific, *i.e.* the stereochemical information (*E* or *Z*) of the diene and the dienophile is transferred into the product. Interestingly, the reaction is thermally reversible when the reactants are stable molecules or when one can be consumed in a side reaction. The reverse reaction is known as the retro Diels–Alder reaction.

A variant is the hetero Diels-Alder, in which either the diene or the dienophile contains a heteroatom, most often nitrogen or oxygen. This alternative constitutes a powerful synthesis of six-membered ring heterocycles. C. Barner-Kowollik and M. H. Stenzel introduced in 2008 the use of RAFT hetero Diels-Alder especially in polymer science as a powerful tool for synthesis.^[44] The combination of RAFT chemistry and the hetero Diels–Alder (HDA) cycloaddition was successfully utilized in the synthesis of poly(styrene) (PS) star polymers with up to 4 arms. This variant of the “coupling onto” method of star polymer synthesis was investigated for two different RAFT end groups (diethoxyphosphoryldithioformate and pyridin-2-ylthioformate) and coupling agents bearing 2, 3, or 4 diene functional groups.^[45] Recent papers have shown the huge potential of hetero Diels-Alder reaction in polymer science to produce block copolymer, graft copolymer network and highly complex architecture polymer.^[46-52]

The application of Diels–Alder (DA) click chemistry for hydrogel formation has recently grown, because of the efficient chemical bonding and the mild biological reaction conditions. The primary example of Diels-Alder coupling reaction to form a hydrogel was published in 1990.^[53] In this paper, Chujo *et al.* described the synthesis of poly(oxazoline) hydrogel by the means of Diels-Alder reaction between furan modified poly(N-acetyylethyleimine) (PEAI) and a maleimide-modified PEAi. Some years after this work, a growing amount of papers using Diels-Alder for the synthesis of hydrogel was published.

An injectable hyaluronic acid/PEG (HA/PEG) hydrogel was successfully synthesized for the first time through two crosslinking processes: the first one being enzymatic crosslinking and the second being a subsequent DA click chemistry crosslinking. The enzymatic crosslinking resulted in a fast gelation of HA/PEG in 5 min, leading to the formation of an injectable material. In addition, the DA click reaction crosslinking outstands the properties of the hydrogel giving high shape memory and anti-fatigue

properties.^[54] Later, furan-modified HA derivatives were synthesized and crosslinked via dimaleimide poly(ethylene glycol) to achieve an easy one step setup in an aqueous based system. By controlling/changing the furan to maleimide molar ratio, both mechanical and degradation properties of the resulting Diels–Alder crosslinked hydrogels can be tuned. These HA crosslinked hydrogels were shown to be cytocompatible and might represent a promising material for soft tissue engineering.^[55] Later, Shoichet and coworkers demonstrated the use of a Diels–Alder click reaction to create a stable and biocompatible hyaluronic acid hydrogels by modifying the carboxylic group of HA with furfurylamine to create furan-functionalized HA. Finally, the modified HA was crosslinked with a maleimide PEG crosslinker to form hydrogels.^[55] The mechanical and degradation properties of these hydrogels can be modulated using various molar ratio of furan to maleimide. Using a similar approach, Marra and coworkers prepared HA-based hydrogels for controlled release application.^[56] HA was functionalized by either a maleimide or a furan group and crosslinked in PBS at 37 °C within ~40 minutes. Insulin (negatively charged) or lysozyme (positively charged) were encapsulated as model proteins within these HA-based hydrogels. The release profiles showed slight or no burst release depending upon the protein, owing to electrostatic interactions. Moreover, the hydrogels were cytocompatible and maintained the viability of the entrapped cells. Furthermore, polysaccharides were derivatized into precursor able to react through aqueous Diels–Alder chemistry without the involvement of catalysts and coupling reagents. It allowed direct encapsulation of positive and negative proteins within biodegradable hydrogels and demonstrated that aqueous Diels–Alder chemistry provides an extremely selective reaction and proceeds with high efficiency for polysaccharide bioconjugation.^[56]

Recently, the tetrazine–norbornene inverse electron demand Diels–Alder reaction has been used as a new crosslinking chemistry for the formation of cell laden hydrogels. Indeed, when multifunctional PEG-tetrazine macromer was reacted with a dinorbornene peptide, the fast reaction rate and irreversible nature of this reaction allowed hydrogel formation within minutes.^[57] Moreover, the specificity of the tetrazine–norbornene reaction was exploited for sequential modification of the network via thiol–ene photochemistry. These advantages, combined with the synthetic accessibility of the tetrazine molecule, make this crosslinking chemistry interesting and powerful for the development of new cell-instructive hydrogels for tissue engineering

applications.^[58] Taken together, all these examples indicate that the Diels–Alder crosslinking is a promising strategy for the design of cell-compatible hydrogels allowing potential applications and new promising strategies for soft tissue engineering, regenerative medicine and controlled release applications.

II.2.1.2.5. TAD Chemistry

Triazolinedione molecules (TAD) are heterocyclic compounds with an azo moiety connected to two carbonyl functionalities. TAD chemical structure presents an overall resemblance with the well-known maleimides. However, TAD compounds react much faster than maleimides and can also participate in a larger variety of reactions with a wider range of substrates.^[59-61] While many maleimide-based reactions are reversible, most TAD-based reactions are irreversible due to their higher intrinsic thermodynamic driving force. TAD reagents present an important characteristic, indeed they show a relative lack of (controlled) reactivity toward typical nucleophiles such as thiols and amines. In terms of reactivity, TAD compounds have often been compared with singlet oxygen which is highly reactive but unstable reagents with very short lifetimes.^[62] Indeed, TAD molecules have a very similar reactivity profile to that of singlet oxygen, and favor ultrafast Diels–Alder and ene-type, and 2+2 cycloadditions reactions as depicted in Figure II.11.

However, an important distinction differs a TAD compound from the singlet oxygen: their lifetime. Many TAD compounds can be isolated and stored for prolonged period while singlet oxygen has a half-life of a few microseconds in most organic solvent. Moreover, TAD reagents allow the possible introduction of a wide range of functionalities and offer a range of selective covalent linking reaction with high yield under equimolar conditions at low temperature without the need of a catalyst (Figure II.11). Although TADs can undergo a very wide range of reactions with many different functional groups as depicted in Figure II.12, these reactions are usually not observed in the presence of suitable Diels–Alder or ene reaction partners and, moreover, TAD compounds show high kinetics preferences for electron-rich π systems, which allows for good selectivity between alternatively substituted (di)enes. TAD compounds are highly reactive toward electron-rich delocalized π -cloud-type substrates, including simple alkenes. A qualitative empirical reactivity scale is shown in Figure II.13.

Additionally, the resulting urazole-type adducts are robust heterocyclic scaffolds, compatible with a large number of solvents, reaction conditions and applications. An additional benefit of these reactions is the intense red color of TAD compounds, which provides a visual feedback system, as most of the corresponding urazoles are colorless.^[63, 64] More information can be found in the recent review of De Bruycker *et al.*^[65]

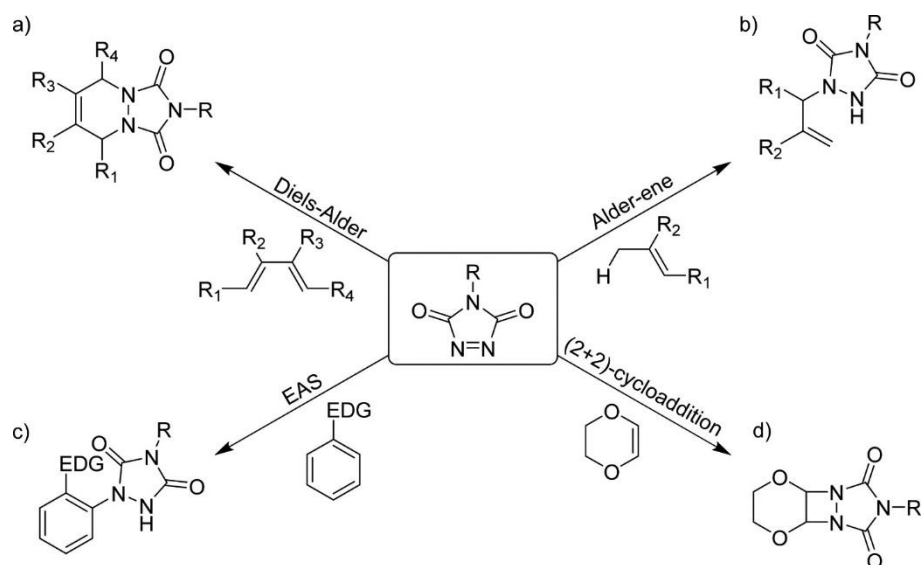


Figure II.11: Reactivity of TAD towards various substrates.

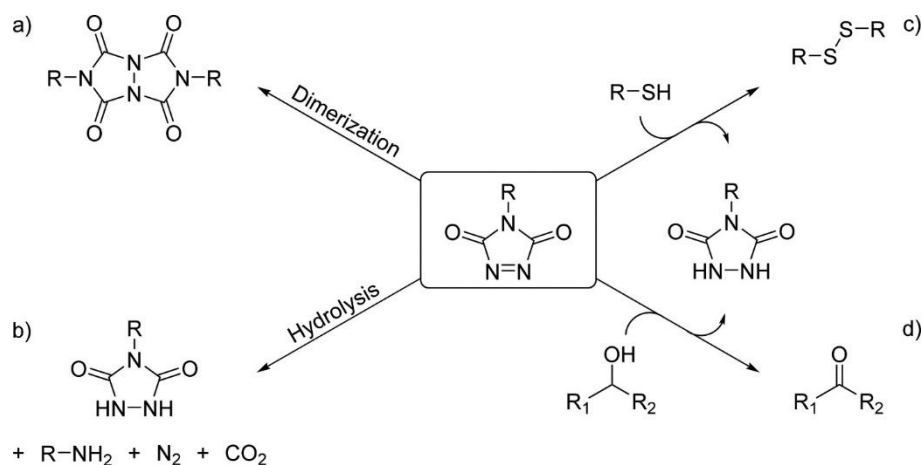


Figure II.12: Important side reactions involving TAD: (a) dimerization of TAD under UV irradiation or when heated above 160 °C, (b) hydrolysis of TAD, (c) oxidation of thiols, and (d) oxidation of alcohols to aldehydes or ketones.

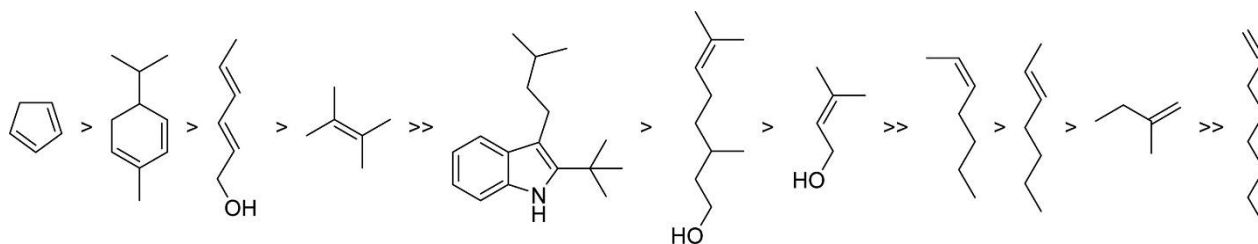


Figure II.13: Relative reaction rates as observed in a head-to-head analysis (in DMSO- d_6) of different representative reaction partners for triazolinediones. The symbol “>” indicates that a selectivity for the left substrate is observed (>50% adduct formation), while the symbol “>>” indicates a complete selectivity.^[66]

II.2.1.3. Synthesis by radical polymerization process

Free radical polymerization (FRP) has been an important technological area for seventy years. As a synthetic process it has enabled the production of materials that have enriched the lives of millions of people on a daily basis. Free radical polymerization was driven by technological progress, and its commercialization often preceded scientific understanding.^[67] For example, polystyrene and poly(methyl methacrylate) were in commercial production before many of the facets of the chain polymerization process were understood. The period 1940–1955 was particularly fruitful in laying down the basis of the subject; eminent scientists such as Mayo and Walling laid the framework that still appears in many textbooks. This success led some scientists at the time to conclude that the subject was largely understood.^[68] Since then, conventional free radical polymerization became the most important commercial process used for the production of commodity materials with various molecular weight and also hydrogels.

This success of the free radical polymerization (FRP) owes it to its robust process allowing the polymerization of a wide range of functional monomers both in organic and in aqueous media, under relative mild conditions.^[69] In contrast to ionic processes, the FRP tolerates the presence of protic impurities and can be carried out in waterborn systems. However, FRP requires the absence of oxygen to prevent peroxide formation. The FRP occurs following a mechanism of chain reactions including 4 steps: initiation, propagation, termination and chain transfer as illustrated in Figure II.14.

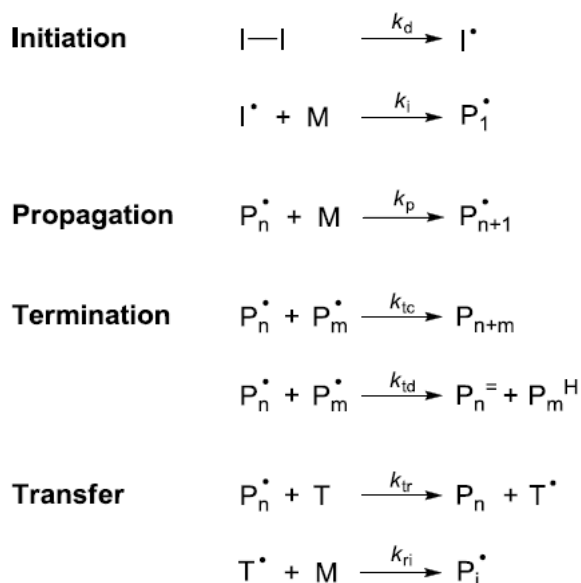


Figure II.14: The elementary four steps of a free radical polymerization process.

Initiation consists of two steps. The first step is the generation of primary radicals, commonly achieved through thermal or photochemical homolytic cleavage of an initiator molecule such as azo- or peroxy compounds. The second step is the addition of a primary radical to the C=C double bond of the monomer to form a growing radical. Successive addition of the growing radical to the double bond is called the propagation. The propagation process is extremely rapid with typical constant values of $k_p \approx 10^{3 \pm 1} \text{ M}^{-1} \text{ s}^{-1}$. Termination of two growing radicals can occur during the entire process by combination or disproportionation. Termination rate coefficients are chain length dependent and controlled by diffusion with typical constant of ($k_t \approx 10^{8 \pm 1} \text{ M}^{-1} \text{ s}^{-1}$). An additional process that generates dead polymer chains is transfer to the monomer, polymer, solvent or a transfer agent. In the case of transfer to polymer, intramolecular transfer (backbiting), which produces short chain branches, has to be distinguished from intermolecular reaction where long chain branches are formed. Transfer reactions do not change the overall radical concentration and only influence the molecular weight distribution and not the kinetics if reinitiation is fast. Slow reinitiation, however, results in retardation/inhibition of the polymerization.

A radical chain growth process can never be living in the strict sense because it is impossible to completely suppress termination reactions. However, several methods have been developed which drastically reduce the proportion of terminated chains in radical polymerization providing efficient control over molecular weight and end-group

functionality. Such reversible deactivation radical polymerizations (RDRP) can be achieved by reversible termination or degenerative chain transfer mechanism. The most widely employed CRP methods are the nitroxide mediated polymerization (NMP), atom transfer radical polymerization (ATRP) and reversible addition-fragmentation chain transfer (RAFT) polymerization.[70] These mechanisms are beyond the scope of this thesis, for further information see Matyjaszewski [69, 71, 72] for ATRP, Chiefari, Moad and Chong [73-75] for RAFT, and Moad, Rizzardo, Hawker, Nicolas and Sciannamea [76-79] for NMP.

Radical polymerization has been a crosslinking technique with several advantages: low energy, free solvent requirements. It also implies a rapid reaction with mild conditions which is highly desired in the design of polymer hydrogels for biomedical as it could be performed in aqueous system. Indeed, nontoxic components are commercially available. In the frame of cell-encapsulating, many efforts have been made to develop radical precursors that can decompose chemically at r.t. or photochemically at biocompatible wavelength. Typically, ammonium persulfate/N,N,N',N'-tetramethylethylenediamine (APS/TEMED) or APS/ascorbic acid have been used as redox-initiating system. Synthetic polymers such as poly(propylene fumarate-co-ethylene glycol) [80], PLA-poly(ethylene glycol) (PEG)-PLA [81], PLA-Pluronic® [82-85], PCL-Pluronic® [86], and oligo[poly(ethylene glycol) fumarate] [87, 88] were crosslinked using the redox-system. Few examples using natural derivatized macromers such as acrylate-functionalized dextran [89], and methacrylate functionalized chitosan [90] were also studied as biocompatible hydrogels.

Recently, the photoinitiated process gains more attention thanks to spatio-temporal control ability. Eosin/triethanolamine, Irgacure 2959 or even light visible initiator like camphorquinone have been used as photoinitiator to promote the formation of hydrogels. Photo-polymerization systems investigated for *in situ* hydrogel formation include synthetic polymers such as PEG diacrylate [91-93], PEG dimethacrylate [94, 95], methacrylate end-capped PLA-PEG-PLA [96, 97], and natural polymers such as methacrylated chondroitin sulfate [98, 99], methacrylated hyaluronic acid (HA) [100-102], PLA-methacrylated HA [103], methacrylated glycol chitosan [104-106], heparin methacrylamide [107], methacrylated alginate [108], and methacrylated gelatin.[109]

II.2.2. Physical crosslinking: generalities on physical stimuli

Hydrogels are called ‘reversible’ or ‘physical’ gels when the networks are held together by molecular entanglements, and/or secondary forces including ionic, H-bonding, hydrophobic forces or even stereocomplexes.^[110, 111] Physical hydrogels are not homogeneous, since clusters of molecular entanglements, or hydrophobically- or ionically-associated domains, can create inhomogeneities. Free chain ends or chain loops also represent transient network defects in physical gels. A typical physically induced hydrogel can be realized by ionic association of polyelectrolyte with multivalent ions of the opposite charge (ionotropic gel) or by mixing two polyelectrolyte of opposing charges (complex coacervate). Other associations are depicted in Figure II.15.

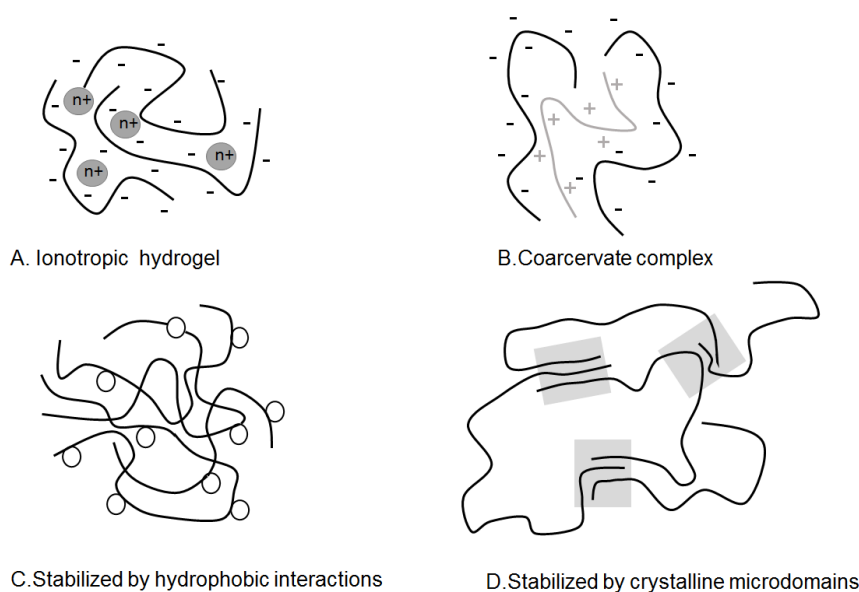


Figure II.15: Representation of the different physical associations in hydrogels.

Electrostatic interactions as well as other secondary interactions stabilizing the hydrogels can be triggered by various physical stimuli as ionic strength, pH, temperature, application of stress or addition of specific solutes.^[112] Interestingly, as all these interactions are weak and reversible, they can also be disrupted by application of the right trigger to recover a liquid/viscous solution. Physical crosslinking methods provide simple and safe approaches for preparing injectable *in situ* forming hydrogels. The absence of potentially toxic crosslinkers or catalysts is a great advantage for biomaterial design and *in vivo* hydrogels applications, with a particular interest for cell or sensitive drug encapsulation. For example, Bhattarai *et al.* synthesized a thermo-

sensitive polymer based on PEO-b-chitoson as injectable hydrogel for the delivery of protein.^[113] In the same range of ideas, Park *et al.* developed an injectable hydrogel made of chitosan-Pluronic for cell delivery.^[114] More examples can be found in these reviews.^[115, 116] Finally, as these secondary interactions are subject to change with initial polymer concentration or environmental conditions (pH, temperature, ionic strength,...), the production of physical hydrogels with optimal properties require a good control of the experimental conditions.

II.3. Doubly crosslinked networks

A common limitation for many hydrogels is that they are constructed by polymerizing small monomers. This method might limit their potential for biomaterial applications because such preparations may not be suitable for *in vivo* use. Therefore, a new approach for hydrogels construction has recently emerged using covalent inter-linking of swellable microgel (MG) particles.^[117] By definition, microgels are crosslinked polymer colloids able to swell in a good solvent. Concentrated dispersions of swollen microgels can be covalently inter-linked to form doubly crosslinked MGs (DX MGs).^[118-121] In this kind of system, microgel particles are used as building block for the formation DX MG hydrogels. Saunders' team is one of the pro-active research group studying this particular hydrogel system obtained mostly by radical coupling reactions. Recently, they developed a system where they could precisely control the extent of vinyl functionalization of the microgel (MG) particles which act as the colloidal building blocks for hydrogel assembly. In their paper, they constructed a new class of DX MG using MG particles that were vinyl functionalized by copper catalyzed azide-alkyne cycloaddition (CuAAC). Finally the concentrated suspension of the modified microgels were crosslinked using APS.^[122] In their following paper, they studied for the first time the effects of intra-MG crosslinking on the swelling of the MGs and the mechanical properties of the DX MGs. It was shown that good tuneability of the DX MG properties could be obtained simply by controlling the DVB and BDDA contents within the MG particles.^[123] Another example demonstrating the possibility of such hydrogel system can be found in the paper from Cui *et al.* where they studied conductive gel composites because of their interesting electrical and mechanical properties. In their study, conductive gel composites were prepared from mixed dispersions of vinyl-functionalised pH-responsive microgel particles (MGs) and multi-walled carbon

nanotubes (CNTs).^[120] Further details describing all the various synthetic strategy to prepare such system will be detailed later.

II.4. Advantages and limitations of the crosslinking methods

Table II.1: Advantages and limitations of crosslinking methods.

Crosslinking methods	Advantages	Disadvantages
Self-assembly	No crosslinker required; reversible; mild gelation upon exposure to external stimuli (e.g. pH,T,...)	Typically mechanically weak gels
Photocrosslinking	Spatiotemporal control over gelation	Light source and initiator required
Thiol/acrylate Michael reaction	High specificity; controllable gelation kinetics; mild gelation under physiological conditions	Sometimes organic bases (<i>i.e.</i> triethanolamine) used
Disulfide formation	High specificity; controllable gelation kinetics under physiological conditions	Oxidizing agents often required
Schiff's base reaction	Controllable gelation kinetics; mild gelation under physiological conditions	Lack of specificity: aldehyde groups can react with amine of bioactive factor and tissue extracellular matrix molecules
Enzyme-mediated reaction	High specificity; gelation in mild conditions	Instability of some enzymes: active enzymes may remain following gelation
Click reaction	High specificity; high reaction efficiency; controllable gelation rate	Toxic Cu(I) catalyst often required and Cu(I) free system synthetically difficult

Ionic crosslinking	Gelation in mild conditions; potentially reversible	Charged therapeutics might interfere with crosslinking
Molecular recognition	High specificity; gelation in mild conditions	Sometimes mechanically weak gels and rapid degradation

Generally, physical hydrogels present weaker properties than their homologue chemical system. Moreover, in a particular system such as system based on ionic crosslinking, interference with therapeutics may occur. However, these systems are highly interesting for the delivery of sensitive system like DNA, protein, cells. Chemical hydrogels are often associated with strong gel and with highly controlled mechanical properties making them highly desirable for bone regeneration. The main problem of chemical injectable hydrogels is the presence of moieties (initiator, copper, oxidizing agent,...) that could be problematic for biomedical applications as the substances added can present toxicity. Schiff base system presents lack of specificity. The case of enzyme mediated hydrogel is very interesting and studied as it presents many advantages and few drawbacks. However, the enzyme could be instable and their activities could remain after hydrogels synthesis. In the present work, we are interested in a system presenting the philosophy of click reaction being highly specific, fast with controllable kinetics. To get rid of the problem of copper, this work proposes to use Diels-Alder as crosslinking reaction as it is a very promising crosslinking method. In the same range of ideas, DX-gels will be targeted as it is a promising new way to form gel presenting several advantages compared to conventional gel made of monomers crosslinking.

II.5. Shape and size designed hydrogels: the case of nano and microgels

II.5.1. Nano and microgels: description and applications

Recent advances realized in hydrogel synthesis to make them compatible with biomedical fields have led researchers to meet new challenges to design the biomaterials at the size and shape corresponding to the targeted application.

Notwithstanding the positive features displayed by radical polymerization processes and Click coupling reactions in the design of materials, the recent challenges were to set up fabrication methods allowing to broaden the range of available materials according to their size. Owing to those fabrications techniques, hydrogels ranging from nano- to micro-sized were developed and optimized to meet satisfaction. Microgels are microscopic three-dimensional networks dispersed in a proper solvent and characterized by average diameters between 50 nm to several μm . The microgels are stabilized by the crosslinking and can therefore swell in a good solvent. The term 'microgel' was first introduced by Baker in 1949 in a publication entitled: 'microgel, a new macromolecule'. However, Staudinger and Huseman were the first to synthesize microgel particles by polymerizing divinylbenzene in high dilute conditions and in a good solvent to obtain swollen crosslinked polymer particles.^[124] Baker emphasized that microgels consisted of very high molecular weight polymer networks. In other words, each gel particle is an individual polymer molecule. Lately, microgels are defined as a colloidal dispersion of gel particles.

Although microgels present same chemical compositions and thermodynamic properties compared to their corresponding macrogels, they show many distinguished differences. For example, micro-sized and nano-sized hydrogel particles are low viscosity dispersions while macrogels are viscoelastic solids. In addition, micro-sized hydrogels respond faster to environmentally triggered changes in swelling and molecule binding allowing their use in controlled and regulated applications.^[125, 126]

Generally, microgels don't aggregate because the surface often bears electrical charge and dangling surface chains. Moreover, microgels present high colloidal stability as illustrated by the ability to freeze-dry or to be redispersed spontaneously in water after ultracentrifugation, which is unusual. For example, dry coagulated polystyrene latex is almost impossible to redisperse completely in water. In general, microgels tend to be more colloidally stable at the swollen state where Van Der Waals attraction is diminished and surface chains can sterically stabilize the microgel particles.

The volume fraction of dispersion occupied by microgel particles (Φ_d) is an important parameter for industrial applications and rheological studies. The value of Φ_d is

proportional to the volume fraction of polymer in the dispersion (Φ_p) and is independent of particle size. The relationship between Φ_d , Φ_p and Φ_2 is simply:

$$\Phi_d = \frac{\Phi_p}{\Phi_2}$$

where

$$\Phi_p = \frac{\frac{m_p}{\rho_p}}{\frac{m_p}{\rho_p} + \frac{m_s}{\rho_s}}$$

m_p , m_s are the mass of polymer and solvent, respectively; ρ_p and ρ_s are the densities of polymer and solvent. Φ_2 is the volume fraction of polymer in each particle. The most important property for microgel particles is the extent of swelling which is usually determined from changes in the hydrodynamic diameters measured using PCS. It is experimentally convenient to measure swelling changes relative to the fully swollen hydrodynamic diameter (d_0). The extent of particle deswelling is expressed as the deswelling ratio (α) which is simply: $\alpha = (d/d_0)^3$, where d is the measured hydrodynamic diameter at a given temperature. The deswelling ratio and Φ_2 are related by: $\alpha = (d_c/d_0)^3/\Phi_2$ where d_c , is the diameter of the particles in the fully collapsed state.

Swelling behavior of microgels

$$\mu_1 - \mu_{1,0} = \Delta\mu_{\text{elastic}} + \Delta\mu_{\text{mix}}$$

Where :

- μ_1 is the chemical potential of the swelling agent within the gel and,
- $\mu_{1,0}$ is the chemical potential of the pure fluid.

The extent of network swelling is usually described by the polymer volume fraction Φ_2 obtained at equilibrium ($\Phi_2 = 1$ in the collapsed state). Using the appropriate thermodynamic relationships, Flory's theory leads to:^[127]

$$\text{Equation 1: } \Phi_2 = \left(\frac{Xv_1}{V_c \left(\frac{1}{2} - \chi_{12} \right)} \right)^{3/5}$$

Where X is the number of crosslinks presents within a collapsed network volume V_c . The subscripts 1 and 2 refer to the solvent and network polymer, respectively; v_1 is

the molar volume of the solvent and χ_{12} represents the Flory solvent-polymer interaction parameter. The term (X/V_c) represents the average density of crosslinked units in the collapsed particle.

Usually, microgels contain a higher proportion of non-crosslinked polymer segments (monomer B) and a (normally) minor proportion of difunctional crosslinking segments (A). Generally, the mole fraction of the latter X_A being typically less than 0.1. Therefore, if it is assumed that the molecular weights of the A and B segments are the same and that each mole of di-functional crosslinking introduces 2 moles of crosslinked units, it can be shown that:

$$\text{Equation 2: } \frac{X}{V_c} = \frac{2X_A \rho_b}{M_b}$$

Where M_b and ρ_b are the molecular weight and density of the B segments, respectively. Substitution of Equation 2 into Equation 1 and assuming $\rho_b = 1$ leads to a simple expression describing the dependence of the volume fraction of the microgel particles on the network composition and solvency:

$$\text{Equation 3: } \Phi_2 = \left(\frac{2X_A v_1}{M_B v_{12}} \right)^{3/5}$$

Where the excluded volume parameter $v_{12} = (0.5 - X_{1,2})$. The polymer volume fraction increases (particles deswell) if the crosslink density increases or the solvency becomes poorer (v_{12} decreases).

The intrinsic viscoelasticity of microgel particles leads to a large amount of interesting suspension properties. Microgels can be made responsive to external stimuli, *i.e* as pH, temperature, magnetic and electric fields, flow, or osmotic pressure. The kinetics of the response can be well controlled and properties such as the timescale of swelling or the microgel elasticity can be well tuned. Therefore, by adjusting the properties of the microgel particles during synthesis, bulk suspension properties, rheology, dynamics, and structure can be tuned.

Recent advancements in synthesis have led to a broad range of complicated microgel morphologies, including core-shell structures, interpenetrating polymer networks, microgels containing nanoparticles, Janus particles and functionalized microgels designed as sensor or for pharmaceutical delivery applications. By choosing the right

monomers, functional microgels can be designed to be biodegradable or biocompatible, making them valuable in many biomedical applications. The tunability of the physical properties of microgels allows an extent use in a wide variety of industrial applications where they can provide new functionalities. Recently, new applications for microgels have emerged, most notably in stem cell research, tissue engineering, and *in vitro* diagnostics.^[126, 128]

II.5.2. Synthetic processes for nano and microgels

Depending on the pathological conditions and actual needs to be tackled, systemic administration of micro- and nanogels is undoubtedly a prerequisite to successful administration of new therapeutics (drugs or cells). Owing to their small size, the microgels possess a high surface area that can be exploited for drug targeting, after surface modification with bio ligands. In contrast to their bulk counterpart that presents some limitations of their applicability in reason of a lack of injectability or slow response rates to their environmental changes, microgels display fast-acting behavior owing to their thinner and smaller size. Their high surface ratio affords fast response and release behavior. While their high potential as drug carrier is clear in the scientific community, the synthesis of hydrogels as drug carriers for *in vivo* applications must be carefully planned. Particles shape plays an important role in specific applications. Therefore, controlling the shape of particles gained tackled the development of various physicochemical and mechanical techniques of fabrications. A large amount of progresses has been done during the past years in the field of particles synthesis encompassing molecular association, atomization, and emulsion based-processes. However, a complete understanding of the role of the shape remains a major challenge. As surface tensions are dominant compared to all the others forces during the synthesis, all the particles are naturally spherical. However, unspherical particles like sticks^[129, 130], disks^[130], colloidal particles with a shape like an acorn^[131], spongy structures^[131], torus, irregular structures^[132], Janus particles^[130, 133], but even more complex geometry^[134] able to offer special properties and a better packaging compare to their spherical homologue have also been reported so far. Such unique structures can have a huge potential application in cosmetics^[135], biotechnology^[136] or pharmaceuticals.^[137] In 2010, Yoo and Mitragotri showed that particles of PLGA were able to change their shape (from elliptical to spherical) in response to an external

stimulus (pH, temperature, chemical additives).^[138] Biological or chemical functionalities that need to be introduced on particle surfaces deserve also particular attention through adapted (well thought) synthetic strategies. The next sections will present the various fabrication techniques of microgels, categorized into molecular association-based procedures and mechanical methods. The last section will describe synthetic strategies that allow easy decoration of microgel surfaces.

II.5.2.1. Molecular association

Microgels synthesized by molecular association are a particular strategy compared to emulsion techniques involving two strategies: the first one being using self-assembled components and the second using complex coacervation. Self-assembled microgels are formed from single biopolymer under appropriate prevailing conditions using either thermal denaturation, crosslinking, desolvation or simple coacervation that promote self-association. Coacervation is a water-based phase separation process of preformed polymers offering new ways to prepare hydrogel microparticles.^[139, 140] Coacervation involves the phase separation of an aqueous polymer solution into two immiscible liquid phases: a polymer-rich phase (coacervate phase) and a polymer-lean phase (equilibrium phase).^[141] Coacervation can be induced either by polyelectrolyte complexation (complex coacervation) or by decreasing the polymer-solvent interactions by changing the solvent composition or the temperature (simple coacervation) as mentioned above.^[142] Further informations can be found in this short review.^[143]

II.5.2.2. Mechanical methods

Mechanical methods imply that particle formation is driven by a specific mechanical device and a crosslinking process arising from physicochemical methods. This combination has proven to be efficient to fabricate well-defined microgels from natural and synthetic polymers. While various techniques are reported in the state of the art ^[143], this section will focus on the main exploited techniques as suspension polymerisation, emulsion polymerisation, and in that frame, an attention to microfluidic devices.

Suspension polymerisation

Suspension polymerization can be considered as the easiest technique of all heterogeneous polymerization processes for the production of particles. A suspension

polymerization in a water-in-oil emulsion where droplets of monomers are dispersed into a continuous organic phase as depicted in Figure II.16. Droplets of water soluble monomers (or reactive polymers) are stabilized by the use of surfactants. An initiator soluble in the monomer phase is added to kick off the polymer chain growth in the droplets. The size of the produced microspheres reaches up from micrometers to several hundred micrometers and – thanks to the addition of porogens such as solvents or polymers – a porosity can be achieved. Suspension polymerization can be applied to monomers and mixture of monomers with crosslinkers. Surfactants or stabilizers are often added to the reaction mixture to stabilize the suspension. The size of the particles is easily tuned by changing the stirring rate as well as the shape of the magnetic stirrer and size and shape of the glassware. Beyond those mechanical parameters, the viscosity of both phases and the nature and concentration of the surfactant is of prime importance for optimizing the surface tension. The degree of porosity is adjustable over several orders of magnitude by varying the concentration and the nature of the porogen. Various solvents, oligomers, polymers can be use as porogen such as toluene ^[144], heptane ^[145], or even linear polymers such as PMMA ^[146], PS ^[147], PEO ^[148], PDMS.^[149] Prior and during the polymerization, a continuous stirring is required to form and maintain the suspension, leading to collisions of the droplets, thus being the major reason for the polydispersity observed in most particles derived from suspension polymerization. Even though polydispersity is a major drawback, this technique is greatly used in industrial process because of its low cost.

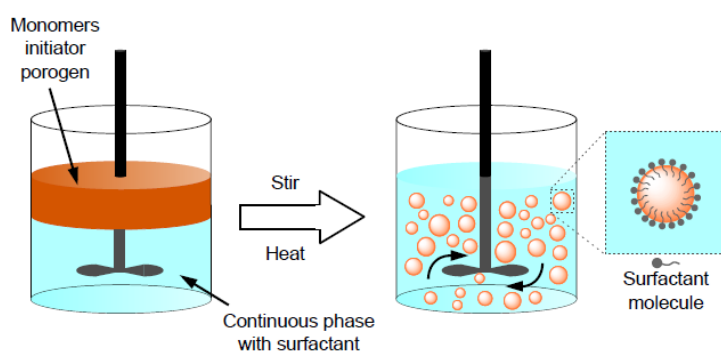


Figure II.16: Schematic representation of a suspension polymerization. Adapted with permission from [150].

This cheap and easy technique allows the production of microgels which are currently under development for multiple applications in the biomedical fields. For example, Freemont and Saunders described the design of injectable microgel dispersions

containing MAA able to provide structural support for damaged soft tissue such as intervertebral discs and enable tissue regeneration in the longer term.^[151] Saunders *et al.* demonstrated the ability of pH-responsive microgel particles to restore the mechanical properties of load-bearing soft tissue.^[152] Gan *et al.* investigated the potential of poly(NIPAM-co-2-hydroxyethyl methacrylate-co-acrylic acid) microgels to act as injectable cell scaffolds with promising results on cells culture and proliferation.^[153] Hopkins *et al.* modified poly(NIPAM) microgels with a cell-adhesive peptide (GRGDS), which bound to cell surface integrins on dermal fibroblasts and endothelial cells. Above their LCST, the microgels removed the cells from their normal culture substrate, then, on cooling, released the viable cells to grow on new substrates.^[154] Further informations on potential applications can be found in this review.^[155]

Emulsion polymerization

Emulsion polymerization is very similar to the suspension polymerization procedure. The difference is the location of the initiator: the chosen initiator has to be soluble in the continuous phase (oil phase), not in the monomer (Figure II.17). As a consequence, the initiation takes place out of the monomer droplets, stabilized by emulsifiers. Particles synthesized via emulsion polymerization can be described as nanoparticles, as they normally feature a size range of 0.05 to 0.2 μm . Depending on the solubility of the monomer, the polymerization can be conducted as either an oil-in-water emulsion, or for hydrophilic monomers, as a water-in-oil emulsion. In both cases a surfactant is added to keep the phases emulsified, which is supported by intensive stirring. The synthesized particles are non-porous and relatively disperse. If the monomer is diluted with a solvent, the reaction is termed 'diluted emulsion polymerization'. If the polymerization is carried out without added emulsifier (named emulsifier free emulsion polymerization) the particles are stabilized by steric effects, solvated surface layers or electro-repulsive forces between ionic fragments. Since these forces are less effective stabilizers than an emulsifier, the final particles reach up to 1 μm in size. Synthesis of nano- and microparticles via emulsion polymerization is a very versatile and extensively investigated area of research. Since the current thesis mainly uses suspension polymerization, the reader is instead referred to the general reviews and books by Landfester,^[30] Ballauff and Lu,^[31] Thickett and Gilbert,^[32] as well as Mittal.

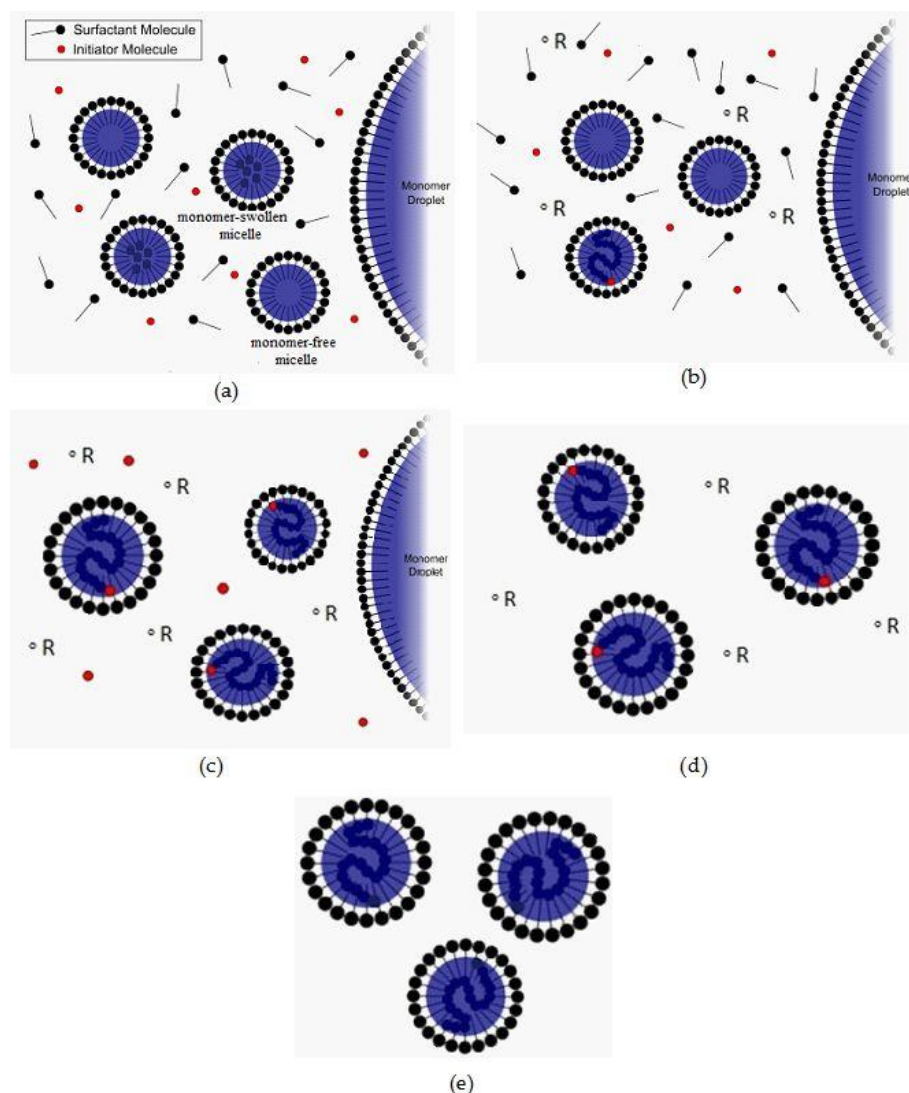


Figure II.17: Schematic representation of the mechanism of emulsion polymerization. (A) before the reaction; (B) nucleation; (C) growth; (D) after the reaction; (E) polymer particles stabilized by surfactant. Adapted with permission from [156].

Precipitation and dispersion polymerization

Opposite to other methods, dispersion or precipitation polymerization begins with a complete homogenous solution. However, they are classified as heterogeneous polymerization procedures because the phase separation occurs during the first step of the polymerization. Even though these 2 methods look pretty similar, two major differences allow to make the distinction:

1. A surfactant is used in dispersion polymerization but not in precipitation polymerization;

2. A crosslinking agent is required and used in large proportion in precipitation polymerization while a crosslinking agent is often omitted in dispersion polymerization. As a consequence, dispersion polymerization is often used for uncrosslinked particles.

These 2 procedures allow the production of monodisperse particles with size ranging from 0.1 μm to 10 μm .

Precipitation polymerization

Precipitation polymerization is a technique widely used for the preparation of monodisperse highly crosslinked polymer microspheres. Precipitation polymerization with acetonitrile as solvent was first proposed by Li and Stover for the preparation of highly crosslinked poly(divinylbenzene), poly(DVB), microspheres.^[157] Precipitation polymerization begins as a solution of initiator, crosslinker and dispersive phase (solvent solubilize moderately the crosslinker) and if wanted a porogen. Solvent will become the continuous phase as the precipitation occurs. Precipitation polymerization requires a large quantity of crosslinkers. Methacrylate polymerization can be realized by precipitation polymerization using a low quantity of added monomers.^[158, 159] As a consequence, particles are rich of double bond allowing functionalization after polymerization.^[160] At the beginning of the polymerization, oligomers and nuclei are formed (Figure II.18). Oligomers remain soluble and nuclei precipitate giving therefore a heterogeneous mixture. Although no surfactant is used, nuclei are stabilized by a layer of oligomers. Polymerization continues at the interface of the particles. Particles size from 1 to 5 μm can be obtained. Recently the synthesis of nanoparticles was also reported by precipitation polymerization.^[158] Precipitation polymerization requires a high dilution of monomers (2 to 5%) which consists of several drawbacks. Moreover polymerization is slow compared to suspension polymerization where a high local monomer concentration is obtained.

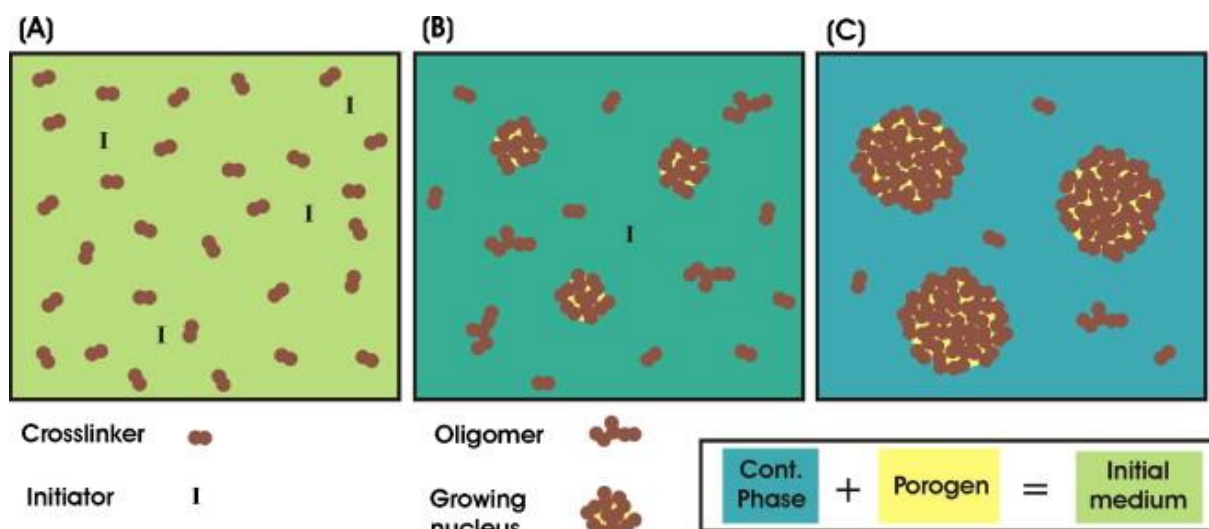


Figure II.18: Schematic description of the stages of precipitation polymerization for porous particle production. (A) Initially, only crosslinker and initiator molecules are in the medium. (B) Oligomers and nuclei are being formed because of radical polymerization. (C) As the reaction continues, nuclei grow by adding monomers and oligomers from the medium. In reality, there is a swollen layer of oligomers around the nuclei.^[150]

Dispersion polymerization

Dispersion polymerization is comparable to the precipitation polymerization approach in many aspects: both techniques start from a homogeneous phase and the reaction consists of nuclei formation with subsequent growth. The main differences between dispersion polymerization and precipitation polymerization is that for the former, the addition of a stabilizer is required, and the amount of crosslinking agent can be significantly lower. Monomers, initiator and surfactant are generally dissolved in an alcohol under stirring. With temperature increases, the initiator forms radical and oligomers still soluble are formed. Oligomers grow and precipitate, forming nuclei of the final particles. Nuclei are stabilized by surfactant added in the beginning of the process. Monodisperse particles can be achieved with the addition of the crosslinker after the nucleation as explained in the paper of Winnik.^[161] The achievable sizes range from less than 1 μm up to around 15 μm (Figure II.19).

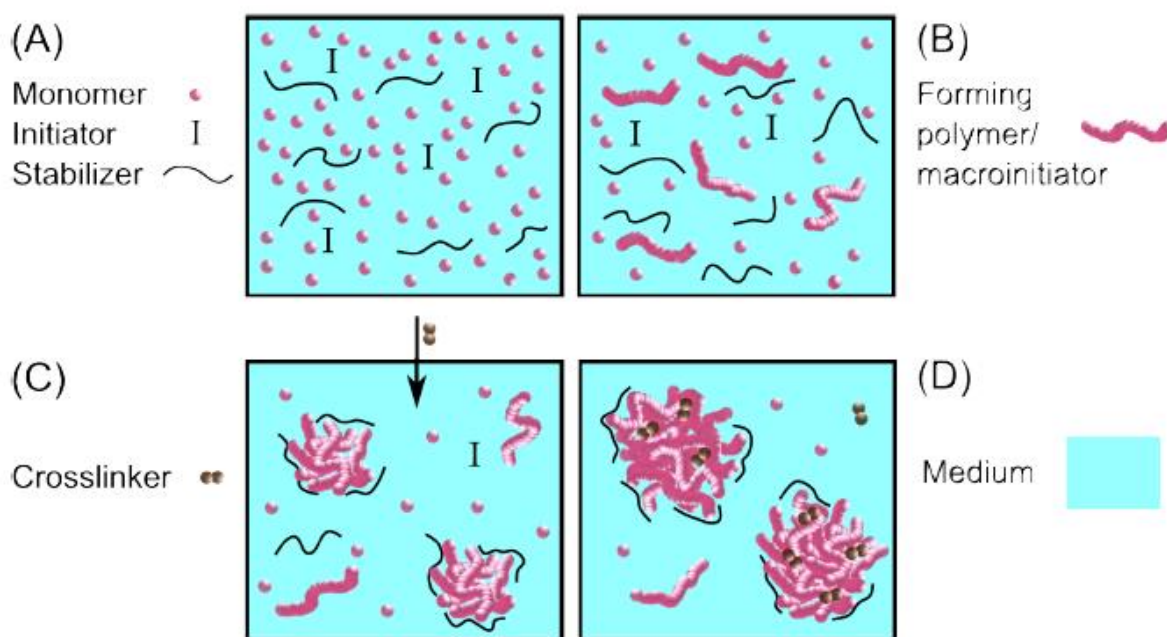


Figure II.19: Schematic description of the stages of dispersion polymerization. (A) Initially, monomer, initiator, porogen and polymeric stabilizer are dissolved in the medium. (B) Oligomers are forming, which are still soluble in the medium. (C) Nucleation stage at around 1% monomer conversion. As their length increases, polymer chains precipitate and form the nuclei that are stabilized by the stabilizer. At this stage, a crosslinker may be added if desired. (D) Particles grow by capturing monomers and oligomers from the medium.^[150]

II.5.2.3. Polymerization in microfluidic device

Microfluidic principle

Microfluidics offer the highest degree of control over the size and dispersity of microparticles. This technique is the newest one and can be considered as a miniaturization of the emulsification microchannel where flow plays an essential key role. Uniform monomer droplets are produced in the center of a flowing continuous phase by a nozzle, which are subsequently crosslinked, most of the time by the use of UV-sensitive initiators. Spherical particles with very low coefficient of variation (CV) (<2%) can be achieved by microfluidics.

The sophisticated and miniaturized design of microchannel emulsification reactors allows not only the synthesis of monodisperse spherical particles but also complex

structures difficult to achieve before like Janus particles^[162-164], regular non-spherical shapes.^[165-168] The main drawback is the difficulty to upscale small achievable samples hindering the mass production and therefore the commercial use.

Droplet formation in the microfluidic tube

The core of the microfluidics is the droplet formation in the tube. For the production of particles with very low CV, the transition from “jetting-dripping” is critical. There is different geometry of the microfluidic tubes: the “T-junction”, “co-flow” and the flow focusing (see Figure II.20). The mechanism of the droplet formation will be discussed in the most used geometry named “co-flow” geometry. In a “co-flow” microfluidic setup, orifice of the discrete phase is localized in the middle of the continuous phase. Continuous and discrete phase flows have the same direction. The droplet formation can occur in “dripping regime” or in “jetting regime” (Figure II.21). The jetting regime is characterized by a long liquid shape before the droplet formation. To achieve better control and then obtain particles with low CV, the dripping regime is needed. Even so, some examples can be found in the literature where the jet is controlled, allowing the production of uniform fibers, tubes.^[169-171] In a “co-flow” geometry, the inside and outside liquid are pressurized with the help of a syringe pump.

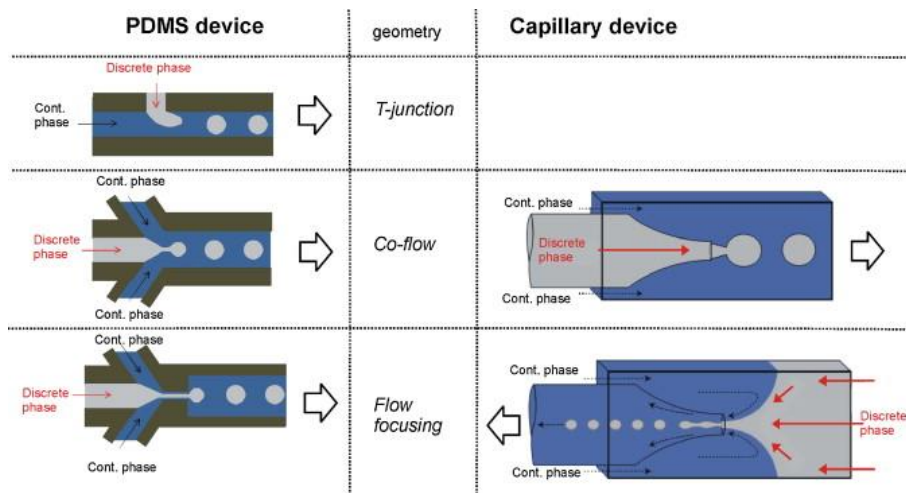


Figure II.20: The different tube geometry in microfluidics.

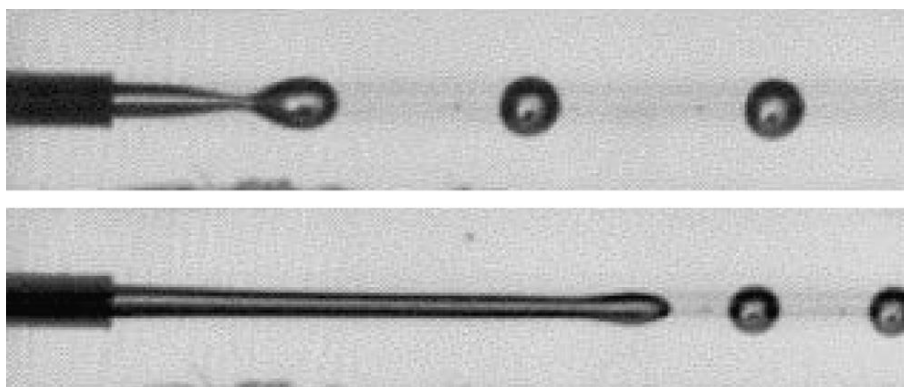


Figure II.21: Picture of dripping (top) and jetting regime (below). Adapted from [150]

Surface tension between the two immiscible liquids allows the growing and formation of the droplet from the discrete phase at the end of the orifice. In a first step, more liquid enters in the droplet resulting in the growth of the droplet. Thus the growing droplet occupies a rising space from the available microchannel, therefore the pressure of the surrounding outer liquid increases. When a critical size for the droplet is reached, the pressure of the outer liquid overcomes the interfacial tension and forces the droplet to pinch off from the orifice, which is the second and the last stage of droplet formation in microfluidics. Thus, flow rates are important to achieve the transition from jetting regime to dripping regime. Indeed, when the flow rate of the outer liquid is too high, the proper droplet growth is restrained, so that the first step is compromised. On the other hand, too high flow rates of the inner liquid contribute at increasing the amount of the discrete phase into the forming jet thus the outer liquid can't narrow the thread, resulting in the blockage of the second step of the droplet formation. Therefore there is a safe zone where both flow rates are low. On the other hand, low flow rates have their inherent problem. First, a lower flow rate for the discrete phase means a lower droplet production rate, which is the main drawback of the microfluidics. Second, an increase of the flow rate in the discrete phase will generally lead to an increase of the synthesized particles which might be not desirable for the application. The continuous phase flow rate can be increased (without exceeding the critical jetting velocity) to keep the particle size lower, without decreasing the discrete phase flow rate. However, an increase in the continuous phase flow rate would result in a higher consumption of continuous phase liquid, and more importantly in a higher ratio of continuous phase over discrete phase droplets that might lead to monomers loss into the continuous phase.

In addition to flow rate, another important factor affects the dripping-jetting transition: the polarity of both phases. For an oil-in-water emulsion, polarity effect can be important for porous particles. Indeed it's the interfacial tension, therefore the polarity difference between the two phases that allows the droplet to growth at the end of the orifice of the inner liquid. An increase in polarity of the monomer phase will lead to smaller droplets and a smaller value of critical jetting velocity which is undesired. The last internal factor affecting the dripping-jetting transition is the viscosity. A highly viscous inner liquid would prefer jetting instead of dripping due to viscous attraction of the inner liquid molecules, thus suppressing the breakup.^[169] This behavior can also be explained by the stabilization of the interface between the two phases.

II.5.3. Surface modifications

Although many different functionalities can be introduced during the synthesis of particles such as carboxylic acid, hydroxyl, bromide, alkene, alkyne, amino groups, a major focus was dedicated to the surface modification of preformed microparticles with easy and upscalable strategies. It should be noticed beforehand that reactions on solid phase are much slower and give lower yields in comparison to homogeneous reactions. These constraints necessitate the use of high yielding reactions on solid phase such as click reactions.^[241]

The four main techniques to realize efficient surface modification are the following one: epoxide ring opening, Copper-catalyzed azide-alkyne cycloadditions (CuAAC), RAFT-HDA and thiol-ene. Epoxide ring opening method is more commonly used to introduce click reaction function for subsequent coupling. The three other methods are generally exploiting functional groups from functional monomers after particles synthesis. Moreover, quantitative detection of unreacted remaining groups may not be straightforward. In addition, it is not always possible to use a large excess of an expensive reagent to achieve complete conversion. All these reasons have led to the use of high yielding reactions on solid phase. As previously discussed "click chemistry" is a term associating high yield reactions in mild conditions without any offensive subproducts making these reactions well appreciated for the particles functionalization.

Epoxide ring opening

The possibility to synthesize microspheres mainly based on the epoxide containing glycidyl methacrylate monomer (GMA) or copolymerized with GMA makes ring-opening of epoxides a facile and versatile grafting reaction on microparticles. Due to the ring strain, the three-membered ring is very reactive and can react with a range of nucleophiles as well as electrophiles ^[172] as illustrated in Figure II.22. Epoxide has been widely used to modify surface of particles to introduce new functions, specially azide moieties for subsequent coupling using CuAAC.

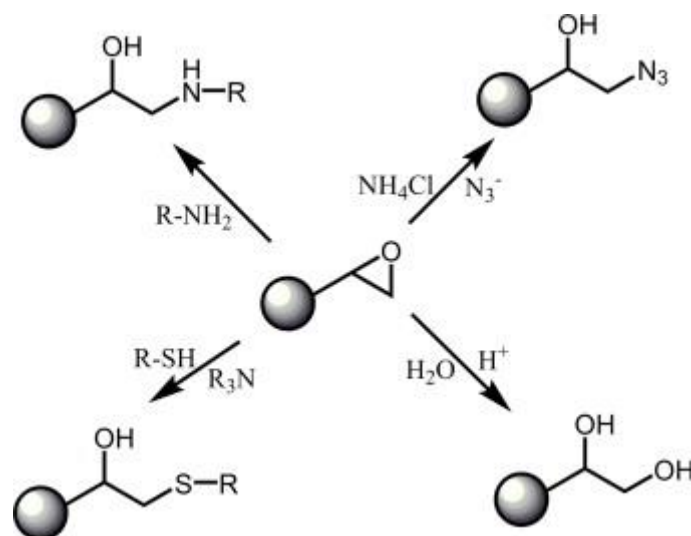


Figure II.22: example of effective modifications of epoxy particles. Only the attack to the less hindered carbon atom is considered.

Commercially available polymers such as poly(ethylene glycol) (PEG) or poly(ethylene imine) can directly be grafted onto particles containing GMA utilizing their nucleophilic end groups^[173, 174]. Moreover, a range of proteins and enzymes can be also immobilized on GMA containing or epoxide functionalized microparticles. ^[78–81]

Copper-catalyzed azide-alkyne cycloadditions (CuAAC)

The first example of CuAAC on microsphere was published in 2006 by Slater *et al.* ^[175] following later by Kacprzak.^[176] In Slater's paper, short aliphatic chains were grafted onto particles previously functionalized with azide as well as alkyne groups. Common approaches to introduce alkyne into a particle are the following one: epoxide opening using sodium azide as discussed above, substitution of Br group from Copper

controlled radical polymerization by NaN_3 copolymerization with an alkyne containing monomer which allows direct grafting of azide functionalized moieties. Glycomoiety can be grafted on microspheres as a monolayer or on polymeric chains previously grafted from the spheres by ATRP.^[63] Natural polymers, such as previously alkyne-functionalized proteins, can also be grafted on microspheres via CuAAC.^[64] Azide functionalized spheres were grafted with several polymers synthesized via RDRP techniques.

RAFT HDA

The RAFT hetero Diels-Alder approach is the reaction between a $\text{C}=\text{S}$ double bond of the thiocarbonyl thio moiety, coming from special RAFT-agents, and a diene. RAFT-functionalities can be attached to microparticles by the addition of a RAFT agent during the synthesis of the particles. Since the RAFT-HDA concept is rather novel, there are only few reports in the literature on microparticles. Recent examples were published by MacroARC (KIT) group where they grafted diene-functionalized poly(ϵ -caprolactone) synthesized via ring-opening polymerization on RAFT-functionalized spheres. In a second approach polystyrene synthesized using a RAFT process was grafted onto cyclopentadiene-functional microspheres.^[177] In another paper, poly(isobornyl acrylate) was directly immobilized onto PDVB particles, employing the most reactive RAFT agent towards HDA, which contains a sulfonyl as Z group. The sulfonyl enables the $\text{C}=\text{S}$ bond to even react with many vinylic monomers, but therefore strongly minimizing the possible applications.^[178] However, small challenges exist as to overcome the devouring of submicron particles by macrophages and other lymphatic cells. In the frame of drug release, their small size may induce an undesirable faster release of the drug than what could be observed from macrogels.

Thiol-ene/yne chemistry

Ligations utilizing thiols are ideal for the grafting of polymers prepared via RAFT-polymerization onto microspheres exhibiting residual double (or triple) bonds, e.g., microspheres synthesized from radical polymerization procedure (usually PDVB microspheres). Indeed, RAFT-polymers can be easily functionalized with thiol moieties by the simple addition of an amine to the dissolved polymer (aminolysis). The first published paper using thiol-ene chemistry showed the efficient grafting of poly(*N*-

isopropylacrylamide) prepared by RAFT polymerization onto double bonds of PDVB microspheres after aminolysis.^[179] Other examples can be found in literature where small thiol-functionalized sugar molecules ^[180, 181], glycopolymers ^[182] are graft onto vinyl functionalized particles. Du Prez *et al.* have shown that thiol-ene/yne chemistry can be utilized to synthesize microparticles via a microfluidic approach allowing the production of either thiol functionalized particles or ene functionalized particles.^[183] They furthermore performed several reactions on thiol-functionalized particles and azide-functionalized particles and compared the grafting density reached on alkyne functionalized spheres via thiol-yne chemistry and CuAAC. They showed that thiol-yne ligation was superior in this context.^[184]

II.6. Doubly-crosslinked hydrogels as new injectable materials

II.6.1. Injectable hydrogels: breakthrough and challenges

Pressure arising from the increasing incidence of severe diseases, together with the need to bring healthcare solutions, have pushed the research community to develop more creative and efficient materials that could improve treatments. Among the various strategies developed in the literature, *in situ* forming hydrogels, also called injectable hydrogels, are gaining an increasing deal of interest these past few years owing to their ability to deliver locally and in a minimally invasive manner therapeutics or living cells upon direct injection. *In situ* forming hydrogels are polymer materials that spontaneously gelify in physiological conditions to form three-dimensional structures, and potentially into sites that are not accessible surgically. Furthermore, injectable hydrogels can easily adapt their shape to a complex geometry and can adhere to the surrounding tissues during hydrogel formation, without altering natural tissue structure.^[185, 186] More interestingly, gelification can occur in the presence of therapeutics (drugs, bioactive molecules or cells), leading to a drug delivery device with controlled release profile at the site of application, overcoming biological obstacles and for particular cases the dose-limiting toxicity.^[186, 187]

From polymer chemistry viewpoint, polymer materials should meet some criteria to be used for *in situ* hydrogel applications, such as adequate viscosity allowing an easy injection, a fast transition from liquid/viscous solution of polymer precursors to a solid,

biocompatibility and finally appropriate physical and mechanical properties for the targeted application. Injectable hydrogels can be divided into two categories according to their gelation process: chemical crosslinking or physical crosslinking. The latter arises from secondary weak interactions as electrostatic interaction^[188-192] host guest interaction^[193-197], stereo-complexation^[198-200] or sol-gel transition induced upon subtle changes of environmental conditions.^[201-203] Physical hydrogels offers a gentle gelation process limiting the denaturation of incorporated drug/proteins and damage embedded cells and surrounding tissues.

For example, PAE-PCL-PEG-PCL-PAE block copolymer was investigated as physical gel for insulin delivery owing to the sol-gel transition with increasing temperature and pH.^[204] A thermo-responsive chitosan with pendant poly (N-isopropylacrylamide) (PNIPAM) has been synthesized by grafting PNIPAM-COOH on chitosan through amide bond linkages. The copolymer exhibited temperature-responsive sol-gel transition around 30°C and formed a porous hydrogel with interconnected pores. [205] More examples can be found in these reviews.^[206-209] While less attractive at its infancy, chemically crosslinked injectable hydrogels are gaining interest as well usually prepared by UV irradiation^[210-213] or covalent bonding^[214-216] undergo large volume change during the transition phase. A large number of studies have been realized to address potential issues of injectable hydrogels including needle clogging, acidic degradation products, degradation rate and burst release. However, several challenges need to be mentioned for further developments of injectable system. First, the initial burst release of therapeutic agents (DNA, protein, low molecular weight and hydrophilic drug) is a concern. Second, the degradation rate of the network is essential for controlled drug delivery and tissue formation. Degradation rate of hydrogels must be considered for specific applications and can be controlled by varying the composition, crystallinity, and topology of the polymers. Third, the cytotoxicity of hydrogels containing cytotoxic moieties may cause inflammation at the injection site. The structures of copolymers containing cytotoxic moieties should be well-defined so as to minimize inflammation. Fourth, multiblock copolymers possess complicated structures that might make it difficult to obtain approval from the Food and Drug Administration. Thus, the development of polymers with simple, well-defined structures remains an ongoing challenge. In this context, starting from surface reactive microgels

opens the doors to new synthetic approaches alleviating the problems usually met in this field, while preserving the outstanding features of the injectable hydrogels.

II.6.2. The case of doubly crosslinked networks

Major attention has been devoted to understand the relationship between sophisticated structures and properties in order to open up and design the range of applications of injectable hydrogels. In this context, doubly crosslinked (DX) gels are a new class of injectable hydrogels that brings two levels of structural hierarchy.^[217-221] Indeed, DX-gels that consist of internally crosslinked particles (micro- or nano-sized gels) are able to establish connections with their partners through an inter-crosslinking process. Unique properties such as fine tuning of mechanical properties, DX-gel mesh size, high specific surface area, controlled heterogeneity at the nanoscale as well as moldable hydrogels that flows on applied stress are all benefits that can emerge from this network construction.^[218, 222] The first paper describing DX-gels was published in 2000 by Hu *et al*.^[223] In their report, they described the synthesis of a new class of nanostructured polymer gels by bonding crosslinked hydroxypropyl cellulose nanoparticles with divinyl sulfone in solution at 55°C. This increasing level of structural complexity offers also great promises for regenerative medicine in which injectable DX-gels were investigated for degenerative intervertebral disc treatment^[121], vocal fold restoration^[218] or mesenchymal stem cells differentiation.^[219] Owing to the existence of two levels of crosslinking, degradation and mechanical properties of the resulting hydrogel can be adjusted independently and therefore the responsivity of the materials increases greatly. A typical example of DX-gel synthesis can be found in Figure II.23. Several examples are detailed below.

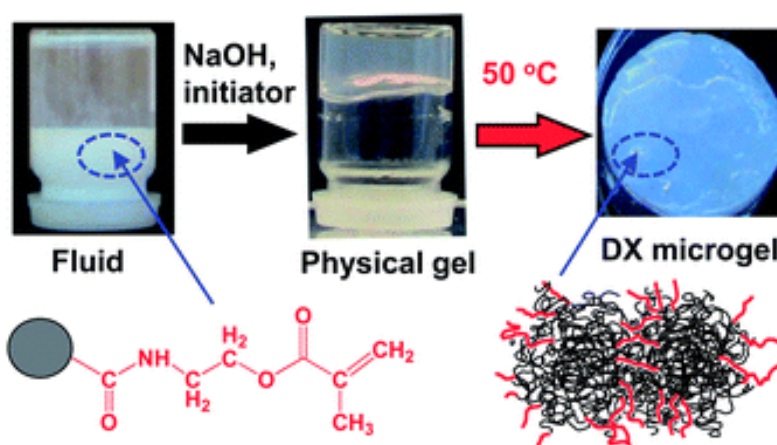


Figure II.23: Reaction figure for preparing DX-gels from [222].

II.6.3. From microgels to macrogels: gelation mechanisms

II.6.3.1. Physical gelation

Only few examples report physical intercrosslinking whilst still being efficient enough to produce hierarchized injectable networks embedding micro- to nanoparticles. Saunders *et al.* developed injectable dispersions of microgels that provide structural support for damaged soft tissue and enable regeneration of tissue. The concentrated dispersions exhibit a strong fluid-to-gel transition when the pH is increased above 6.^[152] Gan *et al.* proposed a PNIPAM microgel dispersion that can be used as a new type of injectable cell scaffolds upon heating. However, the *in situ* hydrogel formed shrank with time, which is undesirable for their use as cell scaffolds.^[153] Continuing on their previous results, they fabricated 2D films and 3D aggregates using PNIPAM microgels as building block.^[224] Moreover, they prepared thermosensitive (P(NIPAM-HEMA)) microgels as a thermal gelling injectable scaffold for three-dimensional cell culture.^[225] Another strategy using oppositely charged dextran microgels was studied by Van Tomme for the release of proteins.^[226]

II.6.3.2. Chemical gelation

Various strategies to synthesize DX-gels have been published so far. Mostly, DX-gels are obtained by covalent coupling via a free-radical polymerization process of pending vinyl bonds localized at the particle surfaces.^[117-119, 121, 219, 222, 227-232] An alternative method was presented by McCann *et al.*, which utilized the imine bond-forming reaction between the aldehyde groups of partially oxidized dextran and the primary amine groups of poly(vinylamine-co-bis(ethyl vinylamine) ether) cationic microgel particles.^[233] The network degradation was induced through an acidic cleavage of the imine bonds at low pH. Saunders group has been successful in preparing double crosslinked microgel systems based on particles of methacrylic acid copolymerised with either methyl methacrylate or ethyl acrylate as a structural monomer and ethyleneglycol dimethacrylate or butanediol diacrylate as a crosslinker.^[220, 222, 234] These particles were functionalized using glycidyl methacrylate (GMA) in order to introduce exposed methacrylate groups to the microgel periphery for future radical coupling. Lowering the pH induced particle swelling and triggered the formation of a physical gel as the peripheries of swollen microgel particles overlapped. This led the pendant methacrylate groups of neighbouring particles into close proximity. Heating these physical gels in the presence of ammonium persulphate (APS) initiator caused

the formation of a permanent, covalently bonded double crosslinked microgel.^[220, 222, 234, 235] These gels have been developed towards the use in specific biomedical applications of restoring structure and function of load bearing tissue, such as damaged or degenerated intervertebral discs.^[121] Lately, Saunders' group studied for the first time the effects of intra-MG crosslinking on the swelling of the MGs and the mechanical properties of the DX MGs. It was shown that good tuneability of the DX MG properties could be obtained simply by controlling the DVB and BDDA contents within the MG particles.^[123] The average strain-at-break value for the DVB-containing DX MGs was 76% which represents the highest value yet reported for a DX MG prepared using commercially available monomers. Analysis of the swelling and compression data enabled relationships between the volume-swelling ratio of the MGs and either the modulus or strain-at-break values for the DX MGs.

In a variation of this theme, colloidal graphene oxide was introduced to anionic poly[(ethyl acrylate)-co-(methacrylic acid)] and significantly improved the mechanical properties of the double crosslinked microgel network.^[231] Later, Cui *et al.* studied conductive gel composites because of their interesting electrical and mechanical properties. In their study, conductive gel composites were prepared from mixed dispersions of vinyl-functionalised pH-responsive microgel particles (MGs) and multi-walled carbon nanotubes (CNTs).^[120] TEM data showed evidence for strong attraction between the MG and the CNTs which facilitated CNT dispersion. The gels formed were electrically conductive and possessed a low percolation threshold (0.15%). The DX gel composites were also pH-responsive and had modulus values that increased linearly with MG–CNT interfacial contact area. A cationic DX-gel network based on the GMA functionalisation of poly(vinyl amine) microgel particles has also been reported with interesting porosity features and may also have biomedical applications.^[227] DX-gels present many advantages over classical polymer networks obtained through chemical or physical crosslinking. The ability to fine tune the final mechanical properties owing to the hierarchical level of reticulation involving a primary crosslinking in the microbeads and an intercrosslinking between the beads is the particular benefit of this method. This freedom of action in tuning mechanical properties is particularly interesting in the field of injectable hydrogels for tissue engineering as the injected material must present equivalent mechanical properties than the hosting tissue.

Moreover, they offer fine tuning of the mesh size, high specific surface area, controlled heterogeneity at the nanoscale as well as moldability.^[218, 222]

The heat released during the polymerization process and/or polymerization conditions (temperature higher than body temperature) are not always compatible with *in vivo* prerequisites. As a consequence, covalent coupling reactions that occur fast and at room temperature are really desirable. The realm of click chemistry reactions offers a large choice for fast coupling reaction at room temperature.^[236-240] However, while being a valuable tool for many coupling reactions, this family of reactions has never been investigated so far in DX-gel formation, except to introduce vinyl functions onto microparticle surfaces as reported recently by Saunders *et al.*^[122]

Therefore, investigation of click coupling reactions to promote the synthesis of DX-gels are very interesting as it could form gels with fast kinetics and easy setup. In order to avoid the toxicity of copper, copper free click chemistry should be targeted.

II.7. Bibliography

1. Wichterle, O. and Lim, D., *Hydrophilic Gels for Biological Use*. Nature, 1960. **185**(4706): p. 117-118.
2. Otto, W., *Reshaping a xerogel by mechanical removal and swelling to form a hydrogel contact lens*, 1968, Google Patents.
3. Dreifus, M., Wichterle, O., and Lim, D., *[Intra-cameral lenses made of hydrocolloidal acrylates]*. Cesk Oftalmol, 1960. **16**: p. 154-159.
4. Dreifus, M., et al., *[Tolerance of orbital implants made of hydrocolloid acrylate]*. Sb Lek, 1960. **62**: p. 212-218.
5. Ahmed, E.M., *Hydrogel: Preparation, characterization, and applications: A review*. Journal of Advanced Research, 2015. **6**(2): p. 105-121.
6. Shu, X.Z., et al., *In situ crosslinkable hyaluronan hydrogels for tissue engineering*. Biomaterials, 2004. **25**(7-8): p. 1339-1348.
7. Gosal, W.S., A.H. Clark, and S.B. Ross-Murphy, *Fibrillar beta-lactoglobulin gels: Part 2. Dynamic mechanical characterization of heat-set systems*. Biomacromolecules, 2004. **5**(6): p. 2420-2429.
8. Kolb, H.C., M.G. Finn, and K.B. Sharpless, *Click chemistry: Diverse chemical function from a few good reactions*. Angewandte Chemie-International Edition, 2001. **40**(11): p. 2004-2021.
9. Jiang, Y.J., et al., *Click hydrogels, microgels and nanogels: Emerging platforms for drug delivery and tissue engineering*. Biomaterials, 2014. **35**(18): p. 4969-4985.
10. Rostovtsev, V.V., et al., *A stepwise Huisgen cycloaddition process: Copper(I)-catalyzed regioselective "ligation" of azides and terminal alkynes*. Angewandte Chemie-International Edition, 2002. **41**(14): p. 2596-2599.

11. Tornøe, C.W., C. Christensen, and M. Meldal, *Peptidotriazoles on solid phase: [1,2,3]-triazoles by regioselective copper(I)-catalyzed 1,3-dipolar cycloadditions of terminal alkynes to azides*. Journal of Organic Chemistry, 2002. **67**(9): p. 3057-3064.
12. Nandivada, H., X.W. Jiang, and J. Lahann, *Click chemistry: Versatility and control in the hands of materials scientists*. Advanced Materials, 2007. **19**(17): p. 2197-2208.
13. Lutz, J.F., *1,3-dipolar cycloadditions of azides and alkynes: A universal ligation tool in polymer and materials science*. Angewandte Chemie-International Edition, 2007. **46**(7): p. 1018-1025.
14. Fournier, D., R. Hoogenboom, and U.S. Schubert, *Clicking polymers: a straightforward approach to novel macromolecular architectures*. Chemical Society Reviews, 2007. **36**(8): p. 1369-1380.
15. Binder, W.H. and C. Kluger, *Azide/alkyne-"click" reactions: Applications in material science and organic synthesis*. Current Organic Chemistry, 2006. **10**(14): p. 1791-1815.
16. Worrell, B.T., J.A. Malik, and V.V. Fokin, *Direct Evidence of a Dinuclear Copper Intermediate in Cu(I)-Catalyzed Azide-Alkyne Cycloadditions*. Science, 2013. **340**(6131): p. 457-460.
17. Malkoch, M., et al., *Synthesis of well-defined hydrogel networks using Click chemistry*. Chemical Communications, 2006(26): p. 2774-2776.
18. Mespouille, L., et al., *Synthesis of adaptative and amphiphilic polymer model conetworks by versatile combination of ATRP, ROP, and "Click chemistry"*. Journal of Polymer Science Part a-Polymer Chemistry, 2008. **46**(15): p. 4997-5013.
19. Hu, X.H., et al., *Biological hydrogel synthesized from hyaluronic acid, gelatin and chondroitin sulfate by click chemistry*. Acta Biomaterialia, 2011. **7**(4): p. 1618-1626.
20. Koschella, A., M. Hartlieb, and T. Heinze, *A "click-chemistry" approach to cellulose-based hydrogels*. Carbohydrate Polymers, 2011. **86**(1): p. 154-161.
21. Agard, N.J., J.A. Prescher, and C.R. Bertozzi, *A strain-promoted [3+2] azide-alkyne cycloaddition for covalent modification of biomolecules in living systems (vol 126, pg 15046, 2004)*. Journal of the American Chemical Society, 2005. **127**(31): p. 11196-11196.
22. DeForest, C.A., B.D. Polizzotti, and K.S. Anseth, *Sequential click reactions for synthesizing and patterning three-dimensional cell microenvironments*. Nature Materials, 2009. **8**(8): p. 659-664.
23. DeForest, C.A., E.A. Sims, and K.S. Anseth, *Peptide-Functionalized Click Hydrogels with Independently Tunable Mechanics and Chemical Functionality for 3D Cell Culture*. Chemistry of Materials, 2010. **22**(16): p. 4783-4790.
24. DeForest, C.A. and K.S. Anseth, *Cytocompatible click-based hydrogels with dynamically tunable properties through orthogonal photoconjugation and photocleavage reactions*. Nature Chemistry, 2011. **3**(12): p. 925-931.
25. McKinnon, D.D., et al., *Design and Characterization of a Synthetically Accessible, Photodegradable Hydrogel for User-Directed Formation of Neural Networks*. Biomacromolecules, 2014. **15**(7): p. 2808-2816.
26. DeForest, C.A. and D.A. Tirrell, *A photoreversible protein-patterning approach for guiding stem cell fate in three-dimensional gels*. Nature Materials, 2015. **14**(5): p. 523-531.
27. Jiang, H.F., et al., *An injectable and fast-degradable poly(ethylene glycol) hydrogel fabricated via bioorthogonal strain-promoted azide-alkyne cycloaddition click chemistry*. Soft Matter, 2015. **11**(30): p. 6029-6036.
28. Hoyle, C.E., T.Y. Lee, and T. Roper, *Thiol-enes: Chemistry of the past with promise for the future*. Journal of Polymer Science Part a-Polymer Chemistry, 2004. **42**(21): p. 5301-5338.
29. Hoyle, C.E. and C.N. Bowman, *Thiol-Ene Click Chemistry*. Angewandte Chemie International Edition, 2010. **49**(9): p. 1540-1573.
30. Truong, V.X., et al., *Preparation of in situ-forming poly(5-methyl-5-allyloxycarbonyl-1,3-dioxan-2-one)-poly(ethylene glycol) hydrogels with tuneable swelling, mechanical strength and degradability*. Journal of Materials Chemistry B, 2013. **1**(2): p. 221-229.

31. Aimetti, A.A., A.J. Machen, and K.S. Anseth, *Poly(ethylene glycol) hydrogels formed by thiol-ene photopolymerization for enzyme-responsive protein delivery*. *Biomaterials*, 2009. **30**(30): p. 6048-6054.
32. Quick, A.S., et al., *Rapid Thiol-Yne-Mediated Fabrication and Dual Postfunctionalization of Micro-Resolved 3D Mesosstructures*. *Advanced Functional Materials*, 2015. **25**(24): p. 3735-3744.
33. Hoyle, C.E., T.Y. Lee, and T. Roper, *Thiol-enes: Chemistry of the past with promise for the future*. *Journal of Polymer Science Part A: Polymer Chemistry*, 2004. **42**(21): p. 5301-5338.
34. Griesbaum, K., *Problems and Possibilities of the Free-Radical Addition of Thiols to Unsaturated Compounds*. *Angewandte Chemie International Edition in English*, 1970. **9**(4): p. 273-287.
35. Lin, C.-C., A. Raza, and H. Shih, *PEG hydrogels formed by thiol-ene photo-click chemistry and their effect on the formation and recovery of insulin-secreting cell spheroids*. *Biomaterials*, 2011. **32**(36): p. 9685-9695.
36. Buwalda, S.J., P.J. Dijkstra, and J. Feijen, *In Situ Forming Poly(ethylene glycol)- Poly(L-lactide) Hydrogels via Michael Addition: Mechanical Properties, Degradation, and Protein Release*. *Macromolecular Chemistry and Physics*, 2012. **213**(7): p. 766-775.
37. McCall, J.D. and K.S. Anseth, *Thiol-Ene Photopolymerizations Provide a Facile Method To Encapsulate Proteins and Maintain Their Bioactivity*. *Biomacromolecules*, 2012. **13**(8): p. 2410-2417.
38. Kharkar, P.M., K.L. Kiick, and A.M. Kloxin, *Design of thiol- and light-sensitive degradable hydrogels using Michael-type addition reactions*. *Polymer Chemistry*, 2015. **6**(31): p. 5565-5574.
39. Kharkar, P.M., A.M. Kloxin, and K.L. Kiick, *Dually degradable click hydrogels for controlled degradation and protein release*. *Journal of Materials Chemistry B*, 2014. **2**(34): p. 5511-5521.
40. Alconcel, S.N.S., A.S. Baas, and H.D. Maynard, *FDA-approved poly(ethylene glycol)-protein conjugate drugs*. *Polymer Chemistry*, 2011. **2**(7): p. 1442-1448.
41. O'Shea, T.M., et al., *Synthesis and Characterization of a Library of In-Situ Curing, Nonswelling Ethoxylated Polyol Thiol-ene Hydrogels for Tailorable Macromolecule Delivery*. *Advanced Materials*, 2015. **27**(1): p. 65-72.
42. Diels, O. and K. Alder, *Synthesen in der hydroaromatischen Reihe*. *Justus Liebigs Annalen der Chemie*, 1928. **460**(1): p. 98-122.
43. Sauer, J. and R. Sustmann, *Mechanistic Aspects of Diels-Alder Reactions: A Critical Survey*. *Angewandte Chemie International Edition in English*, 1980. **19**(10): p. 779-807.
44. Sinnwell, S., et al., *A Study into the Stability of 3,6-Dihydro-2H-thiopyran Rings: Key Linkages in the RAFT Hetero-Diels-Alder Click Concept*. *Macromolecules*, 2008. **41**(21): p. 7904-7912.
45. Inglis, A.J., et al., *Reversible Addition Fragmentation Chain Transfer (RAFT) and Hetero-Diels-Alder Chemistry as a Convenient Conjugation Tool for Access to Complex Macromolecular Designs*. *Macromolecules*, 2008. **41**(12): p. 4120-4126.
46. Schenzel, A.M., et al., *Reversing Adhesion: A Triggered Release Self-Reporting Adhesive*. *Advanced Science*, 2016. **3**(3).
47. Bousquet, A., C. Barner-Kowollik, and M.H. Stenzel, *Synthesis of Comb Polymers via Grafting-Onto Macromolecules Bearing Pendant Diene Groups via the Hetero-Diels-Alder-RAFT Click Concept*. *Journal of Polymer Science Part a-Polymer Chemistry*, 2010. **48**(8): p. 1773-1781.
48. Espinosa, E., et al., *Synthesis of Cyclopentadienyl Capped Polyethylene and Subsequent Block Copolymer Formation Via Hetero Diels-Alder (HDA) Chemistry*. *Macromolecular Rapid Communications*, 2011. **32**(18): p. 1447-1453.
49. Glassner, M., et al., *(Ultra)Fast Catalyst-Free Macromolecular Conjugation in Aqueous Environment at Ambient Temperature*. *Journal of the American Chemical Society*, 2012. **134**(17): p. 7274-7277.
50. Langer, M., et al., *Amphiphilic block copolymers featuring a reversible hetero Diels-Alder linkage*. *Polymer Chemistry*, 2014. **5**(18): p. 5330-5338.

51. Oehlenschlaeger, K.K., et al., *Adaptable Hetero Diels-Alder Networks for Fast Self-Healing under Mild Conditions*. *Advanced Materials*, 2014. **26**(21): p. 3561-3566.
52. Quick, A.S., et al., *Fabrication and Spatially Resolved Functionalization of 3D Microstructures via Multiphoton-Induced Diels-Alder Chemistry*. *Advanced Functional Materials*, 2014. **24**(23): p. 3571-3580.
53. Chujo, Y., K. Sada, and T. Saegusa, *A Novel Nonionic Hydrogel from 2-Methyl-2-Oxazoline .4. Reversible Gelation of Polyoxazoline by Means of Diels-Alder Reaction*. *Macromolecules*, 1990. **23**(10): p. 2636-2641.
54. Yu, F., et al., *An injectable hyaluronic acid/PEG hydrogel for cartilage tissue engineering formed by integrating enzymatic crosslinking and Diels-Alder "click chemistry"*. *Polymer Chemistry*, 2014. **5**(3): p. 1082-1090.
55. Nimmo, C.M., S.C. Owen, and M.S. Shoichet, *Diels–Alder Click Cross-Linked Hyaluronic Acid Hydrogels for Tissue Engineering*. *Biomacromolecules*, 2011. **12**(3): p. 824-830.
56. Tan, H., J.P. Rubin, and K.G. Marra, *Direct Synthesis of Biodegradable Polysaccharide Derivative Hydrogels Through Aqueous Diels-Alder Chemistry*. *Macromolecular Rapid Communications*, 2011. **32**(12): p. 905-911.
57. Alge, D.L., et al., *Synthetically Tractable Click Hydrogels for Three-Dimensional Cell Culture Formed Using Tetrazine–Norbornene Chemistry*. *Biomacromolecules*, 2013. **14**(4): p. 949-953.
58. Alge, D.L., et al., *Synthetically Tractable Click Hydrogels for Three-Dimensional Cell Culture Formed Using Tetrazine–Norbornene Chemistry*. *Biomacromolecules*, 2013. **14**(4): p. 949-953.
59. Williams, A.G. and G.B. Butler, *Mechanistic Studies of the Reaction of 4-Substituted 1,2,4-Triazoline-3,5-Diones with Beta-Dicarbonyl Compounds*. *Journal of Organic Chemistry*, 1980. **45**(7): p. 1232-1239.
60. Furdik, M., et al., *Synthesis of Azodicarboxylic Acid Imide Its N-Substituted Derivatives and Their Use as Dienophiles in Diels-Alder Reaction*. *Chemické Zvesti*, 1967. **21**(6): p. 427-&.
61. Billiet, S., et al., *Triazolinediones enable ultrafast and reversible click chemistry for the design of dynamic polymer systems (vol 6, pg 815, 2014)*. *Nature Chemistry*, 2014. **6**(9).
62. Rádl, S., *1 2, 4-Triazoline-3,5-Diones*, in *Advances in Heterocyclic Chemistry*, R.K. Alan, Editor 1996, Academic Press. p. 119-205.
63. Korobitsyna, I.K., et al., *"4-Phenyl-1,2,4-Triazoline-3,5-Dione in the Organic-Synthesis*. *Khimiya Geterotsiklicheskikh Soedinenii*, 1983(2): p. 147-169.
64. Turunc, O., et al., *From plant oils to plant foils: Straightforward functionalization and crosslinking of natural plant oils with triazolinediones*. *European Polymer Journal*, 2015. **65**: p. 286-297.
65. De Bruycker, K., et al., *Triazolinediones as Highly Enabling Synthetic Tools*. *Chemical Reviews*, 2016. **116**(6): p. 3919-3974.
66. De Bruycker, K., et al., *Triazolinediones as Highly Enabling Synthetic Tools*. *Chemical Reviews*, 2016.
67. Matyjaszewski, K., *Controlled radical polymerization*. *Current Opinion in Solid State and Materials Science*, 1996. **1**(6): p. 769-776.
68. K. Matyjaszewski et al., *Hanbook of radical polymerisation*, John Wiley and Sons, Inc., Hoboken, 2002 p Vii
69. Matyjaszewski, K., *Transition metal catalysis in controlled radical polymerization: Atom transfer radical polymerization*. *Chemistry-a European Journal*, 1999. **5**(11): p. 3095-3102.
70. Goto, A. and T. Fukuda, *Kinetics of living radical polymerization*. *Progress in Polymer Science*, 2004. **29**(4): p. 329-385.
71. Matyjaszewski, K., *Atom Transfer Radical Polymerization (ATRP): Current Status and Future Perspectives*. *Macromolecules*, 2012. **45**(10): p. 4015-4039.
72. Patten, T.E., et al., *Polymers with very low polydispersities from atom transfer radical polymerization*. *Science*, 1996. **272**(5263): p. 866-868.

73. Chiefari, J., et al., *Living free-radical polymerization by reversible addition-fragmentation chain transfer: The RAFT process*. Macromolecules, 1998. **31**(16): p. 5559-5562.
74. Chong, Y.K., et al., *A more versatile route to block copolymers and other polymers of complex architecture by living radical polymerization: The RAFT process*. Macromolecules, 1999. **32**(6): p. 2071-2074.
75. Moad, G., et al., *Living free radical polymerization with reversible addition-fragmentation chain transfer (the life of RAFT)*. Polymer International, 2000. **49**(9): p. 993-1001.
76. Moad, G. and E. Rizzardo, *Alkoxyamine-initiated living radical polymerization: Factors affecting alkoxyamine homolysis rates*. Macromolecules, 1995. **28**(26): p. 8722-8728.
77. Hawker, C.J., *Molecular-Weight Control by a Living Free-Radical Polymerization Process*. Journal of the American Chemical Society, 1994. **116**(24): p. 11185-11186.
78. Nicolas, J., et al., *Nitroxide-mediated polymerization*. Progress in Polymer Science, 2013. **38**(1): p. 63-235.
79. Sciannamea, V., R. Jerome, and C. Detrembleur, *In-situ nitroxide-mediated radical polymerization (NMP) processes: Their understanding and optimization*. Chemical Reviews, 2008. **108**(3): p. 1104-1126.
80. Behraves, E., K. Zygourakis, and A.G. Mikos, *Adhesion and migration of marrow-derived osteoblasts on injectable in situ crosslinkable poly(propylene fumarate-co-ethylene glycol)-based hydrogels with a covalently linked RGDS peptide*. Journal of Biomedical Materials Research Part A, 2003. **65A**(2): p. 260-270.
81. Zhu, W. and J.D. Ding, *Synthesis and characterization of a redox-initiated, injectable, biodegradable hydrogel*. Journal of Applied Polymer Science, 2006. **99**(5): p. 2375-2383.
82. Zhang, Y., et al., *A novel microgel and associated post-fabrication encapsulation technique of proteins*. Journal of Controlled Release, 2005. **105**(3): p. 260-268.
83. Zhu, W., et al., *Preparation of a thermosensitive and biodegradable microgel via polymerization of macromonomers based on diacrylated Pluronic/oligoester copolymers*. European Polymer Journal, 2005. **41**(9): p. 2161-2170.
84. Zhang, Y., et al., *Postfabrication encapsulation of model protein drugs in a negatively thermosensitive hydrogel*. Journal of Pharmaceutical Sciences, 2005. **94**(8): p. 1676-1684.
85. Zhang, Y., W. Zhu, and J.D. Ding, *Preparation of thermosensitive microgels via suspension polymerization using different temperature protocols*. Journal of Biomedical Materials Research Part A, 2005. **75A**(2): p. 342-349.
86. Wang, B., et al., *Synthesis of a chemically-crosslinked thermo-sensitive hydrogel film and in situ encapsulation of model protein drugs*. Reactive & Functional Polymers, 2006. **66**(5): p. 509-518.
87. Park, H., et al., *Effect of Swelling Ratio of Injectable Hydrogel Composites on Chondrogenic Differentiation of Encapsulated Rabbit Marrow Mesenchymal Stem Cells In Vitro*. Biomacromolecules, 2009. **10**(3): p. 541-546.
88. Guo, X., et al., *In vitro generation of an osteochondral construct using injectable hydrogel composites encapsulating rabbit marrow mesenchymal stem cells*. Biomaterials, 2009. **30**(14): p. 2741-2752.
89. Ferreira, L., et al., *Biocompatibility of chemoenzymatically derived dextran-acrylate hydrogels*. Journal of Biomedical Materials Research Part A, 2004. **68A**(3): p. 584-596.
90. Hong, Y., et al., *Covalently crosslinked chitosan hydrogel: Properties of in vitro degradation and chondrocyte encapsulation*. Acta Biomaterialia, 2007. **3**(1): p. 23-31.
91. Bahney, C.S., et al., *Visible Light Photoinitiation of Mesenchymal Stem Cell-Laden Bioresponsive Hydrogels*. European Cells & Materials, 2011. **22**: p. 43-55.
92. Burdick, J.A. and K.S. Anseth, *Photoencapsulation of osteoblasts in injectable RGD-modified PEG hydrogels for bone tissue engineering*. Biomaterials, 2002. **23**(22): p. 4315-4323.
93. Sharma, B., et al., *In vivo chondrogenesis of mesenchymal stem cells in a photopolymerized hydrogel*. Plastic and Reconstructive Surgery, 2007. **119**(1): p. 112-120.

94. Villanueva, I., et al., *Static and dynamic compressive strains influence nitric oxide production and chondrocyte bioactivity when encapsulated in PEG hydrogels of different crosslinking densities*. Osteoarthritis and Cartilage, 2008. **16**(8): p. 909-918.
95. Nicodemus, G.D., S.C. Skaalure, and S.J. Bryant, *Gel structure has an impact on pericellular and extracellular matrix deposition, which subsequently alters metabolic activities in chondrocyte-laden PEG hydrogels*. Acta Biomaterialia, 2011. **7**(2): p. 492-504.
96. Bryant, S.J., et al., *Encapsulating Chondrocytes in degrading PEG hydrogels with high modulus: Engineering gel structural changes to facilitate cartilaginous tissue production*. Biotechnology and Bioengineering, 2004. **86**(7): p. 747-755.
97. Martens, P.J., S.J. Bryant, and K.S. Anseth, *Tailoring the degradation of hydrogels formed from multivinyl poly(ethylene glycol) and poly(vinyl alcohol) macromers for cartilage tissue engineering*. Biomacromolecules, 2003. **4**(2): p. 283-292.
98. Li, Q., et al., *Photocrosslinkable polysaccharides based on chondroitin sulfate*. Journal of Biomedical Materials Research Part A, 2004. **68A**(1): p. 28-33.
99. Bryant, S.J., J.A. Arthur, and K.S. Anseth, *Incorporation of tissue-specific molecules alters chondrocyte metabolism and gene expression in photocrosslinked hydrogels*. Acta Biomaterialia, 2005. **1**(2): p. 243-252.
100. Nettles, D.L., et al., *Photocrosslinkable hyaluronan as a scaffold for articular cartilage repair*. Annals of Biomedical Engineering, 2004. **32**(3): p. 391-397.
101. Fedorovich, N.E., et al., *The effect of photopolymerization on stem cells embedded in hydrogels*. Biomaterials, 2009. **30**(3): p. 344-353.
102. Burdick, J.A., et al., *Controlled degradation and mechanical behavior of photopolymerized hyaluronic acid networks*. Biomacromolecules, 2005. **6**(1): p. 386-391.
103. Sahoo, S., et al., *Hydrolytically degradable hyaluronic acid hydrogels with controlled temporal structures*. Biomacromolecules, 2008. **9**(4): p. 1088-1092.
104. Park, H., et al., *Injectable chitosan hyaluronic acid hydrogels for cartilage tissue engineering*. Acta Biomaterialia, 2013. **9**(1): p. 4779-4786.
105. Hu, J.L., et al., *Visible light crosslinkable chitosan hydrogels for tissue engineering*. Acta Biomaterialia, 2012. **8**(5): p. 1730-1738.
106. Amsden, B.G., et al., *Methacrylated glycol chitosan as a photopolymerizable biomaterial*. Biomacromolecules, 2007. **8**(12): p. 3758-3766.
107. Seto, S.P., M.E. Casas, and J.S. Temenoff, *Differentiation of mesenchymal stem cells in heparin-containing hydrogels via coculture with osteoblasts*. Cell and Tissue Research, 2012. **347**(3): p. 589-601.
108. Jeon, O., et al., *Photocrosslinked alginate hydrogels with tunable biodegradation rates and mechanical properties*. Biomaterials, 2009. **30**(14): p. 2724-2734.
109. Hu, X.H., et al., *Gelatin Hydrogel Prepared by Photo-initiated Polymerization and Loaded with TGF-beta 1 for Cartilage Tissue Engineering*. Macromolecular Bioscience, 2009. **9**(12): p. 1194-1201.
110. Hoffman, A.S., *Hydrogels for biomedical applications*. Advanced Drug Delivery Reviews, 2012. **64**, **Supplement**: p. 18-23.
111. Nagahama, K., et al., *Irreversible temperature-responsive formation of high-strength hydrogel from an enantiomeric mixture of starburst triblock copolymers consisting of 8-arm PEG and PLLA or PDLA*. Journal of Polymer Science Part a-Polymer Chemistry, 2008. **46**(18): p. 6317-6332.
112. Qiu, Y. and K. Park, *Environment-sensitive hydrogels for drug delivery*. Advanced Drug Delivery Reviews, 2001. **53**(3): p. 321-339.
113. Bhattarai, N., et al., *PEG-grafted chitosan as an injectable thermosensitive hydrogel for sustained protein release*. Journal of Controlled Release, 2005. **103**(3): p. 609-624.
114. Park, K.M., et al., *Thermosensitive chitosan-Pluronic hydrogel as an injectable cell delivery carrier for cartilage regeneration*. Acta Biomaterialia, 2009. **5**(6): p. 1956-1965.

115. Lee, K.Y. and D.J. Mooney, *Hydrogels for tissue engineering*. Chemical Reviews, 2001. **101**(7): p. 1869-1879.
116. Jeong, B., S.W. Kim, and Y.H. Bae, *Thermosensitive sol-gel reversible hydrogels*. Advanced Drug Delivery Reviews, 2012. **64**: p. 154-162.
117. Liu, R., et al., *Doubly crosslinked pH-responsive microgels prepared by particle inter-penetration: swelling and mechanical properties*. Soft Matter, 2011. **7**(10): p. 4696-4704.
118. Lane, T., et al., *Double network hydrogels prepared from pH-responsive doubly crosslinked microgels*. Soft Matter, 2013. **9**(33): p. 7934-7941.
119. Milani, A.H., et al., *Swelling and mechanical properties of hydrogels composed of binary blends of inter-linked pH-responsive microgel particles*. Soft Matter, 2015. **11**(13): p. 2586-2595.
120. Cui, Z.X., et al., *A study of conductive hydrogel composites of pH-responsive microgels and carbon nanotubes*. Soft Matter, 2016. **12**(18): p. 4142-4153.
121. Milani, A.H., et al., *Injectable Doubly Cross-Linked Microgels for Improving the Mechanical Properties of Degenerated Intervertebral Discs*. Biomacromolecules, 2012. **13**(9): p. 2793-2801.
122. Farley, R., et al., *Using click chemistry to dial up the modulus of doubly crosslinked microgels through precise control of microgel building block functionalisation*. Polymer Chemistry, 2015. **6**(13): p. 2512-2522.
123. Cui, Z.X., et al., *Using intra-microgel crosslinking to control the mechanical properties of doubly crosslinked microgels*. Soft Matter, 2016. **12**(33): p. 6985-6994.
124. H. Staudinger, E.H., Ber. 68 (1935) 1618.
125. Wang, J., et al., *Temperature-Jump Investigations of the Kinetics of Hydrogel Nanoparticle Volume Phase Transitions*. Journal of the American Chemical Society, 2001. **123**(45): p. 11284-11289.
126. Guan, Y. and Y. Zhang, *PNIPAM microgels for biomedical applications: from dispersed particles to 3D assemblies*. Soft Matter, 2011. **7**(14): p. 6375-6384.
127. Flory, P.J., in: *Principles of Polymer Chemistry*, Cornell, 1953.
128. Gan, T., Y. Guan, and Y. Zhang, *Thermogelable PNIPAM microgel dispersion as 3D cell scaffold: effect of syneresis*. Journal of Materials Chemistry, 2010. **20**(28): p. 5937-5944.
129. Champion, J.A., Y.K. Katare, and S. Mitragotri, *Making polymeric micro- and nanoparticles of complex shapes*. Proceedings of the National Academy of Sciences of the United States of America, 2007. **104**(29): p. 11901-11904.
130. Bhaskar, S., et al., *Towards Designer Microparticles: Simultaneous Control of Anisotropy, Shape, and Size*. Small, 2010. **6**(3): p. 404-411.
131. Misra, A. and M.W. Urban, *Acorn-Shape Polymeric Nano-Colloids: Synthesis and Self-Assembled Films*. Macromolecular Rapid Communications, 2010. **31**(2): p. 119-127.
132. Pawar, A.B. and I. Kretzschmar, *Fabrication, Assembly, and Application of Patchy Particles*. Macromolecular Rapid Communications, 2010. **31**(2): p. 150-168.
133. Trindade, A.C., et al., *Wrinkling Labyrinth Patterns on Elastomeric Janus Particles*. Macromolecules, 2011. **44**(7): p. 2220-2228.
134. Shum, H.C., et al., *Droplet Microfluidics for Fabrication of Non-Spherical Particles*. Macromolecular Rapid Communications, 2010. **31**(2): p. 108-118.
135. Murray, M.J. and M.J. Snowden, *The preparation, characterisation and applications of colloidal microgels*. Advances in Colloid and Interface Science, 1995. **54**: p. 73-91.
136. Yoshida, M., K.-H. Roh, and J. Lahann, *Short-term biocompatibility of biphasic nanocolloids with potential use as anisotropic imaging probes*. Biomaterials, 2007. **28**(15): p. 2446-2456.
137. Shekunov, B.Y., et al., *Particle size analysis in pharmaceuticals: Principles, methods and applications*. Pharmaceutical Research, 2007. **24**(2): p. 203-227.
138. Yoo, J.W. and S. Mitragotri, *Polymer particles that switch shape in response to a stimulus*. Proceedings of the National Academy of Sciences of the United States of America, 2010. **107**(25): p. 11205-11210.

139. Arshady, R., *Microspheres and Microcapsules, a Survey of Manufacturing Techniques .2. Coacervation*. Polymer Engineering and Science, 1990. **30**(15): p. 905-914.
140. Prokop, A., et al., *Water soluble polymers for immunoisolation I: Complex coacervation and cytotoxicity*. Microencapsulation - Microgels - Iniferters, 1998. **136**: p. 1-51.
141. Burgess, D.J., *Practical Analysis of Complex Coacervate Systems*. Journal of Colloid and Interface Science, 1990. **140**(1): p. 227-238.
142. Menger, F.M., et al., *A sponge morphology in an elementary coacervate*. Langmuir, 2000. **16**(24): p. 9113-9116.
143. Farjami, T. and A. Madadlou, *Fabrication methods of biopolymeric microgels and microgel-based hydrogels*. Food Hydrocolloids, 2017. **62**: p. 262-272.
144. Benes, M.J., D. Horak, and F. Svec, *Methacrylate-based chromatographic media*. Journal of Separation Science, 2005. **28**(15): p. 1855-1875.
145. Garcia-Diego, C. and J. Cuellar, *Synthesis of macroporous poly(styrene-co-divinylbenzene) microparticles using n-heptane as the porogen: Quantitative effects of the DVB concentration and the monomeric fraction on their structural characteristics*. Industrial & Engineering Chemistry Research, 2005. **44**(22): p. 8237-8247.
146. Horak, D., et al., *The Effect of Polymeric Porogen on the Properties of Macroporous Poly(Glycidyl Methacrylate-Co-Ethylene Dimethacrylate)*. Polymer, 1993. **34**(16): p. 3481-3489.
147. Ferreira, A., M. Bigan, and D. Blondeau, *Optimization of a polymeric HPLC phase: poly(glycidyl methacrylate-co-ethylene dimethacrylate) Influence of the polymerization conditions on the pore structure of macroporous beads*. Reactive & Functional Polymers, 2003. **56**(2): p. 123-136.
148. Kanamori, K., et al., *Facile Synthesis of Macroporous Cross-Linked Methacrylate Gels by Atom Transfer Radical Polymerization*. Macromolecules, 2008. **41**(19): p. 7186-7193.
149. Macintyre, F.S. and D.C. Sherrington, *Control of porous morphology in suspension polymerized poly(divinylbenzene) resins using oligomeric porogens*. Macromolecules, 2004. **37**(20): p. 7628-7636.
150. Gokmen, M.T. and F.E. Du Prez, *Porous polymer particles—A comprehensive guide to synthesis, characterization, functionalization and applications*. Progress in Polymer Science, 2012. **37**(3): p. 365-405.
151. Freemont, T.J. and B.R. Saunders, *pH-responsive microgel dispersions for repairing damaged load-bearing soft tissue*. Soft Matter, 2008. **4**(5): p. 919-924.
152. Saunders, J.M., et al., *A study of pH-responsive microgel dispersions: from fluid-to-gel transitions to mechanical property restoration for load-bearing tissue*. Soft Matter, 2007. **3**(4): p. 486-494.
153. Gan, T.T., Y. Guan, and Y.J. Zhang, *Thermogelable PNIPAM microgel dispersion as 3D cell scaffold: effect of syneresis*. Journal of Materials Chemistry, 2010. **20**(28): p. 5937-5944.
154. Hopkins, S., et al., *Sub-micron poly(N-isopropylacrylamide) particles as temperature responsive vehicles for the detachment and delivery of human cells*. Soft Matter, 2009. **5**(24): p. 4928-4937.
155. Das, M., H. Zhang, and E. Kumacheva, *Microgels: Old materials with new applications*. Annual Review of Materials Research, 2006. **36**: p. 117-142.
156. H. B. Yamak, E.P.E.o.P.V.o., t.P.o.V.A.B.E.P.i.P. Science, and I. (Ed.: F. Yilmaz), 2013, pp. 35–72.
157. Li, K. and H.D.H. Stöver, *Synthesis of monodisperse poly(divinylbenzene) microspheres*. Journal of Polymer Science Part A: Polymer Chemistry, 1993. **31**(13): p. 3257-3263.
158. Saraçoğlu, B., et al., *Synthesis of Monodisperse Glycerol Dimethacrylate-Based Microgel Particles by Precipitation Polymerization*. Industrial & Engineering Chemistry Research, 2009. **48**(10): p. 4844-4851.
159. Lai, J.-P., et al., *Molecularly imprinted microspheres and nanospheres for di(2-ethylhexyl)phthalate prepared by precipitation polymerization*. Analytical and Bioanalytical Chemistry, 2007. **389**(2): p. 405-412.

160. Goldmann, A.S., et al., *Surface Modification of Poly(divinylbenzene) Microspheres via Thiol-Ene Chemistry and Alkyne-Azide Click Reactions*. *Macromolecules*, 2009. **42**(11): p. 3707-3714.
161. Song, J.-S., F. Tronc, and M.A. Winnik, *Two-Stage Dispersion Polymerization toward Monodisperse, Controlled Micrometer-Sized Copolymer Particles*. *Journal of the American Chemical Society*, 2004. **126**(21): p. 6562-6563.
162. Yuet, K.P., et al., *Multifunctional Superparamagnetic Janus Particles*. *Langmuir*, 2010. **26**(6): p. 4281-4287.
163. Li, W.X., et al., *Controllable microfluidic fabrication of Janus and microcapsule particles for drug delivery applications*. *Rsc Advances*, 2015. **5**(30): p. 23181-23188.
164. Nie, Z., et al., *Janus and Ternary Particles Generated by Microfluidic Synthesis: Design, Synthesis, and Self-Assembly*. *Journal of the American Chemical Society*, 2006. **128**(29): p. 9408-9412.
165. Chang, Z., et al., *Co-axial capillaries microfluidic device for synthesizing size- and morphology-controlled polymer core-polymer shell particles*. *Lab on a Chip*, 2009. **9**(20): p. 3007-3011.
166. Groß, G.A., et al., *Formation of Polymer and Nanoparticle Doped Polymer Minirods by Use of the Microsegmented Flow Principle*. *Chemical Engineering & Technology*, 2007. **30**(3): p. 341-346.
167. Seo, M., et al., *Microfluidics: From Dynamic Lattices to Periodic Arrays of Polymer Disks*. *Langmuir*, 2005. **21**(11): p. 4773-4775.
168. Dendukuri, D., et al., *Controlled Synthesis of Nonspherical Microparticles Using Microfluidics*. *Langmuir*, 2005. **21**(6): p. 2113-2116.
169. Edmond, K.V., et al., *Stable Jets of Viscoelastic Fluids and Self-Assembled Cylindrical Capsules by Hydrodynamic Focusing*. *Langmuir*, 2006. **22**(21): p. 9052-9056.
170. Thangawng, A.L., et al., *A simple sheath-flow microfluidic device for micro/nanomanufacturing: fabrication of hydrodynamically shaped polymer fibers*. *Lab on a Chip*, 2009. **9**(21): p. 3126-3130.
171. Jeong, W., et al., *Hydrodynamic microfabrication via "on the fly" photopolymerization of microscale fibers and tubes*. *Lab on a Chip*, 2004. **4**(6): p. 576-580.
172. Falk, B. and J.V. Crivello, *Synthesis and modification of epoxy- and hydroxy-functional microspheres*. *Journal of Applied Polymer Science*, 2005. **97**(4): p. 1574-1585.
173. Wang, R., et al., *Modification of poly(glycidyl methacrylate-divinylbenzene) porous microspheres with polyethylene glycol and their adsorption property of protein*. *Colloids and Surfaces B: Biointerfaces*, 2006. **51**(1): p. 93-99.
174. Yakup Arica, M., E. Yalçın, and G. Bayramoğlu, *Polyethylenimine-grafted and HSA-immobilized poly(GMA-MMA) affinity adsorbents for bilirubin removal*. *Polymer International*, 2005. **54**(1): p. 153-160.
175. Slater, M., et al., *"Click Chemistry" in the Preparation of Porous Polymer-Based Particulate Stationary Phases for μ -HPLC Separation of Peptides and Proteins*. *Analytical Chemistry*, 2006. **78**(14): p. 4969-4975.
176. Kacprzak, K.M., N.M. Maier, and W. Lindner, *Highly efficient immobilization of Cinchona alkaloid derivatives to silica gel via click chemistry*. *Tetrahedron Letters*, 2006. **47**(49): p. 8721-8726.
177. Nebhani, L., et al., *Efficient Surface Modification of Divinylbenzene Microspheres via a Combination of RAFT and Hetero Diels-Alder Chemistry*. *Macromolecular Rapid Communications*, 2008. **29**(17): p. 1431-1437.
178. Nebhani, L., et al., *Quantification of Grafting Densities Achieved via Modular "Grafting-to" Approaches onto Divinylbenzene Microspheres*. *Advanced Functional Materials*, 2010. **20**(12): p. 2010-2020.
179. Goldmann, A.S., et al., *Surface Modification of Poly(divinylbenzene) Microspheres via Thiol-Ene Chemistry and Alkyne-Azide Click Reactions*. *Macromolecules*, 2009. **42**(11): p. 3707-3714.

180. Gu, W., G. Chen, and M.H. Stenzel, *Synthesis of glyco-microspheres via a thiol-ene coupling reaction*. Journal of Polymer Science Part A: Polymer Chemistry, 2009. **47**(20): p. 5550-5556.
181. Alvarez-Paino, M., et al., *Synthesis and lectin recognition studies of glycosylated polystyrene microspheres functionalized via thiol-para-fluorine "click" reaction*. Polymer Chemistry, 2012. **3**(12): p. 3282-3288.
182. Pfaff, A., et al., *Surface modification of polymeric microspheres using glycopolymers for biorecognition*. European Polymer Journal, 2011. **47**(4): p. 805-815.
183. Prasath, R.A., et al., *Thiol-ene and thiol-yne chemistry in microfluidics: a straightforward method towards macroporous and nonporous functional polymer beads*. Polymer Chemistry, 2010. **1**(5): p. 685-692.
184. Gokmen, M.T., et al., *Revealing the nature of thio-click reactions on the solid phase*. Chemical Communications, 2011. **47**(16): p. 4652-4654.
185. Yang, J.A., et al., *In situ-forming injectable hydrogels for regenerative medicine*. Progress in Polymer Science, 2014. **39**(12): p. 1973-1986.
186. Ko, D.Y., et al., *Recent progress of in situ formed gels for biomedical applications*. Progress in Polymer Science, 2013. **38**(3-4): p. 672-701.
187. Burdick, J.A. and G.D. Prestwich, *Hyaluronic Acid Hydrogels for Biomedical Applications*. Advanced Materials, 2011. **23**(12): p. H41-H56.
188. Yetimoglu, E.K., et al., *Sulfathiazole-based novel UV-cured hydrogel sorbents for mercury removal from aqueous solutions*. Radiation Physics and Chemistry, 2009. **78**(2): p. 92-97.
189. Wang, J.L., et al., *Ion-linked double-network hydrogel with high toughness and stiffness*. Journal of Materials Science, 2015. **50**(16): p. 5458-5465.
190. Ren, Z.Q., et al., *Hydrogen bonded and ionically crosslinked high strength hydrogels exhibiting Ca²⁺-triggered shape memory properties and volume shrinkage for cell detachment*. Journal of Materials Chemistry B, 2015. **3**(30): p. 6347-6354.
191. Park, H., E.K. Woo, and K.Y. Lee, *Ionically cross-linkable hyaluronate-based hydrogels for injectable cell delivery*. Journal of Controlled Release, 2014. **196**: p. 146-153.
192. Sun, J.Y., et al., *Highly stretchable and tough hydrogels*. Nature, 2012. **489**(7414): p. 133-136.
193. Hao, X., et al., *A new class of thermo-switchable hydrogel: application to the host-guest approach*. Journal of Materials Chemistry A, 2013. **1**(46): p. 14612-14617.
194. Chen, Y., X.H. Pang, and C.M. Dong, *Dual Stimuli-Responsive Supramolecular Polypeptide-Based Hydrogel and Reverse Micellar Hydrogel Mediated by Host-Guest Chemistry*. Advanced Functional Materials, 2010. **20**(4): p. 579-586.
195. Wang, J., et al., *Bridged-cyclodextrin supramolecular hydrogels: host-guest interaction between a cyclodextrin dimer and adamantyl substituted poly(acrylate)s*. Rsc Advances, 2015. **5**(57): p. 46067-46073.
196. Cui, H.T., et al., *In Situ Electroactive and Antioxidant Supramolecular Hydrogel Based on Cyclodextrin/Copolymer Inclusion for Tissue Engineering Repair(a)*. Macromolecular Bioscience, 2014. **14**(3): p. 440-450.
197. Li, F., et al., *Injectable supramolecular hydrogels fabricated from PEGylated doxorubicin prodrug and alpha-cyclodextrin for pH-triggered drug delivery*. Rsc Advances, 2015. **5**(67): p. 54658-54666.
198. de Jong, S.J., et al., *Physically crosslinked dextran hydrogels by stereocomplex formation of lactic acid oligomers: degradation and protein release behavior*. Journal of Controlled Release, 2001. **71**(3): p. 261-275.
199. Slager, J. and A.J. Domb, *Biopolymer stereocomplexes*. Advanced Drug Delivery Reviews, 2003. **55**(4): p. 549-583.
200. Hiemstra, C., et al., *In vitro and in vivo protein delivery from in situ forming poly(ethylene glycol)-poly(lactide) hydrogels*. Journal of Controlled Release, 2007. **119**(3): p. 320-327.
201. Nowak, A.P., et al., *Rapidly recovering hydrogel scaffolds from self-assembling diblock copolypeptide amphiphiles*. Nature, 2002. **417**(6887): p. 424-428.

202. Huang, C.C., et al., *3-D self-assembling leucine zipper hydrogel with tunable properties for tissue engineering*. Biomaterials, 2014. **35**(20): p. 5316-5326.
203. Huang, R.L., et al., *Self-assembling peptide-polysaccharide hybrid hydrogel as a potential carrier for drug delivery*. Soft Matter, 2011. **7**(13): p. 6222-6230.
204. Huynh, D.P., et al., *Functionalized injectable hydrogels for controlled insulin delivery*. Biomaterials, 2008. **29**(16): p. 2527-2534.
205. Chen, J.P. and T.H. Cheng, *Thermo-responsive chitosan-graft-poly(N-isopropylacrylamide) injectable hydrogel for cultivation of chondrocytes and meniscus cells*. Macromolecular Bioscience, 2006. **6**(12): p. 1026-1039.
206. Yu, L. and J.D. Ding, *Injectable hydrogels as unique biomedical materials*. Chemical Society Reviews, 2008. **37**(8): p. 1473-1481.
207. Ruel-Gariepy, E. and J.C. Leroux, *In situ-forming hydrogels - review of temperature-sensitive systems*. European Journal of Pharmaceutics and Biopharmaceutics, 2004. **58**(2): p. 409-426.
208. Klouda, L. and A.G. Mikos, *Thermoresponsive hydrogels in biomedical applications*. European Journal of Pharmaceutics and Biopharmaceutics, 2008. **68**(1): p. 34-45.
209. Klouda, L., *Thermoresponsive hydrogels in biomedical applications A seven-year update*. European Journal of Pharmaceutics and Biopharmaceutics, 2015. **97**: p. 338-349.
210. Kurecic, M., M. Sfiligoj-Smole, and K. Stana-Kleinschek, *Uv Polymerization of Poly (N-Isopropylacrylamide) Hydrogel*. Materiali in Tehnologije, 2012. **46**(1): p. 87-91.
211. Bardajee, G.R., et al., *UV-prepared salep-based nanoporous hydrogel for controlled release of tetracycline hydrochloride in colon*. Journal of Photochemistry and Photobiology B-Biology, 2011. **102**(3): p. 232-240.
212. Kim, I.S., S.H. Kim, and C.S. Cho, *Drug release from pH-sensitive interpenetrating polymer networks hydrogel based on poly (ethylene glycol) macromer and poly (acrylic acid) prepared by UV cured method*. Archives of Pharmacal Research, 1996. **19**(1): p. 18-22.
213. Li, B.Q., et al., *Hydrosoluble, UV-crosslinkable and injectable chitosan for patterned cell-laden microgel and rapid transdermal curing hydrogel in vivo*. Acta Biomaterialia, 2015. **22**: p. 59-69.
214. Liu, Z.Q., et al., *Dextran-based hydrogel formed by thiol-Michael addition reaction for 3D cell encapsulation*. Colloids and Surfaces B-Biointerfaces, 2015. **128**: p. 140-148.
215. Dong, Y.X., et al., *A rapid crosslinking injectable hydrogel for stem cell delivery, from multifunctional hyperbranched polymers via RAFT homopolymerization of PEGDA*. Polymer Chemistry, 2015. **6**(34): p. 6182-6192.
216. Kim, K.S., et al., *Injectable hyaluronic acid-tyramine hydrogels for the treatment of rheumatoid arthritis*. Acta Biomaterialia, 2011. **7**(2): p. 666-674.
217. Cho, E.C., et al., *Highly responsive hydrogel scaffolds formed by three-dimensional organization of microgel nanoparticles*. Nano Letters, 2008. **8**(1): p. 168-172.
218. Jia, X.Q., et al., *Hyaluronic acid-based microgels and microgel networks for vocal fold regeneration*. Biomacromolecules, 2006. **7**(12): p. 3336-3344.
219. Jha, A.K., et al., *Controlling the adhesion and differentiation of mesenchymal stem cells using hyaluronic acid-based, doubly crosslinked networks*. Biomaterials, 2011. **32**(10): p. 2466-2478.
220. Liu, R.X., et al., *Doubly crosslinked pH-responsive microgels prepared by particle interpenetration: swelling and mechanical properties*. Soft Matter, 2011. **7**(10): p. 4696-4704.
221. Cho, E.C., et al., *Regulating Volume Transitions of Highly Responsive Hydrogel Scaffolds by Adjusting the Network Properties of Microgel Building Block Colloids*. Langmuir, 2010. **26**(6): p. 3854-3859.
222. Liu, R.X., et al., *Tuning the swelling and mechanical properties of pH-responsive doubly crosslinked microgels using particle composition*. Soft Matter, 2011. **7**(19): p. 9297-9306.
223. Hu, Z.B., et al., *Polymer gel nanoparticle networks*. Advanced Materials, 2000. **12**(16): p. 1173-1176.
224. Guan, Y. and Y.J. Zhang, *PNIPAM microgels for biomedical applications: from dispersed particles to 3D assemblies*. Soft Matter, 2011. **7**(14): p. 6375-6384.

225. Gan, T.T., Y.J. Zhang, and Y. Guan, *In Situ Gelation of P(NIPAM-HEMA) Microgel Dispersion and Its Applications as Injectable 3D Cell Scaffold*. Biomacromolecules, 2009. **10**(6): p. 1410-1415.
226. Van Tomme, S.R., et al., *Mobility of model proteins in hydrogels composed of oppositely charged dextran microspheres studied by protein release and fluorescence recovery after photobleaching*. Journal of Controlled Release, 2005. **110**(1): p. 67-78.
227. Thaiboonrod, S., A.H. Milani, and B.R. Saunders, *Doubly crosslinked poly(vinyl amine) microgels: hydrogels of covalently inter-linked cationic microgel particles*. Journal of Materials Chemistry B, 2014. **2**(1): p. 110-119.
228. Sahiner, N., et al., *Fabrication and characterization of cross-linkable hydrogel particles based on hyaluronic acid: potential application in vocal fold regeneration*. Journal of Biomaterials Science-Polymer Edition, 2008. **19**(2): p. 223-243.
229. Cai, T., et al., *Photonic Hydrogels with Poly(ethylene glycol) Derivative Colloidal Spheres as Building Blocks*. Macromolecules, 2008. **41**(24): p. 9508-9512.
230. Jha, A.K., et al., *Structural Analysis and Mechanical Characterization of Hyaluronic Acid-Based Doubly Cross-Linked Networks*. Macromolecules, 2009. **42**(2): p. 537-546.
231. Cui, Z.X., et al., *A Study of Physical and Covalent Hydrogels Containing pH-Responsive Microgel Particles and Graphene Oxide*. Langmuir, 2014. **30**(44): p. 13384-13393.
232. McParlane, J., et al., *Dual pH-triggered physical gels prepared from mixed dispersions of oppositely charged pH-responsive microgels*. Soft Matter, 2012. **8**(23): p. 6239-6247.
233. McCann, J., et al., *Poly(vinylamine) microgel-dextran composite hydrogels: Characterisation; properties and pH-triggered degradation*. Journal of Colloid and Interface Science, 2015. **449**: p. 21-30.
234. Supasuteekul, C., et al., *A study of hydrogel composites containing pH-responsive doubly crosslinked microgels*. Soft Matter, 2012. **8**(27): p. 7234-7242.
235. Bird, R., et al., *Doubly crosslinked hydrogels prepared from pH-responsive vinyl-functionalised hollow particle dispersions*. Soft Matter, 2012. **8**(11): p. 3062-3066.
236. Tasdelen, M.A., *Diels-Alder "click" reactions: recent applications in polymer and material science*. Polymer Chemistry, 2011. **2**(10): p. 2133-2145.
237. Golas, P.L. and K. Matyjaszewski, *Marrying click chemistry with polymerization: expanding the scope of polymeric materials*. Chemical Society Reviews, 2010. **39**(4): p. 1338-1354.
238. Espeel, P. and F.E. Du Prez, *"Click"-Inspired Chemistry in Macromolecular Science: Matching Recent Progress and User Expectations*. Macromolecules, 2015. **48**(1): p. 2-14.
239. Barner-Kowollik, C., et al., *"Clicking" Polymers or Just Efficient Linking: What Is the Difference?* Angewandte Chemie International Edition, 2011. **50**(1): p. 60-62.
240. Mueller, J.O., et al., *Visible-Light-Induced Click Chemistry*. Angewandte Chemie International Edition, 2015. **54**(35): p. 10284-10288.
241. Binder, W.H. and R. Sachsenhofer, *'Click' chemistry in polymer and material science: An update*. Macromolecular Rapid Communications, 2008. **29**(12-13): p. 952-981.

Chapter III: Synthesis of doubly crosslinked microgels by RAFT Hetero Diels-Alder click conjugation

III.1 Synthesis of click functionalized microgels by free radical suspension polymerization

III.1.1. Introduction to microgel synthesis and their surface modification

Microgels are crosslinked polymer particles able to absorb a large amount of water owing to the hydrophilic nature of polymer chains. Their high water content makes them biocompatible, and contributes to desirable mechanical properties. The most important feature that contributes to a growing interest in the design of hydrogel beads is their applicability in drug delivery systems to encapsulate, protect and release any bioactive agents. Their tunable size from nanometers to micrometers and their large surface area for multivalent biocunjugation allows to reach further challenges in drug targeting delivery but also in many other fields as in textile, biotechnology applications, automotive, food and many others (see Chapter II).

To be effective, microgels must be designed according to targeted applications in order to fulfill the specifications required. The methods employed to produce microgels are numerous. Each method presents particular advantages and is chosen depending on the desired properties or application. The chosen synthetic method is of particular importance when one considers post synthesis modification or bioconjugation of the resulting material, since the location, density and nature of chemoligation sites on the microgel will dictate the function and utility of the grafted conjugate. Generally, microgels are prepared by (surfactant-free) emulsion polymerization, precipitation polymerization or inverse emulsion polymerization.

In emulsion polymerization, monomers and initiator are dissolved in different phases. Oppositely, in suspension polymerizations, monomers and initiator are in the same

phase of a two-phase system. Precipitation polymerizations begin as an initially homogeneous system. During polymerization, phase separation occurs as the formed polymers are insoluble in the polymerization medium and therefore, produces discrete particles. Although the precipitation polymerization technique offers a versatile synthetic route to multifunctional microgels, it suffers from few drawbacks with respect to the high temperature used and the requirements for polymer phase separation during synthesis. These problems can be overcome by using inverse emulsion polymerization, where an aqueous solution of all the monomers is added to an appropriate amount of oil and surfactant and is agitated to form a thermodynamically stable emulsion.

Suspension polymerizations tend to produce larger particles with larger size dispersion compared to emulsion or dispersion polymerizations.^[1] All these techniques have been applied for the synthesis of a large variety of microgels. One of the most studied microgel is PNIPAM based microgels owing to their properties, structure and applications. Schmidt *et al.* reported thermoresponsive poly(*N*-isopropylacrylamide) (PNIPAM) microgel films allowing controlled detachment of adsorbed cells via temperature stimuli.^[2] Tsai *et al.* prepared temperature sensitive PNIPAM microgel particles with metal affinity for selective binding of peptides.^[3] Many other examples can be found in this review.^[4]

Even though PNIPAM is the most used polymer in microgel synthesis, several other polymers are reported in literature specially, MMA and AA. Among them, Lally *et al.* reported the pH dependent swelling of poly(MMA/MAA/EGDMA) microgel dispersion. Such dispersion presents a fluid-to-gel phase by varying the pH. Preliminary results indicate that gelled poly(MMA/MAA/EGDMA) microgel dispersion is biocompatible with human intervertebral discs cells.^[5] Das *et al.* reported a dextrin and poly(methyl methacrylate) (PMMA) based biodegradable and biocompatible microgel for dual drugs carrier. Cytotoxicity assays revealed that the crosslinked microgel is non-toxic. Moreover, the microgels could efficiently encapsulate both ciprofloxacin and ornidazole.^[6] Sahiner *et al.* prepared poly(vinyl carbazole) (P(VC)) particles via surfactant free emulsion polymerization using 9-vinylcarbazole (VC) as functional monomer. This monomer was later used for chemical modification by using modifying agents such as 4-bromonitrile and 1,6-bromohexane.^[7]

Tehrani *et al.* reported the preparation of thermoresponsive PEGMA microgels by precipitation copolymerization and the covalent attachment of horseradish peroxidase

to these microgels. Enzymes immobilized on the PEGMA microgel lost their activity 3.4 times slower than free enzymes against thermal denaturation in the first 5 h of annealing at 50°C.^[8] Zhang *et al.* prepared a novel negatively thermo-sensitive and biodegradable microgel by combination of macromer synthesis and inverse suspension polymerization. Model proteins (hemoglobin, bovine serum albumin and insulin) were encapsulated at low temperature after the preparation of microgels avoiding the use of organic solvent.^[9] Wang *et al.* reported the use of self-assembled microgels to inhibit the bacterial colonization of synthetic surfaces by modulating surface cell adhesiveness at length scales comparable to bacterial dimensions and by locally storing/releasing an antimicrobial compound. Depot of these microgels onto biomedical devices could reduce the rate of biomaterial-associated infection.^[10] Bromberg *et al.* evaluated novel microgels composed of crosslinked copolymers of poly(acrylic acid) and Pluronics as possible permeation enhancers for doxorubicin transport. Pluronic-PAA microgels showed the enhancement of the overall cell absorption of doxorubicin and might be used as formulations for oral delivery owing to their non-irritating nature and mucoadhesive properties.^[11]

Standard techniques for coupling small molecules, peptides, oligonucleotides, and proteins are generally applicable to microgels.^[12] Microgels offer some interesting advantages compared to others particles: first, microgels can be centrifuged and easily redispersed, which facilitates cleaning and their purification; second, subtle changes can be followed by dynamic light scattering, which is sensitive to swelling, and microelectrophoresis, which is sensitive to surface charge; third, microgels are generally more colloidally stable than latexes and other nanosized support particles. The usual starting points for microgel derivatization are carboxyl or amine groups. Biotin,^[13] streptavidin,^[14] proteins,^[15] and oligonucleotides^[16] have been conjugated to microgels. Carbodiimide-based coupling chemistries seem to be the most popular, even if new techniques using click chemistry appear recently.^[17-19]

III.1.2. Synthesis of microgels by free radical suspension polymerization

III.1.2.1. HLB system theory: a time saving empiric law for optimized conditions

Stabilization of an emulsion can be very complicated and time consuming due to the large choice of available emulsifying agents produced by different companies. The choice between the several chemical types of surfactant (anionic, cationic, nonionic or amphoteric) depends largely on the application as the solubility is a critical parameter. Generally, anionic, cationic and amphoteric emulsifiers present high or medium solubility in water and poor solubility in oils. But the case of nonionic emulsifiers is completely different as they can be water-soluble, oil-soluble or in between. Nonionic emulsifiers solubility can be predicted by the HLB (hydrophilic-lipophilic balance), *i.e.* the balance of the size and strength of the hydrophilic (water-loving or polar) and the lipophilic (oil-loving or non-polar) groups of the emulsifier. All emulsifiers consist of a molecule that combines both hydrophilic and lipophilic groups. An emulsifier that is lipophilic in character is assigned a low HLB number (below 9.0), and one that is hydrophilic is assigned a high HLB number (above 11.0). Those in the range of 9-11 are intermediate. When two or more emulsifiers are blended, the resulting HLB of the blend can be easily calculated.^[45] For example, suppose you want to determine the HLB value of a blend comprising 70% of TWEEN 80 (HLB = 15) and 30% of SPAN 80 (HLB = 4.3).

The calculation would be: HLB of the blend: $0.7 \times 15 + 0.3 \times 4.3 = 11.8$

The HLB of an emulsifier is related to its solubility. Therefore, an emulsifier having a low HLB will tend to be oil-soluble, and one having a high HLB will tend to be water-soluble, although two emulsifiers may have the same HLB and yet exhibit quite different solubility characteristics. Concretely, a “water-soluble” is used as an emulsifier when the final product must exhibit *aqueous characteristics*, *i.e.* to be dilute readily with water. Oppositely, a water in oil (W/O) emulsion, stabilize water solution droplets into an oil. Table III.1 shows some interesting general correlations.

Table III.1: Relation HLB and emulsification properties.^[45]

HLB range	Use
4-6	W/O emulsifiers
7-9	Wetting agents
8-18	O/W emulsifiers
13-15	Detergents
10-18	Solubilizers

By knowing the “Required HLB” of the components for the emulsion narrows down the choice of emulsifiers considerably, but the right chemical type for the emulsifiers is as important as the HLB value for an ideal emulsion. As example, optimized conditions for an emulsion requiring an HLB of 12 achieved by a blend of SPAN 60 and TWEEN 60 (stearates) can provide good stability for the emulsion but other families of emulsifiers (laureate, palmitates or oleates) might give better results. Perhaps some chemical family blends outside the popular SPAN-TWEEN class might be even more suitable. HLB ratio is merely an indication of the percentage weight of the hydrophilic portion of the nonionic emulsifier. Therefore, if a nonionic emulsifier was 100% hydrophilic, it will be expected that the HLB value is 100. In the ICI system (system developed by ICI Americas Inc, a chemical company localized in US), such an emulsifier would be assigned with an HLB value of 20 for practical reasons (0/20).

HLB values for most nonionic emulsifiers can be calculated from either their theoretical composition but this method may lead to considerable errors due to approximation in the content of the emulsifiers or by analytical data. Data obtained by actually analyzing the emulsifier are usually a better basis for determining HLB values. For example, HLB values of most polyol fatty acid esters can be calculated with the formula:

$$HLB = 20 \left(1 - \frac{S}{A}\right)$$

Where S = saponification number of the ester (1) and A = acid number of the recovered acid (2).

While the formula given above is satisfactory for many nonionic emulsifiers, certain other nonionic emulsifiers, mainly containing propylene oxide, butylene oxide, nitrogen and sulfur, exhibit behavior unrelated to their composition. Moreover, ionic emulsifiers do not follow this “weight percentage” HLB basis, because, even though the hydrophilic portion of such emulsifiers is low in molecular weight, the fact that it ionizes lends extra

emphasis to that portion, and therefore makes the product more hydrophilic. Therefore, the HLB values of these special nonionics, and of all ionics, must be estimated by experimental methods. The experimental method to determine HLB, while not precise, consists of blending the unknown emulsifier in various ratios with an emulsifier of known HLB, and using the blend to emulsify an oil of known "Required HLB". The blend, which performs best, is assumed to have an HLB value approximately equal to the "Required HLB" of the oil. Therefore, HLB value of the unknown emulsifier can be calculated. In practice, a large number of experimental emulsions have to be made, from which an average HLB value for the unknown emulsifier is finally calculated.

III.1.2.2. Taking advantage of theory to synthesize our microgels by free radical suspension polymerization

In the following section, the synthetic steps and analytical results will be discussed in detail, covering the entire sequence from the microgel preparation to the surface analysis of the final functionalized microgel. In this thesis, we aim at synthesizing PEG-based microgels composed of poly(ethylene glycol)methyl ether methacrylate (PEGMA, $M_n = 500 \text{ g mol}^{-1}$), glycidyl methacrylate (GMA) as monomers and ethylene glycol dimethacrylate (EGDMA) as crosslinker. Their chemical structures are depicted in Figure III.1.

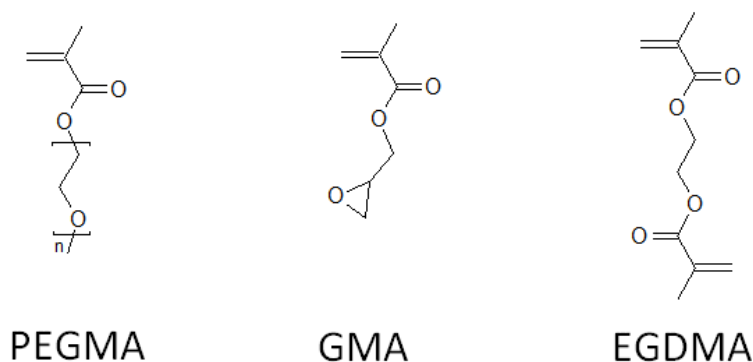


Figure III.1: Chemical structure of the chemical components.

Glycidyl functions will then be ring-opened to install cyclopentadiene (Cp) moieties as reactive click coupling functions. For this purpose, conventional water in oil (W/O) suspension free-radical copolymerization will be employed as synthetic method for the microgels preparation.

Firstly, an emulsion stability study was performed to determine stable conditions for the microgels synthesis. As discussed in the above paragraph, a water in oil suspension polymerization requires an HLB ratio between 4 and 7. A screening of the HLB value in these regions has been investigated by combining different amounts of two emulsifiers: SPAN 80 and TWEEN 80. As depicted in Figure III.2, an HLB ratio around 5.9, obtained by a blend of 85 % of SPAN 80 and 15% of TWEEN 80, led to a stable emulsion as the coalescence effect is limited (see left photograph in Figure III.2). An unappropriated blend of SPAN 80 and Tween 80 resulted in an unstable emulsion where aggregation and then formation of bigger droplets occur (see right photograph in Figure III.2). Among that, nature of the emulsifiers can influence the stability of the emulsion over time. Therefore, for the sake of comparison, the stability of an emulsion presenting the same HLB ratio of 5.9 but prepared using another family of surfactant was investigated. A blend of 55 % of SPAN 85 and 45% of TWEEN 85 (laureate family) with the same HLB ratio of 5.9 was realized. As depicted in Figure III.3, the nature of the surfactants does not impact the stability of the suspension. Since no discrimination can be made between the two emulsion systems, both conditions were used first for the synthesis of GMA-based microgels.

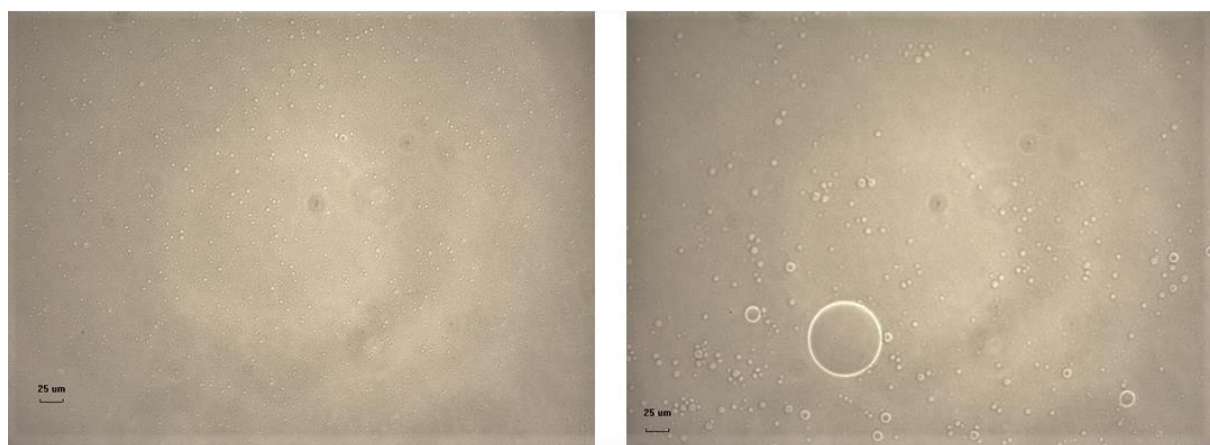


Figure III.2: High magnification of a stable emulsion (left) and an unstable emulsion (right) of monomer solutions in cyclohexane using a blend respectively of 85 % SPAN 80/15 % TWEEN 80 and 80% SPAN 80/ 20 %TWEEN 80.



Figure III.3: High magnification image of an emulsion of monomer solutions in cyclohexane using a blend respectively of 55 % SPAN 85/45 % TWEEN 85.

A glycidyl moiety represents an advantageous function for post-modification reactions as the epoxide group can react in many ways. In this section, series of glycidyl-based microgels were prepared by water-in-oil (W/O) suspension free-radical copolymerization of glycidyl methacrylate (GMA), poly(ethylene glycol) methyl ether methacrylate (PEGMA) and ethylene glycol dimethacrylate (EGDMA). The free-radical polymerization was conducted into water droplets dispersed in cyclohexane under strong stirring with an initial monomer concentration of 40 %. The polymerization was initiated at 70°C using 4,4'-azobis(4-cyanovaleric acid) as free-radical precursor. Small-size and non-aggregated microparticles were achieved by use of a mixture of SPAN 80/TWEEN 80 (5.6/1 molar ratio) surfactants that guarantee stable droplets formation and afterwards, non-aggregated microgels with narrow size distribution (Figure III.4, left). For sake of comparison, the experimental conditions using a mixture of SPAN 85/TWEEN 85 were also investigated as surfactant nature (e.g. oleate, trioleate,...) can influence emulsion stability. However, as depicted in Figure III.4 (right), a bimodal population was obtained. As aggregation might occur after the washing and purification steps, the sample was submitted to ultrasonic bath for several minutes. Size and size distribution were measured again by particle sizer. As no modification in particle size and size distribution were noticed, we postulate that aggregation occurs already during the polymerization process, indicating therefore that our suspension is not stable enough during the polymerization when a blend of SPAN 85/TWEEN 85 is used. Consequently, the blend SPAN 80/TWEEN 80 has been chosen as the emulsifier blend of choice for the preparation of Glycidyl-based microgels in this thesis.

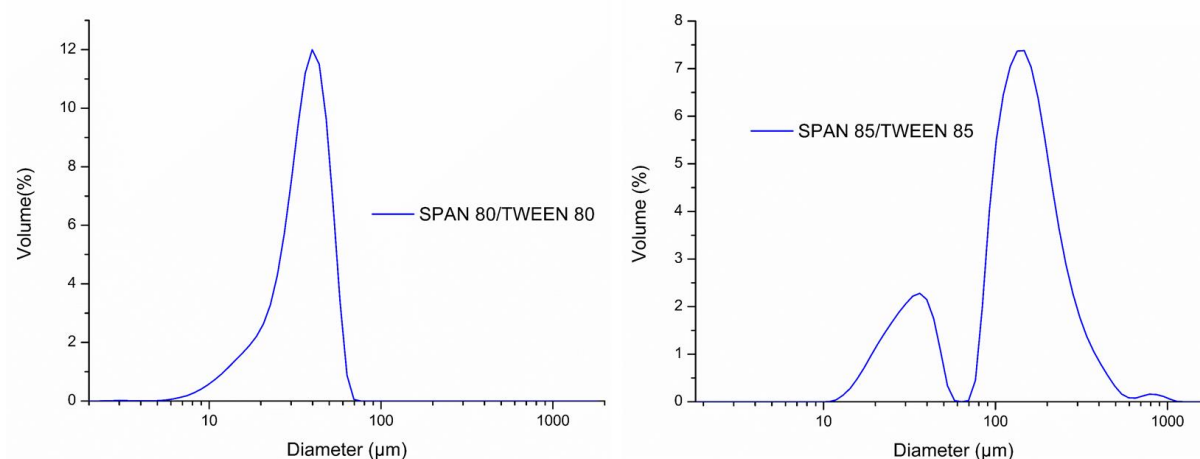


Figure III.4: particle size measurements after 6h reaction using a blend of SPAN 80/TWEEN 80 (left) and (right) a blend of SPAN 85/TWEEN 85 (left).

The initial co-monomer molar ratio $[GMA]_0/[PEGMA]_0/[EGDMA]_0$ was fixed to 3/7/1 and to 3/7/1.5, which led to a molar composition in glycidyl function of 28.1 % and 26.8%, respectively. In the first series of experiments, impact of the stirring rate on particle size was studied by applying stirring rates of 1200, 800, 400 and 200 rpm. Similarly, impact of the crosslinker density in microgels was also varied. The polymerizations were stopped after 6h of reaction and the resulting microgels were purified by extensive washing in ethanol to get rid of any soluble fractions and surfactants. Size and size distribution were investigated by particle size measurements. The morphology of PEG microgels was also characterized by optical microscopy (Figure III.5). Table III.2 shows the evolution of the microgel diameter as a function of the stirring rate and the crosslinker density.

First of all, optical microscopy confirmed the formation of well-defined spherical microgels as well as the stability of the starting droplets as depicted in Figure III.5 (left). As expected, increasing stirring rate led to smaller microgels, ranging from 90 μm (200 rpm) to 12 μm (1200 rpm). In addition, a small increase in the crosslinker molar composition led to a significant decrease of the microgel size. More importantly, size and size distribution measured by both techniques were in good agreement.

TABLE III.2: Evolution of microgel size depending on stirring rate and crosslinker density. All distributions listed in the table were monomodal.

Samples	$[M]_0/[I]_0/[C]_0^a$	Stirring rate (rpm)	Size (μm) ^b
A	1/0.05/0.1	1200	12 \pm 2.5
B	1/0.05/0.1	800	22 \pm 5.2
C	1/0.05/0.15	800	17 \pm 5.7
D	1/0.05/0.1	400	40 \pm 12.6
E	1/0.05/0.1	200	90 \pm 40
F	1/0.05/0.15	200	65 \pm 25

A) $[M]_0/[I]_0/[C]_0$: initial monomer/initiator/crosslinker molar ratio

B) Size and size distribution as measured by particle sizer in distilled water at r. t.

III.1.3. Cyclopentadiene functionalization of microgels

The highly reactive cyclopentadiene (Cp) was chosen as the diene of choice to decorate the microgels since Cp is one of the most reactive dienes for hetero Diels Alder (HDA) reactions.^[21] The Cp-functionalized microgels were synthesized according to a protocol inspired by the work of Barner-Kowollik's team.^[22] In their work, porous glycidyl-based microspheres were produced by suspension polymerization followed by post-modification reaction with sodium cyclopentadienide. In this context, the glycidyl moiety represents an advantageous function for post-modification reactions as the epoxide group can react in many ways.^[20]

In our derivatization synthesis, reactive cyclopentadienyl groups were installed on microgels through nucleophilic addition onto the ring-strained epoxide. Practically, the GMA based-microgels were functionalized in a single step by suspending the microgels in anhydrous THF and subsequently adding a solution of sodium cyclopentadienide (Figure III.7). The cyclopentadienide anion reacted rapidly, following a nucleophilic addition onto the epoxide ring. After only 1h at 0°C and 3h at r.t., the reaction was quenched with a saturated solution of ammonium chloride and the amber-like particles were purified by filtration, followed by extensive washing with saturated aqueous solution of ammonium chloride, acetone, water, acidic water (3% HCl), ethanol/water (1/1), tetrahydrofuran and ethanol to isolate the Cp-functionalized

microgels. Interestingly, no change in size and size distribution was noticed after Cp derivatization, as depicted in Figures III.5 and III.6.

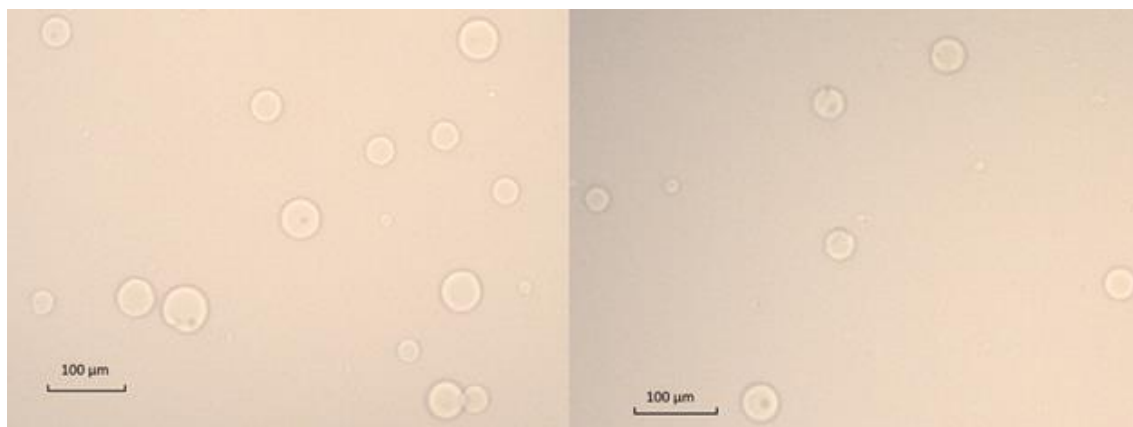


FIGURE III.5: Images of the purified glycidyl-based microgels (Entry C, Table 1) obtained by optical microscopy in deionized water at r.t. before (left) and after functionalization by NaCp (right).

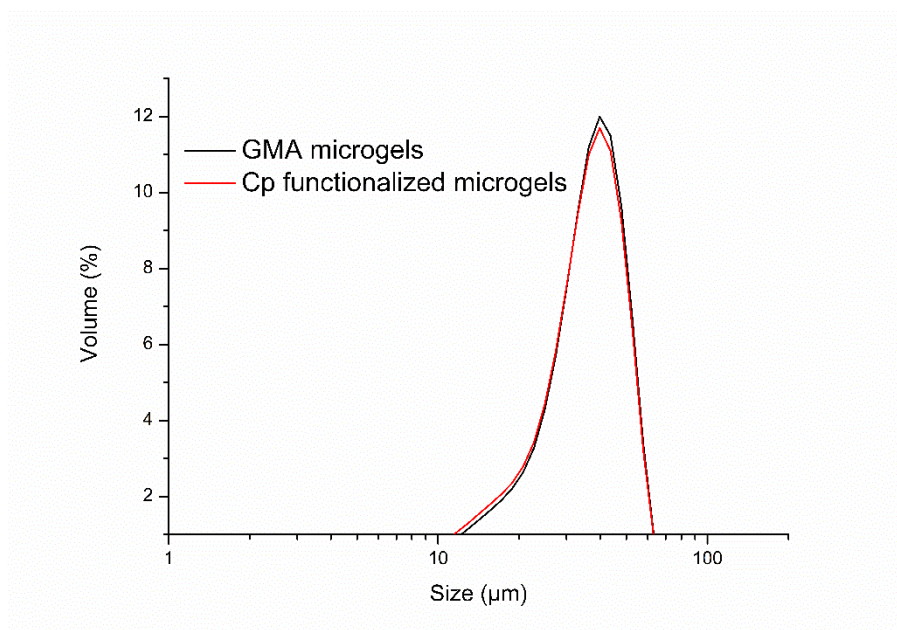


FIGURE III.6: Particle size distribution as measured by particle sizer before (black) and after (red) derivatization by sodium cyclopentadiene (microgels from Entry C, Table III.3).

TABLE III.3: Evolution of the microgels size after functionalization by sodium cyclopentadienide.

Samples	Size before derivatization (μm) ^a	Size after Cp derivatization (μm) ^a
A	12 \pm 2.5	12 \pm 2.5
B	22 \pm 5.2	23 \pm 5.2
C	40 \pm 12.6	41 \pm 12.6

a) Size and size distribution as measured by particle sizer in water at r. t.

Beyond the change of coloration of the microparticles batch after treatment with NaCp, the success of the derivatization can be attested indirectly by fluorescence microscopy. For this purpose, Cp-functionalized microgels were reacted with the fluorescent marker *N*-(1-pyrene) maleimide (Pyr-Mal) via a Diels–Alder reaction at 40°C for 3 hours (Figure III.7). As depicted in Figure III.8, microgels showed fluorescent activity upon irradiation with UV light (366 nm), demonstrating the grafting of pyrene onto the surface of the particles. Moreover, surface functionalization was attested by fluorescent microscopy as shown in Figures III.8 b and c. Both analyses demonstrated unambiguously that microgels were well derivatized with Cp and that Cp surface distribution is homogenous on a micrometer scale. As a control, glycidyl-based microgels submitted to the same washing steps as their Cp-functionalized counterparts did not show any fluorescence.

Controlling the kinetics of DX-gel formation is an important issue that needs to be addressed depending on the targeted application. It can be anticipated that the density of reactive dienes onto the surface will strongly influence the rate of gelation. Herein, tuning Cp density onto the surface is an interesting strategy to set up the kinetics window of gelation. For this purpose, GMA-based microgels were subjected to a post-modification reaction with various quantities of NaCp solution. Cp density modulation and distribution on the microgel can be followed qualitatively by indirect measurements of fluorescence microscopy after derivatization of Cp with *N*-(1-pyrene) maleimide. Indeed, with this DA click reaction being quantitative and fast, it can be assumed that the fluorescence intensity of pyrene can be directly correlated to Cp quantity. For this study, a microgel sample was derivatized with a quantity from 0.08 to 0.4 mmol of NaCp and finally by pyrene-maleimide.

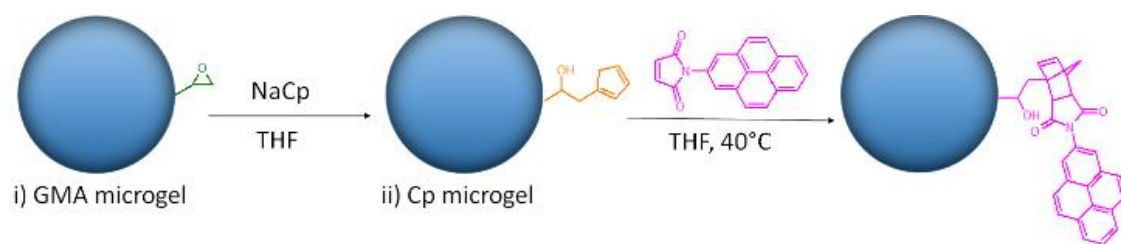


FIGURE III.7: Schematic overview of the functionalization and grafting reactions on microgels. (i) GMA functionalized microgels are functionalized with Cp by the reaction with sodium cyclopentadienide solution in anhydrous THF. (ii) The Cp-functionalized microgels undergo Diels–Alder reactions with the fluorescence marker N-(1-pyrene) maleimide.

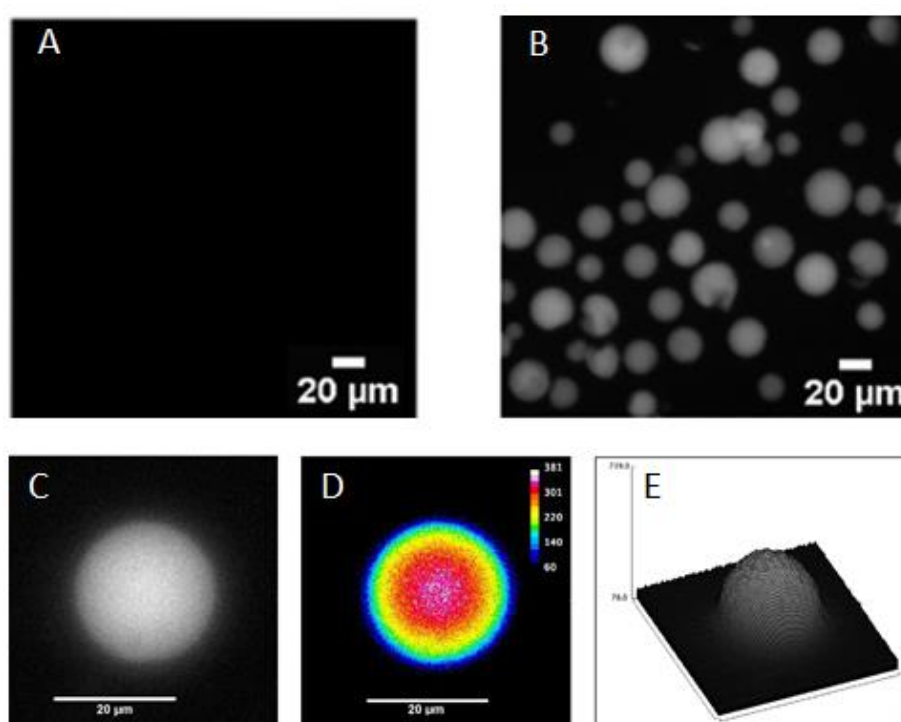


FIGURE III.8: Fluorescence analysis of A) Cp microgels (Negative control), B) Fluorescent image of microgels after N-(pyrene) maleimide functionalization, C) High magnification image of a microgel after N-(pyrene) maleimide functionalization, D) Color-coded fluorescent image with N-(1-pyrene) maleimide and E) Surface plot representation of the fluorescence on a microgel surface (reconstructed from D).

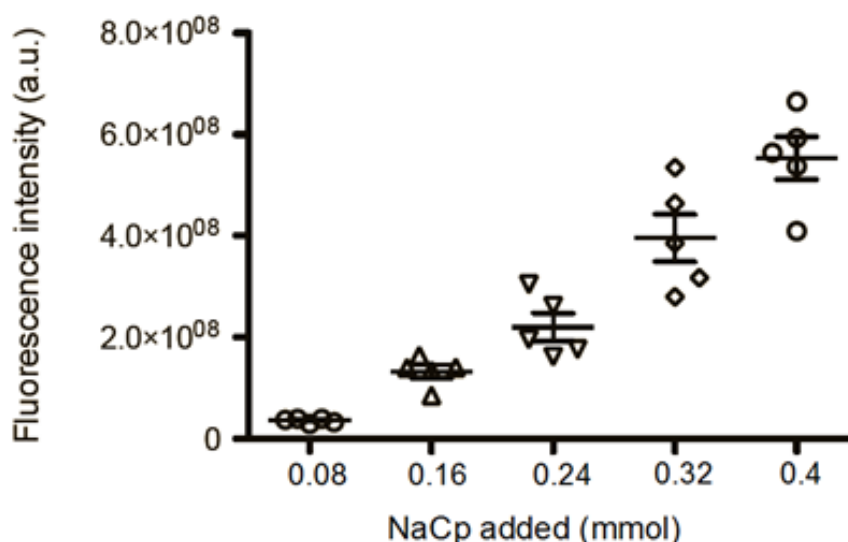


FIGURE III.9: Linear increase of the fluorescence intensity of the Pyr-based microgels in direct correlation with the quantity of the NaCp derivatizing agent.

As depicted in Figure III.9, a linear increase of the fluorescence of the beads as a function of mmol of NaCp derivatizing agent is reported, with a reasonable regression coefficient. This study confirms that we can control the density functionalization of the microgels with a good level of reproducibility, which paves the way towards the on-demand gelation kinetics of DX-gel formation.

As fast inter-crosslinking and a high degree of gelation are prerequisites to some bio-related applications, quantitative estimation of the amount of Cp available on the surface is of utmost importance in order to be able to determine the quantity of crosslinker that should be added to the medium. Quantification of Cp functions was further approached by titration of Cp moieties using an UV sensitive reactant that could react instantaneously and quantitatively with the diene. For that study we took advantage of the recently developed triazolinedione TAD click chemistry (color switch), which fits perfectly with the titration prerequisite. The reaction was performed on two sets of particles, the size of which is centered around 12 ± 2.5 and 41 ± 12.6 μm (Table 1, entries A and C) with available 4-phenyl-1,2,4-triazoline-3,5-dione (PTAD) (Figure III.10, left) as a simple UV-sensitive titration molecule at room temperature in butyl acetate. An excess of PTAD arising after saturation of the Cp-based microgels was measured by UV and quantified by means of a calibration curve ($A = 147.68$, $\lambda = 540$

nm, Figure III.11). Therefore, the Cp content was indirectly determined via quantification of the PTAD amount remaining in solution.

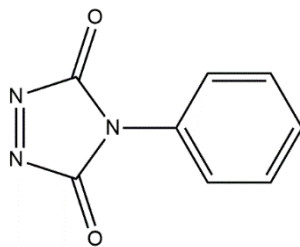


FIGURE III.10: Structure of 4-phenyl-1,2,4-triazoline-3,5-dione (PTAD).

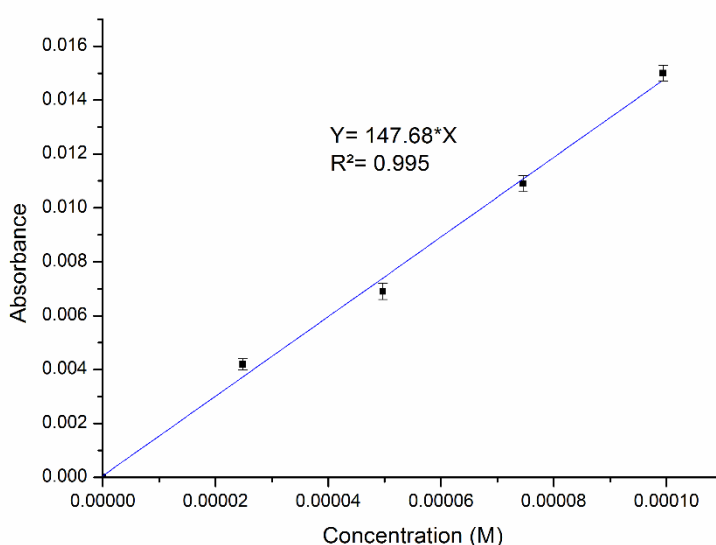


Figure III.11: Calibration curve for the UV titration of Cp functionalized microgels.

As expected for an equal quantity of starting microgels, smaller particles require more PTAD solution to saturate the microgel surfaces as a result of their higher specific surface area. Therefore, it was calculated that 137 nmol *versus* 66 nmol of Cp were required to saturate respectively 80 mg of 12 μm and 41 μm size particles, corresponding respectively to surfaces of $40 \cdot 10^9 \mu\text{m}^2$ and $11.7 \cdot 10^9 \mu\text{m}^2$).

III.1.4. Cytocompatibility of the Cp functionalized microgels

To validate our concept of using PEG based microgels, cytocompatibility tests of the functionalized microgels were performed in collaboration with the University of Louvain-La-Neuve. For that purpose, MTT assay, which is a convenient and rapid method for living cells counting, was realized in the presence of Cp based microgels.

Basically, a tetrazolium salt (3-(4,5-dimethylthiazol-2-yl)-2,5-diphenyltetrazolium bromide, MTT) can be reduced by succinate dehydrogenase of active living cells into a purple formazan crystal in metabolically active cells as illustrated in Figure III.12.

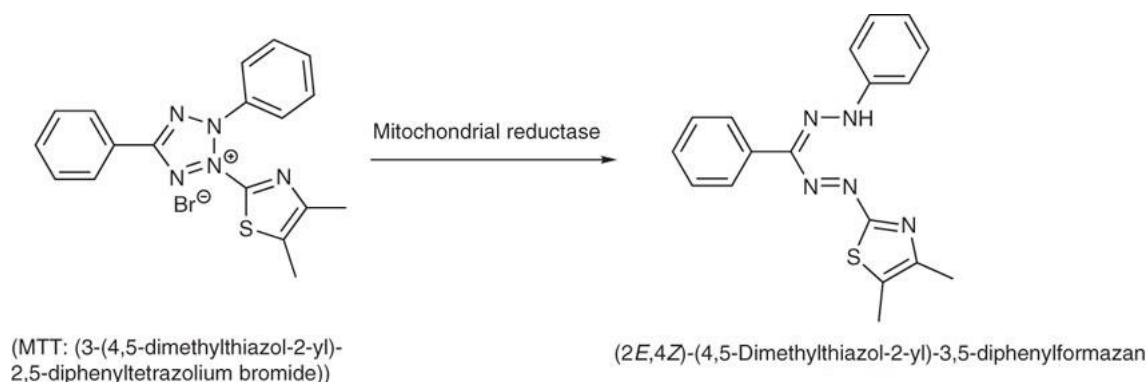


Figure III.12: Illustration of the reaction involved in MTT assay.

After incubation of cells with MTT, the insoluble formazan can be dissolved with DMSO or acidified ethanol, to produce a concentration dependent colorimetric signal measurable at a wavelength of 570 nm, proportional to the cell number and activity. Various concentrations of microgels suspension were prepared and tested using MTT assay as showed in Figure III.13. A triton solution was used as a positive control and a solution containing cells without any other solution added is the reference. Good cell viability was confirmed over the range of concentration investigated (from 0.5 to 25 mg/ml), even at the highest concentration (25 mg/ml) where more than 60 % of cells were still alive 48h later despite a small decrease of cell viability over concentration. This good result was an important information concerning the potential use of Cp-functionalized microgel as a building block for the construction of doubly crosslinked gels networks.

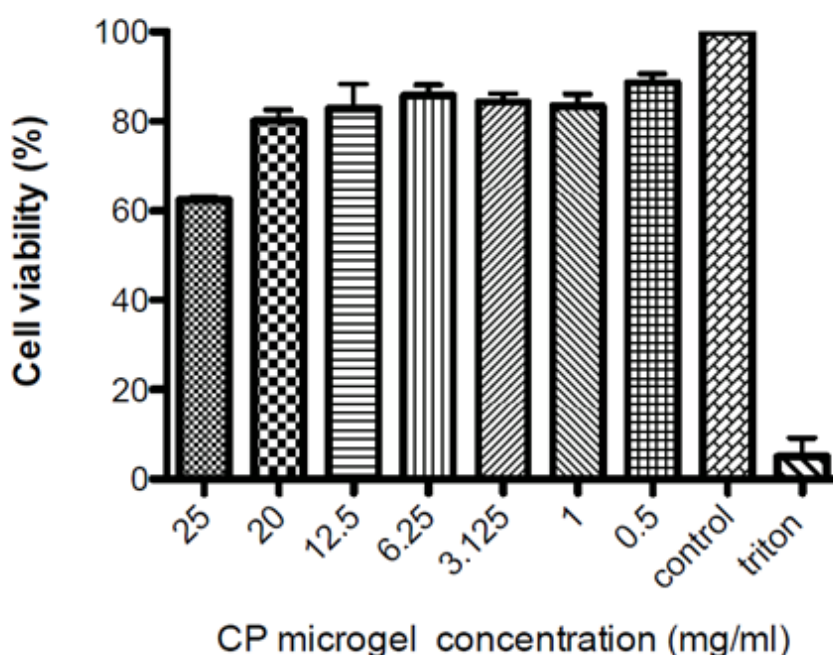


Figure III.13: Cell viability evolution with microgel concentration after 48h.

III.2. Doubly crosslinked microgels by RAFT-HDA click chemistry

III.2.1. Introduction on DX-gel

It was demonstrated above that the ring opening of epoxide reaction can be used to functionalize microgel particles with a high degree of efficiency and without compromising colloidal stability to introduce cyclopentadiene. Quite recently, two emerging classes of polymer gels with impressive mechanical properties have been referred in literature. These two classes are double network (DN) hydrogels and double crosslinked (DX) gels. DN gels consist of two interpenetrating polymer components. The first one is a densely crosslinked polyelectrolyte polymer within a ductile and loosely crosslinked neutral polymer acting as the second component.^[23, 24] On the other hand, DX-gels consist of internally crosslinked particles that are involved in a second level of crosslinking by covalent bonds established between the swollen particles. This kind of hydrogels possess two crosslinking levels: the first one being the intra-particle crosslinking and the second one being the inter-particles crosslinking. Consequently,

these new gels have considerably improved the mechanical properties of traditional polymer hydrogel networks and offer improvements in the biomedical applications of artificial load bearing tissue and muscle tissue engineering.^[25-28] Furthermore, there are several routes towards preparing mechanically strong gel networks. While DN gels have demonstrated their potential to improve mechanical properties of conventional hydrogels since the pioneering works of Gong *et al.* ^[24], the scope of this thesis will focus on DX networks. Indeed, DX-gels present many advantages over classical polymer networks obtained through chemical or physical crosslinking. Particularly the ability to fine tune the final mechanical properties is a great interest owing to the hierarchical level of reticulation involving a primary crosslinking in the microbeads and an intercrosslinking between the beads. This freedom of action in tuning mechanical properties is particularly interesting in the field of injectable hydrogels for tissue engineering as the injected material must present equivalent mechanical properties than the hosting tissue. Moreover, DX-gels offer fine tuning of the mesh size, high specific surface area, controlled heterogeneity at the nanoscale as well as moldability.^[29, 30] For example, Saunders' group has been successful in preparing double crosslinked microgel systems based on particles of methacrylic acid copolymerised with either methyl methacrylate or ethyl acrylate as structural monomers and ethylene glycol dimethacrylate or butanediol diacrylate as crosslinkers.^[30-32] These particles were functionalized using glycidyl methacrylate (GMA) in order to introduce exposed methacrylate groups to the microgel periphery for future radical coupling. Lowering the pH induced particle swelling and triggered the formation of a physical gel as the peripheries of swollen microgel particles overlapped. This brought the pendant methacrylate groups of neighbouring particles into close proximity. Heating this physical gel in the presence of ammonium persulphate (APS) initiator caused the formation of a permanent, covalently bonded double crosslinked microgel.^[30-33] These gels have been developed towards the use in the specific biomedical applications of restoring structure and function of load bearing tissue, such as damaged or degenerated intervertebral discs.^[25] In a variation of this theme, colloidal graphene oxide was introduced to anionic poly[(ethyl acrylate)-co-(methacrylic acid)] and significantly improved the mechanical properties of the double crosslinked microgel network.^[34] A cationic DX-gel network based on the GMA functionalization of poly(vinyl amine) microgel particles has also been reported with interesting porosity features and may also have biomedical applications.^[35] Moreover,

a specific advantage of the “click like” epoxide ring opening approach towards any other functionalization of microgel particles and subsequent DX-gel formation is that the high efficiency of the reaction allows precise quantitative control over the extent of cyclopentadiene functionalization and therefore should enable enhanced tuneability of the mechanical properties of the DX-gels formed. Although click chemistry has been used previously as a tool for microgel and nanoparticle functionalization [36, 37], the cyclopentadiene functionalization of microgel particles using click chemistry has not been reported. The aim of the discussion below is to expand the range of DX-gels from radical coupling DX-gel formation to a new synthetic process using RAFT-HDA click chemistry where the mechanical properties of the gel can be controlled in an easy manner through a click chemistry reaction. In this chapter, various RAFT crosslinkers were synthesized and tested in various conditions.

III.2.2. Synthesis and characterization of RAFT crosslinkers

Three basic RAFT-agent structures available can undergo HDA reactions thanks to the electron-withdrawing nature of their Z-groups (Figure III.14).^[38, 39]

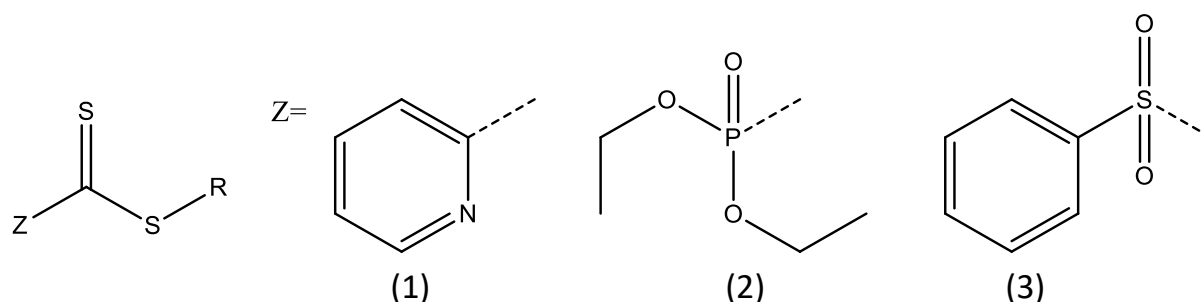


Figure III.14: Z-groups presently available for RAFT-agents that are able to undergo hetero Diels-Alder (HDA) reactions.

RAFT-agents carrying the sulfonyl moiety (3) as Z-group are labile and react readily, even with vinylic monomers in [2+4] cycloadditions,^[40] making them unsuitable for the controlled polymerization of some monomers. The phosphonate group (2) has been employed in the grafting of RAFT-polymers onto microspheres before, making it highly desirable as reactive group to crosslink particles together.^[39] The third class of RAFT agent with a pyridinyl based Z-group (1) is also a very reactive species but presents the only disadvantage of requiring an acid catalyst when employed (1) *e.g.*, trifluoroacetic acid, for facile and fast RAFT-HDA conversion. The acidic catalyst may

be easily removed by applying vacuum. The water solubility of such pyridinyl RAFT-agents could be adjusted by the variation of the R-group, yet establishing the synthesis of a well water soluble RAFT-agent with the Z-group required for RAFT-HDA would be very tedious. Grafting these functional groups to a water soluble polymer e.g. PEG would make the final moieties water soluble, which is highly desirable when targeting biomedical applications.

Multiple crosslinkers with various molecular weights were targeted in this chapter with different RAFT species able to react by HDA. The synthetic procedure to make all the following compounds can be found in the experimental section below. The chosen polymer was a 4 arm polyethylene glycol ($M_n = 5000 \text{ g.mol}^{-1}$, $D = 1.04$). PEG-based polymer was chosen as beyond its water solubility, it is also FDA approved. This polymer was derivatized using DCC/DMAP in one single step. First, 4-((pyridine-2 carbonothioylthio)methyl)benzoic acid (Pyr-RAFT) was grafted using a large excess of the RAFT species to promote the efficient synthesis of the Pyr-RAFT-functionalized 4-arms PEG linker. Full conversion was reached after 16 hours at r.t. by the appearance of the signal b at 4.4 ppm and the respect of ratio 1/1 between signal e and b as attested by ^1H -NMR and ^{13}C -NMR as depicted in Figure III.15 and III.16. Both analyses demonstrated also the good stability towards oxidation of the Pyr-RAFT functionalized 4-arms PEG under the synthetic conditions. Further analysis of the generated Pyr-RAFT functionalized 4-arms PEG polymer via MALDI ionization mass spectrometry allowed for an in-depth investigation of its end group functionality. The chains exhibit the Z-group from the RAFT-agent attesting its successful derivatization as it can be seen at signal $m/z = 6310.2$ corresponding to the macromolecule ionized with a sodium ion. However and surprisingly, a second population centered on 3000 m/z was noticed and ascribed to the corresponding Pyr-RAFT-functionalized PEG linker with 2 missing arms, as shown in Figure III.17. In fact, this second population come from the PEG (5000 g.mol^{-1}) commercial product. As the MALDI-ToF technique discriminates higher molecular weight, in depth analysis of the starting 4-arms PEG was carried out by SEC in THF to evidence whether a second population ascribed to the 2-arms compounds could be detected. Monomodal distribution characterized by a M_n around 7500 g/mol and a narrow dispersity of 1.06 was measured as showed in Figure III.18, attesting that only one distribution was present in our sample and in the commercial product in the conditions explored above. Table III.4 summarizes the macromolecular characteristics

of the obtained polymer. From this analysis and keeping in mind that lower M_n polymers are over expressed in MALDI-ToF analysis, we can approximate that the 2-arms based compound is not much present in the sample as its presence is not seen on SEC.

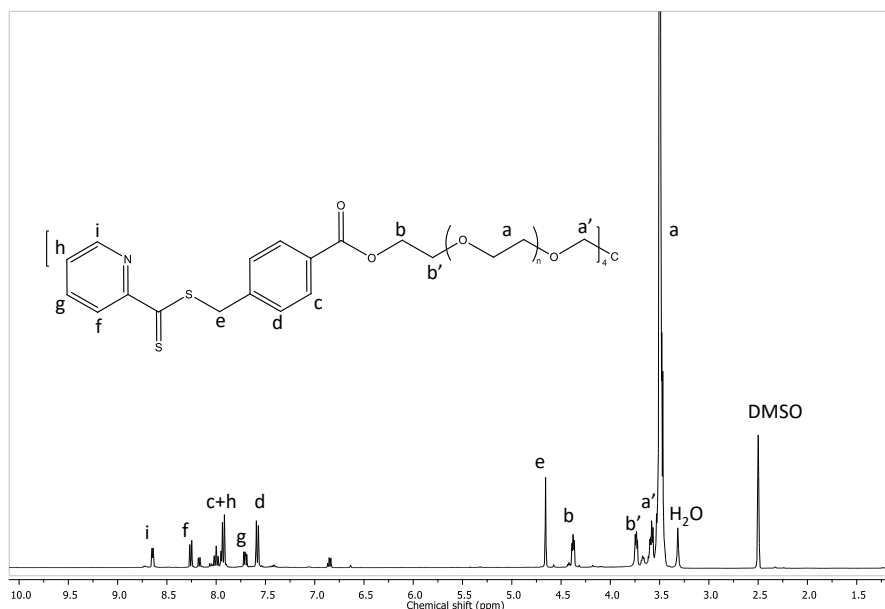


Figure III.15: ^1H -NMR of a Pyr-RAFT functionalized 4-arms PEG linker ($M_n = 7500 \text{ g.mol}^{-1}$) in DMSO-d_6 .

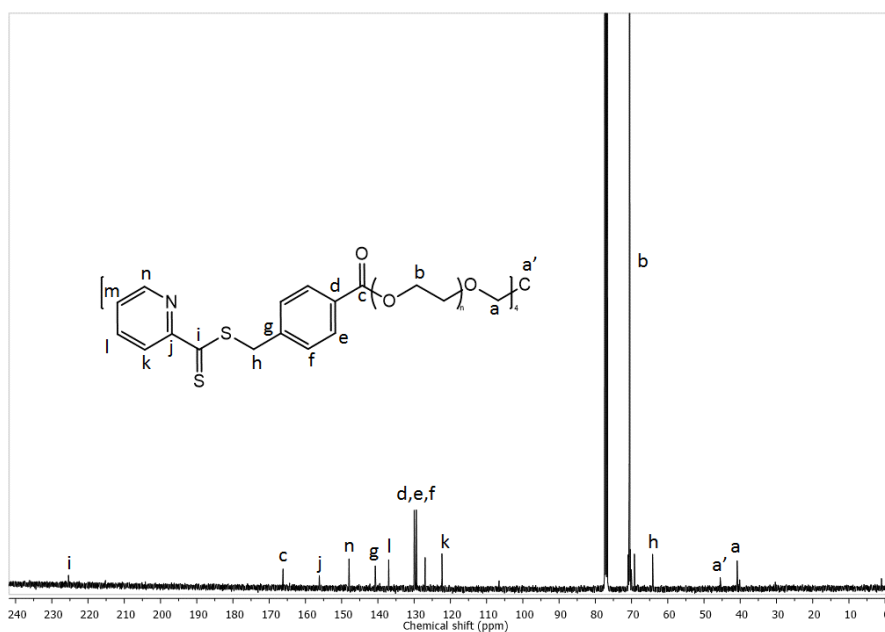


Figure III.16: ^{13}C -NMR of a Pyr-RAFT functionalized 4-arms PEG linker in DMSO-d_6 ($M_n = 7500 \text{ g.mol}^{-1}$).

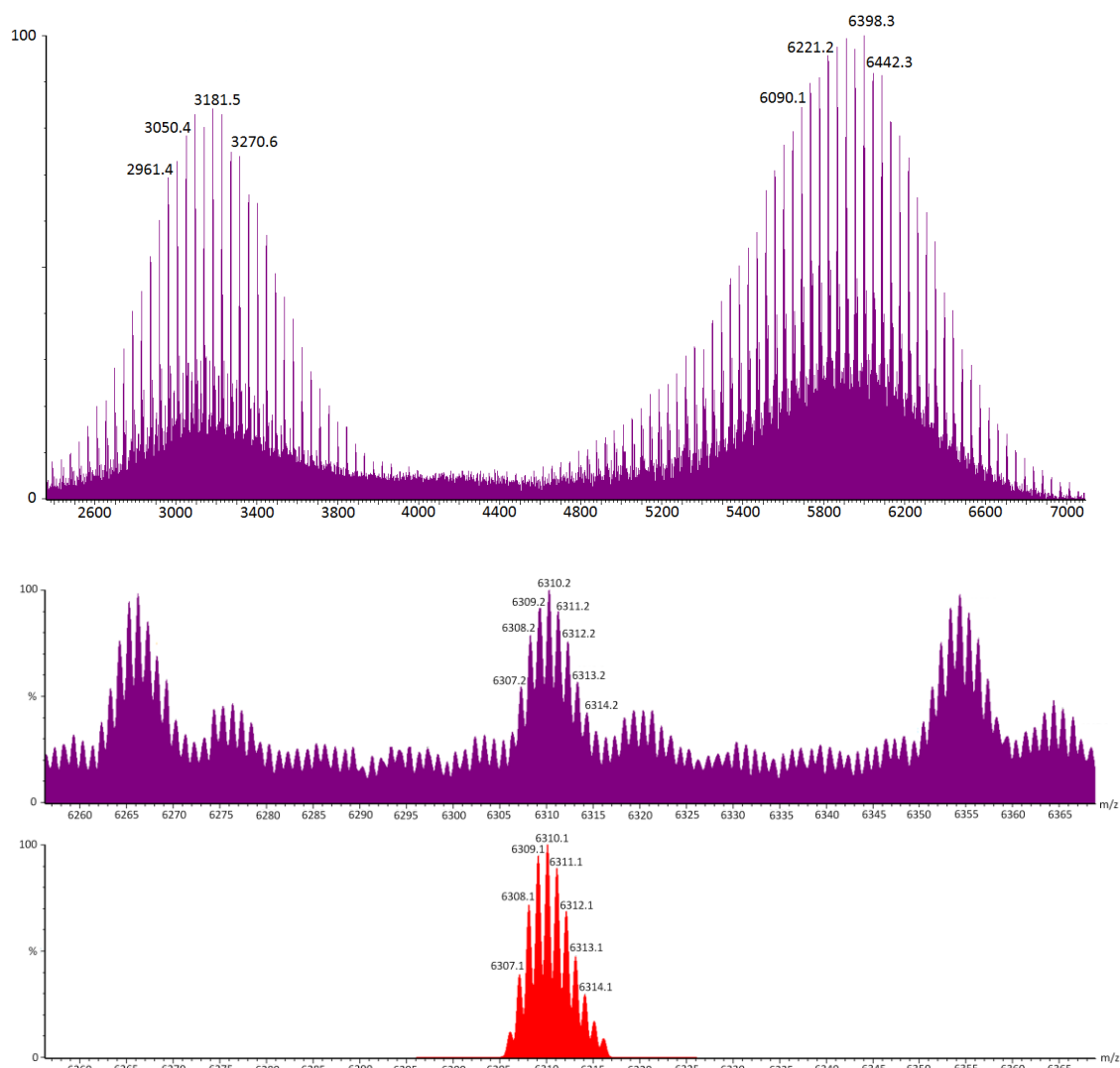


Figure III.17: MALDI Mass spectrum of the Pyr-RAFT functionalized 4-arms PEG (top) and the isotopic model of the corresponding product (below).

Table III.4: Macromolecular parameters obtained by SEC in THF at 35°C using PS as polymer standards of the 4-arm PEG and the Pyr-RAFT-functionalized 4-arms PEG obtained after esterification reaction with the 4-((Pyridine-2 carbonothioylthio)methyl)benzoic acid (Pyr-RAFT).

Samples	M_p	M_n	\bar{D}
	(g/mol)	(g/mol)	
4-arms PEG (Reference)	7200	6500	1.04
DEP-RAFT 4-arms PEG	8200	7500	1.06

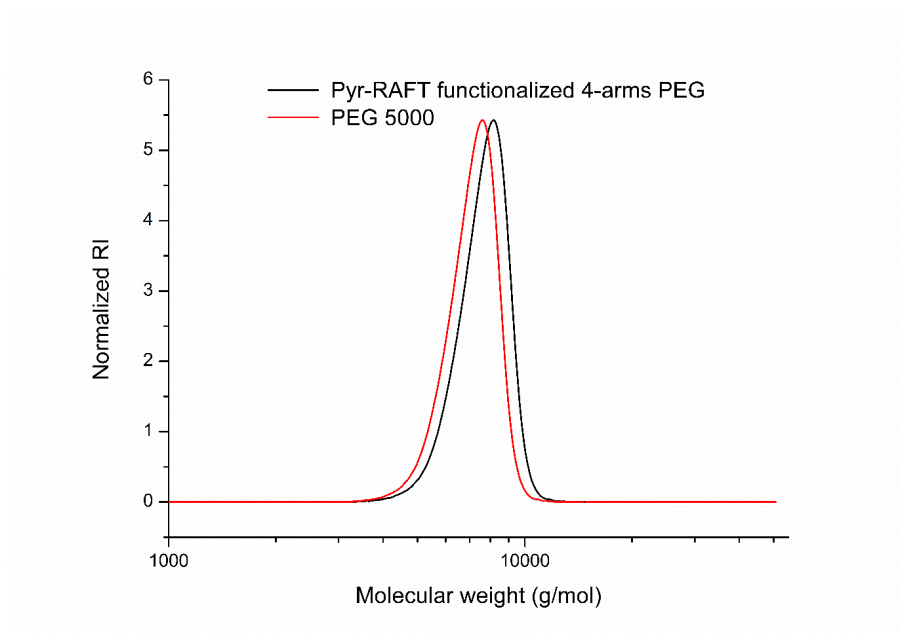


Figure III.18: SEC traces of 4-arms PEG (M_n reference supplier: 5000 g.mol⁻¹) and Pyr-RAFT functionalized 4-arms PEG obtained by SEC in THF at 35°C using PS as polymer standards.

In the following paragraph, the synthesis of another RAFT-functionalized PEG linker retaining a phosphoryldithioester compounds is discussed. This RAFT molecule is particularly interesting for HDA click reaction as it presents higher reaction kinetics compared to 4-((Pyridine-2 carbonothioylthio)methyl)benzoic acid (Pyr-RAFT)(Pyr-RAFT). While Barner-Kowollik *et al.* demonstrated that it could be used without any catalyst, a very small amount of ZnCl accelerates drastically the kinetics of the reaction.^[41]

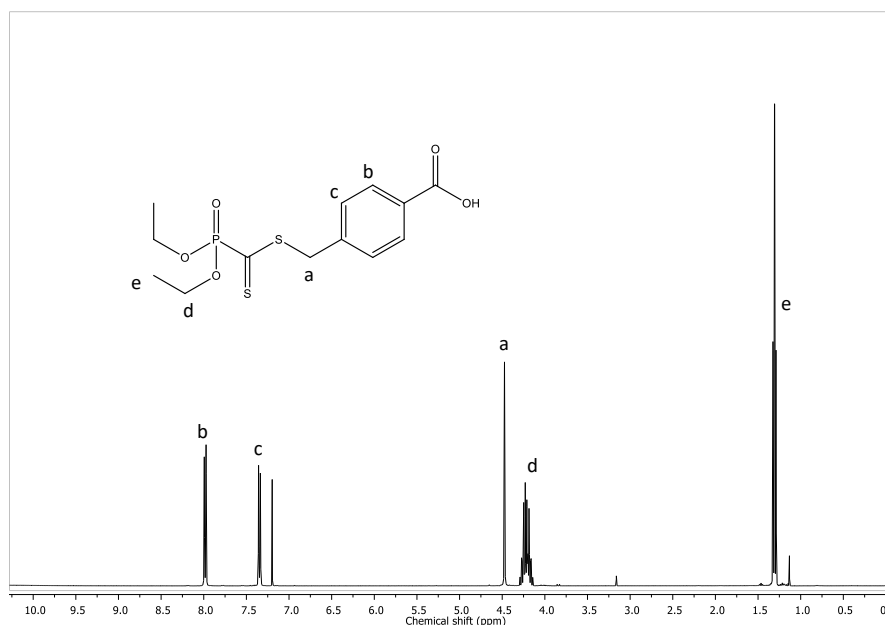


Figure III.19: ^1H -NMR of 4-(((Diethoxyphosphoryl)carbonothioyl)thio)methyl) benzoic acid (DEP-RAFT) in CDCl_3 .

DEP-RAFT was synthesized according to a reported procedure from Barner-Kowollik's group^[42] and characterized by H^1 -NMR as showed in Figure III.19. In a next step, DEP-RAFT was used to esterify the 4 hydroxyl end groups of the 4-arms PEG ($M_n = 5000 \text{ g.mol}^{-1}$, $\bar{D} = 1.04$) using a similar synthetic procedure as the one employed with the Pyr-RAFT agent. However, SEC analysis evidences the presence of side reactions during the synthesis as a multimodal population is obtained. Moreover, H^1 -NMR showed that a complete conversion was not achieved as the integration of signals g and d does not respect the ratio of 1/1 (Figures III.20 and III.21). It was suspected that dimers of PEG by disulfide bond are formed from the RAFT moieties degradation during the synthesis leading to an increase of molecular weight and dispersity. Table III.5 summarizes the macromolecular characteristics of the obtained polymer.

Table III.5: Macromolecular parameters obtained by SEC in DMAc at 50°C using PS as polymer standards of the 4-arm PEG and the DEP-RAFT-functionalized 4-arms PEG obtained after esterification reaction DEP-RAFT.

Samples	M_p	M_n	\bar{D}
	(g/mol)	(g/mol)	
4-arms PEG (Reference)	11800	11000	1.03
DEP-RAFT 4-arms PEG	13300	15400	1.6

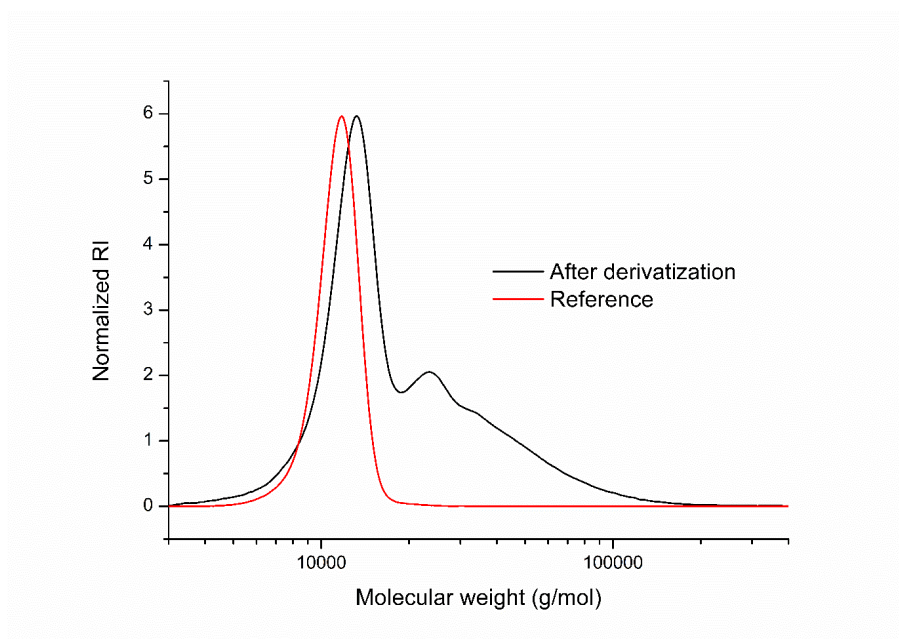


Figure III.20: SEC traces of 4-arms PEG (M_n reference supplier: 5000 g.mol⁻¹) and DEP-RAFT-functionalized 4-arms PEG obtained by SEC in DMAc at 50°C using PS as polymer standards.

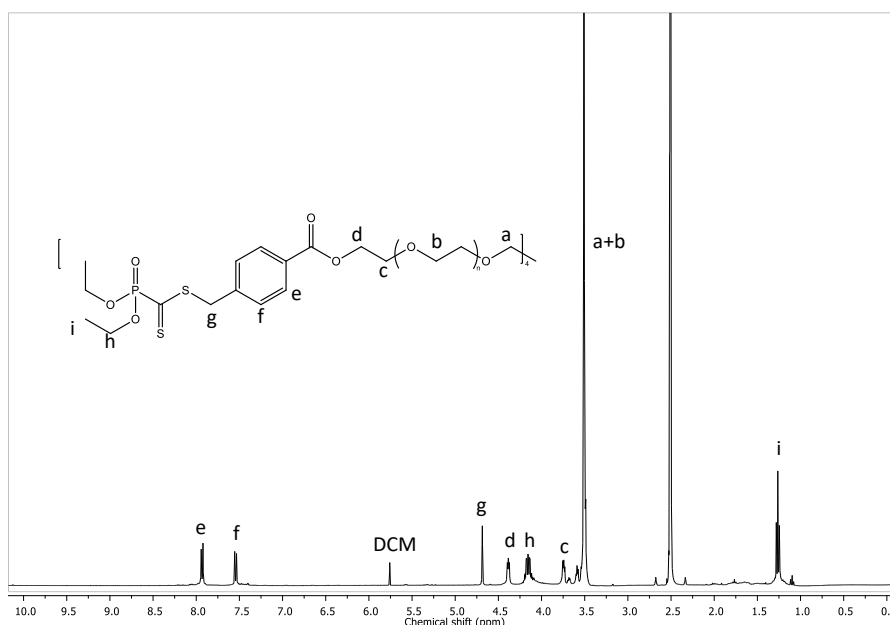


Figure III.21: ¹H-NMR of the DEP-RAFT functionalized 4-arms PEG linker in DMSO-d₆.

Several trials performed in absence of DMAP catalyst or using oxalyl chloride as activating agent were explored to prepare the DEP-RAFT-functionalized 4-arms PEG

linker. Unfortunately, for unknown reasons those reactions failed also. Indeed, SEC analysis evidences the presence of side reactions during the synthesis as a multimodal population is obtained. Since PEG 5000 dissolves slowly in water, the same experiment was conducted on a PEG presenting a lower molecular weight ($M_n = 1500 \text{ g.mol}^{-1}$, $\bar{D} = 1.05$). The synthesis of the DEP-RAFT PEG linker was successfully achieved as attested by ^1H -NMR even though a small proportion of the polymer underwent dimerization as attested by SEC analysis, respectively depicted in Figure III.22 and III.23. Indeed, ^1H NMR spectrum presents an intensity ratio of 1/1 between the signals c and f confirming the complete conversion. Carbon NMR and phosphor NMR were also carried out to assess that the RAFT end group is not oxidized under the synthetic conditions investigated. As presented in Figures III.24 and III.25, only the signals of the characteristic product are present, which therefore attest that oxidation does not occur. All these analysis tend to confirm the successful synthesis of the DEP-RAFT PEG linker. Therefore, this linker will be employed in the next section for the preparation of DX-gels.

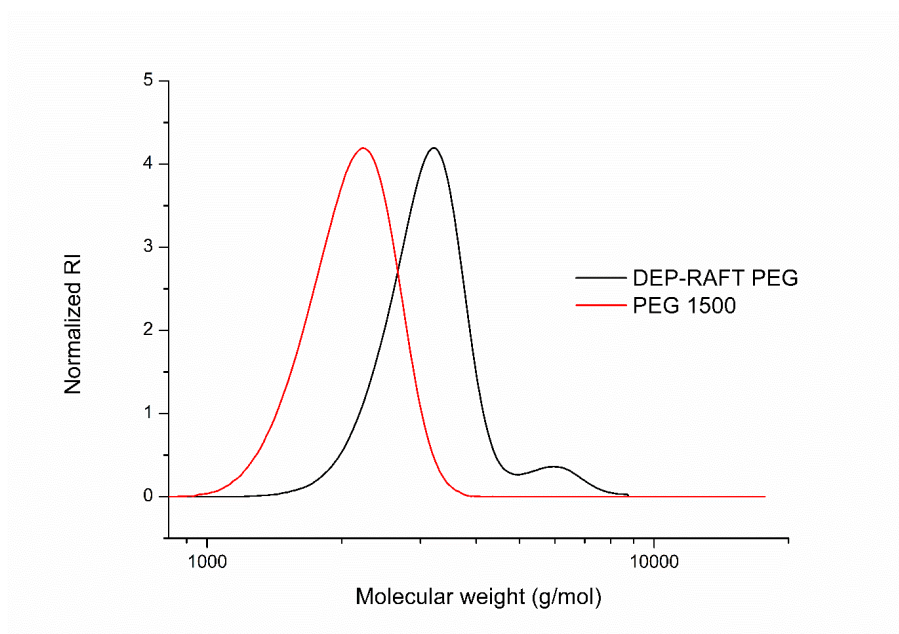


Figure III.22: SEC traces of PEG (M_n reference supplier: 1500 g.mol^{-1}) and DEP-RAFT PEG linker obtained by SEC in THF at 35°C using PS as polymer standards.

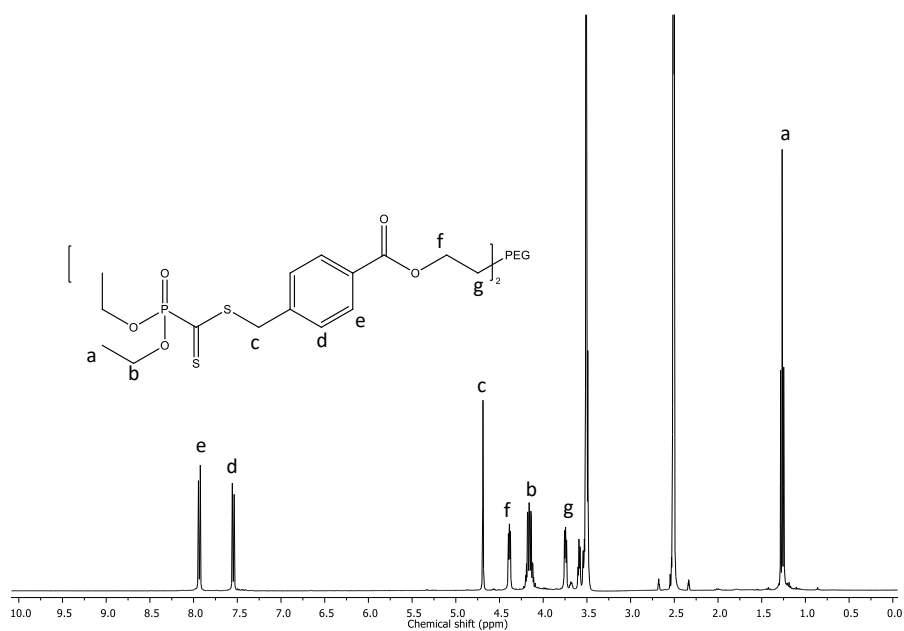


Figure III.23: ^1H -NMR spectrum of the DEP-RAFT PEG linker in $\text{DMSO}-d_6$.

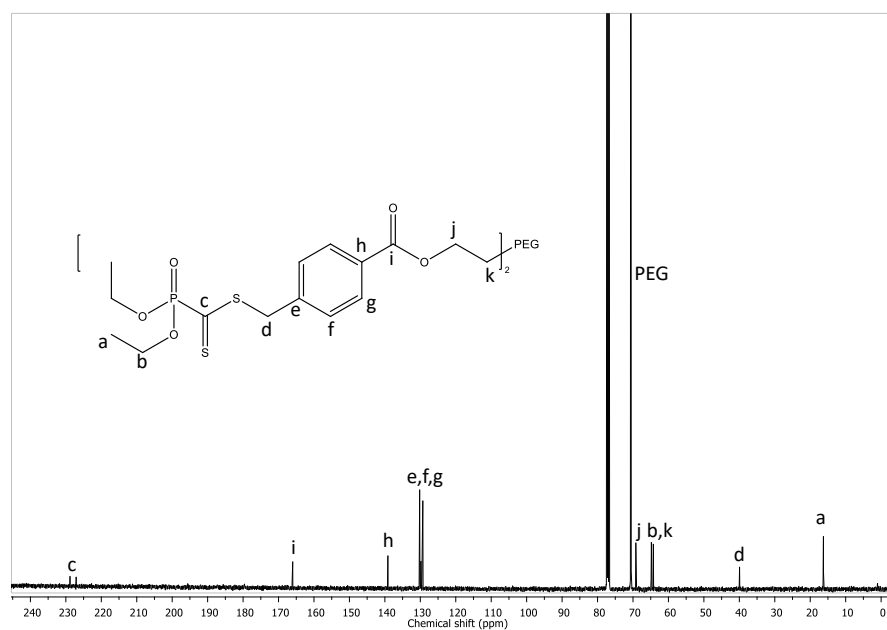


Figure III.24: ^{13}C -NMR spectrum of the DEP-RAFT PEG linker in CDCl_3 .

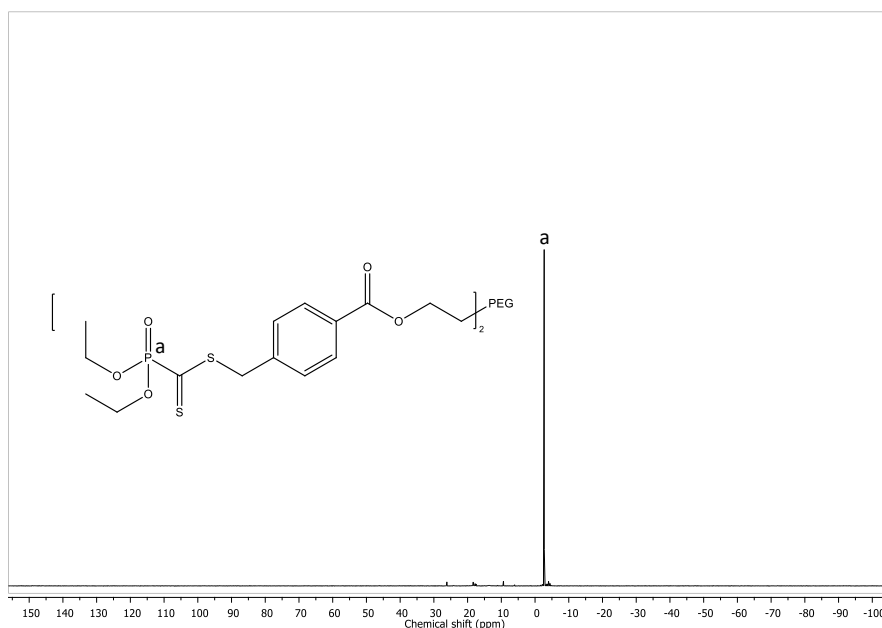


Figure III.25: ^{31}P -NMR of spectrum of the DEP-RAFT PEG linker in CDCl_3 .

III.2.3. Reactivity tests of various RAFT crosslinkers

Dithiothiester- and trithiocarbonate-based RAFT agents are bright colored compounds that turn colourless when the thiocarbonyl bond has reacted with a diene through a HAD reaction. This color switch was exploited to investigate the reactivity of the RAFT-functionalized PEG linkers synthesized in the previous section with small diene molecules. Discoloration tests of the mixture solutions will then be evaluated to qualitatively demonstrate the reactivity of our PEG linkers (Figure III.26). For this purpose, trans,trans hexadiene-1-ol was chosen as a model diene (3 equivalent added) and reactions were carried out in ethyl acetate at 25°C for an initial concentration of 10 mg/ml, under atmospheric conditions. A discoloration from pink to yellow was observed for the Pyr-RAFT-functionalized 4-arms PEG linker and from pink to colorless for the DEP-RAFT PEG within a time frame ranging from 10 to 30 min, attesting of the reactivity between the RAFT agent of the PEG linker and the diene. Following these promising results, samples were characterized by ^1H NMR to quantify the conversion of RAFT agent into the clicked adduct. Figures III.27 and III.28 display the ^1H NMR spectrum of the polymers resulting from the click reaction between the trans,trans hexadien-1-ol (HD-OH) with the Pyr-RAFT functionalized 4-arms PEG linker and the DEP-RAFT PEG linker, respectively. Characteristic protons of the adducts are clearly visible in the 7-8.5 ppm region while the characteristic protons of

the diene at 5.5ppm and 6 ppm, bringing further evidences of the good click reactivity of the synthesized linkers as intensities of signals j and k are in the ratio of 1/1 compared to signal b.

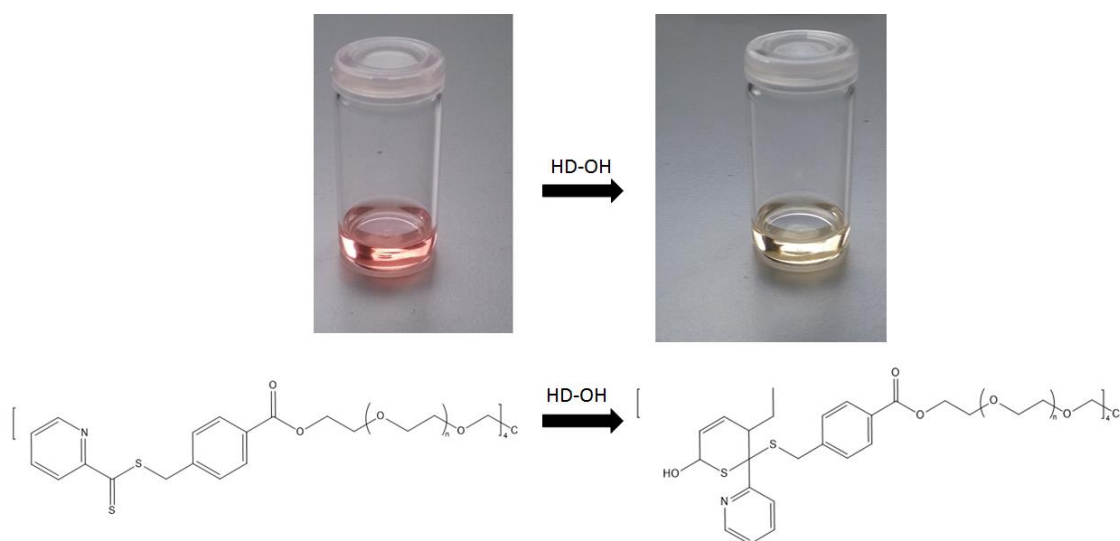


Figure III.26: Discoloration test to qualitatively evidence the reactivity of the Pyr-RAFT-functionalized 4-arms PEG linker with trans,trans hexadiene-1-ol (HD-OH) molecule at r.t. in EA using TFA as catalyst.

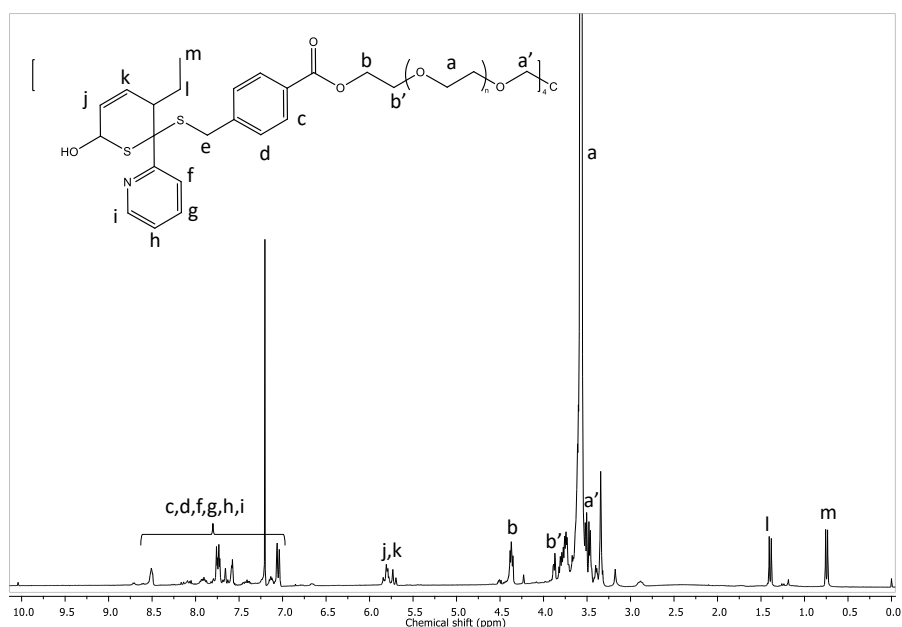


Figure III.27: ^1H NMR of the Pyr-RAFT-functionalized 4-arms PEG linker after reaction with trans,trans-hexadiene-1-ol.

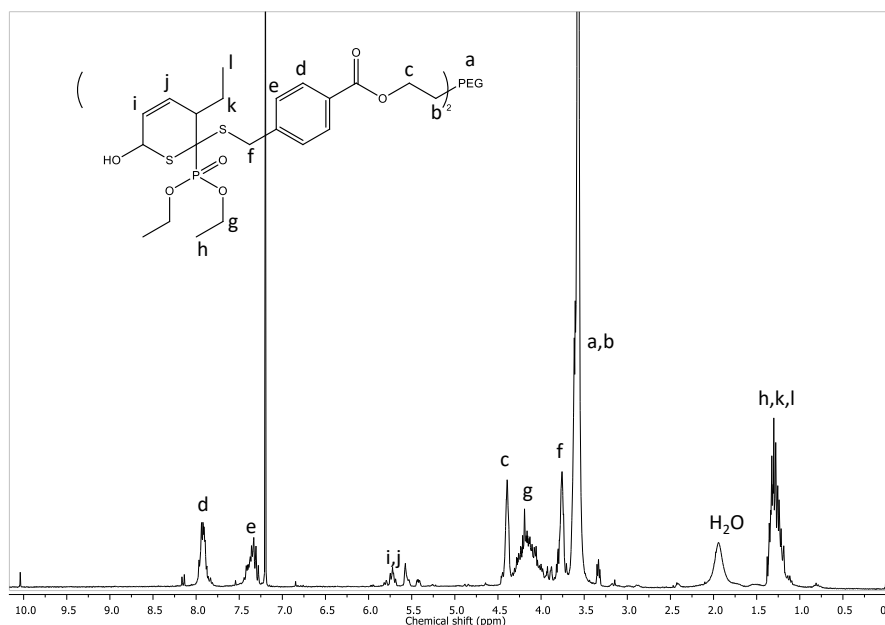


Figure III.28: ^1H NMR of the DEP-RAFT PEG linker after reaction with trans,trans hexadiene-1-ol.

A final reactivity test was also performed on the DEP-RAFT PEG linker with 1,10-DiCp-decane to demonstrate the validity of our approach to form DX-gel. 1,10-DiCp-decane was kindly given by Alexander Schenzel from KIT and was synthesized according to a reported procedure from Barner-Kowollik's group.^[42] For that purpose, to a DEP-RAFT-functionalized 2-arms PEG solution in ethyl acetate was added various amounts of 1,10-DiCp-decane to realize a "step-growth" polymerization, as illustrated in Figure III.29. The resulting polymer was recovered by precipitation in cold diethyl ether after 15 minutes of reaction. SEC analysis (Figure III.30) revealed a multimodal population composed of dimers, trimers and even tetramers, supporting the reactivity of the PEG dilinker towards a diene.

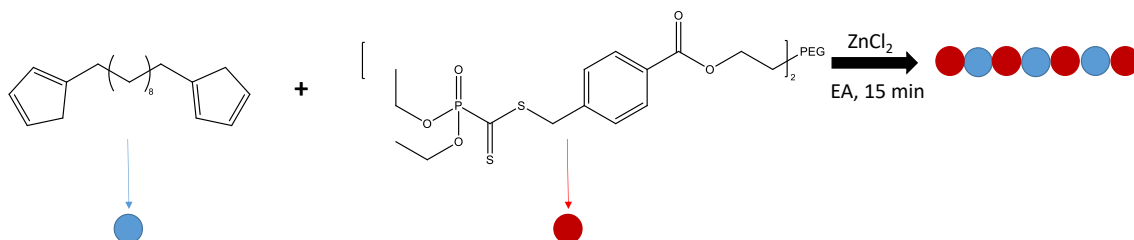


Figure III.29: Schematic representation of the reactivity test carried out between DEP-RAFT- PEG linker.

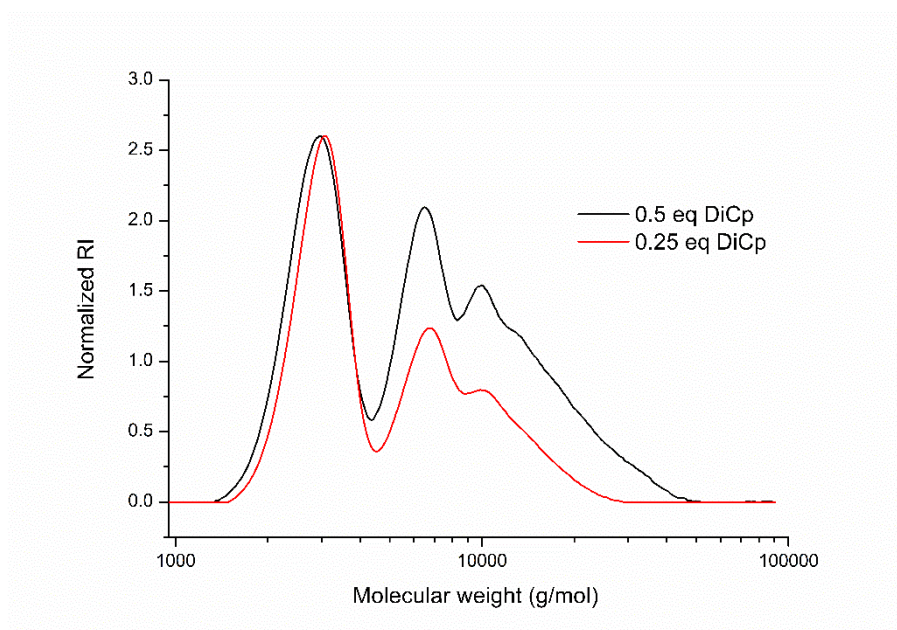


Figure III.30: SEC traces in THF at 35°C of DEP-RAFT PEG linker after reaction with 0.25 (red curve) and 0.5 (black curve) equivalent of 1,10-DiCp-decane using PS as polymer standards.

As evidenced by SEC and NMR analyses, we can conclude that in principle all the synthesized RAFT-based PEG linkers can be employed to crosslink Cp-functionalized microgels.

III.2.4. DX gel synthesis

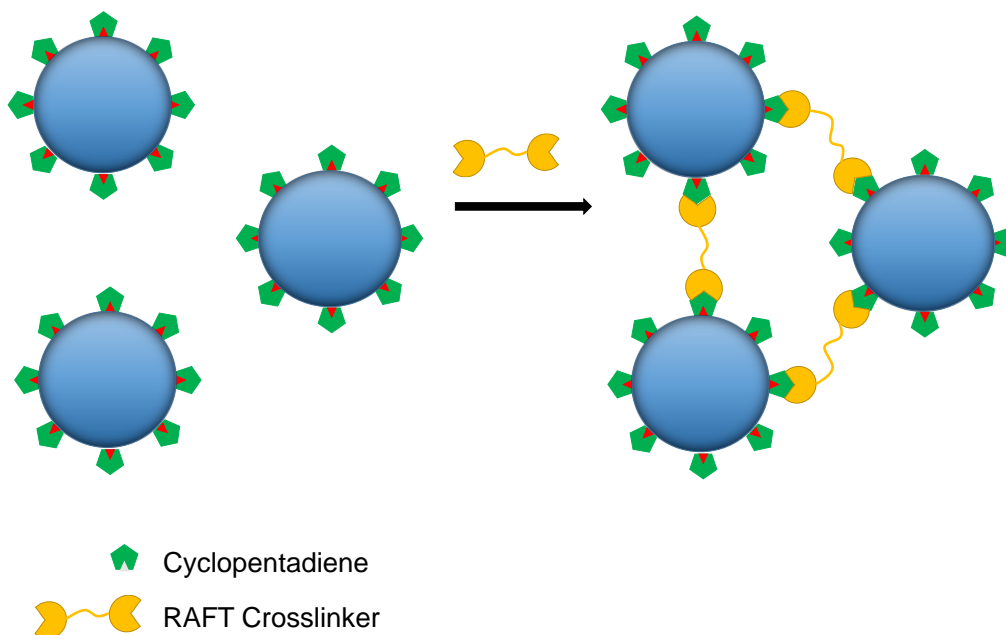


Figure III.31: Schematic representation of the formation of DX-gels from Cp-microgels and a RAFT-based crosslinker.

The advantage of our strategy compared to other systems previously developed by Sanders *et al.* in the state of the art is that our approach does not involve radical coupling for the preparation of DX-gels, which are more adequate to the specificities of the biomedical field. Moreover, this metal-free and fast click coupling reaction occurring in mild conditions presents the supplementary advantages to be monitored by a color shift of the reaction as the starting materials are brightly colored while the adduct is colorless, providing a visual feedback to evaluate the progress of the reaction, or at least, if it proceeds properly. Therefore, in this series of experiments, the 2 RAFT PEG crosslinkers synthesized above and listed in Table III.6 were tested in various conditions with the Cp-functionalized microgels to promote the formation of DX gels.

Another crosslinker was also employed for sake of comparison: the 2-(methylthio)-2-thioxoacetate (MTTA, Figure III.32). Indeed, this short and reactive crosslinker employed in HDA reactions ^[43] was tested to demonstrate whether the molecular weight limits the DX-gels synthesis. This crosslinker was kindly given by Kai Pahnke from KIT, according to a reported procedure from Barner-Kowollik's group.^[43] The various parameters investigated involve the solvent nature, the temperature of

reaction, the relative ratio between cyclopentadiene, the RAFT species and the RAFT type chain transfer agent.

Table III.6: Experimental conditions investigated for the synthesis of DX-gels by RAFT HDA click reaction.

Samples	Solvent	Linker	[Cat] ₀ /[RAFT] ₀	T (°C)
A	EA	Pyr-RAFT 4-arms PEG	1/1 ; 5/1	25
B	EtOH	Pyr-RAFT 4-arms PEG	1/1 ; 5/1	25
C	EA	Pyr-RAFT 4-arms PEG	1/1 ; 5/1	40
D	EtOH	Pyr-RAFT 4-arms PEG	1/1 ; 5/1	40
E	THF	DEP-RAFT PEG	1/1 ; 5/1	25
F	EA	DEP-RAFT PEG	1/1 ; 5/1	25
G	EtOH	DEP-RAFT PEG	1/1 ; 5/1	25
H	EA	DEP-RAFT PEG	1/1 ; 5/1	40
I	EtOH	DEP-RAFT PEG	1/1 ; 5/1	40
J	THF	MTTA	-	25
K	THF	MTTA	-	40
L	EA	MTTA	-	25

Experiments were realized with a [RAFT]₀/[Cp]₀ ratio of 0.2 to 0.8

Experiments were stopped after a reaction time of 6 days

EA, EtOH, THF correspond respectively to ethyl acetate, ethanol and tetrahydrofuran

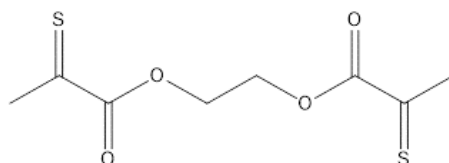


Figure III.32: Chemical structure of the 2-(methylthio)-2-thioacetate (MTTA).

Unfortunately, none of the tested conditions resulted in the formation of doubly crosslinked gels, even after 6 days of reaction, an increase of the reaction temperature from room to 40°C or the addition of 1 to 5 equivalents of catalyst. A test in a rheometer (strain 0.5%, f: 1Hz) to monitor in real time the reaction by measuring the evolution of

storage modulus (G') has been carried out to further investigate these observations (Figure III.33).

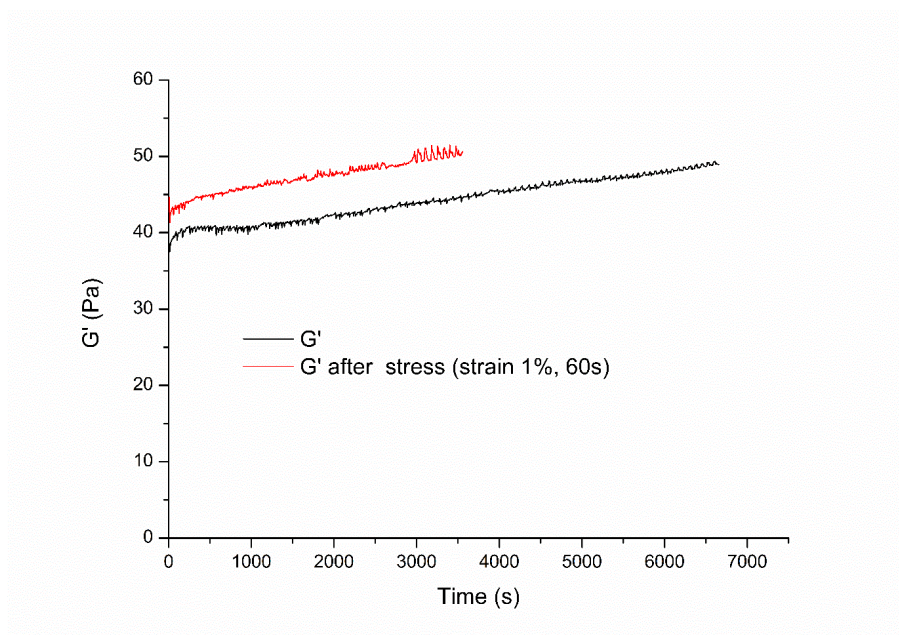


Figure III.33: Evolution of the storage modulus G' versus time of the Cp-based microbeads in the presence of DEP-RAFT PEG linker (conditions: strain 0.5%, f : 1Hz, r.t.).

A small evolution of G' over time is noticed. Such a behavior is probably due to aging of the sample. Aging is a phenomenon closely associated with the slow cooperative relaxation of defects and stresses accumulated during the initial preparation and trapped inside interlocked neighboring particles. Indeed, a small stress was applied onto the sample to demonstrate the aging of the sample. G' came back close to the original value after the stress, attesting the aging behavior of the sample. Moreover, particle size analyses demonstrate that no coupling occurs between the particles as depicted in Figure III.34.

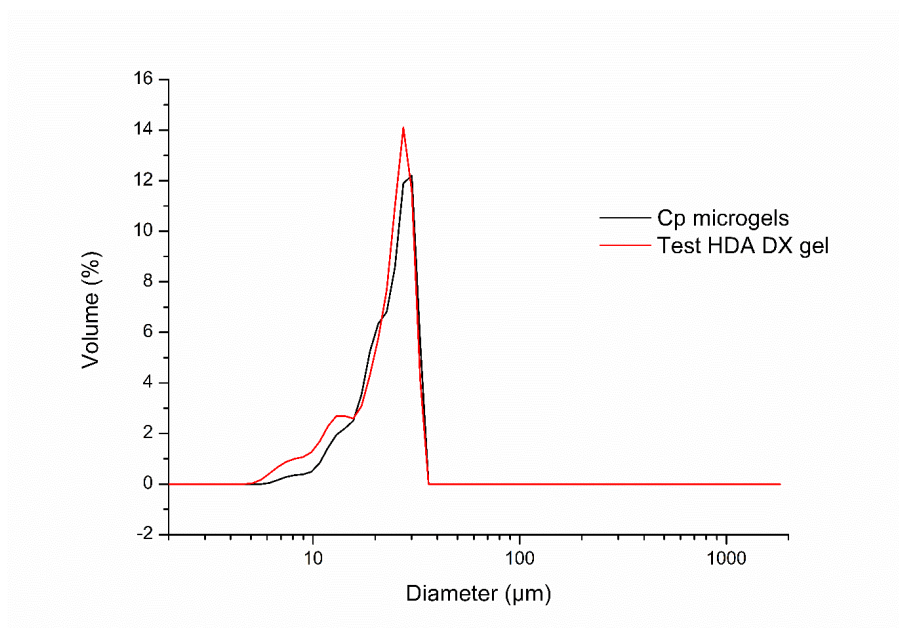


Figure III.34: Particle size distribution as measured by particle sizer before (black) and after (red) HDA reaction.

While Cp-based particles and RAFT-functionalized crosslinkers have both demonstrated their respective reactivity towards HDA click coupling reactions, no DX-gels were obtained when the two reactants are mixed together. An explanation could not be proposed for these observations. Therefore, to achieve DX-gels efficiently, our strategy developed in the next chapter relies on the use of a more reactive dienophile agent: the triazolinedione (TAD) function as employed for evidencing Cp-derivatization quantitatively.

III.3. Conclusions

The results discussed in this chapter demonstrate the ability to prepare cyclopendadiene-bearing microgels via a simple radical suspension co-polymerisation method using glycidyl-based comonomer and its subsequent derivatization to introduce the desired Cp moiety on their periphery. Particles varying in size and crosslinking density were achieved by optimizing various parameters including the surfactant nature, the surfactant quantity, the surfactant HLB ratio, the reaction time, the stirring rate and the monomers/crosslinker ratio. The surface modification surprisingly does not modify the swelling properties of the microgels as attested by particle size measurements. This unchanged swelling behavior might be due to the

release of a hydroxyl group after the surface modification that compensates the introduction of the cyclopentadiene group. Tuning of cyclopentadiene density onto particle surface can be achieved by a simple adjustment of the experimental parameters. Moreover, successful HDA click chemistry reactions were performed onto microgel particles previously swollen in THF with pyrene-maleimide. The fluorescence of pyrene-derivatized microparticles followed a linear emission evolution. Therefore, it was assumed that the reactions follow a fast and quantitative process. While fluorescent measurements confirm qualitatively the grafting of Cp and its reactivity, UV measurements offer an accurate measurement of Cp content, which will be also applied in the upcoming chapters. Moreover, fluorescence microscopy measurements give an additional information concerning the homogeneous distribution of the Cp reactive functions onto the microgel surface for all tested samples. Also, cell biocompatibility of the starting PEG-composed microbeads was assessed by a MTT test, validating our materials in the outlook of biomedical applications. Finally, to prepare DX gels, various RAFT-functionalized PEG crosslinkers were successfully synthesized as proven by SEC, NMR and MS. Moreover, reactivity of these crosslinkers towards HDA reaction was efficiently demonstrated by reaction with a commercial diene molecule (trans,trans hexadiene-1-ol). Surprisingly, mixing of Cp-based microgels with the synthesized RAFT-based crosslinkers for an initial molar ratio $[RAFT]_0/[Cp]_0 = 0.8$, did not yield DX-gels even though reactions run for days, with or without catalyst and at 40°C. This unexplained behavior of our system was unexpected as every component is reactive separately. Therefore, a new strategy using a more reactive click chemistry will be investigated in the next chapter.

III.4. Experimental section

Materials

Polyethylene glycol methyl ether methacrylate (PEGMA, M_n : 500 g/mol), glycidyl methacrylate (97%) and ethylene glycol dimethacrylate (98%), *N*-(1-pyrene) maleimide, butyl acetate (99.7%), aluminium oxide basic, molecular sieves dry THF, molecular sieves dry DCM were purchased from Sigma Aldrich Fluka. All monomers were passed over basic aluminum oxide before use. 4,4'-azobis(4-cyanovaleric acid) (98%>) (ABCVA), Span 80, Tween 80, sodium cyclopentadienide (2M in THF), ammonium chloride (99.5%>), dicyclohexylcarbodiimide (99%),

dimethylaminopyridine (99%>), diethyl phosphite (98%), carbon disulphide (99.9%>), 4-bromomethylbenzoic acid (97%), sodium sulfate (99%>), zinc chloride (99.99%), were purchased from sigma and were used as received. Cyclohexane, hexane, tetrahydrofuran, ethanol, acetonitrile, hydrochloric acid were purchased from VWR. Solvents were used as received unless precise.

Emulsion study

Emulsion studies were realized by mixing PEGMA (M_n : 500 g/mol, 0.7 g, 0.0014 mol), glycidyl methacrylate (GMA, 90 mg, 0.63 mmol), ABCVA (25 mg, 0.089 mmol), and ethylene glycol dimethacrylate (EGDMA, 42 mg, 0.212 mmol) (molar ratio 0.7/0.3/0.05/0.1) in a 1.2 mL mixture of water/acetonitrile 5/1 (40% w/w). The solution was transferred into a separated flask containing 20 mL of cyclohexane containing various mixture of Span 80 and Tween 80. Solutions were stirred for 10 minutes and were analysed by optical microscopy.

Preparation of PEG-Co-GMA microgel

The PEG-co-GMA microgels were synthesized by suspension radical polymerization with ABCVA as an initiator in a 500 mL round bottom flask with temperature and stirring control. First, PEGMA (M_n : 500 g/mol, 7 g, 0.014 mol), glycidyl methacrylate (GMA, 900 mg, 6.3 mmol), ABCVA (250 mg, 0.89 mmol), and ethylene glycol dimethacrylate (EGDMA, 420 mg, 2.12 mmol) (molar ratio 0.7/0.3/0.05/0.1) were dissolved in a mixture of 12 mL water/acetonitrile 5/1 (40% w/w) and the solution was transferred into a separate flask containing 200 mL of cyclohexane and the surfactant (mixture of Span 80 and Tween 80 HLB : 5.9). The flask was degassed with N_2 for 30 min. Polymerization was carried out at 70°C under stirring at 400 rpm for 6 h. The particle size is controlled by the stirring speed. Microgels were dried after washing by ethanol.

Preparation of Cp functionalized PEG microgels

PEG microgels (3 g) were suspended in 200 mL of dry THF in a round bottom flask and cooled down in an ice-salt bath to -10°C. A solution of sodium cyclopentadienide (2M in THF, 4.8 mL, 12 mmol) diluted into 25 mL of dry THF was added dropwise to the microgel solution. After 1 h at -10°C, the ice-salt bath was removed and the mixture was slightly stirred for extra 3 hours at ambient temperature. The reaction was quenched by pouring the reaction mixture into 200 mL of saturated NH_4Cl solution.

Subsequently, the microgels were filtered off and washed successively by 200 mL of acetone, ethanol-water (1/1), 3% HCl in water, water, THF and hexane. Microgels were kept in ethanol for better storage.

Derivatization for fluorescence microscopy

Cp-PEG microgels (50 mg) and *N*-pyrene maleimide (20 mg, 68×10^{-3} mmol) were suspended in 2.5 mL of dry THF in flask and were stirred for 4 hours at 40°C. The microgels were washed thoroughly (3 x 25 mL of THF and 3 x 25 mL of ethanol) to remove the physically absorbed pyrene moiety.

UV quantitative study

A stock fresh solution of 4-phenyl-1,2,4-triazoline-3,5-dione (PTAD) (M_w : 175.14 g/mol, 4.35 mg into 5 mL, 0.497M) in butyl acetate was used as titration species. A calibration curve was made using 5 different concentrations of PTAD solutions. The following titration procedure was used: 100 μ L of a suspension of microgels were added into a vial with 2.4 mL of butyl acetate. A defined volume of PTAD solution stock (50 μ L) was added into the vial and the mixture was stirred for 5 minutes. The solution was filtered on a micro-disk with a pore size diameter of 0,5 μ m. Filtered solution was characterized by UV to determine the remaining PTAD after reaction with the cyclopentadienyl function onto the microgel surface.

MTT test

SH-SY5Y cells were grown in DMEM supplemented with 10% (v/v) fetal bovine serum and 100 IU/ml of penicillin G sodium and 100 μ g/ml of streptomycin sulfate. The cells were maintained in an incubator supplied with 5% CO₂/95% air humidified atmosphere at 37 °C. SH-SY5Y cells were seeded in 96-well plates at the density of 10000 viable cells per well and incubated 24 h to allow cell attachment. The cells were then incubated with Cp-microgels particles (microgels concentration concentrations of 0.5, 1, 3.125, 6.25, 12.5, 20 and 25 mg/ml at), for 48 h.

At determined time, the formulations were replaced with DMEM containing MTT (5 mg/ml) and cells were then incubated for additional 4 h. MTT was aspirated off and DMSO was added to dissolve the formazan crystals. Absorbance was measured at 560 nm using an ELISA microplate reader. Untreated cells were taken as control with

100% viability and cells without addition of MTT were used as blank to calibrate the spectrophotometer to zero absorbance. Triton X-100 1% was used as positive control of cytotoxicity. The results were expressed as mean values \pm standard deviation of 5 measurements.

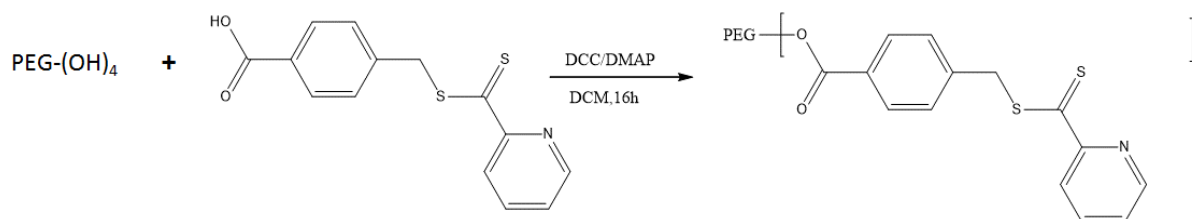
Synthesis of 4-((Pyridine-2-carbonothioylthio)methyl)benzoic acid

4-((Pyridine-2-carbonothioylthio)methyl)benzoic acid was synthesised according to procedure described by C. Barner Kowollik's team and was given by researchers from KIT.^[44]

Synthesis of MTTA

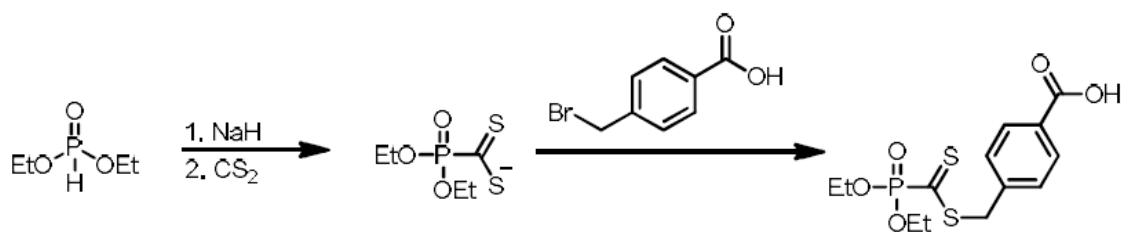
Synthesis of 2-(methylthio)-2- thioacetate was realized according to procedure developed by C. Barner-kowollik's team and was given by researchers from KIT.^[43]

Synthesis of the a 4 arm PEG crosslinker based on 4-((Pyridine-2-carbonothioylthio)methyl)benzoic acid



In a round bottom flask dried overnight at 120°C in the oven, 500 mg of 4 arm-PEG (n: 0.1 mmol ; Mw : 5000 g/mol), 0.326 g of DMAP (n : 2.25 mmol, Mw : 122 g/mol) were dissolved into 25 ml of THF. A solution of 20 ml of DMF containing 1.12 g of 4-((Pyridine-2-carbonothioylthio)methyl)benzoic acid(3.88 mmol, Mw : 289 g/mol) and 0.825 g (n : 4 mmol) of DCC were added to the solution and the reaction is carried on for 72 h. After 72 h, the precipitate was filtered off and the solvent is evaporated under vacuum and finally the polymer is precipitated into cold ether. The solid was recovered by filtration on Buchner. The solid was therefore solubilized again in DCM and the solution was filtered to eliminate the residual 4-((Pyridine-2-carbonothioylthio)methyl)benzoic acid in excess and the polymer is recovered by precipitation in cold ether.

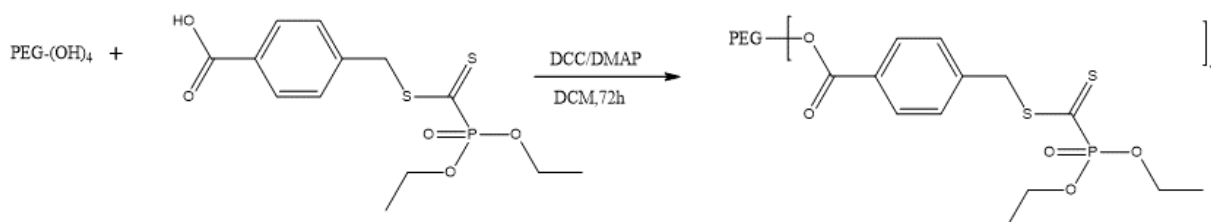
Synthesis of 4-(((Diethoxyphosphoryl)carbonothioyl)thio)methyl) benzoic acid (PDTMBA)



Procedure:

A solution of 5.3 mL diethyl phosphite (1.0 eq. 41 mmol, 5.7 g) in 40 mL of dry THF is added to a stirred suspension of 1.5 g NaH (1.5 eq., 62 mmol) in 20 mL of dry THF at ambient temperature. Completion of the addition is assessed when no more H₂ bubbles form in the medium. The reaction mixture is heated to reflux for 15 min. Subsequently, the solution is cooled down to -90 °C and 12.3 mL of CS₂ (5.0 eq., 205 mmol, 15.6 g) are added dropwise. It is stirred for 2 h, whereat the reaction mixture turns brown. After the addition of 750 mL of THF to facilitate the stirring, a solution of 10.0 g of 4-bromomethylbenzoic acid (1.1 eq., 46 mmol) in 75 ml THF is added dropwise at ambient temperature. After stirring for 16 h, the solvent is removed from the purple reaction mixture. DCM and H₂O are added in a ratio of 1:1 until all residue is dissolved. The water phase is washed with DCM and the combined organic layers are dried over Na₂SO₄. After removal of the solvent, the crude product is purified via column chromatography (cyclohexane/EA/acetic acid = 1/1/0.01) and finally a recrystallization in tertbutyl methyl ether was realized to give a purple solid of PDTMBA.

Synthesis of A PEG crosslinker based on PDTMBA



In a round bottom flask dried overnight at 120 °C in the oven, 500 mg of 4 arm-PEG (n: 0.1 mmol ; Mw: 5000 g/mol), 46 mg of DMAP (n: 0.05 mmol, Mw: 122 g/mol) were dissolved into 10 ml of dry DCM. A solution of 5 ml of DMF containing 175 mg of 4-(((Diethoxyphosphoryl)carbonothioyl)thio)methyl) benzoic acid (0.515 mmol, Mw :

348.43 g/mol) and 154 mg (n: 0.75 mmol, 206.32 g/mol) of DCC were added to the solution and the reaction is carried on for 72 h. After 72 h, the precipitate was filtered off and the solvent is evaporated under vacuum and finally the polymer is precipitated into cold ether. The solid was recovered by filtration on Buchner.

Equipment

UV spectrometer

UV measurements were performed on a UV spectrometer Analytic-Jena Specord 200.

Optical microscopy

Optical microscopy measurements were performed on an Olympus Optical microscopy equipped with a Canon camera.

Particles size measurements

Particle size measurements were recorded on a Beckman Coulter LS 200 particles sizer.

Fluorescence microscopy

Microgels were observed in epifluorescence mode with an inverted Nikon Eclipse Ti-E motorized microscope (Nikon, Japan) equipped with x10 Plan Apo (NA 1.45), x40 Plan Apo (NA 1.45, oil immersion) and x60 Plan Apo (NA 1.45, oil immersion) objectives, two lasers (Ar-ion 488 nm; HeNe, 543, 543 nm) and a modulable diode (408 nm). Epifluorescence images were captured with a Roper QuantEM: 512SC EMCCD camera (Photometrics, Tucson, AZ) using NIS Elements AR (Nikon, Japan). To quantify the fluorescent signal, microgels were observed in epifluorescence with similar conditions (objective, light intensity, gain, and camera frequency). The microbead outline was automatically detected with NIS element using a mask obtained from a thresholded fluorescent image. The microbead area, the raw integrated density and the mean gray value were obtained for each microbead. In addition, five random background regions were taken near each microbead to obtain a mean gray value of the fluorescent background. The corrected microgel fluorescence was calculated using the following relation: corrected microgel fluorescence = raw integrated density – (microgel section x mean fluorescence background).

Nuclear Magnetic Resonance (NMR)

¹H-spectra were recorded with a Bruker Avance 300 (300 MHz) FT-NMR spectrometer in CDCl₃ (Eurisotop) or DMSO-*d*₆ solution at room temperature. Chemical shifts are presented in parts per million (*ppm*) relative to CHCl₃ (7.26 ppm for H¹-NMR) and DMSO (2.50 ppm for H¹-NMR) as an internal standard. The resonance multiplicities are described as [br. (broad)] s (singlet), d (doublet), t (triplet), q (quadruplet), quin (quintuplet), sext (sextuplet) or m (multiplet).

MALDI-MS

Matrix assisted laser desorption ionization time of flight (MALDI-ToF) mass spectra were recorded using a spectrometer equipped with a nitrogen laser, operating at 337 nm with a maximum output of 500 J.m⁻² delivered to the sample in 4 ns pulse at 20 Hz repeating rate. Time-of-flight mass analyses were performed in reflection mode at resolution of 100000. Polymer samples were dissolved in acetonitrile to obtain 1 mg/ml⁻¹ solutions.

SEC

Size exclusion chromatography (SEC/GPC) was performed in THF or in THF + 2wt% NEt₃ at 35°C using either a Polymer Laboratories liquid chromatograph equipped with a PL-DG802 degasser, an isocratic HPLC pump LC 1120 (flow rate = 1 ml/min), a Rheodin manual injection (loop volume = 200 µL, solution conc. = 1 mg/mL), a PL-DRI refractive index detector and four columns: a PL gel 10 µm guard column and three PL gel Mixed-B 10µm columns (linear columns for separation of MWPS ranging from 500 to 10⁶ daltons).

Mechanical characterization by dynamic rheology

Dynamic rheology measurements were performed using an Anton Paar Physica MCR 310 Rheometer in oscillary mode with a temperature-controlled rheometer equipped with solvent trap. A 20 mm diameter plate geometry with a solvent trap was used. A strain of 1 % was used for the frequency sweep measurements.

The extent of linear viscoelastic regime was determined by performing a strain sweep from 0 % to 15 % to define the linear viscoelastic region in which the modulus *G'* and

G'' are independent of the applied strain. In our experiment, the strain amplitude was set as 0.5 %

III.5. Bibliography

1. Arshady, R., *Preparation of Polymer Nanospheres and Microspheres by Vinyl Polymerization Techniques*. Journal of Microencapsulation, 1988. **5**(2): p. 101-114.
2. Schmidt, S., et al., *Adhesion and Mechanical Properties of PNIPAM Microgel Films and Their Potential Use as Switchable Cell Culture Substrates*. Advanced Functional Materials, 2010. **20**(19): p. 3235-3243.
3. Tsai, H.Y., et al., *Synthesis of poly(N-isopropylacrylamide) particles for metal affinity binding of peptides*. Colloids and Surfaces B-Biointerfaces, 2014. **114**: p. 104-110.
4. Guan, Y. and Y.J. Zhang, *PNIPAM microgels for biomedical applications: from dispersed particles to 3D assemblies*. Soft Matter, 2011. **7**(14): p. 6375-6384.
5. Lally, S., et al., *Microgel particles containing methacrylic acid: pH-triggered swelling behaviour and potential for biomaterial application*. Journal of Colloid and Interface Science, 2007. **316**(2): p. 367-375.
6. Das, D., et al., *Biocompatible amphiphilic microgel derived from dextrin and poly(methyl methacrylate) for dual drugs carrier*. Polymer, 2016. **107**: p. 282-291.
7. Sahiner, N. and S.B. Sengel, *Surfactant free synthesis and characterization of poly(vinyl carbazole) microgel and its chemical modifications*. Colloids and Surfaces a-Physicochemical and Engineering Aspects, 2017. **514**: p. 243-250.
8. Tehrani, S.M., Y.J. Lu, and M.A. Winnik, *PEGMA-Based Microgels: A Thermoresponsive Support for Enzyme Reactions*. Macromolecules, 2016. **49**(22): p. 8711-8721.
9. Zhang, Y., et al., *A novel microgel and associated post-fabrication encapsulation technique of proteins*. Journal of Controlled Release, 2005. **105**(3): p. 260-268.
10. Wang, Q.C., et al., *Self-Assembled Poly(ethylene glycol)-co-Acrylic Acid Microgels to Inhibit Bacterial Colonization of Synthetic Surfaces*. Acs Applied Materials & Interfaces, 2012. **4**(5): p. 2498-2506.
11. Bromberg, L. and V. Alakhov, *Effects of polyether-modified poly(acrylic acid) microgels on doxorubicin transport in human intestinal epithelial Caco-2 cell layers*. Journal of Controlled Release, 2003. **88**(1): p. 11-22.
12. Hermanson, G.T., *Bioconjugate Techniques*. Academic Press, San Diego, CA, 1996.
13. Nayak, S. and L.A. Lyon, *Ligand-functionalized core/shell microgels with permselective shells*. Angewandte Chemie-International Edition, 2004. **43**(48): p. 6706-6709.
14. Su, S.X., et al., *Microgel-based inks for paper-supported biosensing applications*. Biomacromolecules, 2008. **9**(3): p. 935-941.
15. Hamerska-Dudra, A., J. Bryjak, and A.W. Trochimczuk, *Immobilization of glucoamylase and trypsin on crosslinked thermosensitive carriers*. Enzyme and Microbial Technology, 2007. **41**(3): p. 197-204.
16. Delair, T., et al., *Amino-containing cationic latex-oligodeoxyribonucleotide conjugates: application to diagnostic test sensitivity enhancement*. Colloids and Surfaces a-Physicochemical and Engineering Aspects, 1999. **153**(1-3): p. 341-353.
17. Tiwari, R., et al., *A Versatile Synthesis Platform To Prepare Uniform, Highly Functional Microgels via Click-Type Functionalization of Latex Particles*. Macromolecules, 2014. **47**(7): p. 2257-2267.
18. Farley, R., et al., *Using click chemistry to dial up the modulus of doubly crosslinked microgels through precise control of microgel building block functionalisation*. Polymer Chemistry, 2015. **6**(13): p. 2512-2522.

19. Farley, R. and B.R. Saunders, *A general method for functionalisation of microgel particles with primary amines using click chemistry*. Polymer, 2014. **55**(2): p. 471-480.
20. Falk, B. and J.V. Crivello, *Synthesis and modification of epoxy- and hydroxy-functional microspheres*. Journal of Applied Polymer Science, 2005. **97**(4): p. 1574-1585.
21. Blinco, J.P., et al., *Dynamic Covalent Chemistry on Surfaces Employing Highly Reactive Cyclopentadienyl Moieties*. Advanced Materials, 2011. **23**(38): p. 4435-4439.
22. Kaupp, M., et al., *Modular design of glyco-microspheres via mild pericyclic reactions and their quantitative analysis*. Polymer Chemistry, 2012. **3**(9): p. 2605-2614.
23. Gong, J.P., et al., *Double-network hydrogels with extremely high mechanical strength*. Advanced Materials, 2003. **15**(14): p. 1155-1158.
24. Gong, J.P., *Why are double network hydrogels so tough?* Soft Matter, 2010. **6**(12): p. 2583-2590.
25. Milani, A.H., et al., *Injectable Doubly Cross-Linked Microgels for Improving the Mechanical Properties of Degenerated Intervertebral Discs*. Biomacromolecules, 2012. **13**(9): p. 2793-2801.
26. McCann, J., et al., *Poly(vinylamine) microgel-dextran composite hydrogels: Characterisation; properties and pH-triggered degradation*. Journal of Colloid and Interface Science, 2015. **449**: p. 21-30.
27. Yasuda, K., et al., *A Novel Double-Network Hydrogel Induces Spontaneous Articular Cartilage Regeneration in vivo in a Large Osteochondral Defect*. Macromolecular Bioscience, 2009. **9**(4): p. 307-316.
28. Tanabe, Y., et al., *Biological responses of novel high-toughness double network hydrogels in muscle and the subcutaneous tissues*. Journal of Materials Science-Materials in Medicine, 2008. **19**(3): p. 1379-1387.
29. Jia, X.Q., et al., *Hyaluronic acid-based microgels and microgel networks for vocal fold regeneration*. Biomacromolecules, 2006. **7**(12): p. 3336-3344.
30. Liu, R.X., et al., *Tuning the swelling and mechanical properties of pH-responsive doubly crosslinked microgels using particle composition*. Soft Matter, 2011. **7**(19): p. 9297-9306.
31. Liu, R.X., et al., *Doubly crosslinked pH-responsive microgels prepared by particle inter-penetration: swelling and mechanical properties*. Soft Matter, 2011. **7**(10): p. 4696-4704.
32. Supasuteekul, C., et al., *A study of hydrogel composites containing pH-responsive doubly crosslinked microgels*. Soft Matter, 2012. **8**(27): p. 7234-7242.
33. Bird, R., et al., *Doubly crosslinked hydrogels prepared from pH-responsive vinyl-functionalised hollow particle dispersions*. Soft Matter, 2012. **8**(11): p. 3062-3066.
34. Cui, Z.X., et al., *A Study of Physical and Covalent Hydrogels Containing pH-Responsive Microgel Particles and Graphene Oxide*. Langmuir, 2014. **30**(44): p. 13384-13393.
35. Thaiboonrod, S., A.H. Milani, and B.R. Saunders, *Doubly crosslinked poly(vinyl amine) microgels: hydrogels of covalently inter-linked cationic microgel particles*. Journal of Materials Chemistry B, 2014. **2**(1): p. 110-119.
36. Kar, M., et al., *Synthesis and Characterization of Poly-L-lysine-Grafted Silica Nanoparticles Synthesized via NCA Polymerization and Click Chemistry*. Langmuir, 2010. **26**(8): p. 5772-5781.
37. Meng, Z.Y., G.R. Hendrickson, and L.A. Lyon, *Simultaneous Orthogonal Chemoligations on Multiresponsive Microgels*. Macromolecules, 2009. **42**(20): p. 7664-7669.
38. Inglis, A.J., et al., *Reversible addition fragmentation chain transfer (RAFT) and hetero-Diels-Alder chemistry as a convenient conjugation tool for access to complex macromolecular designs*. Macromolecules, 2008. **41**(12): p. 4120-4126.
39. Nebhani, L., et al., *Quantification of Grafting Densities Achieved via Modular "Grafting-to" Approaches onto Divinylbenzene Microspheres*. Advanced Functional Materials, 2010. **20**(12): p. 2010-2020.
40. Nebhani, L., et al., *Strongly Electron Deficient Sulfonyldithioformate Based RAFT Agents for Hetero Diels-Alder Conjugation: Computational Design and Experimental Evaluation*. Journal of Polymer Science Part a-Polymer Chemistry, 2009. **47**(22): p. 6053-6071.

41. Glassner, M., et al., *(Ultra)Fast Catalyst-Free Macromolecular Conjugation in Aqueous Environment at Ambient Temperature*. Journal of the American Chemical Society, 2012. **134**(17): p. 7274-7277.
42. Schenzel, A.M., et al., *Reversing Adhesion: A Triggered Release Self-Reporting Adhesive*. Advanced Science, 2016. **3**(3).
43. Pahnke, K., et al., *A mild, efficient and catalyst-free thermoreversible ligation system based on dithiooxalates*. Polymer Chemistry, 2016. **7**(19): p. 3244-3250.
44. Inglis, A.J., et al., *Rapid Bonding/Debonding on Demand: Reversibly Cross-Linked Functional Polymers via Diels-Alder Chemistry*. Macromolecules, 2010. **43**(13): p. 5515-5520.
45. Griffin W C. *Classification of Surface-Active Agents by "HLB"*. J. Soc. Cosmet. Chem. 1949; **1**: 311–326.

Chapter IV: Synthesis and characterization of DX hydrogels by TAD click chemistry in organic conditions

IV.1. Introduction

In Chapter III, we have demonstrated that the ring opening reaction of epoxide is an efficient synthetic approach to functionalize the microgel particle shell with cyclopentadiene (Cp) functions without compromising the colloidal stability. In this previous chapter, we tried to use the RAFT based-HDA click chemistry to promote the formation of doubly crosslinked network but for unknown reasons, we could not achieve a macrogel formation. The aim of this chapter is to replace the RAFT-based function by more reactive click moieties that will enable the crosslinking between Cp functionalized beads. For this purpose, we aim at exploiting the TAD chemistry, a powerful coupling reaction developed by some of us few years ago.^[1-3] The overall synthetic scheme of this chapter (Figure IV.1) comprises the preparation of Cp functionalized microgels by suspension polymerization and subsequent derivatization followed by their crosslinking with a bi-functionalized TAD compound. The use of this metal-free, click coupling reaction has been optimized in order to ensure reproducibility of the synthetic protocol and a high quality of DX-gels.

TAD chemistry is a promising approach as it displays an extremely high reactivity towards enes and dienes, favoring ultrafast Diels-Alder and ene-type reactions. Typically, these reactions occur in a time scale of seconds at room temperature with high conversion and without the need of any catalyst or stimuli. More interestingly, the reddish color of the TAD compound disappears after ene-coupling to resulting in a colorless product, offering a visual feedback for the progress of the reaction.^[4] According to these outstanding properties, it is believed that TAD-based coupling reaction may provide an advantageous tool to prepare DX-gels with an easy setup, a fast processability at r.t., injectability and variation of the DX-gel modulus. After demonstrating the proof of concept of using this interesting chemistry, several batches of microgels were used to demonstrate the various possibilities of tuning the mechanical properties by changing experimental parameters during the DX-gels

synthesis. The present study is based on reasonable hypotheses. We assumed that the ductility of the MG building blocks and DX-gels were intimately correlated as well as the concentration and the size of the microgels in the network. In the following sections, we test these hypotheses using MGs and DX-gels that are constructed from commercially available materials using methods that are scalable and versatile with very easy setup. Various size microgels containing different crosslinker contents were synthesized using suspension polymerization followed by click derivatization. The morphologies and mechanical properties of physical and doubly crosslinked gels were examined using SEM and dynamic rheology respectively.

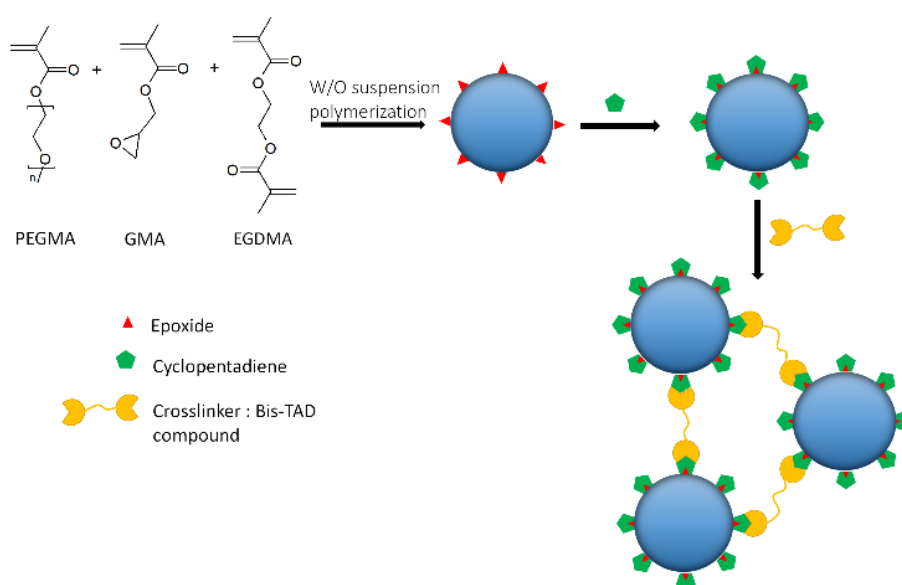


Figure IV.1: Experimental scheme for the preparation of DX-gels by TAD click chemistry.

IV.2. DX-gel synthesis using TAD click chemistry in organic medium and characterization

Doubly crosslinked (DX) gels arise from covalent bonding between microgels, resulting in a permanent monolithic hydrogel. An efficient conjugation process is therefore required to link soft microbeads all together. In the field of this work where beads are in the size range of microns, it is of importance to select a conjugation process that ensures the coupling of localized functions in an additive-free way. Hetero Diels Alder click reactions involving Cp have already been demonstrated as a powerful technique in terms of efficiency, allowing to obtain very high molecular weight block copolymers in less than 10 minutes, starting from end-functional high molecular weight polymer

precursors.^[5, 6] Herein, we take advantage of the ultrafast TAD-based HDA click chemistry to interconnect the microgels. For that purpose, a bis-TAD functional crosslinker, 4,4'-(4,4'-diphenylmethylene)-bis-(1,2,4-triazoline-3,5-dione) (MDI-TAD, Figure IV.2), was synthesized according to a reported procedure.^[1]

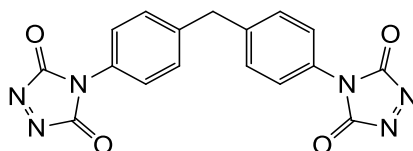


Figure IV.2: Structure of 4,4'-(4,4'-diphenylmethylene)-bis-(1,2,4-triazoline-3,5-dione) (MDI-TAD).

Practically, a concentrated suspension of Cp-functionalized microgels (as prepared in the Chapter III, Table II.4, entry B, $d = 23 \mu\text{m}$) was stirred at r.t. and MDI-TAD was added directly into the suspension. Different amounts of crosslinker were added, based on the Cp content retained by the beads as determined by UV titration, to check the influence of the crosslinker quantity on the gel formation. Hydrogel formation begins immediately after addition of the MDI-TAD. On the one hand, at too low MDI-TAD concentration, there is insufficient amount of crosslinker and ill-defined materials are obtained. On the other hand, when a too high concentrations of MDI-TAD is used, gelation did not occur. Obviously, the first HDA reaction is faster than the second reaction step, which results in saturation of the Cp moieties at higher crosslinker concentrations. Only at intermediate MDI-TAD concentrations closer to the stoichiometric composition, homogenous hydrogels were formed within seconds, as shown in Figure IV.3 and Table IV.1. As described in chapter III, we were never able to obtain such hydrogels with the Cp RAFT-HDA approach. Then, Cp microgels and DX-gels were characterized by high resolution MAS NMR to attest the formation of the Diels-Alder adduct from the reaction of the diene with the TAD species. As showed in Figure IV.4, signals corresponding to the microgels can be easily seen (between 0.5 and 4.5 ppm), but unfortunately cyclopentadiene and its corresponding clicked adduct aren't noticed. To better understand this, the actual Cp content (in mass) is compared to the relative mass of the microgels taking into account the respective amount of bis-TAD crosslinker added. Therefore, it was calculated that the weight content of the adduct represents around 0.12 % of the DX-gel system, which is then very difficult to see by NMR, specially due to the relative poor sensitivity of diene in NMR. This

proportion is calculated by using the Cp content determined by UV assuming that all the MDI-TAD used is consumed.

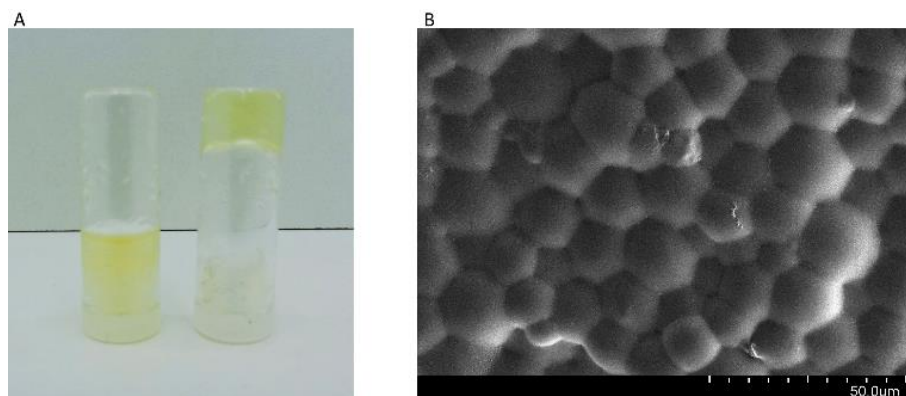


Figure IV.3: A) Picture of gel (right) formed within 2 minutes after addition of the MDI-TAD onto a microgel suspension (entry D table IV.1) and (left) microgel suspension (Entry A table IV.1) B) SEM image of a DX-gel.

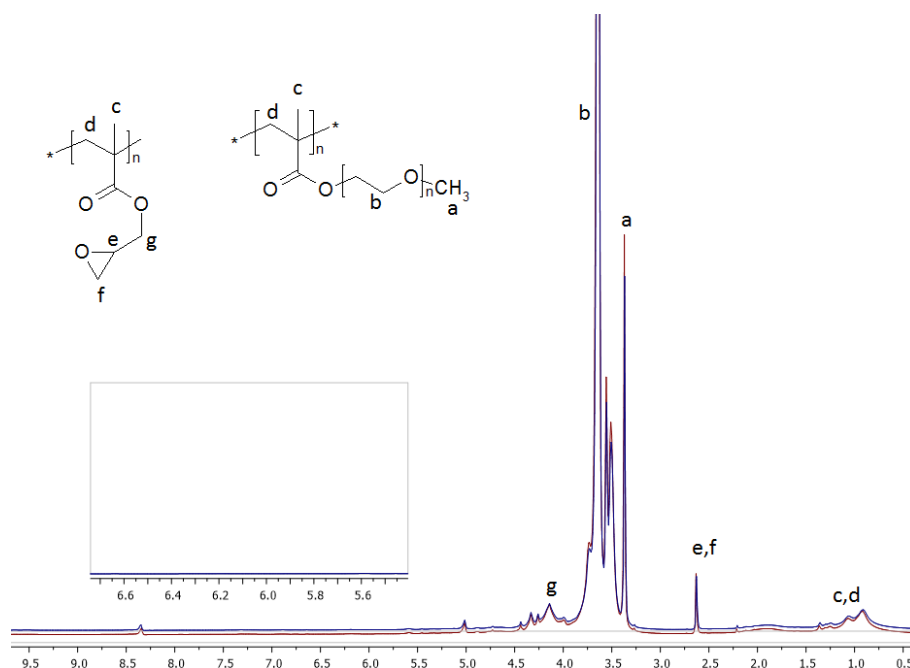


Figure IV.4: ^1H -MAS NMR of respectively in blue and red Cp functionalized microgel and doubly crosslinked gels (entry D, table IV.1) and a zoom in the region where the TAD-Cp adduct should be localized.

TABLE IV.1: G' evolution of the DX-gels with the TAD/Cp ratio.

Samples	Ratio TAD/Cp	Gelation Time (s)	G' (Pa)
A	0	No gel	25 ± 3
B	0.7	300	86 ± 8
C	0.8	15	90 ± 9
D	0.875	15	112 ± 10
E	1.05	15	92 ± 9
F	1.22	30	84 ± 8
G	2.5	No gel	24 ± 3

Dynamic rheology was used to probe the mechanical properties of the DX-gels using parallel plate geometry. The data were compared to the precursor microgel suspension at the swollen state. The microgel suspension was homogeneously dispersed before DX-gel formation to promote homogenous density of microgel in the resulting DX-gel. The storage modulus, G' , reflects the solid-like component of the rheological behavior, which is thus low at solution stage but increases drastically after gelation (G'' is the loss modulus and $\tan \delta = G''/G'$). Samples are first subjected to a strain sweep from 0 % to 15 % to define the linear viscoelastic region in which the modulus G' and G'' are independent of the applied strain. In our experiment, the strain amplitude was set as 0.5 % and G' and G'' of the different DX-gels were probed over a period of measurements of a duration of 5 minutes to verify the influence of the crosslinker quantity on G' of the resulting DX-gel.

For both DX-gels and microgel suspension, the storage modulus (G') values are higher than the loss modulus, indicating a gel-like behavior as defined in Winter and Chambon criteria.^[7] This data shows that the precursor microgel suspension exists as physical gels prior to the second level of crosslinking as also stated in the paper of Saunders *et al.*^[8] The variation of G' for the DX-gels as a function of the crosslinker quantity is demonstrated in Figure IV.5.

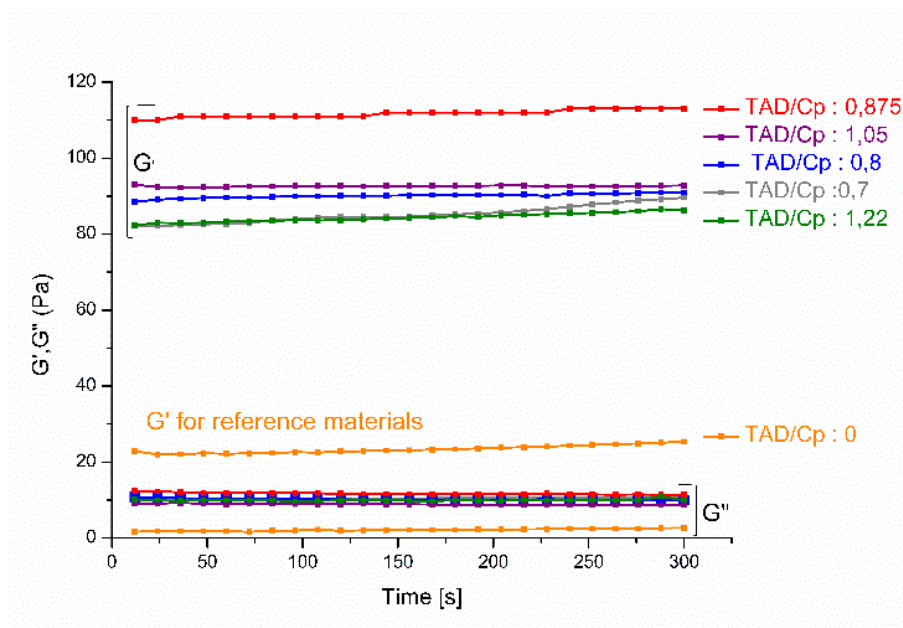


Figure IV.5: Mechanical properties characterizations of DX-gels obtained at various TAD/Cp ratios and of the starting microgel suspension by rheology at r.t.

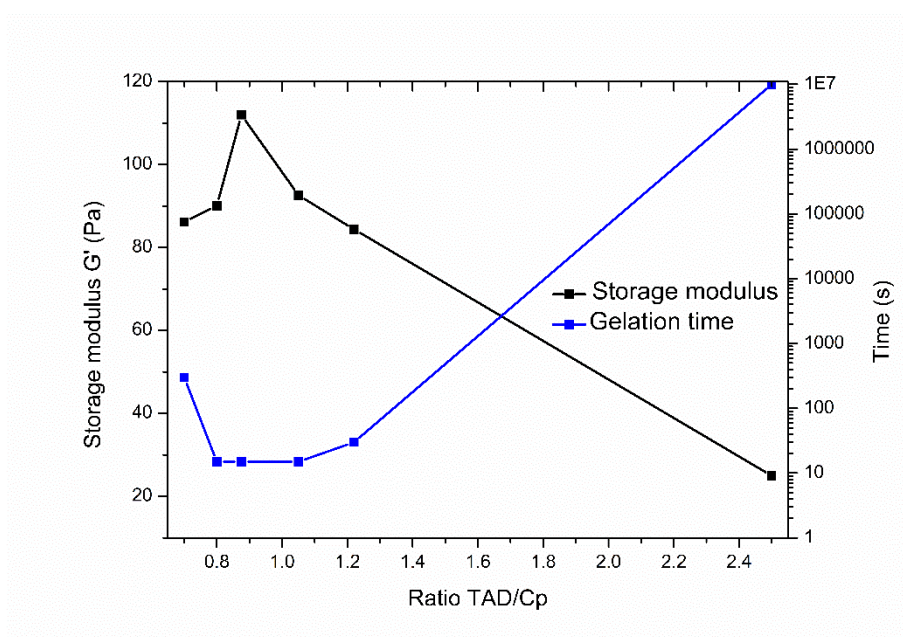


Figure IV.6: Comparative evolution of G' (in black) and gelation time (in blue) with TAD/Cp ratio.

This data reveal that the DX-gels had consistently higher G' values than the precursor microgel suspension (25 Pa, entry A) and that the G' value increased by approximately a factor of 4 for the DX-gel (see Table IV.1). The increased G' values can be attributed to the additional covalent crosslinking adducts from the cyclopentadiene/TAD reaction. It was expected that increasing the crosslinker quantity will lead to a higher value of G'

but interestingly, a maximum in G' is observed after adding an amount of MDI-TAD, corresponding to a ratio of TAD/Cp of 0.875. Confirming previous observations, a further increase in the quantity of MDI-TAD leads to a decrease of the storage modulus and even to no gelation if a large amount of MDI-TAD is added as depicted in Figure IV.6.

This decrease in G' and gelation time can be explained by the saturation of the microgel surface by the MDI-TAD, reducing drastically the amount of Cp available to be enrolled in the formation of the second network. This data nicely validates our approach to prepare DX-gels by click chemistry. As the gelation time can be varied from seconds to minutes, moldability tests of microgels suspension were performed as depicted in Figure IV.7 as a proof of concept of injectability. Depending on the mold shape, square or triangle-shaped hydrogels have been obtained in few minutes.



Figure IV.7: Moldability tests performed using the conditions presented in table IV.1, entry B. Square (top) or triangle shaped (bottom) DX-gel.

Samples were completely moldable and various shapes could be prepared using these conditions. This procedure thus provides a great flexibility in designing the shape of the hydrogel structure. The fast kinetic of gelation is an additional advantage as it takes its final 3D shape in a minute, which is sometime a prerequisite in biomedical field. However, mechanical properties of these gels are not adapted for any biomedical applications as they are too brittle. Indeed, they broke easily under small handlings. Therefore, we studied below the influence of various parameters that could modulate

the final properties of the gels. For this purpose, we have adopted the same philosophy than the one used to prepare conventional networks: variation of the monomer concentration and the crosslinking density in the primary beads. Also, the impact of testing conditions can be investigated.

IV.3. Investigation of the mechanical properties of doubly crosslinked gels

IV.2.1. Introduction and generalities

We demonstrated above the potential of using TAD click chemistry for the synthesis of doubly crosslinked networks with a very easy setup and fast kinetics of reaction. However, when compared to high ductility gels such as double network hydrogels [9], our doubly crosslinked microgels were relatively brittle. The motivation behind this subsection is to establish and improve our DX-gels system by studying effects of various parameters on the synthesis of a DX-gel. This present section is based on reasonable hypothesis. We assumed that the ductility of the microgel building blocks and DX-gels were intimately correlated as well as the concentration and the size of the microgels in the network. In the following section, we test these hypotheses using microgels and DX-gels that are constructed from commercially available materials using methods that are scalable and versatile with easy setup. As depicted in Figure IV.8, various size microgels containing different crosslinker contents were synthesized using suspension polymerization followed by click derivatization as discussed in Chapter III. In our approach PEG-GMA MG particles containing a small proportion of crosslinker (EGDMA) were functionalized with cyclopentadiene via ring opening of the epoxide. Concentrated Cp functionalized PEG-GMA MG dispersions were covalently crosslinked using bis-TAD moieties to give PEG-GMA-DX MGs (Figure IV.1). In this section, we first determine the compositions of Cp content of MG particles using UV to quantify the extents of Cp functionalization. Particle size measurements and optical microscopy images were used to determine the diameter of microgel particles and their morphologies. Doubly crosslinked gels were synthesized as described above. The morphologies of the various obtained DX-gels are investigated using SEM and the mechanical properties were probed using dynamic rheology.

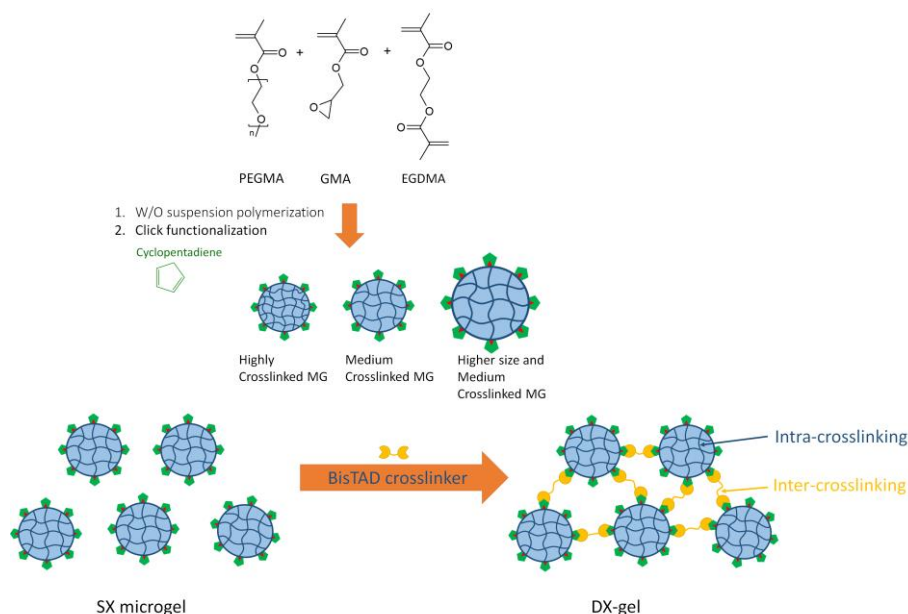


Figure IV.8: Depiction of the method used to prepare microgels (MG) and DX-gels for this study.

Suspension radical polymerization was used to produce a series of microgels varying in terms of size and crosslinking density. Two batches of microgels with an initial $[M]_0/[I]_0/[C]_0$ ratio of 1/0.05/0.1 but presenting respectively diameter sizes around 25 μm and 45 μm were synthesized by adapting the stirring rate from 800 to 400 rpm, respectively. A batch with more crosslinked beads was obtained by applying the same process to a monomer solution presenting a higher concentration in EGDMA crosslinker to reach an initial ratio $[M]_0/[I]_0/[C]_0$ of 1/0.05/0.15. The resulting beads are characterized with a size around 20 μm . Subsequently, the method used for cyclopentadiene functionalization of the microgels involved epoxide ring-opening through reaction with sodium cyclopentadiene and was described in details in the previous chapter. After functionalization, microgels were washed successively by a saturated solution of ammonium chloride, acetone, ethanol-water (1/1), 3% HCl in water, water, THF and hexane. Optical microscopy was used to verify the spherical morphology of the Cp-microgels as depicted in Figure IV.9. Particle size measurements determined the number-average diameters and the size polydispersities. The diameters were in the range of 25 μm and any significant change can be noticed after functionalization. The coefficients of variation were in the range of 20–30 % and were consistent with earlier reports. To determine the extent of functionalization of cyclopentadiene (Cp), the Cp contents were determined using UV

titration and varied from 8.7 $\mu\text{mol/g}$ of swollen microgels to 15.2 $\mu\text{mol/g}$ depending on the experimental conditions used for the batch synthesis. Characteristics of the microgels used for this study are detailed in Table IV.2.

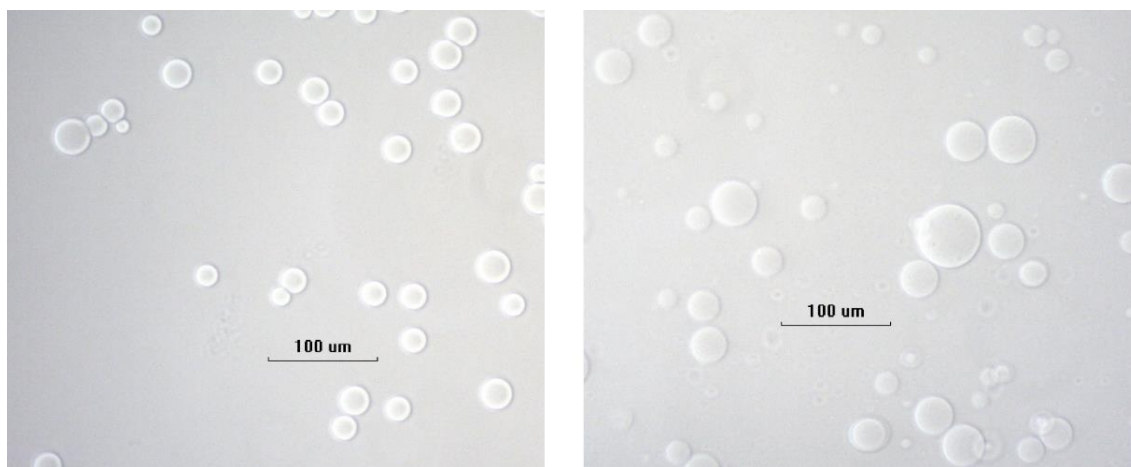


Figure IV.9: Image of purified microgels entry A (left) and C (right) swollen in water (Table IV.2).

Table IV.2: Characteristics of the microgel batches prepared by suspension radical polymerization.

Samples	$[M]_0/[I]_0/[C]_0$	Stirring rate (rpm)	Size (μm) ^a	Swelling ratio ^b	Cp Loading capacity ($\mu\text{mol/g}$) ^c
A	1/0.05/0.1	800	25 ± 6.9	14.3 ± 0.6	10.9
B	1/0.05/0.15	800	17 ± 5.7	11.4 ± 0.6	15.2
C	1/0.05/0.1	400	44.6 ± 14.9	13 ± 0.3	8.7

- a) As attested by particles size measurements.
- b) Measured and calculated by gravimetric measurements in water.
- c) As calculated by UV titration measurements using PTAD.

Mechanical properties of a single microgel from entry A and B Table IV.2 were probed using nanoindentation and AFM in tapping mode to demonstrate the correlation of mechanical properties at microgels level towards the DX-gels level. Unfortunately, none of these experiments were successful as the microgels were respectively too soft to make a good indent by nanoindentation and too large for the AFM equipment.

As we believe that concentration of the building block *i.e.* microgel concentration plays an important role in the final properties, viscosities of solutions containing various concentrations of microgels were analyzed to demonstrate this behavior. Literature refers an exponential evolution of viscosity for suspension of microgels with increasing

concentration.^[10-12] As expected, increasing microgels concentration from 0.05 w% to 5 w% increases drastically the relative viscosity of the medium as depicted in Figure IV.10, which therefore comforts our idea that microgels concentration will impact the properties of the colloidal suspension as well as of the resulting DX material. Literature refers similar values of viscosity for other microgel suspensions.^[10-12]

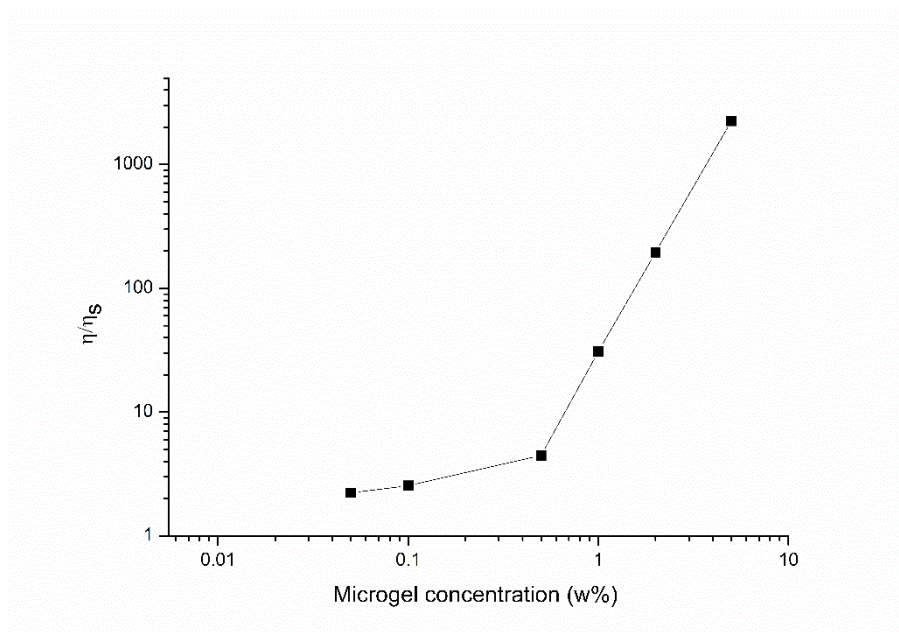


Figure IV.10: Evolution of the relative viscosity with microgels concentration (w%).

IV.2.2. Morphology of DX-gels and their swelling properties

The DX-gel formation involved a covalent interlinking of the particles to form a permanent gel as depicted in Figure IV.3. As previously noticed, microgels suspension behaves already like a gel due to their high concentration and high swelling ratio. DX-gels morphologies were first studied in their swollen state (in butyl acetate) by conventional optical microscopy as depicted in Figures IV.11 and IV.12. As expected, Figure IV.12 highlights a monolithic structure composed of interconnected beads (Table IV.2, entry A). Optical microscopy is limited due to the different height into the samples. Therefore, DX-gels morphologies of freeze dried DX-gels were imaged using SEM as presented in Figure IV.13. SEM analyses confirmed also that DX-gels were the result of interlinking of the spherical microgels. A closer look at the SEM images allowed to notice that some beads are also deformed to maximize the surface contact with the beads in their neighborhood. This is making possible owing to their soft nature allowing deformation of their morphology. The SEM images also show that the DX-

gels packing was disordered for the macroscopic gel in contrast to other DX-gels prepared where they presented a hexagonal array of points.^[13] For these DX-gels, it was suggested that such a behavior is favored for DX gels composed of microgel particles with low size polydispersity (<10%) which was not the case here.



Figure IV.11: Morphology of a DX-gel by optical microscopy (Table IV.2, entry A).

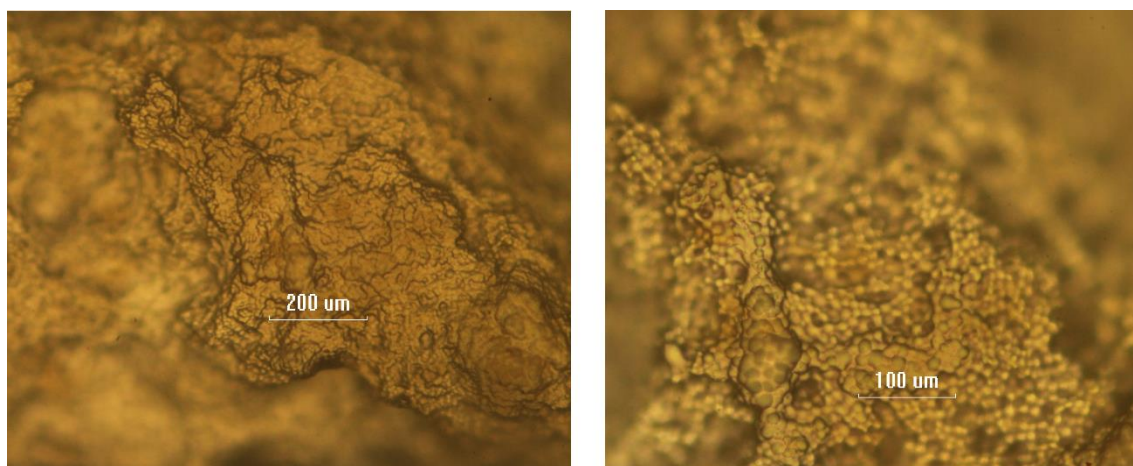


Figure IV.12: Picture of a swollen DX-gel swollen in butyl acetate upon magnification (10x).

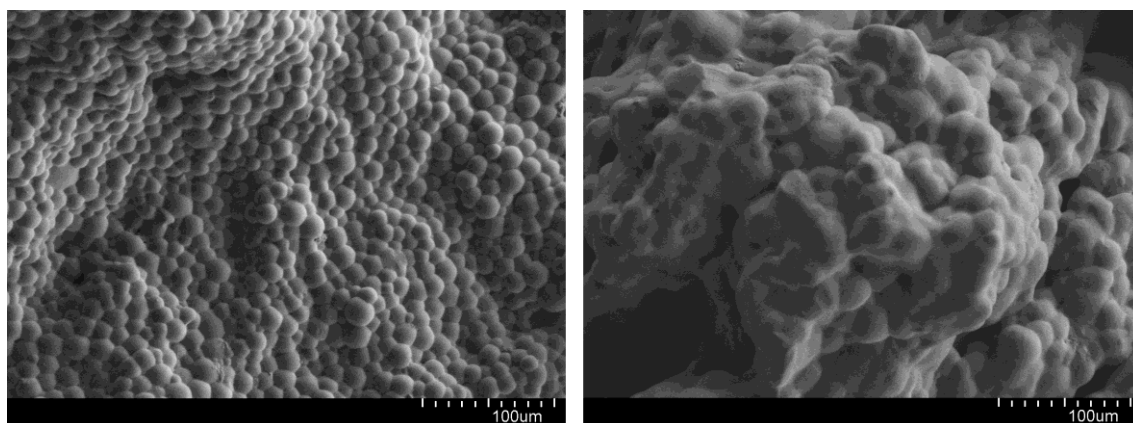


Figure IV.13: Morphologies of covalent DX-gels after click coupling of Cp-microgels with BisTAD (prepared from microgel table IV.2 entry A (left) and entry C (right) with a TAD/Cp ratio of 0.8).

As expected for any crosslinked systems, the swelling degree is an important parameter to evaluate. The swelling of a gel is controlled by the affinity of the polymer with the solvent and the density of reticulation. The crosslinking brings retractile forces that limit the expansion of the network in the solvent. For this study, slabs of 2 DX-gels, distinct in terms of initial crosslinking ratio in the primary beads, were immersed in butyl acetate and their swelling degrees were measured versus time in triplicate. As depicted by Figure IV.14, no more than 30 minutes are required in both cases to reach an equilibrium. This fast swelling kinetic is often observed in the case of DX-gels.^[14] Indeed, these remarkably faster kinetics arise from the small dimensions of the microgel particles that form the scaffold structure; the smaller size speeds the diffusion of fluid through the microgel particles and also in voids created by the interlinking, thereby reducing the relaxation time of the gel (variation of size versus time) in favor to a large engulfment of water at the beginning of the swelling process. Obviously, the DX-gels made from less crosslinked microgels (M/I/C of 1/0.05/0.1) swell more than the DX-gels prepared with more crosslinked microgels (M/I/C ratio of 1/0.05/0.15) to reach a S_{eq} of 8 and 10.5, respectively.

$$S_{eq} = \frac{M_s - M_d}{M_d}$$

Where S_{eq} , M_s , M_d are respectively the swelling ratio, the mass swollen and the dry mass.

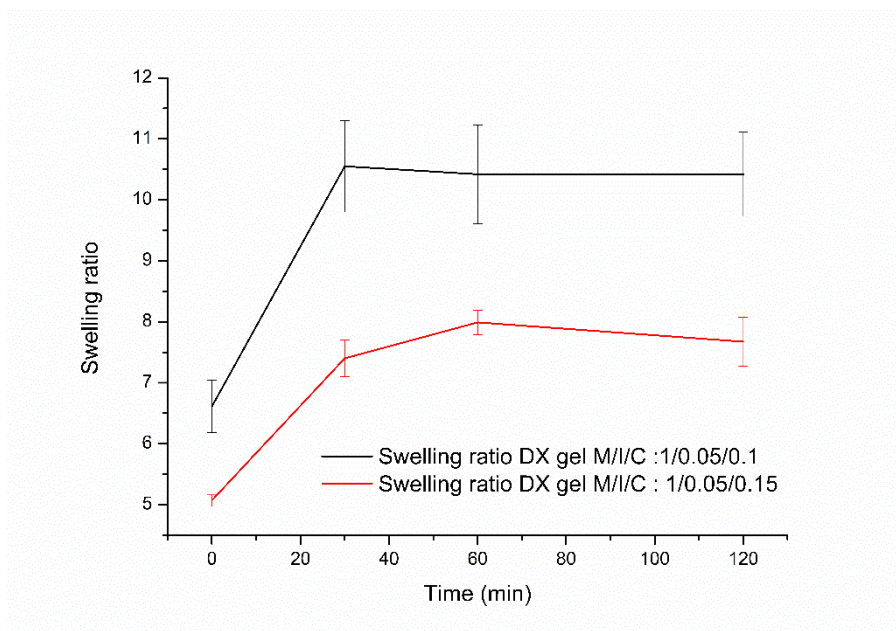


Figure IV.14: Swelling behavior in butyl acetate of two covalent DX gels prepared from microgels presenting two different densities of crosslinking (table IV.2, entry A and C, TAD/Cp ratio of 0.8).

IV.2.3. Investigation of mechanical properties of the DX-gels

IV.2.3.1. Comparison of the mechanical properties of the microgels with their DX-gels counterpart

Concentrated SX MG dispersions of 8.75 w% were first prepared in butyl acetate at room temperature. For this study, microgels from Table IV.2, entry A were chosen. The swollen microgel suspensions present physical gel properties. Indeed, a physical gel forms because the microgels are unable to move past each other's due to excluded volume effects. This explains why G' is higher than G'' in Figure IV.15. Furthermore, the Cp groups are believed to be present mostly at the periphery of the MG particles. The crosslinker (Bis-TAD) with an initial TAD/Cp ratio of 0.8 was added to the concentrated microgel dispersions and stirred to homogenize. Conversion of SX microgels into DX-gels operates within a minute. Since this strategy presents key advantages in the biomedical field to inject soft materials able to fill ill-defined voids, it is important to evaluate their rheological properties. First, strain sweep measurements were realized to determine the linear region where G' and G'' were independent from the strain applied. All strain-sweep data exhibited linear G' and G'' regions at low strain values. When the SX microgels and DX-gels are compared, it can be seen that the G'

values in this region increased from 300 up to 1000 Pa with the second level of crosslinking, which was expected.

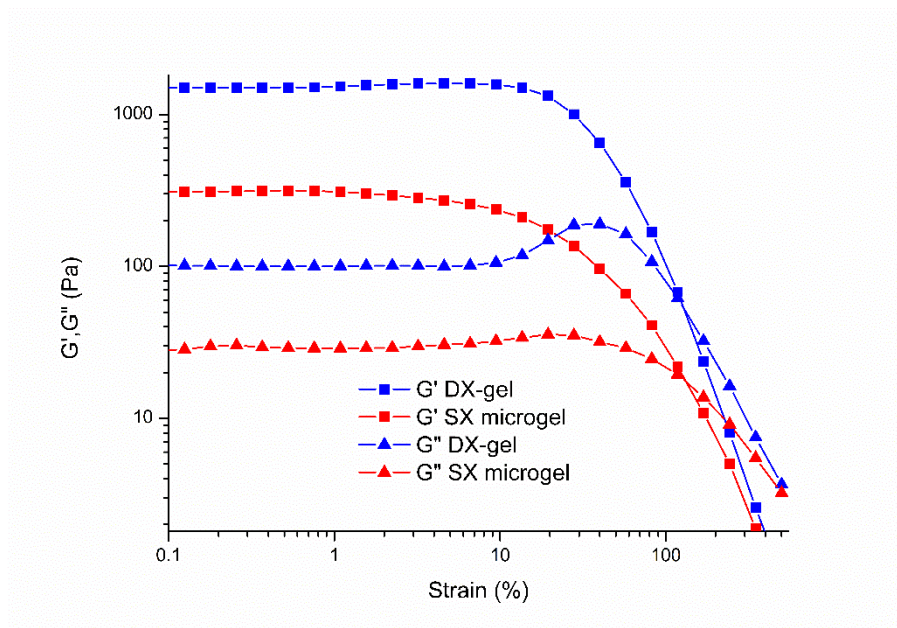


Figure IV.15: Strain sweep evolution of SX microgel and DX-gel.

When strain increases, it can be noticed that the G' values decreased and an increase of G'' occurred at intermediate strains. Finally the G' data passed through a point where $G'' = G'$. The strain when $G'' = G'$ is the critical strain (γ_c) which is a measure of the strain at which the gel fails. After passing this point the DX-gels look like the original suspension of microgels before crosslinking. In this context, the critical strain γ_c can be used as a measure of the ductility of the gels.

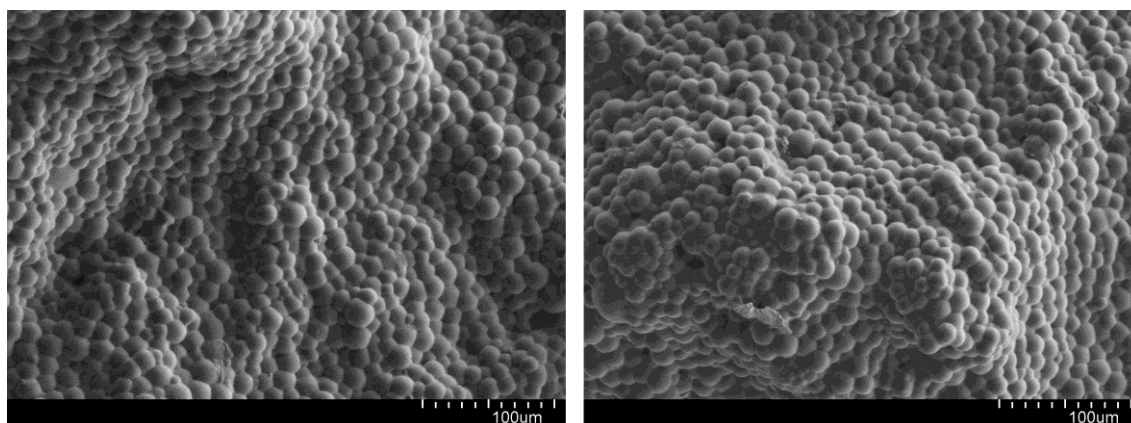


Figure IV.16: SEM image of DX microgels before and after the strain sweep.

In the case of SX microgels, the behavior is slightly different. The strain-induced breaking of the SX microgels can be explained using the cage breaking theory, which is often used to describe the rheology of concentrated dispersions.^[15] In this theory, each particle is trapped in a cage made of the nearest neighbor particles.^[16] Therefore, the γ_c value for the SX microgels can be considered as the minimum strain for a particle to escape from the cage. By contrast, the cages were locked together by relatively strong inter-microgel crosslinks for the DX-gels. In their recent paper, Saunders *et al.* proposed that internal failure of the intra-particle network within the microgels determined the γ_c values.^[17] SEM pictures (Figure IV.16) showed that the microgels remain intact and maintain the structure of the microgel components after gel failure for DX-gels prepared with high concentration of microgels, meaning that the intercrosslinking determined the γ_c value of the gel.

When the highly concentrated microgels suspension and DX-gels are compared, it can be seen that the G' values are increased by approximately a factor of 3 for the DX-gels compared to the SX microgels, as expected due to the creation of new covalent crosslink between the microgels. G' values were almost frequency independent. This behavior was also observed for the SX microgel (not doubly crosslinked). Consequently, the low frequency dependence for the G' values was attributed to the close packed nature of the microgel particles within the gels, rather than the inter-microgel linking as depicted in Figure IV.17.

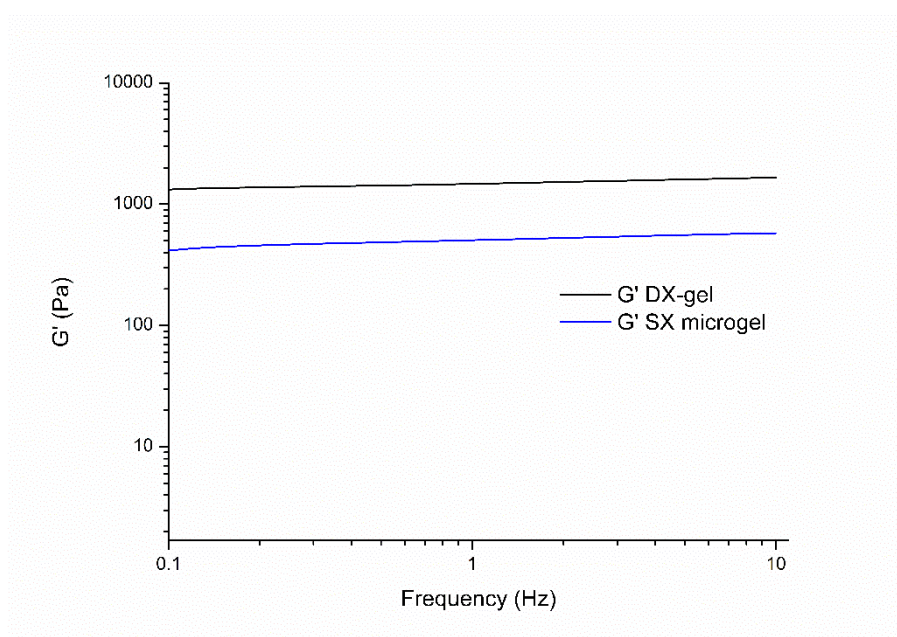


Figure IV.17: Frequency sweep evolution of G' for SX microgels and the corresponding covalently DX-gels.

Figure IV.18 shows that DX-gel formation decreases the $\tan \delta$ value ($\tan \delta = G''/G'$), which has been reported for acrylate based DX-gels^[18] as well as for divinyl benzene-based and a mix of acrylate and divinyl-benzene based crosslinker.^[17] This decrease of $\tan \delta$ and increase of G' compared to SX microgel are attributed to the formation of elastically effective linkages between neighbouring particles. The new inter-particle elastically effective chains resist shear and hold the network together. The frequency dependences of $\tan \delta$ are slightly different for the DX-gel and SX microgels at higher frequency. The $\tan \delta$ value increases over frequency for SX microgels while the trends are less frequency dependent for the DX-gel. Such difference of behavior arises from the interconnections between the beads that bring elasticity, indicating therefore extended covalent network formation within the DX-gel. All of the microgels produced in this study satisfy the most widely invoked criterion to be considered as gels *i.e.*, $\tan \delta < 1.0$.

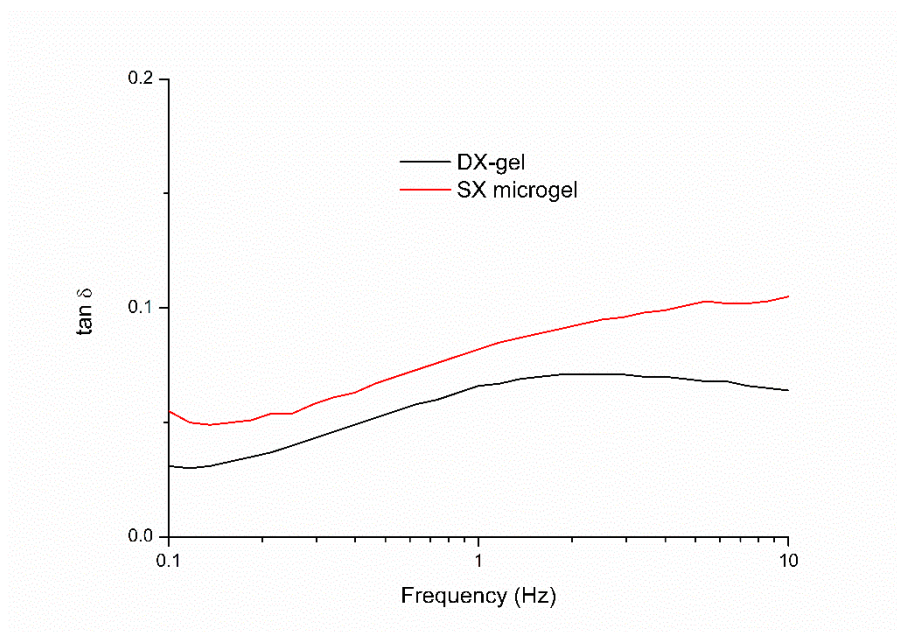


Figure IV.18: Frequency sweep data evolution of $\tan \delta$ for SX microgels and the corresponding covalently DX-gel (Table IV.2 entry A).

IV.2.3.2. Effect of microgel concentration (CMG) on the dynamic rheological properties

DX-gels attract great interest in the biomedical field as injectable biomaterial for tissue engineering or drug release. Depending on the injection site, surrounding tissues are characterized by different mechanical strength. Therefore, it is of prime interest to

design materials with adapted properties able to support biomechanical meaningful loads or to prevent important frictional effects. In that field, Saunders *et al.* investigated the impact of the pH on acid methacrylic-based DX-gels ^[18] but no relationship has been established yet between morphology and final mechanical properties of DX gels. Since our DX-gels are brittle, we aim at investigating the tuning of the mechanical properties by modification of several parameters. First, the effect of initial microgel concentration was studied by dynamic rheology. Frequency-sweep dynamic rheology measurements were obtained for gels prepared using a range of microgels concentrations ranging from 7,5 w% to 12 w% and are shown in Figures IV.19 and Figure IV.20. The G' (storage modulus) values have very low frequency dependence for all investigated concentrations and the gels exhibited solid-like viscoelastic behavior, which is a common characteristic for DX-gels.^[19, 20] The $\tan \delta$ values ($= G''/G'$) were less than 0.10 showing therefore that the DX-gels presented mostly elastic behavior. Moreover, the $\tan \delta$ values were in the range 0.02 to 0.08 for the gels containing a microgel concentration ≤ 12 wt%. These values mean that 92 % of the mechanical energy used to deform the DX-gel matrix was stored for these systems. The $\tan \delta$ values for all the different DX-gels were similar and were therefore not impacted by the initial microgel concentration. However, the $\tan \delta$ values increase as a function of frequency, suggesting that the DX-gels were not ideally elastic. An explanation of this behavior has been presented by B. Saunders' group. In their paper, they observed an increase of $\tan \delta$ over frequency for particular DX-gels and claimed that such a $\tan \delta$ behavior comes from the fact that the resulting DX-gels formed elastically ineffective chains that give rise to frequency dependent $\tan \delta$ values. Such chains may result from trapping of microgel particles into structural arrangements that do not allow sufficient movement for interlinking to occur. They observed specially this behavior for highly functionalized microgels or highly swellable microgels.^[13]

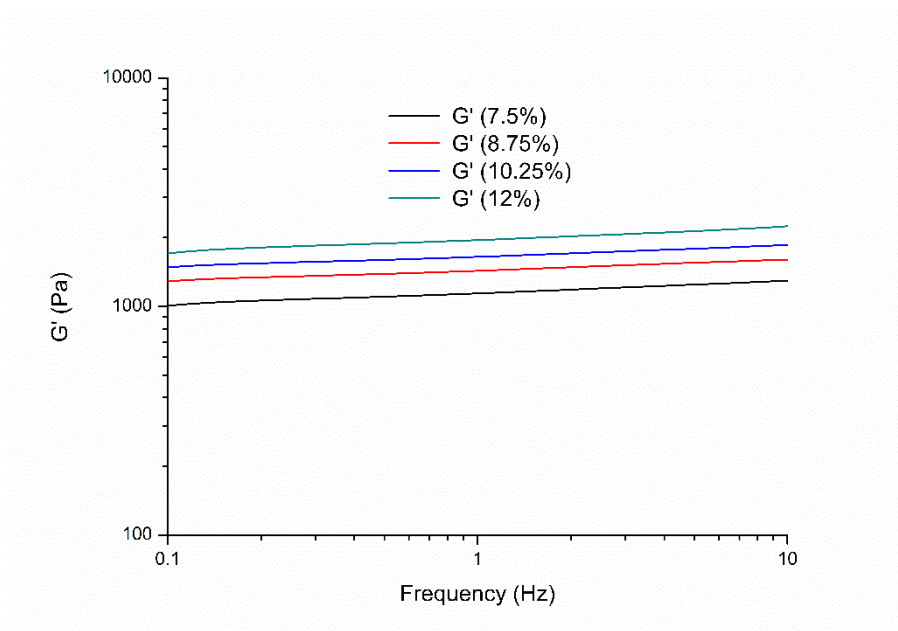


Figure IV.19: Effect of microgel concentration on DX-gels mechanical properties.

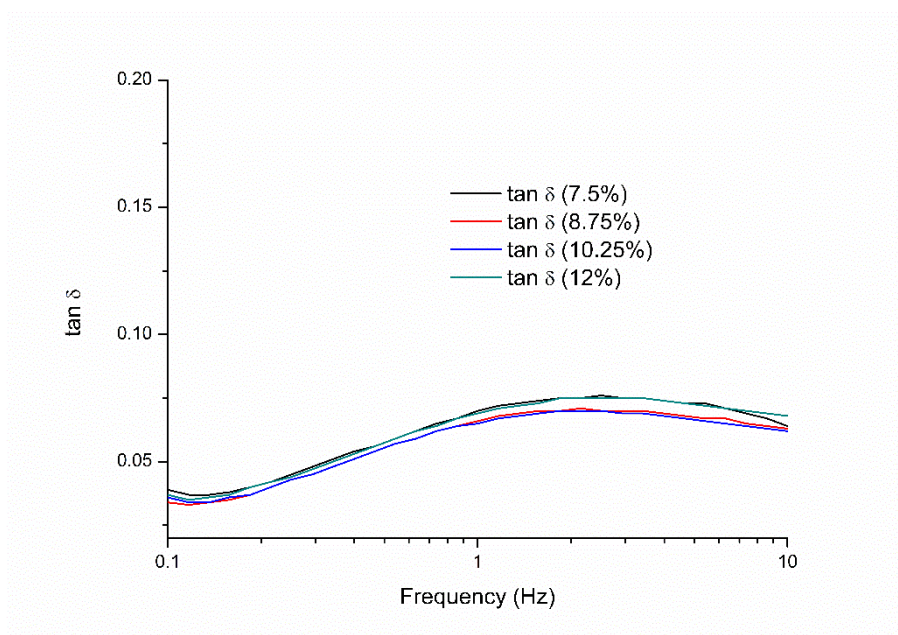


Figure IV.20: Evolution of $\tan \delta$ with MG concentration.

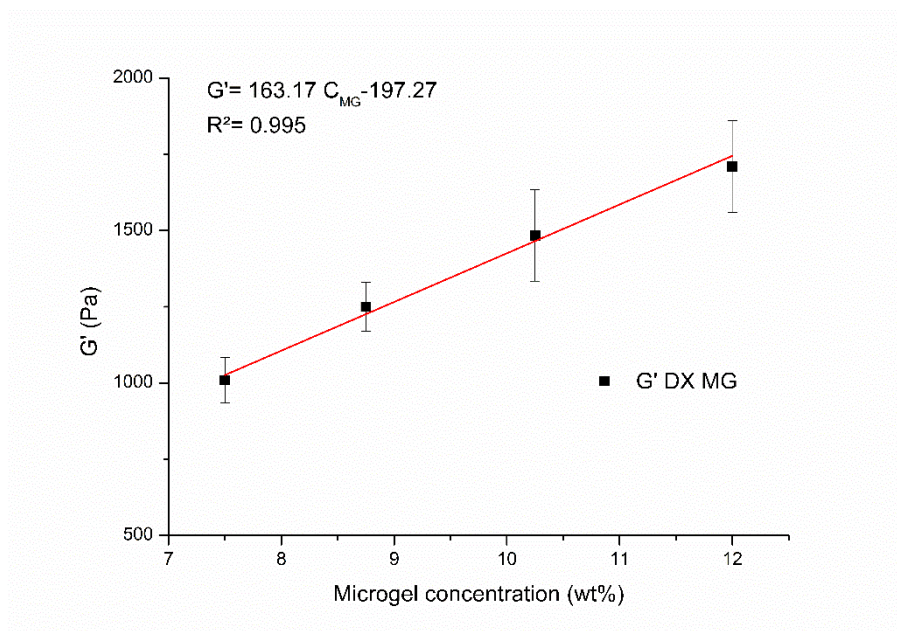


Figure IV.21: Dependence of G' with microgel concentration.

The G' values were plotted as a function of microgels concentration and not as a function of the effective volume fractions as sometime reported in the literature (Figure IV.21). Even though effective volume fraction occupied by microgel are reported for concentrated microgels dispersion, such values usually are determined using low concentration viscosity measurements, which can be very different at high concentration.^[21-23] Indeed, extrapolation of those values to higher concentrations closer to the one use for the preparation of DX-gels often results in effective volume fraction values that are higher than unity. Therefore, such values offer limited insight beyond showing that the microgels particles have deformed. Therefore, weight microgels concentration values were used in this work. It was taken into account that most likely the microgel particles were deformed for covalent gels as depicted in Figure IV.16. Interestingly, the storage modulus (G') data showed a linear increase with microgel concentration as depicted in Figure IV.21. Such a behavior was unexpected and differs completely from conventional acrylate based doubly crosslinked gels. Indeed, acrylate based doubly crosslinked gels have been reported to show exponential dependence of G' with the microgels concentration.^[24] It was assumed that our doubly crosslinked system presents properties close to the doubly crosslinked gels of Saunders' group who observed the same behavior for a methacrylic acid based microgel. In their paper, they synthesized doubly crosslinked gels by radical coupling of vinyl functionalized microgels. While they were not certain of the cause of this

difference that contrasts with conventional acrylate doubly crosslinked microgels, they suggested that the linear behavior observed might be aided by the strong swelling nature of the microgel particles favoring efficient inter microgel covalent bonding.^[13]

IV.2.3.3. Effect of microgel intra-crosslinking density on the dynamic rheological properties

The second parameter investigated was the intracrosslinking density variation. It is well-established by Flory that increasing crosslinking degree will increase stiffness of materials. Therefore, increasing the crosslinking density of the primary beads might impact the mechanical properties of the resulting DX-gels. As showed in Figure IV.22, increasing the microgel intracrosslinking leads to an increase of both the stiffness and the storage modulus. Indeed, by increasing the ratio of microgel intracrosslinkg from 10 to 15 % (compared to monomer) the storage modulus of the resulting DX-gels increases by around 50% for a TAD/cp ratio of 0,8. Interestingly, increasing the crosslinking density leads also to a higher $\tan \delta$ value, suggesting that these DX-gels are less elastic as depicted in Figure IV.23. However, even there are more inelastic linkages, DX-gels produced from more crosslinked microgels present a higher storage modulus.

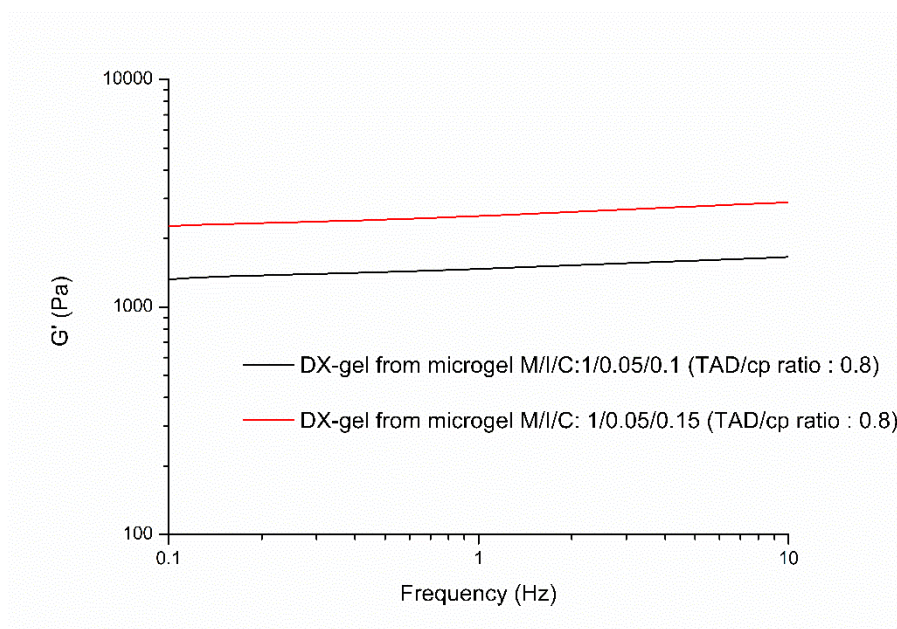


Figure IV.22: Frequency sweep data evolution of G' for DX-gels prepared using microgels with M/I/C of 1/0.05/0.1 and 1/0.05/0.15 (microgel concentration: 8.75%).

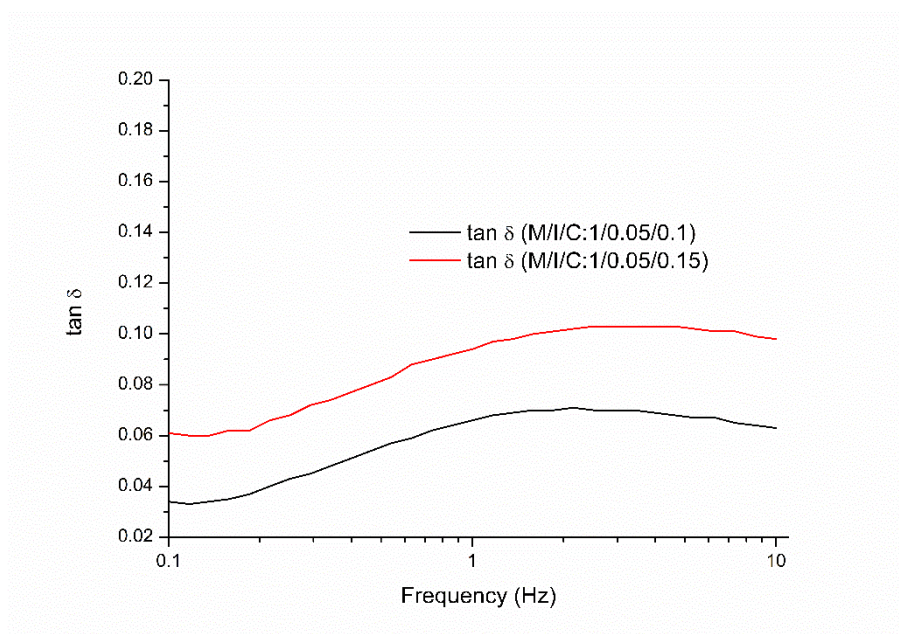


Figure IV.23: Frequency sweep data evolution of $\tan \delta$ for DX-gels prepared from microgels with M/I/C of 1/0.05/0.1 and 1/0.05/0.15 (microgel concentration: 8.75%).

IV.2.3.4. Influence of the microgel size over mechanical properties of DX gels

In a last series of experiments, the size of the “building block” microgels was studied by comparing DX-gels prepared from microgels characterized by the same crosslinking density (M/I/C of 1/0.05/0.1) but varying in size, ranging from 25 to 45 μm . As the size is different, it is expected that smaller microgels will pack better and fill in the interstices to maximise interlinking between the beads in the final DX-gels. This difference of packing might lead to stronger DX-gels. Beads of two different sizes were obtained by free radical polymerization in suspension by modulation of the rate of stirring during the polymerisation. Rates of 400 and 800 rpm led to particles of 45 and 25 μm , respectively. As depicted in Figure IV.24, DX-gels made of smaller microgels present a higher storage modulus with a significative jump of 300 Pa, confirming our postulate of packing density. Surprisingly, $\tan \delta$ evolution differs a lot for these two DX-gels as depicted in Figure IV.25. $\tan \delta$ of the DX-gel produced from 25 μm size microgels presents an increase over frequency while the DX-gel made from 45 μm -size microgels presents a small decrease over frequency, meaning that over frequency the system

tends to be more elastic. This experience demonstrates that playing with micro-bead size allow to modulate the stiffness of DX materials.

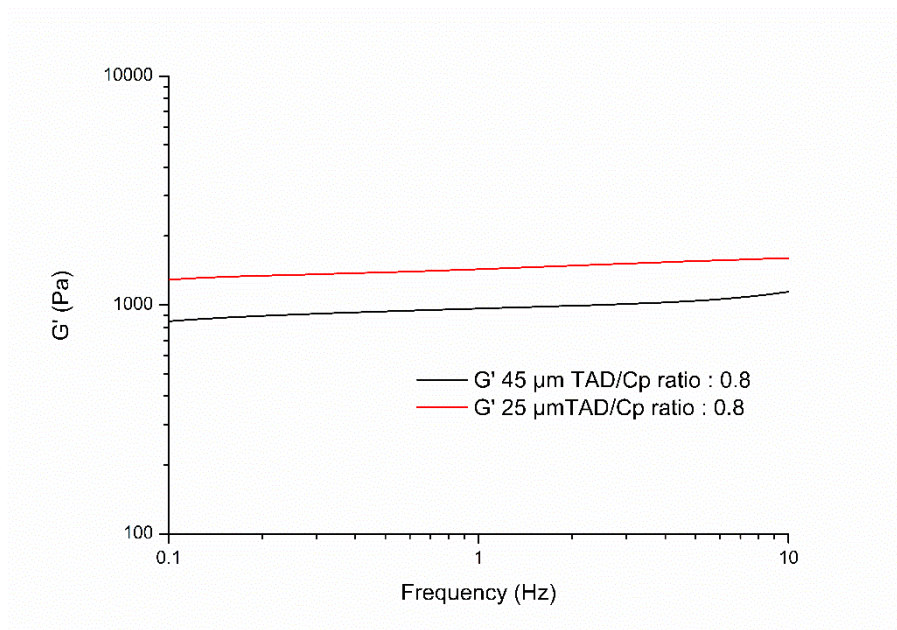


Figure IV.24: Storage modulus of DX-gels prepared from microgels of constant crosslinking density (M/I/C of 1/0.05/0.1), and with a size of the primary beads of 25 μm (red line) and 45 μm (black line). Initial microgel concentration of 8.75%.

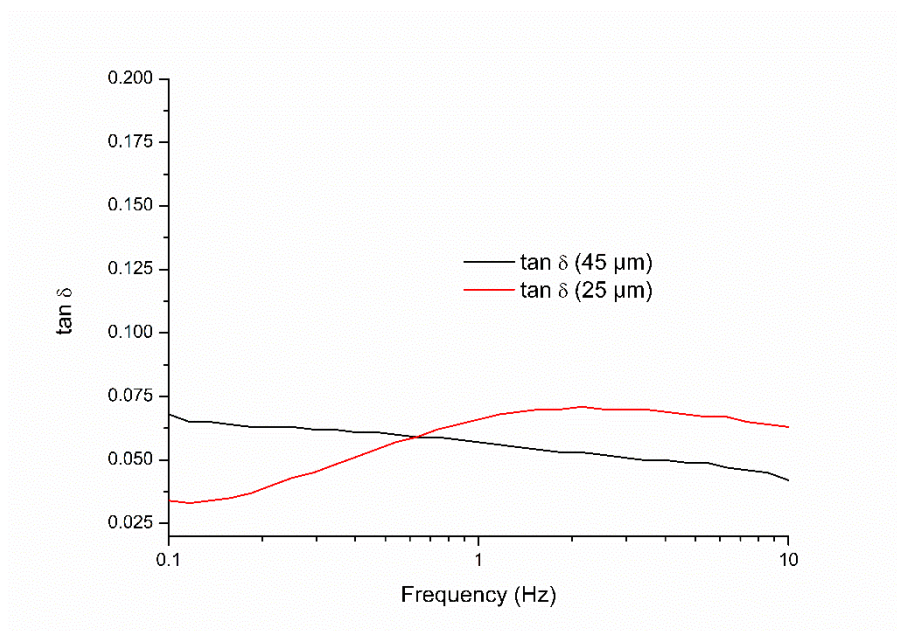


Figure IV.25: $\tan \delta$ of DX-gels prepared with microgels of constant crosslinking density (M/I/C of 1/0.05/0.1) and with a size of the primary beads of 25 μm (red line) and 45 μm (black line). Initial microgel concentration of 8.75%.

This surprising $\tan \delta$ behavior has not been noted yet in the field of DX-gels. As DX-gels are a quite recent topic, only few papers studied their rheological properties. At this stage, we can not put forward a correct explanation of such a behavior.

IV.2.3.5. Impact of an applied force during the gelation process over the mechanical properties of DX-gels

Taking advantage of the soft nature of the microgels, we decided to investigate the benefits of microgels deformability to optimize the contacts between the microgels and increase the intercrosslinking as illustrated in Figure IV.26. In this last series of experiments, we studied the impact of an applied external force during the preparation of the DX-gels and their resulting mechanical properties. To achieve this goal, samples were prepared in a syringe system presenting two pistons and a mass of 200 g was applied on one side for various time length (from 0 minute to 120 minutes, system depicted in figure IV.27). Finally the gels were characterized by rheology.

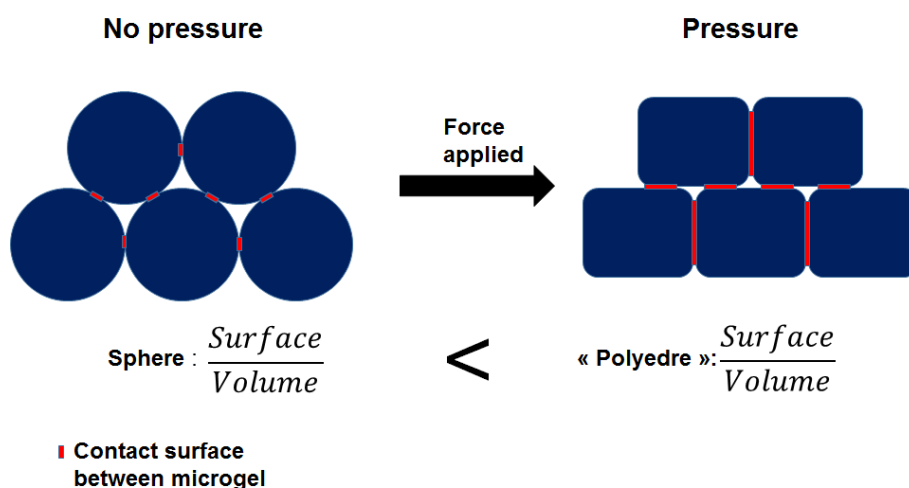


Figure IV.26: Illustration of contact surface increased by deformation of the microgels

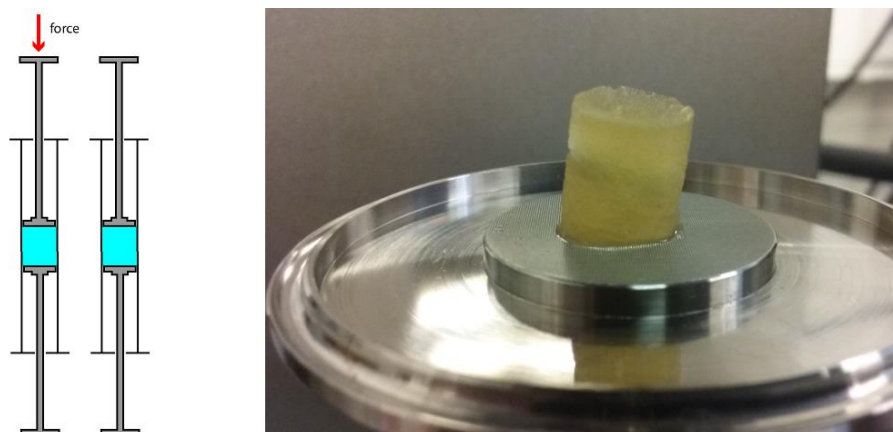


Figure IV.27: Schematic representation of the system applying force (left), photograph of a resulting DX-gels using this setup (right).

As showed in Figure IV.28 and Figure IV.29, increasing the duration of applied pressure led to respectively a decrease of the $\tan \delta$ value and an increase of G' . These $\tan \delta$ and G' evolutions are attributed to the formation of a higher amount of elastically effective linkages between neighboring particles compared to a sample without force applied. These decreases of $\tan \delta$ suggest that, as expected by applying pressure during the DX-gels synthesis, the formation of elastic linkages between neighboring particles is favored by forcing the deformation of microgels and therefore the connections between neighboring particles.

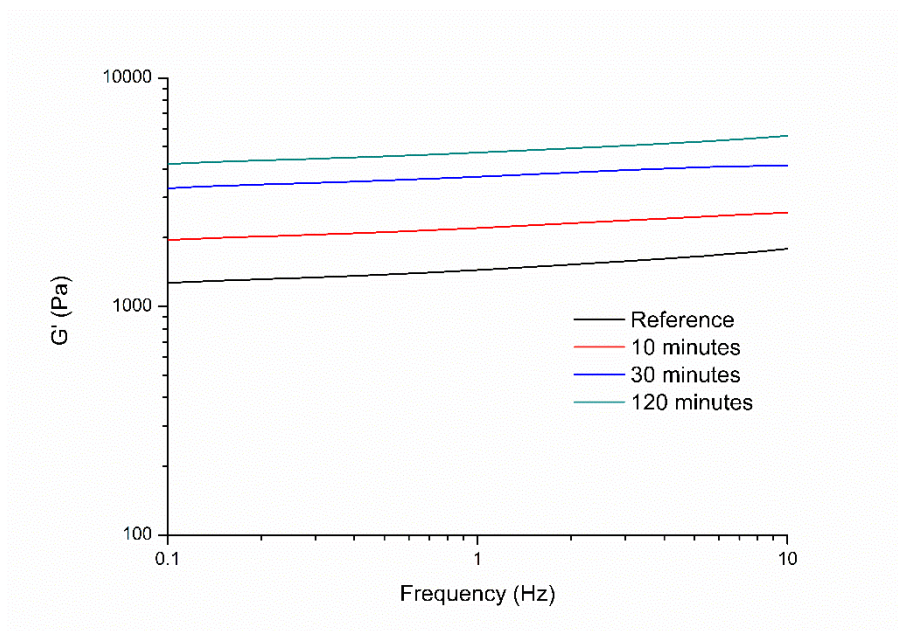


Figure IV.28: Frequency sweep evolution of G' for various time of applied force for DX-gels produced using microgels with M/I/C of 1/0.05/0.15 (microgel concentration 8.75%).

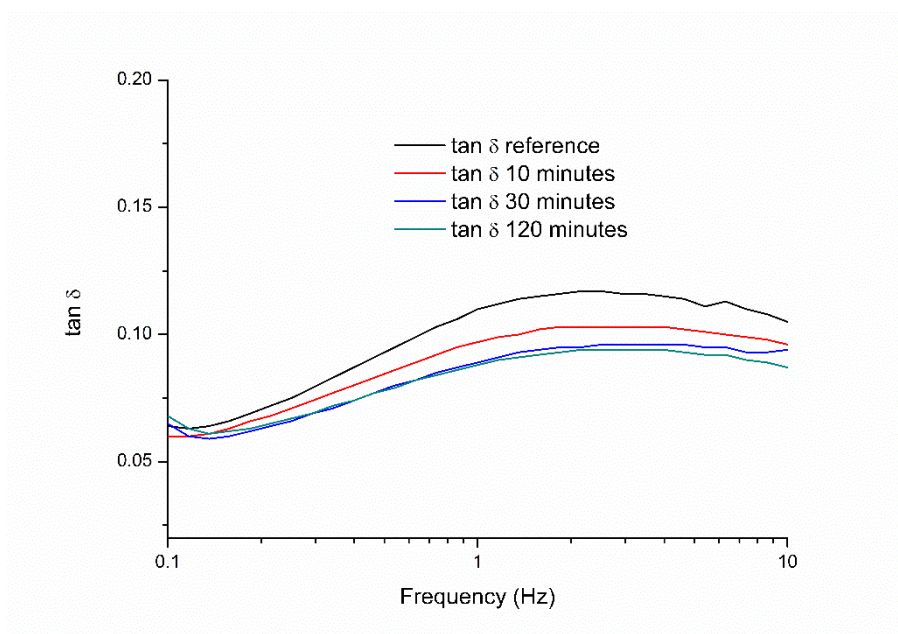


Figure IV.29: Frequency sweep evolution of $\tan \delta$ for various time of applied force for a DX-gel produced from microgels obtained with M/I/C of 1/0.05/0.15 (Table IV.2 entry B).

IV.4. Conclusions

The robustness of our doubly crosslink approach in the design of DX-gels has been fully demonstrated as all specifications in terms of kinetics, reproducibility and tuning of mechanical properties have been demonstrated. Indeed, the TAD-based click chemistry reaction used to form the second level of crosslinking between microgel beads led to well-assembled materials within a minute under mild conditions, and without the need of any catalyst. The mechanical properties of the suspensions and the resulting gels were probed by dynamic rheology. The storage modulus varied with the relative proportion TAD-based crosslinker/microgel functionality and were found the highest for a TAD/Cp ratio close to stoichiometry (TAD/Cp of 0.875), with an improvement of the storage modulus by a factor 4. Mechanical properties of starting microgels as well as the resulting DX-gels have been studied according to various parameters such as the concentration of starting microgels solution, microgels intra-crosslinking density, microgel size and the application of an initial pressure with various time of stress. Figure IV.30 describes the range of mechanical properties of DX-gels achieved so far by TAD click chemistry and the mechanical properties of some human tissues.

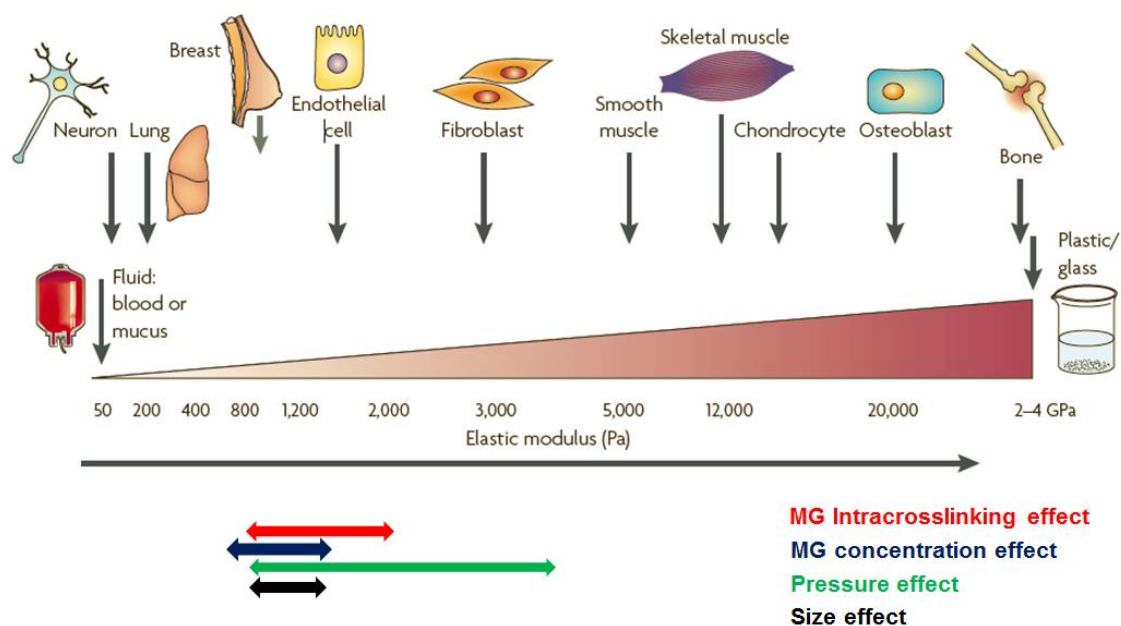


Figure IV.30: Resuming scheme of parameters investigated and their respective effect on mechanical properties.

Moreover, size distribution of the microgels greatly influences the resulting properties of the gel. Finally, the results show that TAD applying TAD chemistry is a highly efficient and versatile method for obtaining DX-gels where modulus values can be tuned precisely. The moduli of the doubly crosslinked gels were sensitive to both particle concentration but also to microgel intracrosslinking density. Increasing both of these parameters resulted in doubly crosslinked microgels with higher moduli. These findings suggest that cyclopentadiene functionalization and subsequent doubly crosslinking may be of particular use in applications in which defined and consistent properties are a requirement. Moreover, it was found that applying a pressure forces the deformation of the microgels and maximizes the contact of the microgels leading to an increase of the moduli of the resulting DX-gels. Adapted mechanical properties, biocompatibility and toxicity tests should be addressed for potential applications *in vivo*.

IV.5 Experimental section

Materials

Polyethylene glycol methyl ether methacrylate (PEGMA, M_n : 500 g/mol), glycidyl methacrylate (97%) and ethylene glycol dimethacrylate (98%), *N*-(1-pyrene) maleimide, butyl acetate (99.7%), aluminium oxide basic were purchased from Sigma Aldrich Fluka. All monomers were passed over basic aluminum oxide before use. 4,4'-azobis(4-cyanovaleric acid) (98%>) (ABCVA), Span 80, Tween 80, sodium cyclopentadienide (2 M in THF), ammonium chloride (99.5%>) were purchased from sigma and were used as received. Cyclohexane, hexane, tetrahydrofuran, ethanol, acetonitrile, hydrochloric acid were purchased from VWR. Solvents were used as received.

Preparation of Cp functionalized PEG microgels

The method used for click functionalizing the microgels involved epoxide ring-opening through reaction with sodium cyclopentadiene is represented in Figure IV.1 and directly comes from our previous work.^[25] Different microgels with various sizes and crosslinker quantities were prepared for the future DX-gel mechanical studies. Briefly, a mixed monomer solution (M_n : 500 g/mol, 7 g, 0.014 mol) of polyethylene glycol, ((GMA, 900 mg, 6.3 mmol) glycidyl methacrylate, (EGDMA, 420 mg, 2.12 mmol) ethylene glycol

dimethacrylate and ABCVA (250 mg, 0.89 mmol) into 12 ml of a solution of water/acetonitrile (5/1). This solution was transferred into a 500 ml flask containing 200 ml of cyclohexane. This solution was purged by nitrogen for 30 minutes. Microgels were formed at 70°C with mechanical stirring under nitrogen atmospheres within 6h. The microgels were extensively washed using the same method as described in the paper referred above. The method for functionalizing the microgels particles with cyclopentadiene was identical to that reported elsewhere.

UV quantitative study

A stock fresh solution of 4-phenyl-1,2,4-triazoline-3,5-dione (PTAD) (M_w : 175.14 g/mol, 4.35 mg into 5 mL, 0.497M) in butyl acetate was used as titration species. A calibration curve was made using 5 different concentrations of PTAD solutions. The following titration procedure was used: 100 μ L of a suspension of microgels were added into a vial with 2.4 mL of butyl acetate. A defined volume of PTAD solution stock (50 μ L) was added into the vial and the mixture was stirred for 5 minutes. The solution was filtered on a micro-disk with a pore size diameter of 0,5 μ m. Filtered solution was characterized by UV to determine the remaining PTAD after reaction with the cyclopentadienyl function onto the microgel surface.

Synthesis of bisTAD

Synthesis of the 4,4'-(4,4'-diphenylmethylene)-bis-(1,2,4-triazoline-3,5-dione) crosslinker come directly from a paper in the PCR-group published in Nature Chemistry.^[1] Briefly the TAD species we used are done by reacting 4,4'-Methylenebis(phenyl isocyanate) with ethyl carbazate. Then the 4,4'-(4,4'-diphenylmethylene)-bis (carbethoxysemicarbazide) formed is refluxed in aqueous potassium hydroxide solution and finally the end product (urazole) of the previous reaction is oxidized to form the 4,4'-(4,4'-diphenylmethylene)-bis-(1,2,4-triazoline-3,5-dione).

Viscosity measurements

Solution of microgels of various concentrations were prepared by mixing microgels with butyl acetate and viscosity measurements were measured using an Anton Paar Physica MCR 310 Rheometer. A 20 mm diameter plate geometry with a solvent trap was used

Equipment

Mechanical characterization by dynamic rheology

Dynamic rheology measurements were performed using an Anton Paar Physica MCR 310 Rheometer in oscillary mode with a temperature-controlled rheometer equipped with solvent trap. A 20 mm diameter plate geometry with a solvent trap was used. A strain of 1 % was used for the frequency sweep measurements.

UV Spectrometer

UV measurements were performed on a UV spectrometer Analytic-jena Specord 200.

Optical microscopy

Optical microscopy measurements were performed on an Olympus Optical microscopy with a Canon camera.

Particles size measurements

Particle size measurements were recorded on a Beckman Coulter LS 200 particles sizer.

HR-MAS NMR

HR-MAS analyses were performed on a Bruker Avance II 700 spectrometer (700 MHz). The samples were prepared as follows: dry material was cut into small pieces and put in a 4 mm rotor (80 μ L). Next, solvent (CDCl_3) was added to allow the material to swell. This removes most of the dipolar line broadening typically associated with the solid state, while residual line broadening caused by susceptibility differences can be handled by spinning at the magic angle. The sample was homogenized by stirring within the rotor. All ^1H NMR spectra were recorded using a HR-MAS probe equipped with a ^1H , ^{13}C , ^{119}Sn , and gradient channel. Samples were spun at a rate of 6 kHz. To characterize the gels, ^1H spectra were recorded.

IV.6. Bibliography

1. Billiet, S., et al., *Triazolinediones enable ultrafast and reversible click chemistry for the design of dynamic polymer systems*. Nature Chemistry, 2014. **6**(9): p. 815-821.
2. Wang, Z.K., et al., *Sustainable thermoplastic elastomers derived from plant oil and their "click-coupling" via TAD chemistry*. Green Chemistry, 2015. **17**(7): p. 3806-3818.

3. De Bruycker, K., et al., *Triazolinediones as Highly Enabling Synthetic Tools*. Chemical Reviews, 2016. **116**(6): p. 3919-3974.
4. Turunc, O., et al., *From plant oils to plant foils: Straightforward functionalization and crosslinking of natural plant oils with triazolinediones*. European Polymer Journal, 2015. **65**: p. 286-297.
5. Inglis, A.J., M.H. Stenzel, and C. Barner-Kowollik, *Ultra-Fast RAFT-HDA Click Conjugation: An Efficient Route to High Molecular Weight Block Copolymers*. Macromolecular Rapid Communications, 2009. **30**(21): p. 1792-1798.
6. Glassner, M., et al., *(Ultra)Fast Catalyst-Free Macromolecular Conjugation in Aqueous Environment at Ambient Temperature*. Journal of the American Chemical Society, 2012. **134**(17): p. 7274-7277.
7. Chambon, F. and H.H. Winter, *Linear Viscoelasticity at the Gel Point of a Cross-Linking Pdms with Imbalanced Stoichiometry*. Journal of Rheology, 1987. **31**(8): p. 683-697.
8. Liu, R., et al., *Tuning the swelling and mechanical properties of pH-responsive doubly crosslinked microgels using particle composition*. Soft Matter, 2011. **7**(19): p. 9297-9306.
9. Gong, J.P., *Why are double network hydrogels so tough?* Soft Matter, 2010. **6**(12): p. 2583-2590.
10. Borrega, R., et al., *Concentration dependence of the low-shear viscosity of polyelectrolyte micro-networks: From hard spheres to soft microgels*. Europhysics Letters, 1999. **47**(6): p. 729-735.
11. Boggs, L.J., M. Rivers, and S.G. Bickel, *Characterization and rheological investigation of polymer microgels used in automotive coatings*. Journal of Coatings Technology, 1996. **68**(855): p. 63-74.
12. Senff, H., et al., *Rheology of a temperature sensitive core-shell latex*. Langmuir, 1999. **15**(1): p. 102-106.
13. Farley, R., et al., *Using click chemistry to dial up the modulus of doubly crosslinked microgels through precise control of microgel building block functionalisation*. Polymer Chemistry, 2015. **6**(13): p. 2512-2522.
14. Cho, E.C., et al., *Highly responsive hydrogel scaffolds formed by three-dimensional organization of microgel nanoparticles*. Nano Letters, 2008. **8**(1): p. 168-172.
15. van der Vaart, K., et al., *Rheology of concentrated soft and hard-sphere suspensions*. Journal of Rheology, 2013. **57**(4): p. 1195-1209.
16. Pham, K.N., et al., *Yielding behavior of repulsion- and attraction-dominated colloidal glasses*. Journal of Rheology, 2008. **52**(2): p. 649-676.
17. Cui, Z.X., et al., *Using intra-microgel crosslinking to control the mechanical properties of doubly crosslinked microgels*. Soft Matter, 2016. **12**(33): p. 6985-6994.
18. Liu, R.X., et al., *Tuning the swelling and mechanical properties of pH-responsive doubly crosslinked microgels using particle composition*. Soft Matter, 2011. **7**(19): p. 9297-9306.
19. Thaiboonrod, S., A.H. Milani, and B.R. Saunders, *Doubly crosslinked poly(vinyl amine) microgels: hydrogels of covalently inter-linked cationic microgel particles*. Journal of Materials Chemistry B, 2014. **2**(1): p. 110-119.
20. Lane, T., et al., *Double network hydrogels prepared from pH-responsive doubly crosslinked microgels*. Soft Matter, 2013. **9**(33): p. 7934-7941.
21. Lyon, L.A., et al., *Microgel colloidal crystals*. Journal of Physical Chemistry B, 2004. **108**(50): p. 19099-19108.
22. Senff, H. and W. Richtering, *Temperature sensitive microgel suspensions: Colloidal phase behavior and rheology of soft spheres*. Journal of Chemical Physics, 1999. **111**(4): p. 1705-1711.
23. Urayama, K., et al., *A simple feature of yielding behavior of highly dense suspensions of soft micro-hydrogel particles*. Soft Matter, 2014. **10**(47): p. 9486-9495.
24. Liu, R.X., et al., *Doubly crosslinked pH-responsive microgels prepared by particle inter-penetration: swelling and mechanical properties*. Soft Matter, 2011. **7**(10): p. 4696-4704.

25. Absil, R., et al., *Click reactive microgels as a strategy towards chemically injectable hydrogels*. Polymer Chemistry, 2016.

Chapter V: Synthesis of doubly crosslinked gels by TAD based HDA click chemistry in aqueous conditions

V.1. Introduction

Injectable biomaterials for tissue engineering and local drug delivery are thoroughly investigated research areas worldwide as many diseases or trauma could be healed with higher level of efficiency compared to transplantations of foreign tissues or traditional systemic administration of drugs. Beyond specificities that the biomaterial must meet to be exploited as injectable material *in vivo*, practical truths unveil the intricate nature of the challenges that polymer chemists have to surmount. Ill-defined location, mechanical properties of the hosting tissue, gelation time together with benign synthetic starting materials are so many locks that cannot be underestimated. In that field, doubly-crosslinked materials have already demonstrated their high potential to self-assemble into a monolithic material within minutes.^[1-3] These two-level of hierarchized crosslinking, combined with the injectable nature of the material, leverage therapeutically outcomes in tissue engineering, in drug delivery and more interestingly for the combination of the two. Indeed, the macroscopic design of the resulting network won't be a limitation to any applications since the route of delivery in the human body bypasses the surgery technical locks. Lately, we demonstrated that Cp-functionalized PEG-based microgels could be interlinked in less than 5 minutes by the mean of Hetero Diels-Alder (HDA) click chemistry using triazolidione (TAD) as dienophile. Interestingly, doubly crosslinked networks presenting storage moduli varying between 800 and 4000 Pa were achieved simply by adjusting particle size, the crosslinking degree of the starting microgels, initial concentration of the microgels or by applying a pressure to deform the soft beads. As shape, architectures and final properties are all important features that will dictate the use of the swollen material, using the injected DX-gel approach allows on-demand tuning of these parameters. In the particular case of our previously developed system, the range of storage moduli reached for the DX-gels coincides with the mechanical properties of natural tissues as brain, fibroblasts and smooth muscles. Though the biocompatibility of the starting Cp-microbeads were demonstrated via a MTT test, the second level of crosslinking induced by TAD click

chemistry as developed in chapter 3 cannot be applied at such *in vivo* as in this proof of concept, the ligation occurs in organic medium, hampering therefore its applicability in the biomedical field. The aim of this chapter is to adapt the protocol towards aqueous solution, which is not straightforward since it is reported that TAD compounds suffer from hydrolysis in aqueous solutions.^[4] We hypothesized that those side reactions being kinetically far slower than the ligation process, the competition between the two reactions should be in favor of the DX-gels formation. This hypothesis is reasonable as our group developed lately the preparation crosslinked plant oil nanoparticles in minutes by TAD chemistry in surfactant-free water based emulsion.^[5] Therefore, water swollen microgels were prepared using the previously described conditions (see Chapter 3) to test this hypothesis.

V.2. DX-gel synthesis using TAD click chemistry in aqueous medium and characterization

In Chapter 3, we demonstrated that TAD click chemistry is a powerful ligation method to link Cp-functionalized microbeads and form a two level hierarchized hydrogel within minutes with a very easy setup. However, in the outlook of biomedical applications, there are several requirements we need to address like the need of a benign solvent for the synthesis of DX-gels by TAD-based HDA ligation. Since the preparation of TAD-functionalized hydrophilic crosslinker is tedious to synthesize, MDI-TAD was chosen for that study. However, this compound being not soluble in water, DMSO was employed as a co-solvent. While the use of DMSO is controversy in medicine and in pharmaceutical fields, many scientific reports showed that this solvent is harmless depending on the concentration used.^[6] Moreover, DMSO is known to increase the rate of absorption of some compounds through some organic tissues, including skin and even in transdermal drug delivery systems.^[7] Some authors reported also its use as antibacterial ^[8] or analgesic property.^[9] Finally, the US Food and Drug Administration has approved its use for the symptomatic relief of patients with interstitial cystitis or as a preservative of organs for transplants. Firstly, reactivity of MDI-TAD in a mix of butyl acetate and DMSO with a ratio of 50/50 volume/volume was carried out for an initial Cp-microgel concentration of 8.5 % and for a TAD/Cp ratio of 0.8. The Cp microgels were characterized by a size of 25 μm (see table III.2, entry A). For this reaction, the microgels were previously swollen in butyl acetate. For sake of

comparison, the same reaction was conducted in parallel in 100% butyl acetate as reference.

DX-gels were obtained within seconds in both experiments with similar kinetics. The red color of the TAD moieties disappears completely in seconds after the gelation. This successful experiment demonstrates that the use of DMSO is not a concern for the synthesis of DX-gel in the above mentioned experimental conditions. While TAD moieties are not stable in hygroscopic DMSO for a prolonged period of time, the kinetics of ligation is so fast that the click reactive compound has not the time to be degraded. In a second series of experiments, DX-gels were prepared in a solution of water and DMSO with initial volume compositions of 50/50 and 80/20 (water/DMSO). In that particular case, microgels were swollen in demineralized water and suspended in a mixture of water and DMSO. The microgels being stored in butyl acetate, a procedure to eliminate the organic solvent was first applied by solvent exchange. For that purpose, ethanol being miscible with both butyl acetate and water was chosen as intermediate solvent. After the consecutive solvent exchanges, microgels were mixed with DMSO to obtain a microgel suspension to reach the desired water/DMSO ratios of 50% and 80%. MDI-TAD (in DMSO) was added to the microgels solution to reach a TAD/Cp ratio of 0.8 and a total microgel concentration of 8.5 %. As presented in the Figure V.1., both conditions led to a very fast gelation, occurring within seconds as attested by the loss of the characteristically red color of the MDI-TAD and the absence of flow by the classical tilting test.

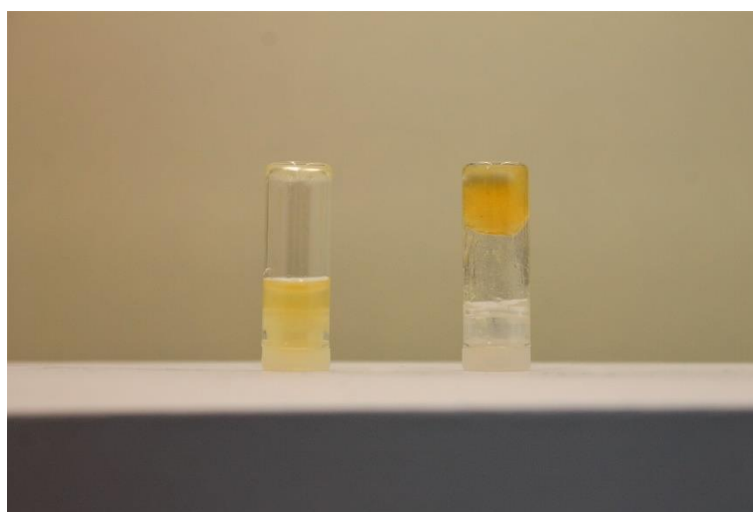


Figure V.1: Picture of microgel suspension (left) and the DX gel (right) formed by click coupling within 30 seconds in a Water/DMSO solution (80/20).

V.2. Morphology of DX-gels and their swelling properties

V.2.1. Morphology investigations by SEM

We probed the morphologies of freeze-dried DX gel produced in water/DMSO mixture (50/50) using SEM. Following the examples of samples produced in organic conditions, morphologies of DX gels synthesized in water solutions show connected microgels. Their soft nature leads to visible deformation of the spherical beads upon interlinking, which is an advantage to increase interfacial contacts and promote more linkages between the microbeads as depicted in Figure V.2. No fundamental differences can be noticed between DX gels made in a water/DMSO mixture or in butyl acetate, as depicted in Figure V.2.

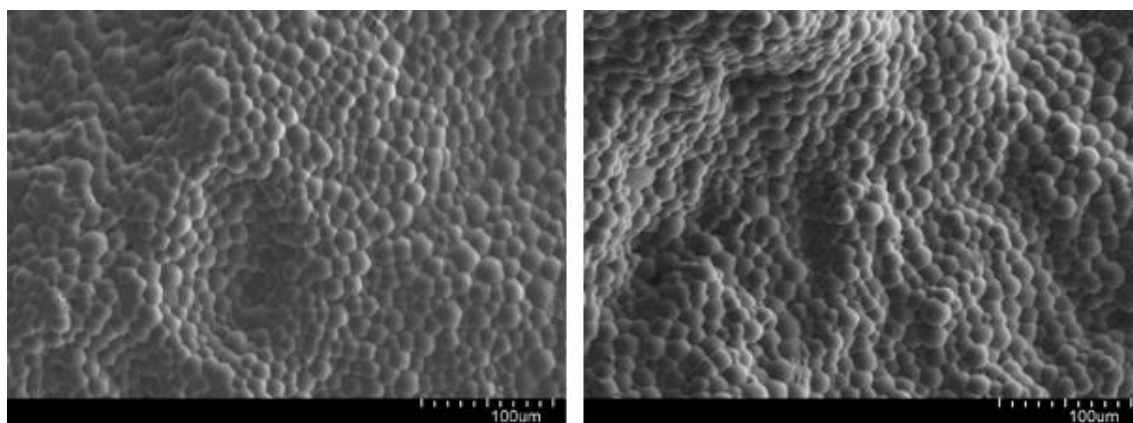


Figure V.2: Morphology of covalent DX gels prepared from Cp-microgels (Table III.2, entry A with a TAD/Cp ratio of 0.8, 25 μm) made in a water/DMSO mixture of 50/50 v/v (left) and of a covalent DX gels prepared from Cp-microgels (Table III.2, entry A with a TAD/Cp ratio of 0.8, 25 μm) made in butyl acetate (right).

V.2.2. Swelling behavior of the DX-gels

By definition, hydrogels are characterized by meshes between crosslinked polymer chains, allowing for liquid and small solutes for diffusion and swelling, without damaging the 3D structure. The swelling property of a gel, being the balance between forces that constrain network deformation and the osmosis favoring water absorption,

is an important feature to evaluate when considering DX-gels for potent biomedical applications. The swelling behavior of the as-obtained DX-gels was simply analyzed in demineralized water while water uptake was followed versus time as depicted in Figure V.3. The DX-gel made with microgels from Table III.2 entry A required only 30 minutes to reach the equilibrium with a swelling ratio S_{eq} of 2200%. This fast swelling is similar to the rapid swelling (minutes) observed for DX gels prepared in butyl acetate. Interestingly, the DX gels made from microgels presenting an initial $[M]_0/[I]_0/[C]_0$ of 1/0.05/0.1 (Table III.2, entry A) swells more than the starting microgels themselves, demonstrating the creation of interconnected channels able to engulf more water in the interstices created by the interlinking of the beads.

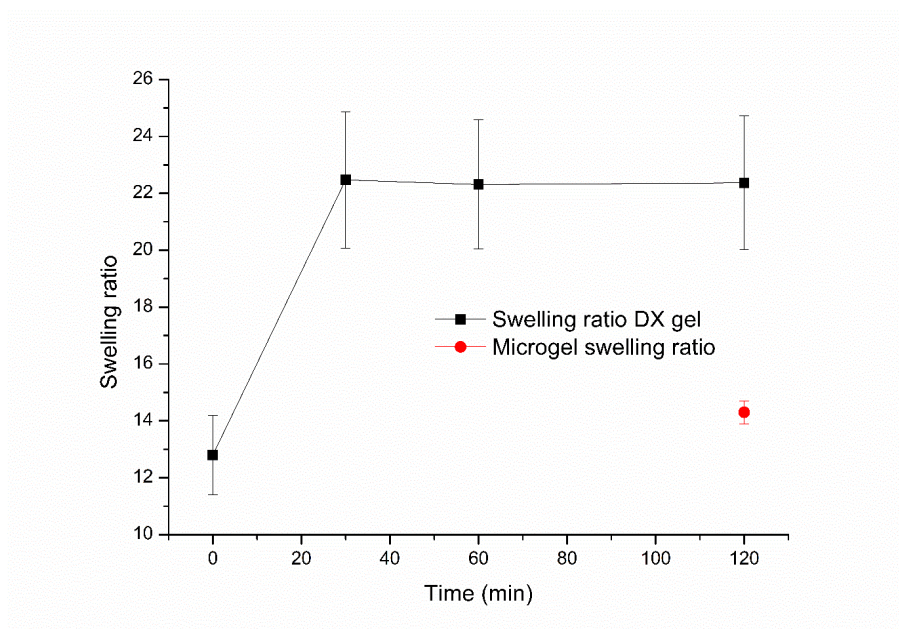


Figure V.3: Swelling ratio evolution versus time of a DX gel made from microgels Table III.2, entry A ($[M]_0/[I]_0/[C]_0$ of 1/0.05/0.1).

V.3 Biocompatibility proof of concept

Short-term tolerability assay

The *in vivo* tolerability of the system was performed using subcutaneous injections as a proof of concept. These experiments were realized in collaboration with the Advanced Drug Delivery and Biomaterials at Université Catholique de Louvain. The principle is to detect a modification in the coloration of the mice skin from pink to red

or black that indicates possible toxicity, inflammation and necrosis reactions, induced by the implanted material. Injections of 50 μ l of DX-gel were realized on 6-week-old female NMRI mice during a period of 7 days ($n=6$).



Figure V.4: *In vivo* tolerability assay assessed by subcutaneous implantation of the DX gel produced in a solution mixture water/DMSO of 80/20: shaved mouse before gel implantation (Left image); mouse 15 minutes after the gel injection (middle); the mouse 7 days after gel injection (right).

As it can be noticed on Figure V.4, the injected gel is still in place and neither inflammation nor necrosis (usually witnessed by a red or black color, respectively) is stated after 7 days of implantation, validating our material could be used for further *in vivo* experiments. *In vivo* tolerability assay in orthotopic conditions (direct implantation of the material in the mice brains) is ongoing.

V.4. Conclusions

Proof of concept demonstrated that TAD click chemistry can be used in a mixture of water/DMSO to synthesize the DX-gels. Such behavior can be explained by the rapid reaction of the cyclopentadiene towards the TAD before complete hydrolysis of the TAD moieties. Swelling tests demonstrated that higher swelling is noticed after creation of the second network. Morphology was studied using SEM and corresponded to randomly interlinked microgels, as it was previously observed for DX-gel made in butyl acetate. Finally, in the scope of biomedical applications, DX-gels were injected in mice. After 1 week, neither inflammation nor necrosis was stated, confirming our concept of

using PEG DX microgels as injectable hydrogels system. Further investigations should be realized to study the properties of DX gels in water/DMSO such as their mechanical properties and toxicity pattern.

V.5. Experimental section

Materials

Polyethylene glycol methyl ether methacrylate (PEGMA, M_n : 500 g/mol), glycidyl methacrylate (97%) and ethylene glycol dimethacrylate (98%), *N*-(1-pyrene) maleimide, butyl acetate (99.7%), aluminium oxide basic were purchased from Sigma Aldrich Fluka. All monomers were passed over basic aluminum oxide before use. 4,4'-azobis(4-cyanovaleric acid) (98%>) (ABCVA), Span 80, Tween 80, sodium cyclopentadienide (2 M in THF), ammonium chloride (99.5%>) were purchased from sigma and were used as received. Cyclohexane, hexane, tetrahydrofuran, ethanol, acetonitrile, hydrochloric acid were purchased from VWR. Solvents were used as received.

Preparation of Cp functionalized PEG microgels

The method used for click functionalizing the microgels involved epoxide ring-opening through reaction with sodium cyclopentadiene is represented in Figure III.1 and directly come from our previous work.[10] Different microgels with various sizes and crosslinker quantities were prepared for the future DX-gel mechanical studies. Briefly, a mixed monomer solution (M_n : 500 g/mol, 7 g, 0.014 mol) of polyethylene glycol, ((GMA, 900 mg, 6.3 mmol) glycidyl methacrylate, (EGDMA, 420 mg, 2.12 mmol) ethylene glycol dimethacrylate and ABCVA (250 mg, 0.89 mmol) into 12 ml of a solution of water/acetonitrile (5/1). This solution was transferred into a 500 ml flask containing 200 ml of cyclohexane. This solution was purged by nitrogen for 30 minutes. Microgels were formed at 70°C with mechanical stirring under nitrogen atmospheres within 6h. The microgels were extensively washed using the same method as describe in the paper referred above. The method for functionalizing the microgels particles with cyclopentadiene was identical to that reported elsewhere.

UV quantitative study

A stock fresh solution of 4-phenyl-1,2,4-triazoline-3,5-dione (PTAD) (M_w : 175.14 g/mol, 4.35 mg into 5 mL, 0.497M) in butyl acetate was used as titration species. A

calibration curve was made using 5 different concentrations of PTAD solutions. The following titration procedure was used: 100 μL of a suspension of microgels were added into a vial with 2.4 mL of butyl acetate. A defined volume of PTAD solution stock (50 μL) was added into the vial and the mixture was stirred for 5 minutes. The solution was filtered on a micro-disk with a pore size diameter of 0,5 μm . Filtered solution was characterized by UV to determine the remaining PTAD after reaction with the cyclopentadienyl function onto the microgel surface.

Synthesis of bisTAD

Synthesis of the 4,4'-(4,4'-diphenylmethylen)-bis-(1,2,4-triazoline-3,5-dione) crosslinker come directly from a paper in our group published in Nature Chemistry.[11] Briefly, the TAD species we used are done by reacting 4,4'-Methylenebis(phenyl isocyanate) with ethyl carbazate. Then the 4,4'-(4,4'-diphenylmethylen)-bis(carbethoxysemicarbazide) formed is refluxed in aqueous potassium hydroxide solution and finally the end product (urazole) of the previous reaction is oxidized to form the 4,4'-(4,4'-diphenylmethylen)-bis-(1,2,4-triazoline-3,5-dione).

Equipment

UV Spectrometer

UV measurements were performed on a UV spectrometer Analytic-jena Specord 200

Particles size measurements

Particle size measurements were recorded on a Beckman Coulter LS 200 particles sizer.

SEM

DX gel was imaged with a field emission gun scanning electron microscope (FEG-SEM Hitachi SU8020).

V.6. Bibliography

1. Milani, A.H., et al., *Injectable Doubly Cross-Linked Microgels for Improving the Mechanical Properties of Degenerated Intervertebral Discs*. *Biomacromolecules*, 2012. **13**(9): p. 2793-2801.
2. Absil, R., et al., *Click reactive microgels as a strategy towards chemically injectable hydrogels*. *Polymer Chemistry*, 2016. **7**(44): p. 6752-6760.
3. Cui, Z.X., et al., *Using intra-microgel crosslinking to control the mechanical properties of doubly crosslinked microgels*. *Soft Matter*, 2016. **12**(33): p. 6985-6994.

4. Roy, N. and J.M. Lehn, *Dynamic Covalent Chemistry: A Facile Room-Temperature, Reversible, Diels-Alder Reaction between Anthracene Derivatives and N-Phenyltriazolinedione*. Chemistry-an Asian Journal, 2011. **6**(9): p. 2419-2425.
5. Chattopadhyay, S. and F. Du Prez, *Simple design of chemically crosslinked plant oil nanoparticles by triazolinedione-ene chemistry*. European Polymer Journal, 2016. **81**: p. 77-85.
6. Capriotti, K. and J.A. Capriotti, *Dimethyl Sulfoxide: History, Chemistry, and Clinical Utility in Dermatology*. The Journal of Clinical and Aesthetic Dermatology, 2012. **5**(9): p. 24-26.
7. Horita, A. and L.J. Weber, *Skin penetrating property of drugs dissolved in dimethylsulfoxide (DMSO) and other vehicles*. Life Sciences, 1964. **3**(12): p. 1389-1395.
8. Salim, A.S., *Removing Oxygen-Derived Free-Radicals Delays Hepatic Metastases and Prolongs Survival in Colonic-Cancer - a Study in the Rat*. Oncology, 1992. **49**(1): p. 58-62.
9. Duimel-Peeters, I.G.P., et al., *A systematic review of the efficacy of topical skin application of dimethyl sulfoxide on wound healing and as an anti-inflammatory drug*. Wounds-a Compendium of Clinical Research and Practice, 2003. **15**(11): p. 361-370.
10. Absil, R., et al., *Click reactive microgels as a strategy towards chemically injectable hydrogels*. Polymer Chemistry, 2016.
11. Billiet, S., et al., *Triazolinediones enable ultrafast and reversible click chemistry for the design of dynamic polymer systems*. Nature Chemistry, 2014. **6**(9): p. 815-821.

Chapter VI: Microfluidics as a new synthetic road towards monodisperse click functionalized microgels

VI.1 Microfluidics: a key technique for monodisperse microgels production

VI.1.1 Introduction

The research on functional particles is extremely important for various applications, including biotechnology ^[1], pharmaceuticals ^[2], cosmetics ^[3], paints ^[4] and structural materials.^[5, 6] Moreover, monodisperse functional particles are highly desired and useful. Indeed, particles exhibit identical properties and behaviors owing to their surface area and volume being identical. Typically, monodisperse polymer particles with sizes from 20 nm to approximately 5 μm can be prepared by miniemulsion, emulsion or dispersion polymerization. The synthesis of larger particles in the range of 5 μm to approximately 200 micrometers with a narrow size distribution is still challenging.^[7] Such microparticles are accessible through miniemulsion polymerization, suspension polymerization, and multistage emulsion polymerization. But, in most cases, the methods are either material-specific or time consuming, or they do not provide a sufficiently narrow size distribution of the resulting particles.^[8] Only recently, microfluidics received an increased attention as a versatile tool for the preparation of monodisperse particles.^[9-11] The basic principle is the following: when two liquids that are immiscible, such as water and oil, are injected into the device at controlled flow rates, a highly monodisperse emulsion can be formed into the device. The size of the resulting droplets is controlled by the fluid flow rates, the dimensions of the microchannels, and the interfacial tension.^[12, 13] Since all these parameters are controllable, the droplet size is monodisperse and can be determined by adequate choice of the experimental parameters. By using this emulsion as a template, monodisperse functional polymer and ceramic particles can be prepared.^[14-17] Actually, several types of microfluidic devices exist such as capillary microfluidic

devices ^[18-20] and more conventional polydimethylsiloxane devices realized by soft lithography ^[21-23] or even lab on chip device avoiding any labor-intensive device preparation techniques such as soft lithography.^[24, 25]

The low cost of capillary microfluidic devices makes them very accessible. They can be fabricated by assembling tapered glass capillaries coaxially in a square capillary, although it can be time consuming to set the positions and sizes of the tapered capillaries precisely. In contrast, the soft lithography technique presents the advantages of accurate control of the positions and sizes of channels in the polydimethylsiloxane (PDMS) device through the design of mask patterns. Moreover, it has the potential for mass production use as once a mask pattern is designed, a large number of PDMS devices can be fabricated by the stamping technique. However, it is difficult to fabricate a device with complex flow channels in three dimensions by soft lithography, which could limit the utility of the device for some applications. Recently, Kanai's team demonstrated the fabrication of a microfluidic device by stereolithography. Stereolithography is a method to build a three-dimensional object layer by layer through the photopolymerization of a liquid monomer resin ^[26], facilitating the construction of complex flow channels in three dimensions.^[27]

The system used in this chapter consists of tubing-needle based "simplified" microfluidic setup and comprises two syringe pumps, one large syringe carrying the continuous phase and another smaller syringe for monomer phase (discrete phase), a flexible and transparent tubing, needles and UV lamps. The large syringe mounted on syringe pump injects from the beginning of the tubing the continuous phase with a relatively high rate compared to the discrete phase. The needle of the second syringe is first bended and punched a little further on the tubing, which injects the monomer phase with a much lower pumping rate using the second syringe pump. As discussed previously, this rate difference provides the droplet formation in the tubing. Monomer droplets travel downstream thanks to the stream of continuous phase and get photopolymerized by UV exposition. Although microgel solidifies in the tubing, extra off-tubing UV curing is applied for approximately 20 minutes to achieve the highest possible monomer conversion. Finally, the obtained particles are washed with different solvents (Figure VI.1.).

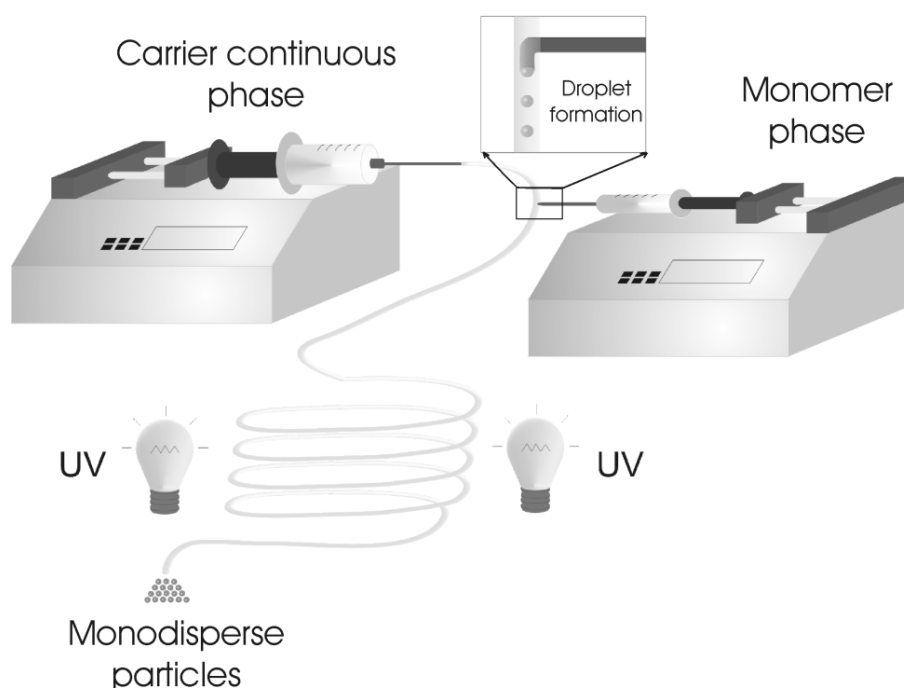


Figure VI.1: Scheme of the tubing-needle based, home-made built microfluidic setup utilized throughout this chapter adapted with permission from [28].

Polymeric microparticles with various diameters ranging from sub-micrometers to hundreds of micrometers have many application fields and can be used for example in purification technologies, immobilization of bioactive materials, or spacer and even calibration standards.^[7, 8, 29-31] Biotechnology and nanotechnology have grown rapidly over the last decade leading to an important development of microparticle-based applications in many fields such as particle based bioassays, flow measurement such as particle image velocimetry (PIV), and microparticle-based display. Moreover, a narrow size distribution of polymeric microparticles is very important to obtain high quality results in the previous cited application fields.^[7, 8, 30, 31] Indeed, monosized microparticles are important to obtain highly efficient results. For example, a column of liquid chromatography having monosized microparticles yields improved separation efficiency.^[7, 30]

Many different groups are working on the development of monosized microgel for various applications by microfluidics. Li *et al.*, developed recyclable poly(polyethylene glycol diacrylate/maleamic acid) (p(PEGDA/MALA)) copolymer hydrogel beads able to

remove heavy metal ions from water using a T junction.^[32] Zhao *et al.* reported a novel method using capture antibody immobilized in porous poly (ethylene) glycol diacrylate (PEGDA) hydrogel microspheres to enable high sensitivity of the vascular endothelial growth factor (VEGF) detection in arrayed microfluidics allowing antibody encapsulation, trapping and flow perfusion on a single device.^[33] Alginate microgels with various shape such as mushroom-like, hemi-spherical, red blood cell-like, and others were prepared by Hu *et al.*. This new method combining microfluidics and external ionic crosslinking allows a continuous fine tuning of the microgel particles shape by simply varying the gelation conditions, e. g. viscosity of the gelation bath, collecting height, interfacial tension.^[34] Hwang *et al.* used a T-junction microfluidic device containing an embedded UV light reflector to prepare spherical and non-spherical hydrogel particles.^[35] Interestingly, the particles prepared by this strategy present paramagnetic behavior when magnetic nanoparticles are uniformly encapsulated in the hydrogel. Kim *et al.* developed a dynamically tunable microlense system based on hydrogel microparticles. In this report, poly(*N*-isopropylacrylamide) hydrogel able to response to external stimuli was used to prepare microlense arrays.^[36] Lately, focus was dedicated to PEGDA hydrogel particles, or “microgels” which are materials of emerging importance to the sensing ^[37], drug ^[38] and tissue engineering ^[39] communities due to intra-particle diffusion, facile antibody ^[40] or oligonucleotide conjugation ^[41] and present high potential for *in vivo* applications.^[42-44]

In this chapter, a preparation method of monodisperse poly(ethylene glycol) (PEG) based microgels using a microfluidics co-flow geometry is presented. Various experimental conditions such as flow rates of the discrete phase (PEG solution) and continuous phase (mineral oil) and concentration of the PEG solution were investigated and optimized to fabricate monosized PEG microparticles presenting epoxide groups onto the surface. In a next step, we will take advantages of the epoxide functions to modify the surface functionality to introduce a very reactive diene onto the surface to promote DX-gels formation made of monodisperse microgels by using TAD-based HDA click chemistry.

VI.1.2. Monodisperse microgels produced by microfluidics

An aqueous solution of poly(ethylene glycol) methacrylate (PEG-MA), glycidyl methacrylate (GMA), ethylene glycol dimethacrylate and the photoinitiator was pressurized by a syringe pump and fed continuously through a blunt needle into a continuous oil stream containing a non-ionic surfactant. The discrete phase was prepared by first dissolving 25 mg of Irgacure 2959 and monomers in 1.2 mL distilled water/acetonitrile (5/1) to achieve a 80% w/w solutions with an initial co-monomer molar ratio $[GMA]_0/[PEGMA]_0/[EGDMA]_0$ of 3/7/1.

After formation of monodisperse aqueous droplets in the oil-stream, the tubing was directed into a UV chamber where radical polymerization of the methacrylate groups was initiated, resulting in the formation of solid monodisperse microgels. The oil stream was collected and the microgels were purified by several washing steps with ethyl acetate to remove the oil and the surfactant and ethanol to remove remaining monomers (Figure VI.2.).

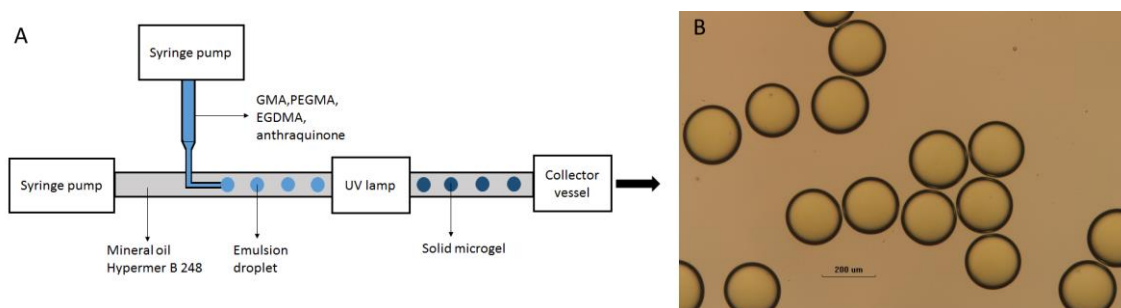


Figure VI.2: A) Schematic representation of the tubing-based microfluidic setup; B) Optical microscopy image of the obtained monodisperse microgels.

First, influence of the solvent nature of the continuous phase, surfactant nature, surfactant concentration and initiator were evaluated. In a first series of experiments, SPAN 80 and Irgacure 2959 were used respectively as surfactant and initiator as they are well referred in literature for the production of particles in aqueous solution.^[45-47] Cyclohexane acted as continuous phase but unfortunately didn't allow a nice dripping regime as the viscosities and surface tension between the two phases of the set-up

were not adapted as observed visually. To overcome this problem, light mineral oil was chosen as a more viscous continuous phase (low viscosity oil).

After this selection, surfactant concentration in the continuous phase was varied from 1% to 20%. For this study, a monomer solution (co-monomer molar ratio $[GMA]_0/[PEGMA]_0/[EGDMA]_0$ of 3/7/1, 80% w/v) in a mixture of water/acetonitrile (5/1) and light mineral oil with various concentrations (20, 10, 5, 2.5, 1.25, 1% w/v) were prepared. Pumping rates of continuous and discrete phases were varied from 0.025 to 0.6 mL/min and from 0.06 mL/h to 0.9 mL/h respectively. As surfactant concentration increased, it was noticed that the jetting regime in droplet formation is more likely to occur leading to a loss of control on the droplet generation (see Chapter II). Therefore, surfactant concentration was limited to 1%. By adapting all these parameters, nice droplet generation was achieved but no polymerization occurred in the droplets, as no solid particles can be collected. Providing longer period time in the tubing or in the collecting flask was unsuccessful. In fact, these unfruitful tests when SPAN 80 surfactant and Irgacure 2959 photoinitiator are used can be explained for different reasons. Concerning the SPAN 80, it appears that SPAN 80 absorbs sufficient amount of light in our setup at 365 nm to prevent the curing of the microgel into the tubing. Therefore no “stable” microparticles can be achieved at the end of the microfluidics process. Absorption spectrum of the SPAN 80 was checked in the literature and compared with the one recorded by our care. Absorbance of SPAN 80 decreases greatly around 350 nm (Figure VI.3) but remains significant (0.2 at 350 nm for 1% SPAN 80 in cyclohexane). By comparing the absorption of SPAN 80 and Hypermer B 246, another surfactant used water-in-oil system, it can be shown that the Hypermer B 246 (HLB: 6) surfactant presents a lower absorption of light at 350 nm (Figure VI.4) for a same composition of surfactants of 1 w% in cyclohexane, minimizing therefore light absorption by the surfactant in the polymerization conditions used (0.2 for SPAN 80 and 0.05 for Hypermer B 246 at 350 nm). Concerning Irgacure 2959, microparticles are not formed when using this initiator for unknown reason as this initiator is largely used in similar conditions in literature.^[48-50] Photopolymerizations were performed outside the microfluidic setup to check potential absorbance of the tubing setup but without success. Therefore, another water-soluble photoinitiator, the anthraquinone-2-sulfonic acid (ASA) was tested. Practically, a monomer solution (co-monomer molar ratio $[GMA]_0/[PEGMA]_0/[EGDMA]_0$ of 3/7/1, 80%) in a mixture of water/acetonitrile (5/1) containing 15 mg/ml of ASA and Hypermer B 246 (1% w/v) in light mineral oil

were prepared. Pumping rates of continuous and discrete phases were varied from 0.3 to 0.6 mL/min and from 0.1 mL/h to 0.2 mL/h respectively.

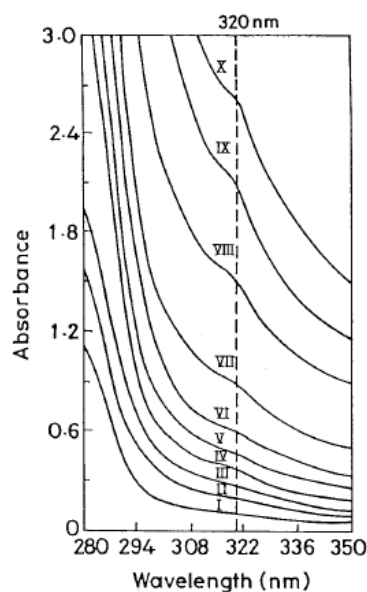


Figure VI.3: UV absorption of Span 80 in cyclohexane (Numerals I to X correspond to 0.25, 0.5, 0.75, 1, 1.25, 1.5, 2, 3, 4, 5 volume% of Span 80 in cyclohexane).^[51]

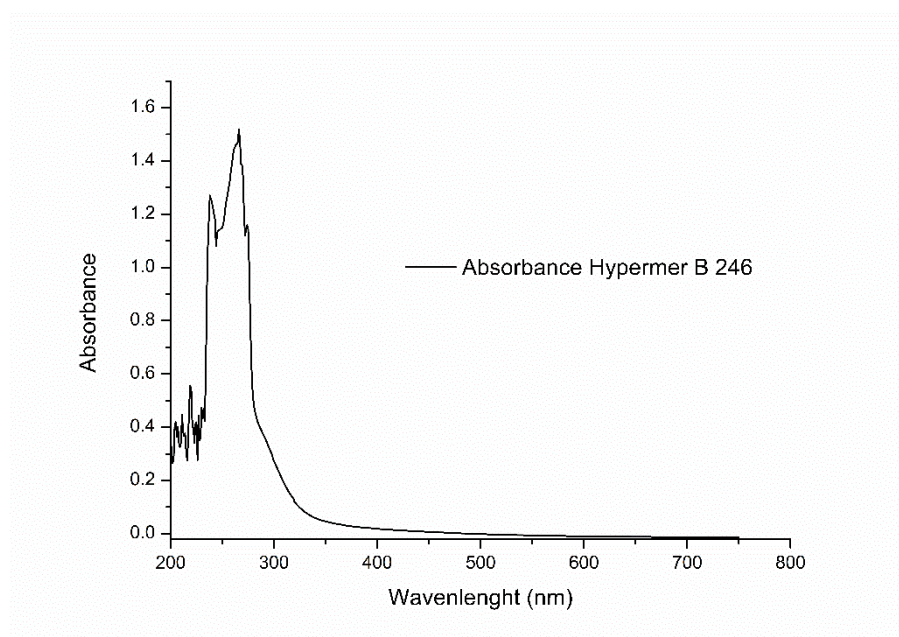


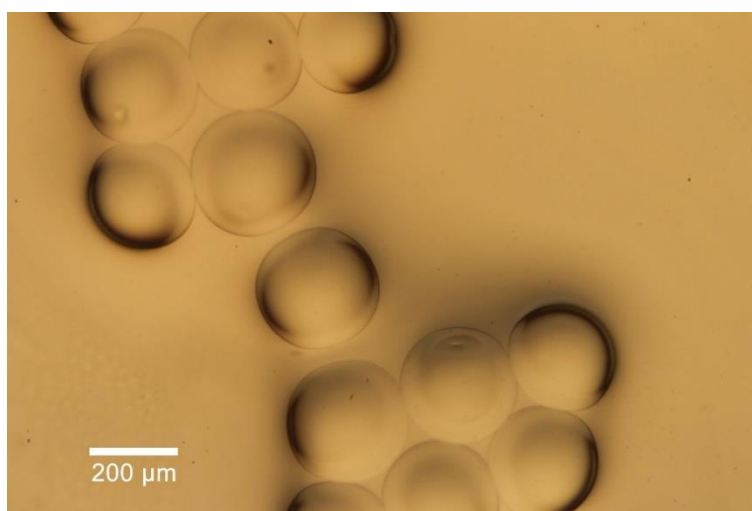
Figure VI.4: UV absorption of Hypermer B 246 in cyclohexane (1% volume).

Various flow speeds were tested to optimized microgels synthesis and are summarized in Table VI.1. Finally, the as-obtained microgels were suspended in ethyl acetate after several washing steps and characterized using optical microscopy (Figure VI.5).

Table VI.1: experimental conditions for microgels synthesis using a 160 μm diameter needle with a monomer concentration of 80% by microfluidics.

Sample	Flow discrete phase (ml/h)	Flow continuous phase (ml/min)	Monomers concentration (%)	Exposition time (s)	Size (μm) ^a
A	0.2	0.3	80	120	350
B	0.2	0.6	80	60	220-250
C	0.1	0.6	80	60	190-200

a) As measured by optical microscopy, swollen in ethyl acetate

**Figure VI.5:** Monodisperse microgels obtained by microfluidics after polymerization at 360 nm (Entry C Table VI.1) after purification with ethyl acetate and ethanol. Microgels swollen in ethyl acetate.

Changing needle size is a trick to modulate considerably the size of particles produced. In a next series of experiments, the same experimental conditions were applied with a smaller needle diameter (110 μm). As showed in Table VI.2, the impact of the speed flow of either the continuous phase or the discrete phase were investigated. It was observed that a high speed flow for the discrete phase resulted in polydisperse microgels distribution while decreasing down to 0.05 ml/h allows to reach smaller particles of 140 μm . The direct negative consequence is that the decrease of the flow rate lowers drastically the production rate of the microgels.

Table VI.2: Experimental conditions using a 110 μm diameter needle.

Sample	Flow discrete phase (ml/h)	Flow continuous phase (ml/min)	Monomers concentration (%)	Exposition time (s)	Size (μm) ^a
A	0.137	0.6	80	60	polydisperse
B	0.07	0.6	80	60	polydisperse
C	0.05	0.6	80	60	140

a) As measured by optical microscopy, swollen in ethyl acetate.

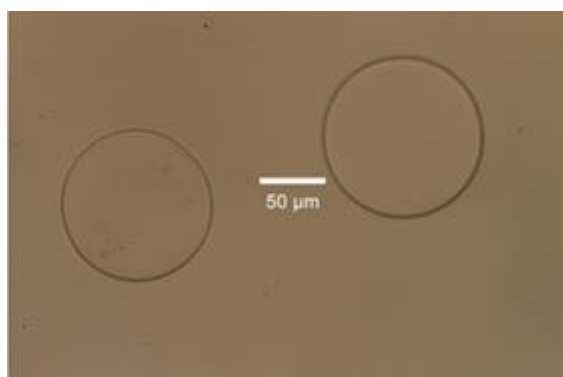


Figure VI.6: Optical picture of ethyl acetate swollen monodispersed microgels produced by microfluidics after polymerization at 360 nm (Table VI.2, entry C) after purification with ethyl acetate and ethanol.

In this series of experiments, monodisperse microparticles with an initial monomer concentration of 80 % in the discrete phase were successfully produced. For sake of comparison towards microgels produced by suspension polymerization, we investigated the synthesis of microgels by microfluidics with a monomer concentration of 40 %. By using adapted flow and needle size, monodisperse microgels with a mean diameter of 200 μm at the end of the tubing were produced with excellent reproducibility within the microfluidic setup as depicted in Figure VI.7. Finally, the as-obtained microgels were suspended in ethyl acetate after several washing steps. The size distribution of the microgels in ethanol is shown in Figure VI.8, indicating a mean diameter of 350 μm and a narrow size distribution.

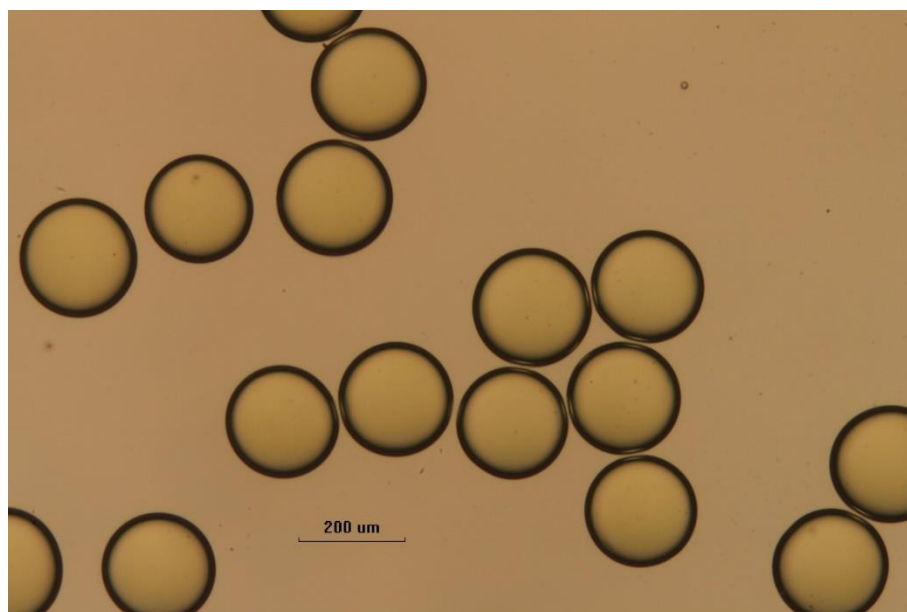


Figure VI.7: Optical microscopy of ethyl acetate swollen microgels produced by microfluidics with a monomer concentration of 40% (needle size 110 μm) after purification with ethyl acetate and ethanol.

Table VI.3. Experimental conditions using a 110 μm diameter needle with a monomer concentration of 40%.

Sample	Flow discrete phase (ml/h)	Flow continuous phase (ml/min)	Monomers concentration (%)	Exposition time (s)	Size (μm) ^a
A	0.2	0.6	40	120	polydisperse
B	0.2	0.4	40	90	polydisperse
C	0.2	0.25	40	60	polydisperse
D	0.2	0.35	40	120	200

a) As measured by optical microscopy, swollen in ethyl acetate

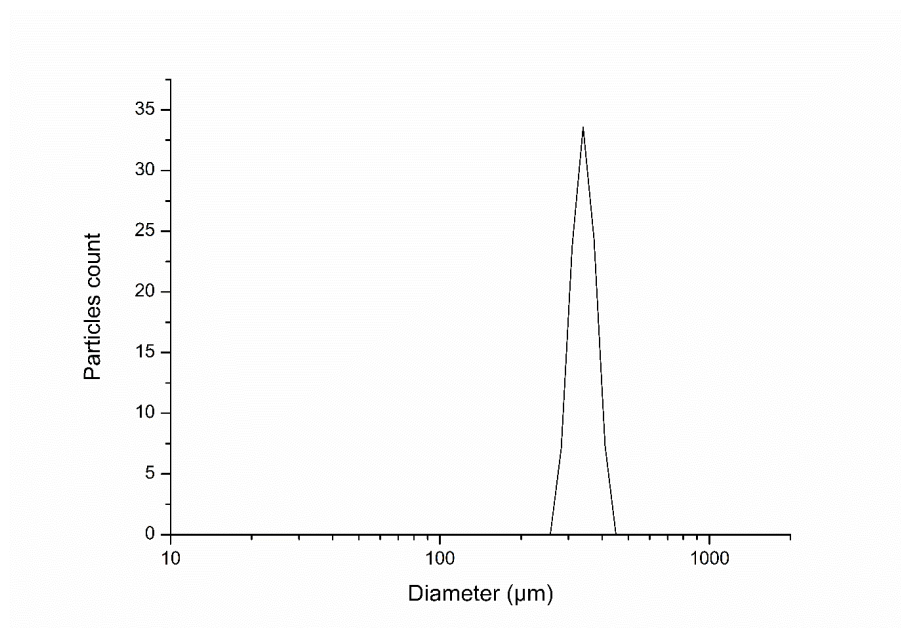


Figure VI.8: Size distribution of the microgels produced by microfluidics in ethanol.

Finally, the monodisperse microgels characterized with a mean diameter of 350 μm were derivatized by taking advantage of epoxide functions present in the microgels shell. Cyclopentadiene functions were introduced by epoxide ring opening using NaCp compounds according to a similar procedure described in Chapter III. The loading Cp content was calculated by UV measurements and correspond to 0.5 $\mu\text{mol/g}$. We note here that the Cp content calculated for polydisperse microgels obtained in Chapter IV was estimated at 11 $\mu\text{mol/g}$.

VI.2. Preparation of DX-gels from monodisperse microgels as-obtained by microfluidics

Doubly crosslinked (DX) gels were synthesized by covalent bonding of the above-obtained monodisperse microgels. Practically, a concentrated suspension of Cp-microgels ($d = 200 \mu\text{m}$, Table VI.3 entry D) in butyl acetate was stirred at r.t. and MDI-TAD in butyl acetate was added directly to the suspension for a relative TAD/Cp ratio of 0.8 as it was previously observed to be the best condition for the synthesis of DX-gels in Chapter IV. As depicted in Figure VI.9, a monolithic gel is formed within few seconds after the addition of the TAD crosslinker. The red color of the TAD moieties disappeared completely in seconds after the gelation. Morphology of the DX-gel was

investigated by SEM. It corresponded to highly deformed spherical objects arranged randomly. As the quantity required to make one sample is important, it is, at this stage, impossible to perform any mechanical testing by rheology. Indeed, our microfluidics set up can only produce 100 mg of microgels a day.



Figure VI.9: Picture of the DX-gel formed within 2 minutes after addition of the MDI-TAD onto monodisperse microgels suspension.

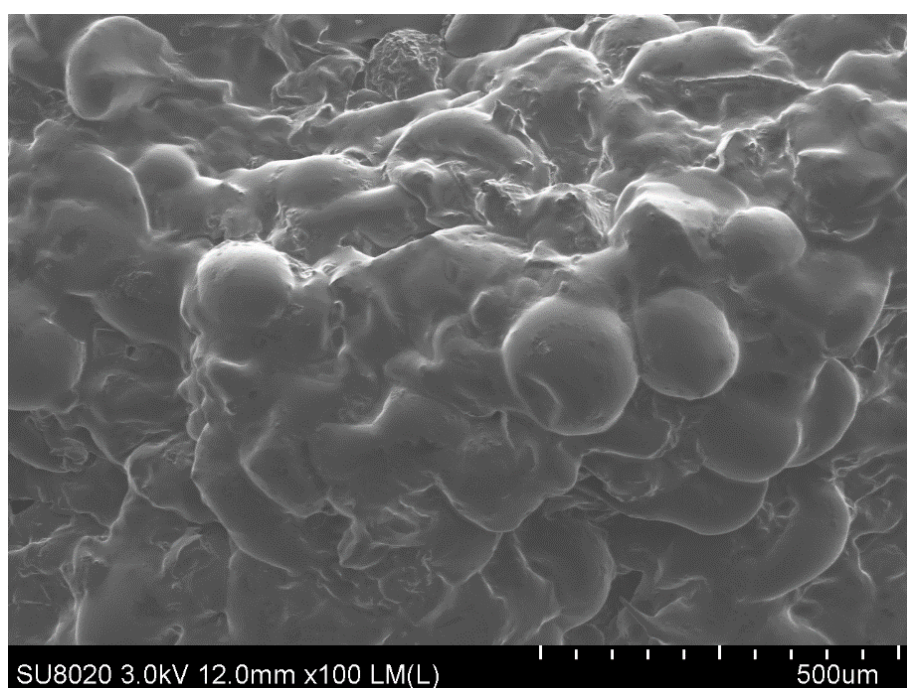


Figure VI.10: Morphologies of covalent DX-gel from monodisperse microgels prepared by microfluidics (Table VI.3 entry D with a TAD/Cp ratio of 0.8).

We probed the morphologies of freeze-dried DX covalent gels using SEM. Morphology of the synthesized DX-gel corresponds to interconnected microgels. Oppositely to DX-

gel obtained from polydisperse microgels, the monodisperse microgels deform a lot upon macroscopic gel formation, probably because of their larger size. To better understand the behavior of these networks, mechanical properties of the microgels deserve to be investigated but an upscaling procedure would be needed first. Indeed, the current microfluidic setup allows only the polymerization of 1 ml of a monomer solution (40%w/v) a day which is very low compared to the suspension setup from which 20 ml of monomer solution (40%w/v) can be polymerized in one single batch.

VI.3. Conclusions

In this work, larger uniform size microgels were synthesized by microfluidics emulsification in a co-flow geometry, allowing large monodisperse microgels to be produced. Size of the microgels can be easily modified by changing monomer concentration or needle size and by adapting the flow of the continuous phase or discrete phase. Derivatization was successfully attested by UV measurements, even though the quantity of grafted cyclopentadiene is far lower compared to microgels produced by suspension. In a final step, a doubly crosslinked gel was synthesized using the microgels produced by microfluidics. Even though the synthesis was successful, morphology differs a lot from our previous DX-gels, synthesized probably due to the size difference and the mechanism of particles production.

VI.4. Experimental section

Materials and Methods

For the microfluidic setup, syringe pumps were KDS Scientific and New Era NE-300 model. Tygon tubing (0.8 mm internal diameter, Saint-Gobain Performance Plastics) were purchased from VWR International. 30G disposable needles were purchased from Becton Dickinson and blunted. A Metalight UV box operating with 12 (320-400 nm) lamps was used for solidification. Light mineral oil, polyethylene glycol methyl ether methacrylate PEGMA (Mn: 550 g/mol), glycidyl methacrylate GMA, ethylene

glycol dimethacrylate EGDMA, Irgacure 2959, anthraquinone-2sulfonic acid and SPAN 80 were purchased from Sigma-Aldrich. Hypermer B 246 were purchased from Croda.

Confocal microscopy images were recorded with the transmission channel on a Nikon EZ-C1.

Microfluidics emulsification

Pumping rates of continuous and discrete phases were 18 and 0.2 mL/h respectively. A 2 m piece of Tygon tubing was used, which allowed the formed droplets to be exposed to UV light for approximately 60 seconds. The tubing makes few loops inside the chamber in which the UV lamps are distributed on the outer circle. These 60 seconds were enough for fixing the structure of the beads but complete conversion was ensured with 20 min of extra off-tubing UV exposure by simply leaving the collected beads in the UV chamber. The continuous phase was prepared by dissolving 1 % (w/v) of surfactant in mineral oil. The discrete phase was prepared by first dissolving 20 mg Irgacure 2959 in 1 mL distilled water/acetonitrile solution (5/1) as initiator stock solution and 600 μ l was added to the monomers (350 mg of MA-PEG, 43 mg of GMA and 20 mg of EGDMA). The mixture was stirred and sonicated, resulting in a 40 % (w/w) monomers solution in water/acetonitrile.

Microgel derivatization

The same procedure as described in Chapter III was used for the cyclopentadiene derivatization of the microgels.

Equipment

UV Spectrometer

UV measurements were performed on a UV spectrometer Analytic-jena Specord 200

Particles size measurements

Particle size measurements were recorded on a Beckman Coulter LS 200 particles sizer.

SEM

DX gel was imaged with a field emission gun scanning electron microscope (FEG-SEM Hitachi SU8020).

Optical microscopy

Confocal microscopy images were recorded with the transmission channel on a Nikon EZ-C1.

VI.5. Bibliography

1. Frykman, S. and F. Srien, *Quantitating secretion rates of individual cells: Design of secretion assays*. Biotechnology and Bioengineering, 1998. **59**(2): p. 214-226.
2. Qiu, Y. and K. Park, *Environment-sensitive hydrogels for drug delivery*. Advanced Drug Delivery Reviews, 2001. **53**(3): p. 321-339.
3. Lademann, J., et al., *Penetration and storage of particles in human skin: Perspectives and safety aspects*. European Journal of Pharmaceutics and Biopharmaceutics, 2011. **77**(3): p. 465-468.
4. McDonald, C.J. and M.J. Devon, *Hollow latex particles: synthesis and applications*. Advances in Colloid and Interface Science, 2002. **99**(3): p. 181-213.
5. Bonderer, L.J., A.R. Studart, and L.J. Gauckler, *Bioinspired design and assembly of platelet reinforced polymer films*. Science, 2008. **319**(5866): p. 1069-1073.
6. Kanai, T., et al., *Air-pulse-drive fabrication of photonic crystal films of colloids with high spectral quality*. Advanced Functional Materials, 2005. **15**(1): p. 25-29.
7. Serra, C.A. and Z.Q. Chang, *Microfluidic-assisted synthesis of polymer particles*. Chemical Engineering & Technology, 2008. **31**(8): p. 1099-1115.
8. Nie, Z.H., et al., *Janus and ternary particles generated by microfluidic synthesis: Design, synthesis, and self-assembly*. Journal of the American Chemical Society, 2006. **128**(29): p. 9408-9412.
9. Shah, R.K., et al., *Designer emulsions using microfluidics*. Materials Today, 2008. **11**(4): p. 18-27.
10. Shum, H.C., J.W. Kim, and D.A. Weitz, *Microfluidic fabrication of monodisperse biocompatible and biodegradable polymersomes with controlled permeability*. Journal of the American Chemical Society, 2008. **130**(29): p. 9543-9549.
11. Kanai, T., et al., *Gel-Immobilized Colloidal Crystal Shell with Enhanced Thermal Sensitivity at Photonic Wavelengths*. Advanced Materials, 2010. **22**(44): p. 4998-+.
12. Chu, L.-Y., et al., *Controllable Monodisperse Multiple Emulsions*. Angewandte Chemie International Edition, 2007. **46**(47): p. 8970-8974.
13. Martin-Banderas, L., et al., *Flow focusing: A versatile technology to produce size-controlled and specific-morphology microparticles*. Small, 2005. **1**(7): p. 688-692.
14. Kim, S.H., et al., *Microspheres with tunable refractive index by controlled assembly of nanoparticles*. Advanced Materials, 2008. **20**(17): p. 3268-+.
15. Lee, D. and D.A. Weitz, *Double emulsion-templated nanoparticle colloidosomes with selective permeability*. Advanced Materials, 2008. **20**(18): p. 3498-+.

16. Kim, J.W., et al., *Fabrication of monodisperse gel shells and functional microgels in microfluidic devices*. *Angewandte Chemie-International Edition*, 2007. **46**(11): p. 1819-1822.
17. Kanai, T., et al., *Fabrication of Tunable Spherical Colloidal Crystals Immobilized in Soft Hydrogels*. *Small*, 2010. **6**(7): p. 807-810.
18. Utada, A.S., et al., *Monodisperse double emulsions generated from a microcapillary device*. *Science*, 2005. **308**(5721): p. 537-541.
19. Ye, C.W., et al., *CNC-loaded hydrogel particles generated from single-and double-emulsion drops*. *Green Materials*, 2015. **3**(1): p. 25-34.
20. Shirk, K., et al., *Assembly of Colloidal Silica Crystals Inside Double Emulsion Drops*. *Langmuir*, 2013. **29**(38): p. 11849-11857.
21. Whitesides, G.M. and A.D. Stroock, *Flexible methods for microfluidics*. *Physics Today*, 2001. **54**(6): p. 42-48.
22. Abate, A.R., et al., *Glass coating for PDMS microfluidic channels by sol-gel methods*. *Lab on a Chip*, 2008. **8**(4): p. 516-518.
23. Romanowsky, M.B., et al., *Functional patterning of PDMS microfluidic devices using integrated chemo-masks*. *Lab on a Chip*, 2010. **10**(12): p. 1521-1524.
24. Dubinsky, S., et al., *Microfluidic synthesis of macroporous copolymer particles*. *Macromolecules*, 2008. **41**(10): p. 3555-3561.
25. Wan, J., et al., *Controllable Microfluidic Production of Microbubbles in Water-in-Oil Emulsions and the Formation of Porous Microparticles*. *Advanced Materials*, 2008. **20**(17): p. 3314-3318.
26. Rosochowski, A. and A. Matuszak, *Rapid tooling: the state of the art*. *Journal of Materials Processing Technology*, 2000. **106**(1-3): p. 191-198.
27. Kanai, T., et al., *Preparation of monodisperse PNIPAM gel particles in a microfluidic device fabricated by stereolithography*. *Polymer Journal*, 2011. **43**(12): p. 987-990.
28. Gokmen, M.T., et al., *Fabrication of Porous "Clickable" Polymer Beads and Rods through Generation of High Internal Phase Emulsion (HIPE) Droplets in a Simple Microfluidic Device*. *Macromolecules*, 2009. **42**(23): p. 9289-9294.
29. Dendukuri, D., et al., *Continuous-flow lithography for high-throughput microparticle synthesis*. *Nature Materials*, 2006. **5**(5): p. 365-369.
30. Nisisako, T., T. Torii, and T. Higuchi, *Novel microreactors for functional polymer beads*. *Chemical Engineering Journal*, 2004. **101**(1-3): p. 23-29.
31. Sugiura, S., et al., *Preparation of monodispersed solid lipid microspheres using a microchannel emulsification technique*. *Journal of Colloid and Interface Science*, 2000. **227**(1): p. 95-103.
32. Li, J., et al., *Facile microfluidic synthesis of copolymer hydrogel beads for the removal of heavy metal ions*. *Journal of Materials Science*, 2016. **51**(23): p. 10375-10385.
33. Zhao, Z.T., et al., *On-chip porous microgel generation for microfluidic enhanced VEGF detection*. *Biosensors & Bioelectronics*, 2015. **74**: p. 305-312.
34. Hu, Y.D., et al., *Shape controllable microgel particles prepared by microfluidic combining external ionic crosslinking*. *Biomicrofluidics*, 2012. **6**(2).
35. Hwang, D.K., D. Dendukuri, and P.S. Doyle, *Microfluidic-based synthesis of non-spherical magnetic hydrogel microparticles*. *Lab on a Chip*, 2008. **8**(10): p. 1640-1647.
36. Kim, J., M.J. Serpe, and L.A. Lyon, *Hydrogel microparticles as dynamically tunable microlenses*. *Journal of the American Chemical Society*, 2004. **126**(31): p. 9512-9513.
37. Pregibon, D.C., M. Toner, and P.S. Doyle, *Multifunctional encoded particles for high-throughput biomolecule analysis*. *Science*, 2007. **315**(5817): p. 1393-1396.
38. Hsu, M.N., et al., *Sustained release of hydrophobic drugs by the microfluidic assembly of multistage microgel/poly (lactic-co-glycolic acid) nanoparticle composites*. *Biomicrofluidics*, 2015. **9**(5).
39. Panda, P., et al., *Stop-flow lithography to generate cell-laden microgel particles*. *Lab on a Chip*, 2008. **8**(7): p. 1056-1061.
40. Sebra, R.P., et al., *Surface grafted antibodies: Controlled architecture permits enhanced antigen detection*. *Langmuir*, 2005. **21**(24): p. 10907-10911.

41. Li, C.Y., et al., *DNA-templated assembly of droplet-derived PEG microtissues*. Lab on a Chip, 2011. **11**(17): p. 2967-2975.
42. Lin, C.C. and K.S. Anseth, *PEG Hydrogels for the Controlled Release of Biomolecules in Regenerative Medicine*. Pharmaceutical Research, 2009. **26**(3): p. 631-643.
43. Burdick, J.A., M.N. Mason, and K.S. Anseth, *In situ forming lactic acid based orthopaedic biomaterials: Influence of oligomer chemistry on osteoblast attachment and function*. Journal of Biomaterials Science-Polymer Edition, 2001. **12**(11): p. 1253-1265.
44. Burdick, J.A. and K.S. Anseth, *Photoencapsulation of osteoblasts in injectable RGD-modified PEG hydrogels for bone tissue engineering*. Biomaterials, 2002. **23**(22): p. 4315-4323.
45. Wu, Y.B., et al., *Injectable biodegradable hydrogels and microgels based on methacrylated poly(ethylene glycol)-co-poly(glycerol sebacate) multi-block copolymers: synthesis, characterization, and cell encapsulation*. Journal of Materials Chemistry B, 2014. **2**(23): p. 3674-3685.
46. Kumachev, A., et al., *High-throughput generation of hydrogel microbeads with varying elasticity for cell encapsulation*. Biomaterials, 2011. **32**(6): p. 1477-1483.
47. Kim, S., J. Oh, and C. Cha, *Enhancing the biocompatibility of microfluidics-assisted fabrication of cell-laden microgels with channel geometry*. Colloids and Surfaces B-Biointerfaces, 2016. **147**: p. 1-8.
48. Ma, S.H., et al., *Fabrication of Microgel Particles with Complex Shape via Selective Polymerization of Aqueous Two-Phase Systems*. Small, 2012. **8**(15): p. 2356-2360.
49. De Geest, B.G., et al., *Synthesis of monodisperse biodegradable microgels in microfluidic devices*. Langmuir, 2005. **21**(23): p. 10275-10279.
50. Tarameshlou, M., et al., *Synthesis of Biocompatible and Degradable Microspheres Based on 2-Hydroxyethyl Methacrylate via Microfluidic Method*. Journal of Applied Polymer Science, 2014. **131**(20).
51. Chatterjee, M. and A. Patra, *Cadmium Sulfide Aggregates through Reverse Micelles*. Journal of the American Ceramic Society, 2001. **84**(7): p. 1439-1444.

Chapter VII: Conclusions and perspectives

VII.1. General conclusions

The aim of this research was to develop injectable and robust hydrogels through a fast and metal-free approach. To meet the specifications of the biomedical fields, our challenge was to develop biocompatible materials that could crosslink in aqueous conditions upon a fast and orthogonal process, free of metal-based catalyst, able to absorb defined quantity of drugs in agreement with a tailor-made posology and with an adequate kinetics of ligation that preserve the injectable character of the material.

To reach our target, doubly crosslinked type networks (referred to as DX-gels) were chosen as the material of choice to build materials with tunable properties that could fill ill-defined shape upon injection.

Primarily crosslinked micro-beads are the building blocks of DX-gels. Functionalization of their shell with the right set of reactive moieties allow promoting intercrosslinking of the microbeads. The originality of our approach relies on the use of a combination of suspension radical polymerization to generate the microbeads and the use of Hetero-Diels Alder click chemistry reactions to build up hierarchized and well-defined materials.

The microgels synthesis incorporated two main facets as described both in chapter III and chapter VI: the optimization of the experimental conditions for the microgels synthesis by either suspension radical polymerization or microfluidics, respectively. To be successful, evaluation of several parameters such as the HLB ratio, monomer concentrations, temperature and time of polymerization needed to be investigated. To be in line with biomedical outlooks, microgels were composed of biocompatible poly(ethyleneglycole methacrylate) (PEGMA) and glycidyl methacrylate (GMA) crosslinked with ethylene glycole dimethacrylate (EGDMA). The epoxide group from GMA introduced in the microgels structure bring the possibility to derivatize the microgels through ring-opening reaction.

In the Chapter III, we have evidenced that well-defined microgels with size ranging from 12 to 90 μm could be obtained by suspension radical polymerization when using a blend of SPAN 80/TWEEN 80 (5.6/1 molar ratio) as surfactants. Optimal synthetic conditions were found for a co-monomer molar ratio $[\text{GMA}]_0/[\text{PEGMA}]_0/[\text{EGDMA}]_0$ of

3/7/1. Cyclohexane was used as continuous phase while water/acetonitrile (5/1) (40% w/v) mixture was employed as discrete phase. Polymerization was performed during 6 h at 70°C using a monomers/crosslinker/initiator molar ratio of 1/0.1/0.1.

In a next step, surface derivatization with cyclopentadiene was achieved by ring-opening the epoxide in the presence of NaCp. The epoxide opening reaction proved to be very successful in modifying microgels. Indeed, successful introduction of cyclopentadiene moieties by epoxide opening is completely controlled as the quantity of cyclopentadiene introduced onto the surface can be fine-tuned by changing the experimental parameters as attested by UV microscopy. Practically, Cp derivatization was assessed by HDA click chemistry reactions performed on microgel particles swollen in THF with pyrene-maleimide derivative. The linear emission evolution of fluorescence measured by UV in agreement with the quantity of Cp introduced on the microgels attests for our ability to fine-tune the functionalization of the beads. The analysis not only allowed for qualitative characterization but also for quantitative determination of the Cp content on the microgel surface. It should be noted that the distribution of click function onto the surface is homogenous. Cell biocompatibility tests confirmed the viability of our approach based on PEG microgels for the DX microgels synthesis. Subsequent crosslinking of the microgels using RAFT-HDA chemistry was investigated from various RAF-functionalized PEG crosslinker. While the synthesis and the reactivity of the RAFT-functionalized PEG have been successfully demonstrated, the preparation of DX through Cp/RAFT HDA remains unsuccessful for unknown reasons.

In chapter IV, TAD click chemistry was studied as a more powerful crosslinking method compared to the RAFT-based HAD reactions. Well-defined DX-gels were successfully obtained within minutes at r.t. in organic medium. Optimized click coupling conditions were found for an initial TAD/Cp ratio of 0.8. The click chemistry used to form the second level of crosslinking worked as a very efficient way to crosslink microgels and presented many advantages: easy handling, fast and no catalyst needed for the gelation reaction. The mechanical properties were probed by dynamic rheology. The storage modulus varied with the relative proportion crosslinker/microgel functionality and can be tuned depending on the crosslinker quantity with an improvement of a factor 4 for a relative ratio TAD/Cp of 0.875 but the doubly crosslinked gels produced were relatively brittle. In the second section of chapter IV, we studied several

parameters influencing the mechanical properties of the DX gels. The effect of microgel composition as well as their concentration on the mechanical properties of double crosslinked microgels were explored in chapter IV. Expanding on the work of chapter IV, various concentrations of microgels were used for the preparation of DX-gel using TAD chemistry. The moduli of the doubly crosslinked gels were sensitive to both particle and cyclopentadiene concentration group concentration. Increasing both of these parameters resulted in double-crosslinked microgels with higher moduli. Moreover, microgel intra-crosslinking and size greatly influence the final properties of the DX-gel. These findings suggest that our synthetic approach offer an easy fine-tuning of the mechanical properties to reach on-demand moduli ranging from 800 to 4000 Pa. Moreover, TAD-based HDA click reaction is a highly powerful method that might be of particular interest anywhere fast ligations in mild conditions is a requirement.

Biomedical applications require the use of a benign solvent for the synthesis of DX-gel by TAD chemistry. As a proof of concept, the organic solvent was replaced by aqueous solutions composed of water and DMSO. While it is well established that TAD functions suffer from hydrolysis in aqueous environment, the kinetics of degradation of the TAD is far slower than the click process. Taking this advantage into consideration, we demonstrated in chapter V that water/DMSO allows for successful preparation of DX-gels within seconds. A swelling test performed in water demonstrates that higher swelling is noticed after creation of the second network, owing to the creation of interstitial voids that allow engulfing more water. Finally, the hydrogel was injected subcutaneously in a mouse and for a first qualitative test of biocompatibility *in vivo*. After 1 week, necrosis or inflammation of tissues were not noticed, tending to assess through this explorative test the biocompatibility of the PEG-based DX gels.

As size distribution might influence the resulting properties of the resulting material, chapter VI focused on the preparation of DX-gel from a monodisperse batch of microgels. This challenge was overcome by the use of a microfluidics system, known to deliver monodisperse beads. Optimization through evaluation of the surfactant type, solvent nature and photoinitiator was carried out to deliver well-defined and monodisperse microgels with size centered around 300 μm . The size of the microgels can be easily modified by changing either the monomer concentration or the needle

size and modulating the flow of the continuous or discrete phase, with very good reproducibility. Finally, cyclopentadiene derivatization and subsequent crosslinking using TAD chemistry were successful to prepare DX gel. Even though the synthesis was successful, morphology differs a lot from our previous DX-gels synthesized probably due to the size difference of the starting beads and the mechanism of particles production.

VII.2. Perspectives

This final section discusses potential improvements to the methods described in this work and possible applications for microgels prepared. As the mechanical properties of hosting tissues vary depending on the place of injection, broadening the range of accessible mechanical properties should be investigated by modulation of various parameters as:

- The use of a higher molecular weight bis TAD crosslinker.
- Modulate the crosslinking density of the primary beads
- Modulate Cp concentration on the surface of the beads
- Mix small (40 μm) and big (200 μm) size particles to fill the interstice left within the materials and promote higher level of crosslinking between the beads.
- Modulate the composition of the microgels by playing with different set of monomers as HEMA for example.

The success of the water-based system opens the doors to in-depth studies of this strategy. As DMSO (named Rimso-50TM) is also recognized as an harmless solvent by the FDA when used in reasonable quantities, direct injection of the microbeads in the presence of bis-TAD linker must be investigated *in vivo*, followed by adequate biocompatibility tests. Since the mechanical properties will dictate the application of the material, dynamic rheology studies on the resulting DX-gels must be studied. Moreover, study of drug loaded microgels and their subsequent interlinking must be performed to evaluate whether the drug does not hamper the crosslinking in the presence of MDI-TAD. As the resulting materials present similar mechanical characteristics than the brain, these DX-gels could be implanted into rat skull as a model study for potential drug loaded material in brain cancer therapy. Microgels functionalized using click chemistry may be beneficial in diagnostic technologies. The high efficiency of the TAD-ene reaction and the ability to introduce multiple useful functionalities to colloidal polymer particles can be particularly useful in microgel and

hydrogel applications. Cp-functionalized microgels can find potential applications in coating and in fiber, textile and surface modification. Indeed the very reactive Cp group could be used to introduce functional group allowing antimicrobial and antifungic properties by grafting adapted moieties onto the particles surfaces.

More generally, the DX gels synthesized by TAD chemistry are worthy of further investigations in the broader context of tissue repair, particularly within tissues that naturally support load. The ability to provide improved ductility through judicious choice of parameters offers considerable benefits for designing and preparing improved injectable DX MG systems in the future and these materials provide a promising route for the fabrication of soft tissue engineering system or regenerative medicine applications. The presence of intact reactive functionalities as Cp onto the MG surface after DX gel formation may offer opportunity to post derivatization of DX gels, leading thus to a new generation of DX gels.

Monodisperse beads of various size were successfully achieved by microfluidics. However, at this stage of the thesis, only small quantities of beads were released, preventing us to study the mechanical properties of the microgels and DX samples. To alleviate this outcome, up-scaling of microgels production might be considered in the future to deliver enough material in a reasonable timeframe.

Curriculum vitae

Date of birth : 10 january 1989

Place of birth : Tournai, Belgium

Nationality : Belgium

Education

- 12.09.2016 Summer school: Plunge in our own business plan : knowledge in economics, business and marketing
- 01.03.2016 3 month scientific visitor in Karlsruhe Institute of technology, in the laboratory of Christopher Barner-Kowollik, Germany
- 24.04.2015 Project management course given by Tom Jacobs (T.O.M)
- 2012-2016 Shared PhD Umons/Ugent in chemistry under the supervision of L. Mespouille and F. Du Prez ; title : "From microparticles to injectable hydrogels : the role of click coupling"
- 2010-2012 Master degree in chemistry, University of Mons (UMons), Mons. Mention : Distinction
- 2007-2010 Bachelor degree in chemistry, University of Mons-Hainaut (UMH), Mons. Mention : Distinction

List of publications

1. R. Absil, S. Çakir, S. Gabriele, P. Dubois, C. Barner-Kowollik, F. Du Prez, L. Mespouille, Click reactive microgels as a strategy towards chemically injectable hydrogels, *Polymer Chemistry*, 2016. **7**(44): p. 6752-6760
2. R. Absil, S. Gabriele, F. Du Prez, L. Mespouille, In depth mechanical characterizations of DX gels produced by TAD click chemistry, *In preparation for Soft Matter*
3. R. Absil, S. Gabriele, L. Mespouille, F. Du Prez, Click functionalized monodispersed microgels as starting building block for doubly-crosslinked hydrogels, *In preparation for a communication in Journal of material chemistry A*

List of poster presentation

1. Synthesis of crosslinkable microgels by suspension polymerization as potent drug carrier for in vivo local delivery" in "Journée scientifique de l'institut Santé", Mons, belgium (2013)
2. Synthesis of crosslinkable microgels by suspension polymerization as potent drug carrier for in vivo local delivery" in "Annual BPG Meeting" , Gent, belgium (2014)

3. Synthesis of crosslinkable microgels by suspension polymerization as potent drug carrier for in vivo local delivery" in "Annual Meeting of the Belgian Polymer Group (BPG 2015)" , Houffalize, Belgium (2015)
4. Synthesis of crosslinkable microgels by suspension polymerization as potent drug carrier for in vivo local delivery" in "International Symposium on amphiphilic polymers, networks, gels, membranes" , Budapest, Hongrie (2015)
5. From reactive microgels to injectable hydrogels : implementation of click coupling reaction for in situ gelation" in "Warwick polymer conference 2016" , Warwick, Angleterre (2016)

List of oral presentation

1. "Synthesis of crosslinkable microgels by suspension polymerization as potent drug carrier for in vivo local delivery" in "IAP DYSCO Study Day" , Leuven, Belgium (2015)
2. Ultrafast gelation of injectable doubly crosslinked microgels by copper-free click chemistry" in "3ème Journée de l'Institut Matériaux" , Mons, Belgique (2016)
3. Ultrafast gelation of injectable reactive microgels : the power of TAD click chemistry" in "Annual Meeting of the Belgian Polymer Group (BPG 2016)" , Hasselt, Belgium (2016)
4. Ultrafast gelation of injectable reactive microgels : the power of TAD click chemistry" in "Polymer Network Group" , Stockholm, Sweden (2016)

Academic Visits

2015	Work in the lab of Prof. Christopher Barner-Kowollik for 1 week, Karlsruhe Institute of Technologie
2016	Work in the lab of Prof. Christopher Barner-Kowollik for 3 months, Karlsruhe Institute of Technologie